Exploitation of Controlled/Living Polymerization Methods and Click Chemistry Approach for Synthesis of Designed Macromolecular Architectures

Thesis Submitted to AcSIR for the Award of the Degree of

DOCTOR OF PHILOSOPHY
In Chemical Sciences

AcSIR

By

Sachin S. Patil

Registration Number: 10CC12J26007

Under the guidance of
Dr. Prakash P. Wadgaonkar

CSIR-National Chemical Laboratory,
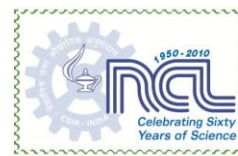Pune-411008, India

DECLARATION

I, hereby declare that all the experiments in this thesis entitled, **"Exploitation of Controlled/Living Polymerization Methods and Click Chemistry Approach for Synthesis of Designed Macromolecular Architectures"** submitted for the degree of **Doctor of Philosophy in Chemical Sciences** to the Academy of Scientific & Innovative Research (AcSIR), has been carried out by me at the Polymer Science and Engineering Division of CSIR-National Chemical Laboratory, Pune, India under the guidance of **Dr. Prakash P. Wadgaonkar**. Research material obtained from other sources has been duly cited and acknowledged in the thesis. The work is original and has not been submitted in part or full by me for any other degree or diploma to other University.

Date: 13-01-2017   **Sachin S. Patil**

Polymer Science and Engineering Division

CSIR-National Chemical Laboratory,

Pune-411 008, India.

Certificate

This is to certify that the work incorporated in this Ph.D. thesis entitled **"Exploitation of Controlled/Living Polymerization Methods and Click Chemistry Approach for Synthesis of Designed Macromolecular Architectures"** submitted by **Mr. Sachin S. Patil** to Academy of Scientific and Innovative Research (AcSIR) in fulfillment of the requirements for the award of the Degree of **Doctor of Philosophy in Chemical Sciences**, embodies original research work under my supervision. I further certify that this work has not been submitted to any other University or Institution in part or full for the award of any degree or diploma. Research material obtained from other sources has been duly acknowledged in the thesis. Any text, illustration, table, etc. used in the thesis from other sources, have been duly cited and acknowledged.

Sachin S. Patil

(Student)

Dr. Prakash P. Wadgaonkar

(Supervisor)

Dedicated to

my parents and teachers

Acknowledgement

I would like to express my sincere thanks to those who supported and contributed partly or significantly to the successful completion of my thesis.

It gives me immense pleasure to express my enormous gratitude to my research supervisor **Dr. Prakash P. Wadgaonkar** *for his continuous and fruitful guidance, encouragement and patience during the completion of research work and achieving the endeavour. He has been open to share and discus his scientific knowledge and experience at all times. I am grateful to him for having shown confidence in me and the freedom he gave me to use my own ideas to perform research work. Working with him was a great pleasure and learning experience for me.*

I express my thanks to the University Grants Commission (UGC) for the research fellowship and financial support. I would also like to express my gratitude to Dr. Ashwinikumar Nangia (Director, CSIR-NCL), Dr. Vijayamohanan Pillai, Dr. Sourav Pal and Dr. Swaminathan Sivaram (former Directors of CSIR-NCL) for giving me the opportunity to work at CSIR-NCL. It's my pleasure to thank Dr. Ashish Lele (Head, Polymer Science and Engineering Division) and Dr. A. J. Varma (former Head of Polymer Science and Engineering Division) for allowing me to work in Polymer Science and Engineering Division and providing the instrumental facilities and infrastructure to perform the research work.

I am thankful to my Doctoral Advisory Committee (DAC) members Dr. Subhash P. Chavan, Dr. S. K. Asha, and Dr. C. V. Avadhani for their yearly assessments of research work, suggestions, valuable advices and fruitful discussions during the DAC meetings. Their valuable suggestions helped me to build and to improve my research skills.

I owe my gratitude to Dr. B. B. Idage and Dr. (Mrs) S. B. Idage for their support during the joining time at CSIR-NCL. I would like to thank Dr. Jayant Khandare, Dr. Ashootosh V. Ambade, Dr. Sachin Mali, Dr. Shivshankar Mane and Professor M. Jayakannan for their suggestions and discussions during the yearly assessments and scientific problems. I also thank Dr. K. Guruswamy, Dr. Sayam Sen Gupta, Dr. J. Nithyanandhan, Dr. K. Krishnamoorthy, Dr. B. L. V. Prasad, Dr. Suresh Bhat, Dr. S. K. Asha, Dr. M. V. Badiger, Dr. Samir Chikkali, Mrs. Deepa Dhoble, Mrs. Poorvi

List of Abbreviations

Abbreviation	Expansion
ATRP	Atom Transfer Radical Polymerization
ATRC	Atom Transfer Radical Coupling
BA_6TREN	Tris(2-bis(3-butoxy-3-oxopropyl)aminoethyl)amine
bpy	2, 2'-Bipyridine
CRP	Controlled Radical Polymerization
CMC	Critical Micelle Concentration
CuAAC	Copper Catalyzed Azide-Alkyne Cycloaddition
dNbpy	4,4'-Di-5-nonyl-2,2'-bipyridine
D_h	Hydrodynamic diameter
DLS	Dynamic Light Scattering
DCM	Dichloromethane
DMF	*N,N*-Dimethyl formamide
DOX	Doxorubicin
DCC	Dicyclohexyl carbodiimide
DMAP	4-(*N,N*-dimethylamino)pyridine
FT-IR	Fourier Transform-Infra Red
GPC	Gel Permeation Chromatography
Hz	Hertz
HMTETA	1, 1, 4, 7, 10, 10-Hexamethyltriethylenetetramine
LCST	Lower Critical Solution Temperature
MALDI-TOF	Matrix Assisted Laser Desorption/Ionization-Time of Flight
MA	Methyl acrylate
MMA	Methyl methacrylate
M_n	Number average molecular weight
M_w	Weight average molecular weight
Me_6TREN	Tris[2-(dimethylamino)ethyl]amine
NIPAAm	*N*-Isopropylacrylamide
NMP	Nitroxide-Mediated Polymerization
nm	Nanometer

NRC	Nitroxide Radical Coupling
NMR	Nuclear Magnetic Resonance
PAN	Poly(acrylonitrile)
PLMA	Poly(lauryl methacrylate)
PCL	Poly(ε-caprolactone)
PC	Polycarbonate
PEGMA	Poly(ethylene glycol methacrylate)
PHEMA	Poly(2-hydroxyethyl methacrylate)
PMA	Poly(methyl acrylate)
PMMA	Poly(methyl methacrylate)
PMDETA	$N, N', N,' N,'' N''$-Pentamethyldiethylenetriamine
PDMAEMA	Poly(N,N-dimethylaminoethyl methacrylate)
PBS	Phosphate Buffer Solution
PVDF	Poly(vinylidene fluoride)
PEO	Poly(ethylene oxide)
PEG	Poly(ethylene glycol)
PS	Polystyrene
PnBA	Poly(n-butyl acrylate)
PtBA	Poly(t-butyl acrylate)
PDI	Polydispersity index (Dispersity)
PNIPAM	Poly(N-isopropyl acrylamide)
PMDETA	N,N,N',N'',N''-Pentamethyldiethylenetriamine
PNIPAAm	Poly(N-isopropylacrylamide)
PDEAEMA	Poly(N,N-diethylaminoethyl methacrylate)
PDEGMA	Poly(diethylene glycol methacrylate)
PDMAEMA	Poly(N,N-dimthylaminoethyl methacrylate)
PHFMA	Poly(hexafluoromethyl acrylate)
P3HT	Poly(3-hexylthiophene)
ROP	Ring Opening Polymerization
ROMP	Ring Opening Metathesis Polymerization
RAFT	Reversible Addition-Fragmentation Chain Transfer
RDRP	Reversible Deactivation Radical Polymerization

SPAAC	Strain Promoted Alkyne-Azide Click
SBS	Styrene-butadiene-styrene
TAD	Triazolinedione
TEM	Transmission Electron Microscopy
*t*BMA	*t*-Butyl methacrylate
THF	Tetrahydrofuran
TLC	Thin Layer Chromatography
TMS	Tetramethylsilane
TEA	Triethylamine
TMS	Trimethyl silyl

Table of Contents

Chapter 1
Introduction

Chapter 2

Functionalized Polystyrene Macromonomers Using
Phenolphthalein-Based ATRP Initiator

Chapter 3

(Poly(ethylene glycol))₂-Poly(ε-caprolactone) and Poly(ε-caprolactone)-Poly(*N*-isopropylacrylamide)-Poly(ethylene glycol) Star Copolymers by the Combination of ROP, ATRP and Coupling Reactions

Chapter 4

Temperature and pH Dual Stimuli Responsive PCL-*b*-PNIPAAm Block Copolymer Assemblies and the Cargo Release Studies

Chapter 5

Healable Network Polymers Bearing Flexible Poly(Lauryl Methacrylate) Chains via Thermo-Reversible Furan-Maleimide Diels-Alder Reaction

Chapter 6
Conclusions and Future Perspectives

Abstract

Well-defined functionally-terminated polymers have attracted a considerable attention due to their usefulness as chain extenders, cross-linkers and as precursors to different macromolecular architectures such as block, star, graft, cyclic, network, cross-linked polymers, etc. Such macromolecular architectures find potential applications in the form of plastics, elastomers, thermosetting resins, viscosity modifiers, compatibilisers in blends, emulsifiers, self healing materials, surface modifiers, lubricants in mechanical and biological systems, drug and gene delivery vehicles and so on. The combination of controlled/living polymerization methods such as ATRP, ROP, RAFT, NMP, etc. and click reactions have made possible the easier access to these macromolecular architectures which would not be otherwise possible by conventional methods of polymer synthesis. These synthetic methods allow the introduction of different number of arms/blocks in a macromolecular architecture with predetermined structural and molecular parameters (chain length) to obtain the control over hydrophilic/hydrophobic balance.

The research work described in the present thesis deals with synthesis of new macromolecular architectures and their properties with respect to the smart behaviour. Towards this end, new ATRP and ROP initiators containing functional groups were designed and synthesized. Furthermore, ATRP and ROP initiators containing functional groups were employed for the synthesis of functionally-terminated polymers and macromonomers. These functionally-terminated prepolymers and macromonomers were subsequently utilized as precursors for synthesis of various macromolecular architectures such as block, star and network polymers.

Chapter 1 gives the detailed introduction and literature survey of different approaches used to synthesize functionally-terminated polymers and the macromolecular architectures therefrom. The exploitation of controlled/living polymerization methods *viz.* NMP, ATRP, RAFT and ROP in combination with different click reactions such as alkyne-azide, thiol-ene, Diels-Alder, etc. have also been highlighted. Smart polymers based on linear block and star copolymers have been briefly discussed with respect to their stimuli-responsive behaviour. Furthermore, the smart materials based on healable polymers for coating applications and their healability has been discussed. Finally, the scope and objectives of present work have been highlighted.

Chapter 2 describes the synthesis of allyl functionalized polystyrene prepolymers

by ATRP and their utility to synthesize macromonomers with functional groups such as acid or hydroxyl. A new ATRP initiator based on commercially available, inexpensive starting material *viz.* phenolphthalein, was synthesized and subsequently employed for ATRP of styrene to obtain bis-allyloxy functionalized polystyrene
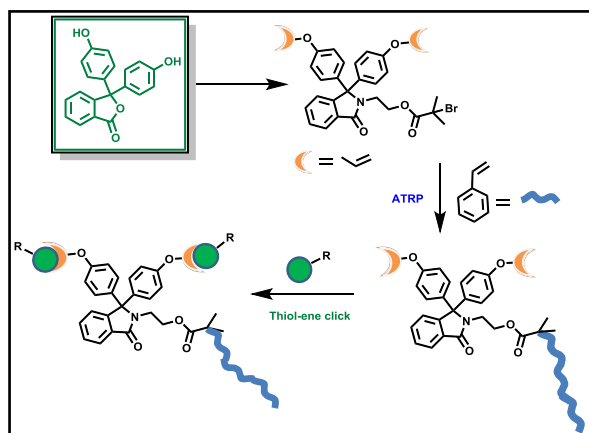
macromonomers. Allyl functionality was specifically selected as it undergoes the reactions such as thiol-ene click, bromination, epoxidation, hydrosilylation, cross-linking, etc. The efficacy of ATRP initiator for the polymerization of styrene was evaluated by carrying out kinetic investigations. Bis-allyloxy functionalized polystyrene macromonomers serve as precursors for the synthesis of star, graft copolymers, etc. Macromonomers with reactive functional groups such as hydroxyl and carboxyl and which are potentially useful for synthesis of graft polymers by polycondensation reactions were obtained by photochemical thiol-ene click reactions of bis-allyloxy functionalised polystyrene with hydroxyl and carboxyl functionalised thiols.

Chapter 3 is concerned with synthesis of star copolymers based on α, α' homo- and α, α' hetero-bifunctionalized poly(ε-caprolactone)s prepared by ROP of ε-caprolactone employing new ROP initiators containing respective functional groups. Two new ROP

initiators containing α-allyl α'-allyloxy or α-allyl α'-propargyloxy groups were synthesized starting from 3-allylsalicyaldehyde. α-Allyl α'-allyloxy and α-allyl α'-propargyloxy bifunctionalized poly(ε-caprolactone)s were synthesized by ROP of ε-caprolactone employing the respective functional initiators. Independently, thiol-terminated poly(ethylene glycol) (PEG)
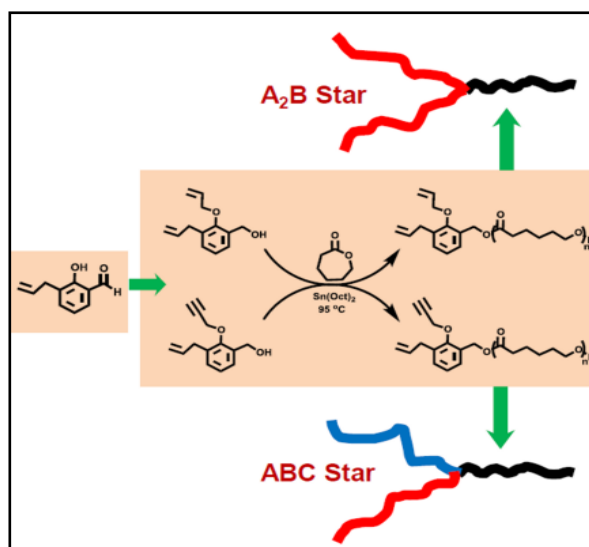
and azido-terminated PNIPAAm were prepared by end group transformations of commercially available mPEG-OH and by ATRP of *N*-isopropylamide using azido-functionalized initiator, respectively. (mPEG)$_2$-PCL star copolymer was synthesized by photochemical thiol-ene coupling reaction of α-allyl α'-allyloxy bifunctionalized poly(ε-caprolactone) with thiol-terminated PEG. PCL-PNIPAAm-mPEG star copolymer was synthesized by alkyne-azide click reaction of α-allyl α'-propargyloxy bifunctionalized poly(ε-caprolactone) with azido-terminated PNIPAAm followed by the photochemical thiol-ene coupling reaction with thiol-terminated PEG. The orthogonality of alkyne-azide and thiol-ene coupling reactions was exploited to obtain the desired star-branched copolymer. The introduction of PNIPAAm arm in PCL-PNIPAAm-mPEG star copolymer imparted thermo-responsive behaviour to polymer whereas the introduction of PEG segment increased the LCST of star copolymer. Morphological changes of the assemblies of PCL-PNIPAAm-mPEG star copolymer in aqueous solution and cargo release profiles of hydrophobic probe *viz.* pyrene from these assemblies were studied under varying conditions of temperature. The aggregates of PCL-PNIPAAm-mPEG star copolymer showed faster release of encapsulated pyrene with increasing temperature.

Chapter 4 deals with the synthesis, self-assembly and cargo release studies of PCL-*b*-PNIPAAm block copolymer. A new ATRP initiator containing both cleavable (*viz* acetal) and clickable (*viz* azido) linkages was designed and synthesized. Azido-terminated PNIPAAm s were synthesized by ATRP employing this initiator to introduce dual stimuli *viz* pH as well as temperature. Independently, propargyl-functionalized PCL was synthesized as a counterpart for alkyne-azide click reaction. PCL-b-PNIPAAm block copolymer bearing acetal as a pH- cleavable linkage close to the junction point was synthesized using alkyne-azide click reaction. The presence of pH-sensitive group and LCST behaviour of PNIPAAm confer the dual-stimuli responsive (pH and temperature) characteristics to the diblock copolymer. These stimuli responsive features were
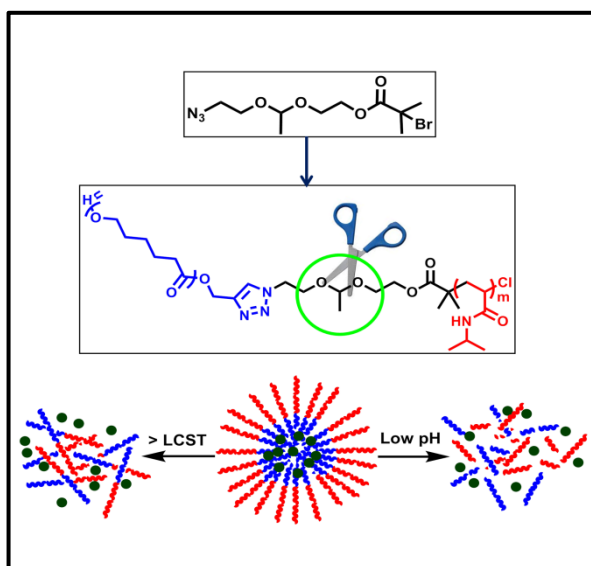
introduced to take the advantage of increased temperature and decreased pH environments of cancer tissues compared to the normal healthy tissues. pH and temperature dependant morphological changes of aggregates of PCL-*b*-PNIPAAm copolymer were studied under conditions of varying pH and temperature. Pyrene release profiles from PCL-*b*-PNIPAAm block copolymer showed the faster release with decreasing pH and increasing temperature.

Chapter 5 deals with the design and synthesis of thermo-reversible network polymers by combination of ATRP and thermo-reversible furan-maleimide Diels-Alder click reaction. A new ATRP initiator containing two furyl rings *viz.* bis(furan-2-ylmethyl) 2-bromopentanedioate was synthesized from glutamic acid as a precursor and was utilised to obtain furyl-terminated poly(lauryl methacrylate) (PLMA) macromonomers by ATRP of lauryl methacrylate. Thermo-reversible network polymer was obtained by furan-maleimide click reaction of PLMA macromonomers with trismaleimide *viz.* 1,1',1''-(nitrilotris(ethane-2,1-diyl))tris(1H-pyrrole-2,5-dione). The obtained network
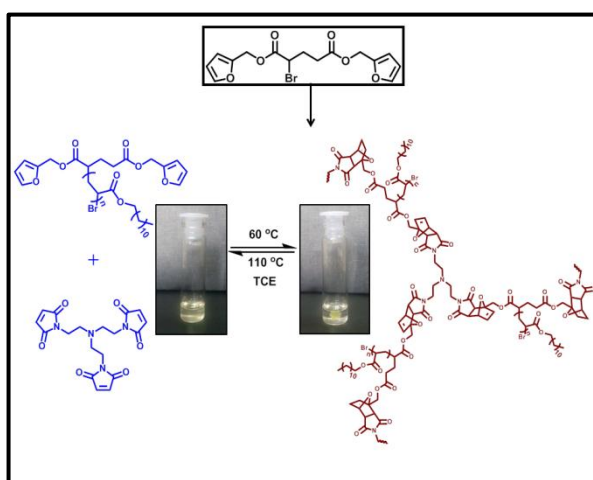
polymer exhibited scratch healing behaviour at moderate temperature (60 °C), thanks to the presence of flexible PLMA chains which induce the chain mobility in these systems due to their low Tg (-40 °C) and Diels-Alder adduct formation. Scratch healing study was performed on the films prepared from this network polymer which showed complete healing at 60 °C after five days with comparable mechanical properties.

Chapter 6 summarizes the results and conclusions of the work included in the thesis with respect to the objectives of design and synthesis of different macromolecular architectures such as macromonomers, block, star, network, etc. The scope for future work is also included in chapter 6.

Chapter 1

Introduction

1.1 Introduction

1.1.1 Polymers

Polymers are very useful class of materials. Various synthetic polymeric materials have been synthesized over the years. The properties of polymeric materials with respect to mechanical strength, thermal properties, optical properties, etc. should match the requirements of properties of materials intended for a given application. The properties of synthetic polymers can be controlled and tailored by varying their chemical structure, molecular parameters and macromolecular architecture.

The sophisticated molecular design of macromolecular architectures through the exploitation of organic reactions and methodologies is a major direction of polymer and materials research with considerable potential for fertilization of concepts between these disciplines. The recent developments in polymer science are based on the progressive synergy between advanced organic chemistry and polymer science. The synthetic approaches employing organic chemistry are the essential requirements to control all facets of macromolecular structures.

Thus, there is a continuing need of synthetic methods and approaches to afford polymers with precise composition, well-defined structure and controlled functionalities to support emerging technologies that demand increasing complexity in the polymer systems. The sophisticated design of macromolecular architectures by exploitation of controlled/living polymerization methods such as nitroxide-mediated polymerization (NMP), atom transfer radical polymerization (ATRP), reversible addition-fragmentation chain transfer (RAFT) and ring opening polymerization (ROP), etc. in combination with different click reactions is highly desirable.

The present chapter deals with the introduction to these synthetic methods with special emphasis on ATRP, ROP and different click reactions *viz*. alkyne-azide, thiol-ene, Diels-Alder, etc. for synthesis of designed macromolecular architectures. The chapter also introduces the potential applications of miktoarm star and block copolymers in the form of stimuli-responsive smart materials and that of network polymers in the form of healable smart materials.

1.1.2 Telechelic polymers

Telechelic polymers are defined as polymers bearing reactive functional group(s) at the chain end(s) which can react selectively with other molecules/reagents to form a new chemical bond. In the last few decades, there have been considerable advancements in synthesis of telechelic polymers and their applications.[1] Telechelic polymers have attracted a considerable attention due to their utility as chain extenders, cross linkers [2, 3] and as precursors to design different macromolecular architectures for various applications in the form of engineering plastics,[4] viscosity modifiers,[5] thermosetting resins and rubbers,[6] compatibilisers in blends,[7] emulsifiers,[8] thermoplastic elastomers,[9] self-healing materials,[2] surfactants,[10] surface modifiers,[11] lubricants in mechanical and biological systems,[12] drug[13] and gene[14] delivery vehicles, *etc*.

Depending on the nature of terminal group(s), telechelic polymers are classified as under:

1) Homo-Telechelic Polymers-[15],[16, 17] [18] [19] Polymers bearing same functional groups at both the terminals are termed as homo-telechelics.

2) Hetero-Telechelic Polymers- [16] [17] [20] [21] [22] [23] [24] [25] Polymers bearing different functional end groups are referred to as hetero-telechelic polymers.

3) Semi-Telechelic Polymers- [26] [27] Polymers bearing functional group only at the one chain end are categorized as semi-telechelic polymers.

4) Star-Telechelic Polymers- Polymers with more than two functional groups along the periphery are termed as star-telechelic polymers.

Schematic representation of different types of telechelic polymers is shown in Figure 1.1.

Homo-telechelic   **Hetero-telechelic**   **Semi-telechelic**

Star-telechelic polymers
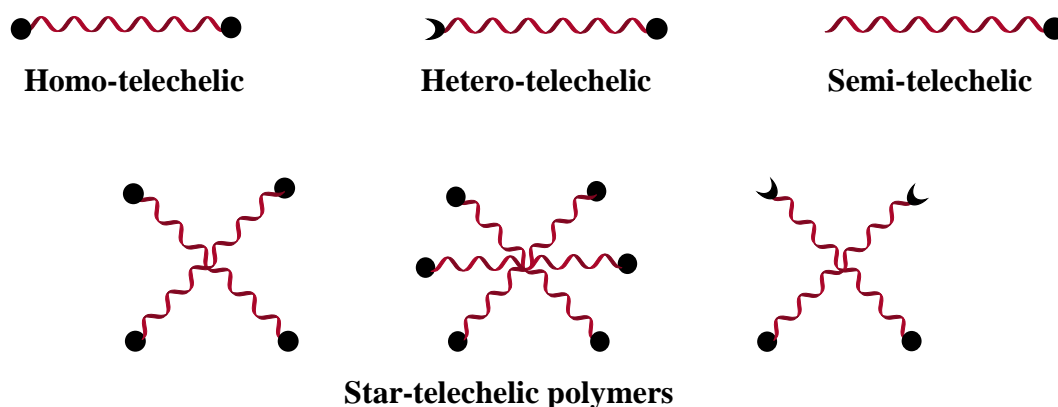
Figure 1.1 Schematic representation of different types of telechelic polymers.

1.1.3 Free Radical Polymerization

The earlier popular methods for synthesis of telechelic polymers involved the conventional free radical polymerization using initiators containing appropriate functional groups. Free radical polymerizations are relatively insensitive to impurities and can be performed at moderate temperatures. However, the disadvantages associated with free radical polymerization methods are 1) poor control over the molecular weight 2) broad molecular weight distribution and 3) difficulties in preparation of well-defined polymers with predetermined functionality. The uncontrolled behaviour of free radical polymerization makes the technique of limited utility with respect to synthesis of well-defined functionally terminated polymers.

1.1.4 Controlled/living polymerization techniques

The essential requirements for utility of polymers in terms of certain applications are the precise control of polymer structure, molecular weight and dispersity. Telechelic polymers with precise control of end functionalities, controlled molecular weight and narrow dispersity can be obtained by various ionic polymerization methods such as anionic,[28] cationic,[29] etc. and controlled/living polymerization methods *viz.* reversible addition-fragmentation chain transfer (RAFT),[30] nitroxide-mediated radical polymerization (NMP),[31] atom transfer radical polymerization (ATRP)[31] and its variants,[32, 33] *etc*. Telechelic polymers prepared by these methods are free from the complications of non-uniformity of molecular weight distribution and hence these methods are mostly preferred to achieve the controlled molecular designs. However, the ionic polymerization methods such as anionic and cationic are highly sensitive to the environmental conditions and other reactive functional groups present in the monomers or initiator involved in the polymerization process and often require the complex reaction set up.

These controlled/living systems usually proceed *via* formation of an intermediate active propagating species, which has a dynamic equilibrium between growing and dormant species. CRPs provide the ability to control the molecular weight, dispersity, composition, functionality and topology of polymers.[34, 35]

1.1.4.1 Nitroxide-Mediated Polymerization (NMP)

NMP technique is based on the principle of reversible termination where the polymer chains are end capped with nitroxide group due to reversible homolytic cleavage.

The mechanism of NMP is shown in Scheme 1.1. The control was obtained due to generation of low concentration of radicals by thermal dissociation of dormant species.

$$P_n\text{-}T \underset{K_{deact}}{\overset{K_{act}}{\rightleftharpoons}} P_n^{\cdot} + T^{\cdot}$$

Monomer K_p — K_t
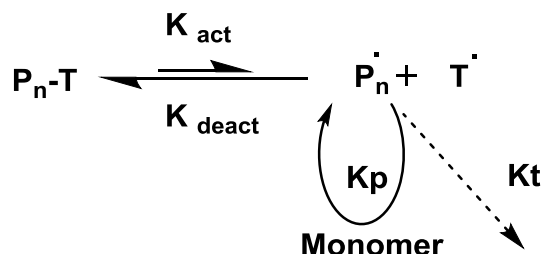
Scheme 1.1 Schematic representation of NMP mechanism.

1.1.4.2 Atom Transfer Radical Polymerization (ATRP)

ATRP is another polymerization method which is based on the principle of reversible termination where the polymer chains retain halide as end-capped group due to reversible homolytic cleavage. In ATRP, halide is reversibly transferred to metal complex. Scheme 1.2 depicts the mechanism of ATRP process. Initiation step involves the abstraction of halide radical from the organic halide (R-X) by transition metal complex, creating a radical which subsequently adds to double bond of the monomer to generate another radical which reversibly deactivates again to form dormant species.[36] Chain transfer and termination reactions have mostly been eliminated in this polymerization method.

$$P_n\text{-}X + Mt^n/L \underset{K_{deact}}{\overset{K_{act}}{\rightleftharpoons}} P_n^{\cdot} + X\text{-}Mt^{n+1}/L$$

Monomer K_p — K_t
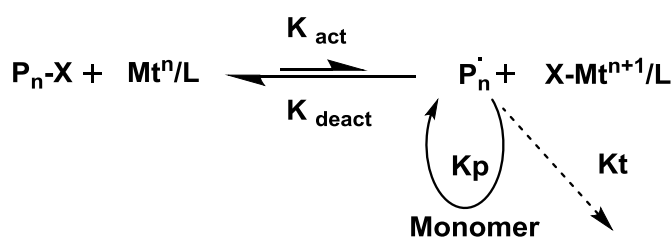
Scheme 1.2 Schematic representation of ATRP mechanism [37]

1.1.4.3 Reversible Addition-Fragmentation Chain Transfer Polymerization (RAFT)

RAFT polymerization method works on the principle of reversible transfer with exchange of active radicals via the transfer agent. Scheme 1.3 depicts the mechanism of RAFT process. The majority of chains in RAFT polymerization are dormant which participate in transfer reactions with low concentration of active radicals. Dithiocarboxylates are mostly used transfer agents in RAFT polymerization method.
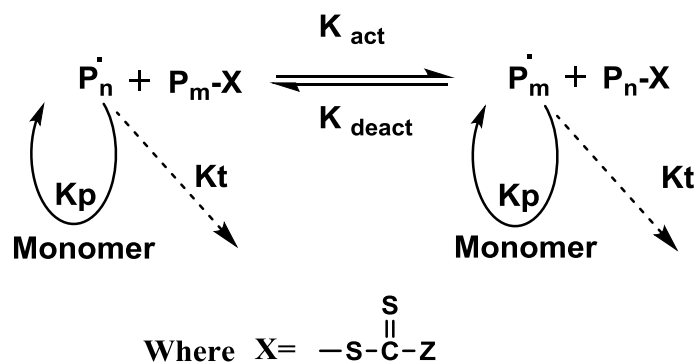
Scheme 1.3 Schematic representation of mechanism of RAFT polymerization.[30]

Amongst all the controlled/living polymerization methods, ATRP is a robust and widely used method due to its tolerance to the environmental conditions and reactive functional groups present on the initiators and monomers involved in the polymerization process. ATRP overcomes the drawbacks of both i.e the sensitivity and reactivity of ionic polymerizations and uncontrolled behaviour of conventional radical polymerizations.[38]

1.2 Atom Transfer Radical Polymerization (ATRP)

ATRP was discovered independently by Matyjaszewski[39] and Sawamoto[40] in 1995. A large number of book chapters, monographs and review articles are available pertaining to the synthesis of macromolecular architectures by ATRP.[35, 41]

To obtain better control on ATRP reaction, initiation step should be faster than the propagation i.e $K_i > K_p$ meaning the initiation rate constant (K_i) should be greater than propagation rate constant (K_p). Polymerization reactions above 95 % conversion may have the chances of radical coupling in ATRP processes that can be avoided by maintaining the conversion of reactions below 95 %. It is well known that less than 5 % terminations are observed in the ATRP reactions.[42] The selection of a suitable catalyst is an important factor in ATRP which enables the system to establish a reversible equilibrium between active and dormant species and in enhancing the rate of initiation by minimizing the possibility of radical-radical terminations.[43] Initiators used in ATRP generally contain active carbon-halide bond, *i.e.* alkyl halides R-X (X = Cl, Br).[42, 44]

The initiator used in ATRP may contain one or more α-halo-ester moieties. The architecture of the prepared polymers can be varied from linear (using alkyl halides with a single halogen atom) to star (multiple halogen atoms in the initiator) depending on the initiator structure and the exact number of halogen atoms present on them.

1.2.1 Main components of ATRP reactions

1.2.1.1 Functional initiators used in ATRP

The main component of ATRP reaction is initiator. Mainly, the activated halides are useful initiators. A range of active halide ATRP initiators to afford telechelic polymers are collected in Table 1.1.

1.2.1.2 Metal-ligand complex in ATRP

Copper (CuCl and CuBr), ruthenium and iron complexes are generally used to catalyze the ATRP reactions.[45] Generally, copper bromide is mainly used metal halide in ATRP to generate stable complex with ligands due to higher reactivity compared to that of copper chloride.[45]

The general order of activity of ligands to form complex with copper is given as tetradentate (Cyclic-bridged) > tetradentate (branched) > tetradentate (cyclic) > tridentate > bidentate.[46]

The electron density on nitrogen atoms of ligands plays an important role in activity of formed copper complexes. Generally alkyl amines are more reactive than pyridines and forms stronger complex with copper.[47] The selective examples of ligands used in ATRP are collected in Figure 1.2.
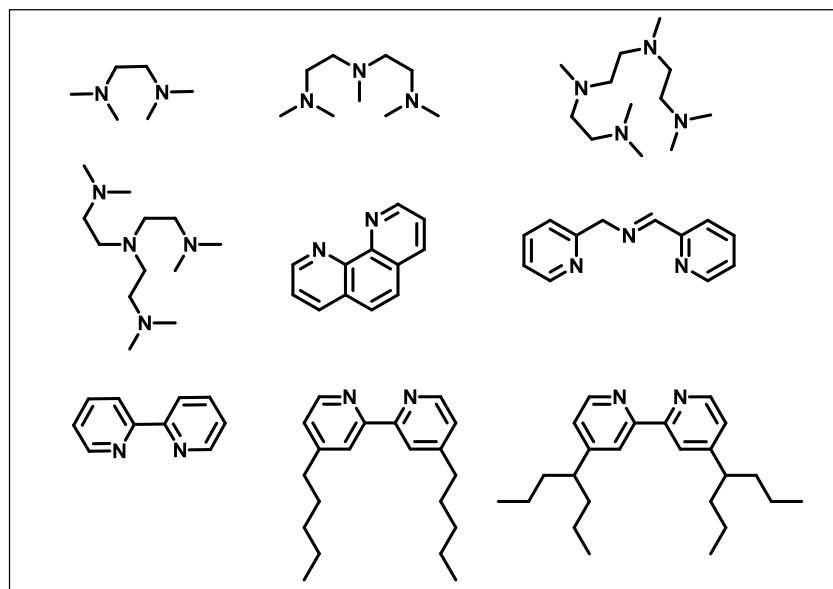
Figure 1.2 Representative ligands used in ATRP.

1.2.1.3 ATRP monomers

Several vinyl group containing monomers were polymerized by ATRP such as styrene(s), (meth) acrylate(s) and acrylamide(s). The order of reactivity of monomers is

acrylonitrile > methacrylates > acrylates = styrenes > acrylamides. [46]

A range of ATRP monomers have been reported in the literature to obtain polymers with different properties based on the criteria of applications (**Figure 1.3**)
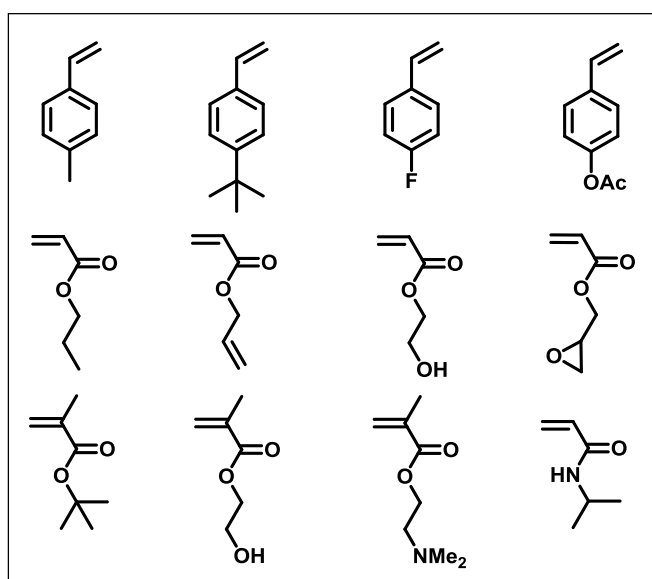
Figure 1.3 Representative monomers used in ATRP.

1.2.2 General observations on the initiator structure in ATRP

Two parameters are important for a successful ATRP initiating system. 1) Initiation should be faster as compared to propagation and 2) Equilibrium has to shift at the dormant side resulting into the minimization of probable side reactions. There are several general considerations for the choice of ATRP initiators: 1) The presence of radical stabilizing group in the order of CN > C(O)R > C(O)OR > Ph > Cl> Me.[48] Multiple radical stabilizing groups increase the activity of the alkyl halide, e.g. carbon tetrachloride, benzhydryl derivatives and malonates. The malonate with two geminal ester groups generate radicals faster than 2-bromoisobutyrate which leads to the lower dispersities. 2) Degree of substitution on generated initiator radical species in the order of primary < secondary < tertiary. Tertiary alkyl halides are better initiators than secondary ones, which are better than primary alkyl halides.[49-51] 3) The presence of weak carbon-halide bond in the ATRP initiator. The order of bond strength in the alkyl halides is R-Cl > R-Br > R-I. Thus, alkyl

chlorides should be the least efficient and alkyl iodides the most efficient initiators due to the faster leaving ability of radical species (Cl < Br < I). However, the use of alkyl iodides requires special precautions. They are light sensitive and can form thermodynamically unstable non-isolable metal iodide complexes (e.g. CuI_2) with an unusual reactivity. The R-I bond may possibly be cleaved heterolytically and there are potential complications in the ATRP process by degenerative transfer.[52, 53] Mostly, bromide and chloride containing initiators are frequently used. In general, halide in the initiator and in the metal salt (e.g., RBr/CuBr) is same; however, the halogen exchange can sometimes be used to obtain better polymerization control.[54] In a mixed halide initiating system (R-X/Mt-Y where X-Br and Y- Cl) the bulk of the polymer chains are terminated with chloride due to the stronger carbon-chloride bond.

1.2.3 Initiator efficiency

The lowering of initiator efficiency for a particular initiating system may be due to the factors such as 1) Side reactions of functionality in the initiator, 2) Initiator concentration in the reaction medium *i.e.* the ratio of monomer to the initiator and 3) The reaction temperature. Xu *et al.*[55] studied the ATRP of styrene in the presence of CuCl/PMDETA as catalyst using 5-chloromethyl-2-hydroxybenzaldehyde as an initiator. The initiator efficiency obtained was in the range 0.08 - 0.66 due to the hydrogen bonding interactions of phenolic hydroxyl group. Similarly, Marsh *et al.*[56] studied the initiator efficiency of unprotected uridine derived initiator in ATRP of MMA using CuBr/ *N-(n-*pentyl)-2-pyridylmethanimine as a catalyst. They found the decrease in initiator efficiency with increasing molecular weight of the polymer. Matyjazewski *et al.*[57] observed the lower initiator efficiency in ATRP of styrene using α-halocarboxylic acids in the presence of CuBr/PMDETA as catalyst, which was attributed to the intra-molecular cyclization resulting in the formation of γ-butyrolactone. Mei *et al.*[58] studied ATRP of styrene in the presence of CuBr/bipyridine as catalyst using coumarin-functonalized initiator. The initiator efficiency was found to decrease at higher temperature.

Furthermore, compatibility of the initiator, monomer and ligand plays an important role to obtain better efficiency. The initiator and ligand with long chains are efficient for polymerization of long chain containing monomers such as lauryl methacrylate and stearyl methacrylate.[59] The structural resemblance of initiator, monomer and catalytic system makes the synthesis more efficient. Polymerization by long chain containing initiators

requires the long chain containing ligand which helps in increasing initiator efficiency by well solubilising the copper catalyst in the reaction medium.[59]

1.3 Synthetic approaches for telechelic polymers by ATRP

Telechelic polymers can be obtained by ATRP using four different approaches: 1) Functional initiator approach by using an appropriate initiator,[60] 2) Use of functional initiator followed by the post-polymerization transformation of terminal halide into other useful functional group[61] 3) Chemical modification of a functional group incorporated *via* functional initiator into other useful functionalities employing the strategies such as deprotection/selective hydrolysis, etc. and 4) Radical-radical coupling process. These approaches lead to the formation of either homo- or hetero-telechelic polymers depending on the choice of initiator.

Figure 1.4 represents the different approaches for synthesis of telechelic polymers by ATRP.
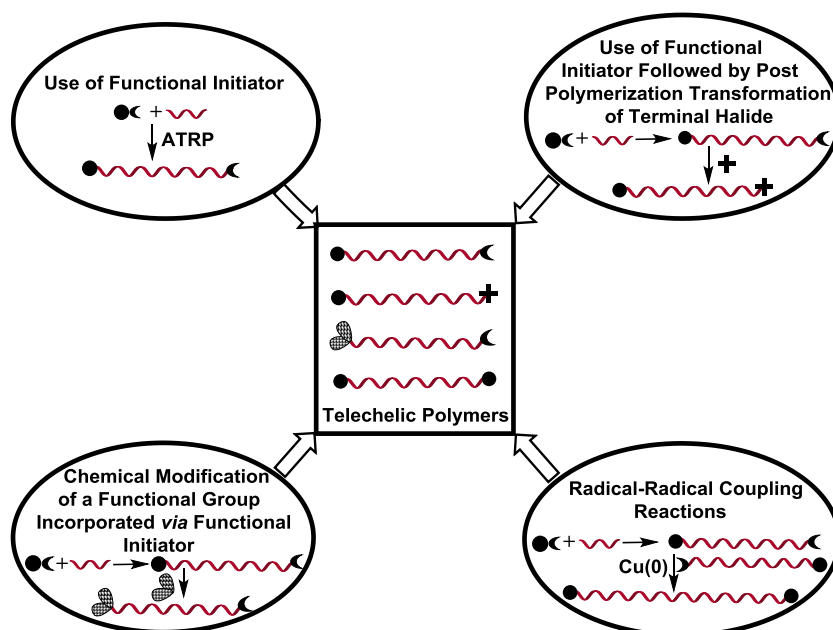
Figure 1.4 Different approaches for synthesis of telechelic polymers by ATRP.

The synthesis of telechelic polymers by the above mentioned approaches are summarized below.

1.3.1 Functional initiator approach

Amongst the above mentioned approaches, functional initiator approach has been considered as highly efficient due to high end group fidelity and the possibility to introduce a wide variety of functional groups by selecting an appropriate functional initiator. The initiator is an important component in ATRP due to its key role in controlling the equilibrium and the rate of initiation. The basic criteria for selection of initiator are the quantitative and fast initiation as compared to the propagation with less probability of side reactions. The amount of initiator determines molecular weight of the polymer and its efficiency determines the number of chains initiated.

The incorporation of functional group at one chain end and halogen at the other chain end provides a route to synthesize end-functional polymers using functional initiator approach. A range of ATRP initiators are commercially available for synthesis of linear and star architectures.[62] In the recent past, clickable functional initiators are frequently used due to the high efficiency, high yields of reactions and requirement of simpler purification methods due to the virtue of their chemistry.[63] The obtained clickable polymers are further modified either to other reactive groups to make them suitable for polycondensations in the form of macromonomers or to perform other organic transformations to synthesize different macromolecular architectures and to change their properties.[64]

The essential requirement of incorporation of a functional group by initiator approach is that the functional group must not interfere with rapid formation of the transition metal catalyst/ligand complex which is required to provide a fast reversible activation and deactivation of the growing polymer chains in ATRP reaction. Most of the successful initiators employed in ATRP are organic halides with a potentially active carbon-halogen bond, which can easily generate a radical species through electronic and steric effects of their substituent.[38] An organic halide with structural similarity to that of the dormant chain end of polymer is preferentially used so that activity of the carbon-halogen bond in the initiator is similar to that of the dormant polymer terminal. A large number of initiators with different functionalities have been compiled in an excellent review article published by Matyjaszewski *et al.* in 2001 [38] and Tasdelen *et al.* in the year 2011.[31] Summarized herein is a plethora of functional ATRP initiators reported in the

literature for the synthesis of functional polymers wherein one of the functional group is either bromide or chloride.

1.3.1.1 Functional ATRP initiators for the synthesis of hetero-telechelic polymers

Polymers obtained using functional ATRP initiators retain halogen (mostly bromide) at one of the terminals hence these polymers are termed as hetero-telechelic (α-ω functionalized) polymers. Polymers with a functionality at the initiation side are called as α-functionalised polymers, if two functional groups are on the same side, those polymers are referred to as α, α'-functionalised polymers. If both the functional groups are same then such polymers are called as α,α' homo- and if they are different, the polymers are termed as α, α' hetero-bifunctionalised polymers. Synthesis of α,α'-homo[60, 65, 66] and α,α'-hetero-bifunctionalized[67] polymers with controlled molecular weight have been reported using functional initiator approach. Furthermore, α,α'-homo-bifunctionalised polymers with functional groups such as dihydroxyl,[68, 69] dicarboxylic acid,[70] aromatic difluoro,[71] aromatic dibromo,[72] and tert-amino[73] have also been prepared successfully using initiator approach.

Halogenated alkanes, such as chloroform, trichloroethanol or carbon tetrachloride (CCl_4) were amongst the first studied ATRP initiators.[74, 75] Benzyl halides are useful initiators for the polymerization of styrene and its derivatives due to the stabilization of generated radical by phenyl ring and their structural resemblance. However, they failed in the polymerization of more reactive monomers such as methyl methacrylate (MMA).[76] Improvement of initiation efficiency for MMA using benzylic halides is possible employing the concept of halogen exchange.[77]

α-Haloesters such as ethyl 2-bromoisobutyrate and ethyl 2-bromopropionate are the widely employed commercial initiators for controlling the ATRP and are considered as the standard initiators. In general, α-haloisobutyrates produce initiating radicals faster than the corresponding α-halopropionates due to better stabilization of the generated radicals after the halogen abstraction step. Thus, slow initiation generally occurs if α-halopropionates are used to initiate the polymerization of methacrylates. In contrast, α-bromopropionates are good initiators for the ATRP of acrylates due to their structural resemblance. Sawamoto and co-workers [78] examined three different α-bromoesters to obtain better control using ruthenium based catalyst. A variety of functionalities, such as hydroxyl, epoxy, allyl, vinyl, lactone, *etc*. have been introduced onto the α-end of the polymer using

α-haloester initiators.[79, 80] Apart from the first studied non-functionalized ATRP initiators, the range of initiators that have been used successfully in ATRP are categorised and discussed below based on the functional groups, while a separate section is devoted to initiators containing 'clickable' groups.

1.3.1.1.1. Hydroxyl-containing initiators

Hydroxyl group containing ATRP initiators are well studied and can be synthesized by esterification or amidation of corresponding dihydroxy or amino-hydroxy precursors. Generally, the hydroxyl groups are well known initiators for ring opening polymerization (ROP) of ε-caprolactone and ethylene oxide. Aliphatic hydroxyl terminated polymers prepared by ATRP have been widely used for the synthesis of diblock copolymers such as polystyrene-*b*-poly(L-lactide),[81] poly(methyl methacrylate)-*b*-poly(ε-caprolactone) [82] and star copolymers such as poly(tBMA)$_2$-poly(ε-caprolactone)$_2$,[83] *etc.* by controlled ROP of corresponding lactides/lactones. The number of arms in the star copolymer depends on the number of hydroxyl groups present at the initiator end. A range of star copolymers with hydroxyl groups at the periphery were also reported by Matyjaszewski [84] and other research groups. [85]

1.3.1.1.2. Acid-containing initiators

It is well known that acid containing ATRP initiators quench the ligands employed for the stabilisation of metal complex which results into the loss of control of molecular weight and dispersity. In such cases, well-defined polymers with terminal acid groups can be prepared *via* the use of protected α-halocarboxylic acid or the initiators with acid and halide groups away from each other.[79] Protection of carboxylic acid or presence of remote halogen suppresses an intra-molecular cyclization reaction between α-halocarboxylic acid and styrene to form γ-butyrolactones. Such reaction is known to occur under ATRA condition.[86, 87]

1.3.1.1.3. Amine-containing initiators

Generally the ligands used for complex formation with the metal catalysts in ATRP reactions are bidentate and multidentate amine derivatives. The preparation of primary amine- functionalized polymers by ATRP requires the indirect methods such as protection-deprotection chemistry. To reduce the possible interaction between the primary amine

group of the initiator and the catalyst system, protected primary amine initiators have been used, which after the deprotection afford primary amine-functionalized polymers.[88-93 94-96 97] Percec *et al.*[98] reported the synthesis of a series of well-defined primary amine end functionalized polymers using different *N*-chloro substituted amides, lactams, carbamates and imides as protected primary amine-functionalized initiators. The synthesis of primary amine end functionalized polymers can also be achieved using phthalimido-functionalized initiators followed by hydrazinolysis of the phthalimido end group.[99-101 102] Primary amine-functionalized polymers can also be prepared using functionalized initiators whereby the functional group is in the form of a precursor of the amine group *viz.* the nitro.[103 104] After the polymerization process, nitro group can easily be converted to the corresponding aromatic amine group by the reduction using zinc/acetic acid.[105-114] Haddleton *et al.*[115] and Blazquez *et al.*[116] reported the use of non-protected aromatic primary amine-functionalized initiators in ATRP for the preparation of amine-functionalized polymers.

1.3.1.1.4. Ketone-containing initiators

Ketone functionalized initiators *viz.* α-bromoketones have been used to initiate the controlled polymerization of MMA catalyzed by Ni$\{o,o'$-(CH$_2$-NMe$_2$)$_2$C$_6$H$_3\}$Br [117] and Ni(PPh$_3$)$_4$.[118] Multi-halogenated alkyl ketones *viz.* CCl$_3$COCH$_3$ and CHCl$_2$COPh are among the best initiators. The stronger electron withdrawing nature of the carbonyl group of ketone induces further polarization of the carbon-halide bond, which is attributed to the faster initiation observed with the ketones than with the ester counterparts.

1.3.1.1.5. Nitrile-containing initiators

Nitrile bearing initiators *viz.* α-halonitriles are the fast radical generators in ATRP of acrylonitrile monomer due to the structural similarity and the presence of strong electron-withdrawing cyano group. Moreover, the radical generated after halogen abstraction is sufficiently reactive, which leads to the fast initiation through rapid radical addition to the monomer. Among the initiators studied for the polymerization of acrylonitrile monomers catalyzed by copper complexes, 2-bromopropionitrile resulted in the polymers with lowest dispersities [119] and is also the initiator of choice in the iron-mediated ATRP of MMA.[120] However, α-halonitriles have not been used in ruthenium-catalyzed ATRP as the cyano group deactivates the catalyst by forming a strong complex with ruthenium.[120]

1.3.1.1.6. Sulfonyl halides as initiators

The halides attached to sulfonyl group *i.e* sulfonyl chlorides yield a much faster rate of initiation than the propagation.[121] The apparent rate constants of initiation are about four (for styrene and methacrylates) and three (for acrylates) orders of magnitude higher than those for propagation. As a result, well-controlled polymerizations of a large number of monomers have been obtained in copper-catalyzed ATRP.[91] Various arenesulfonyl chloride ATRP initiators bearing functional groups such as carboxylic acid, hydroxyl, diazo, amine, *etc.* on the benzene ring have been used for the synthesis of well defined PS, PMMA and PBA.[122] The polymerization reactions were performed using copper (I) chloride and bipyridine as a catalytic system. Aliphatic and aromatic sulfonyl chlorides tolerate other functional groups present in their structures and initiate the polymerization in quantitative manner.

1.3.1.1.7. Initiators containing clickable functionalities:

Click reactions are considered as efficient reactions for polymer modifications due to quantitative yields and simpler purification of the final polymers. The different click reactions such as thiol-ene, copper catalysed alkyne-azide click (CuAAC), Diels-Alder and its variants are widely used for the synthesis of functional polymers and different polymer architectures. Clickable polymers are desirable for efficient synthesis of different macromolecular architectures. The combination of CRP and CuAAC allows the efficient synthesis of a wide range of polymers such as functional, graft, star-shaped polymers, polymeric networks, *etc*. In many cases the catalyst used in ATRP i.e. CuBr/PMDETA (*N, N', N,' N,'' N''* -pentamethyldiethylene triamine) is same as that for the click reaction which allows the simultaneous (one-pot) process of polymerization and click reaction.

1.3.1.1.7.1 Alkyne-functionalized initiators. The first report on the combination of CRP with alkyne-azide click chemistry was published by Van Hest and co-workers [61] in 2005 showing the facile approach towards block copolymers. The alkyne functionality in propargyl 2-bromoisobutyrate initiator was protected with a trimethylsilyl group (TMS)[123] to prevent possible side reactions under the polymerization conditions such as: 1) Complexation with the copper catalyst,[124, 125] 2) Subsequent homo-coupling of alkynes[126] 3) Chain transfer by hydrogen abstraction from the alkyne[127] and interference with propagating radicals leading to crosslinking.[128] Nevertheless, the TMS group was found to

be unstable under the polymerization conditions using CuBr/PMDETA as a catalyst that leads to a loss of protecting group up to 70%. The loss was ascribed to a nucleophilic attack to the TMS group by one of the nitrogen atom of PMDETA. As a consequence, the weak nucleophilic ligand 2,2'-bipyridine (bpy) was chosen to reduce the deprotection though it is not the optimum catalyst for ATRP reactions and does not avoid the decomposition completely.[129] Another strategy uses the more stable tri-isopropylsilyl group (TIPS) instead of TMS revealing no loss during the polymerization. [129] This might be due to the bulky character of the protecting group that hinders the nucleophilic attack of the metal/ligand complex. The alkyne functionalized initiators bearing either chloride or bromide as an initiating species were frequently employed for the polymerization of (meth)acrylates, styrene, and *N*-isopropylacrylamide, wherein the terminal alkyne was protected with TMS [130-132]or in unprotected form.[25, 133-137] Recently, Miller *et al.*[123] showed the requirement of protection of propargyl group with detailed description of side reactions of alkyne group occurring during the ATRP. In these cases, the undesired chain transfer and termination reactions were suppressed by performing the reaction for short time and for lower conversions. Furthermore, side reactions involving the alkyne functionality were suppressed employing lower alkyne concentrations using high monomer to initiator concentration ratio[105] or by performing the reactions at relatively lower temperatures.[138]

1.3.1.1.7.2 Azido-functionalized initiators: The well known method for synthesis of azido-functional ATRP initiator is esterification/amidation of an azide containing alcohol or amine with halo-isobutyryl halide. Since the azide functionality can easily and efficiently be introduced by substitution of the mediating halide with sodium azide, one can avoid the requirement of azide-functionalized initiators. However, the degree of azide functionalization obtained using the initiator approach is higher compared to the transformation route. The reason is the nature of CRPs *i.e* termination reactions occur to some extent and hence the polymer chains cannot retain 100 % of the halide at the ω-terminal. As a consequence, the quantitative azide functionalization at the polymer chain end is difficult. The azide moiety in the initiator can be used without protection during polymerization although some side reactions were described: 1) Cyclization reactions between the azide and the propagating radical that causes low initiator efficiency[139] 2) 1,3-Cycloaddition of azides with the double bond of the monomer occurs in the absence of a catalyst at high temperatures and long reaction times at which the monomer concentration

decreases. The rate of cycloaddition of azide with monomer is in the order of acrylates > acrylamides, methacrylates > styrenes.[140] To reduce the side reactions to a negligible extent, short reaction time [107] and low temperatures [141] are preferably used. It was demonstrated that the side reactions involving the azido group[142] were completely suppressed by performing the ATRP at room temperature.

1.3.1.1.7.3 Maleimido-functionalized initiators: Maleimide is one of the components of Diels–Alder click reaction frequently used in combination with controlled radical polymerizations in the field of materials science.[143-147] Maleimido functionalised ATRP initiators have been used in their protected form because the activated double bond present in maleimide undergoes the ATRP reaction. For example, maleimide has been protected in the form of its adduct with furan.[89] The pre-click approach has been used to protect the maleimido group and the initiator was used for the homo-polymerization of MMA.[148, 149] The protection of maleimido group with anthracene requires comparatively higher temperature which may affect the other thermally unstable groups present in the initiator structure.

1.3.1.1.7.4 Anthracene-functionalized initiators: Like furan, anthracene takes part in the Diels-Alder click reactions as a diene. The anthracene functionalized ATRP initiator was synthesized by esterification of 9-anthracenemethanol with 2-bromoisobutyryl bromide and was used for the polymerization of MMA.[150] Click reaction between anthracene and maleimide requires the higher temperature (110°C) as compared to furan-maleimide reaction (60 ^{o}C). Energy barrier to occur anthracene-maleimide reaction is higher and as a result retro Diels-Alder reaction between anthracene and maleimide requires higher temperature (above 220 ^{o}C).

1.3.1.1.7.5 Pyridyl-disulfide functionalized initiators: The disulfide containing ATRP initiators are mainly used for introduction of redox-sensitive disulfide linkage in the polymers which show the dynamic covalent bond nature. Pyridyl-disulfide functionalised polymers have been reported and are used in pyridyl-disulfide exchange click couplings. The reaction is widely employed in bioconjugations of drug, proteins, *etc*.[151, 152] It is a metal-free reaction and is considered as a click coupling reaction in a broader sense. Thayumanavan and co-workers [153] introduced a disulfide linkage in the PNIPAAm based

block copolymer by using pyridyl-disulfide containing ATRP initiator. However, side reactions in terms of chain coupling and transfer involving the disulfide have been observed at high conversions.

1.3.1.1.7.6 Aminooxy-functionalized initiators: It is known that aminooxy-functional group interferes in the ATRP reactions. To avoid the direct interaction of aminooxy group in the polymerization reaction, it should be protected either by *t*Boc-protection or phthalimido-protection. Aminooxy-functionalized poly(hydroxyethyl methacrylate) (PHEMA), poly(ethylene glycol methacrylate) (PEGMA), PNIPAAm and polystyrene were reported by Maynard and co-workers using *t*-butoxycarbonyl (*t*-Boc) [88, 154] or phthalimido-protected[100] aminooxy-functionalized ATRP initiators, respectively. The absence of termination reactions was found during the polymerization performed using these protected aminooxy-functionalized initiators. The aminooxy group can easily be obtained from *t*Boc protected polymers by reaction with trifluoroacetic acid and from phthalimido-protected polymers by reaction with hydrazine hydrate after the polymerization. Generally, aminooxy-functionalized polymers undergo the rapid aldehyde-aminooxy click reaction without the additional external reagents. The formed oxime linker between the polymers has been considered as dynamic covalent bond [155] and the approach is applicable for synthesis of pH-responsive polymers as the oxime functional group shows pH responsive behaviour[156] and is useful for protein conjugations.[157]

1.3.1.1.7.7 Allyl/vinyl ether/norbornene containing initiators: This class of ATRP initiators contains double bond which can react with thiol or tetrazine in thiol-ene and tetrazine-norbornene click reactions, respectively. Vinyl ethers are electron rich functional groups than simple alkenes. Allyl and vinyl ether containing initiators have been examined for ATRP of methacrylates, styrene and acrylates. It has been found that the vinyl ether undergoes side reactions at higher conversions (above 80 % conversions) for polymerization of methacrylates and styrene while for acrylates side reactions occur even at lower conversions. [158, 159] Thiol-ene reaction is well known and simple coupling tool for conjugation of small organic/drug molecules to the polymer backbone and can be performed thermally or photochemically by irradiating the material with ultra-violet radiations. The reaction is considered as efficient only for the conjugation of small molecules to the polymers but for polymer-polymer conjugations lower efficiency has

been shown by Junkers and coworkers due to the side reactions occurring from the generated thiyl radicals.[160] It is known that norbornene shows higher reactivity for thiol-ene reaction as compared to allyl group.[161] Norbornene containing ATRP initiators have been used for the synthesis of polymers for thiol-ene click reactions with enhanced conjugation efficiencies or for synthesis of graft copolymers by ring opening metathesis polymerization (ROMP).[162] Thiol-norbornene click reaction has been used to develop the materials with high glass transition temperatures (Tg).[163] Furthermore, norbornene functional polymers undergoes the additive-free, inverse electron demand tetrazine-norbornene click reaction.[164] Some of the allyl, vinyl ether and norbornene containing ATRP initiators are summarised in Table 1.1.

1.3.1.1.7.8 Epoxide-containing initiators: Epoxy-terminated polymers can be prepared either by direct esterification of glycidol or by epoxidation of olefin containing alcohols followed by esterification with α-bromo-acid halides. PMMA with mono-, di- and tri-epoxide end groups were prepared by these methods. Thiol-epoxy click reaction of these PMMA with hydroxyl functional thiols was performed to obtain hydroxyl terminated PMMA.[165] Protection and deprotection strategies were avoided due to tolerance of epoxide group in ATRP conditions. Single and multiple epoxide containing ATRP initiators are listed in Table 1.1.

Table 1.1 Representative examples of functional ATRP initiators for synthesis of α, ω-hetero-telechelic polymers.

Sr.No.	Functionality	ATRP Initiator	Polymer (polymerization conditions)	Ref.
1.	Alcohol		PBA, Mn-7100, Dispersity-1.10 (CuBr, CuBr$_2$, PMDETA/ 50 ^{o}C)	84
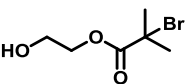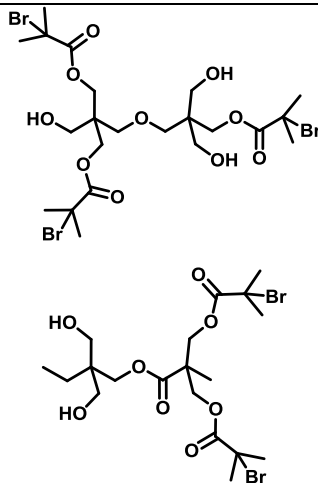
			PDEAEMA and PPEGMA (CuBr$_2$, HMTETA, Sn(Oct)$_2$)	85
			Polystyrene, Mn-8740, Dispersity-1.15 (CuBr, bpy/ 110 ^{o}C)	166
2.	Acid		Polystyrene, Mn-12000, Dispersity-1.10 (CuBr, PMDETA/ 110 ^{o}C).	79
			Polystyrene, Mn-3800-4800, Dispersity-1.18-1.54 (CuCl, bpy/ 110-140 ^{o}C).	167
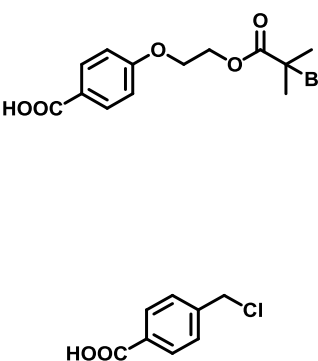
3.	Aldehyde		PMMA, Mn-6440, Dispersity-1.10 (CuBr, *N*-(*n*-octyl)-2-pyridylmethanimine/ 90 ^{o}C).	115
			Polystyrene, Mn-2100, Dispersity-1.38 (CuBr, bpy/ 110 ^{o}C	168
			Polystyrene, (CuCl,PMDETA/ 80-120 ^{o}C	169
4.	Amine		PMMA, Mn-9340, Dispersity-1.19 (CuBr, *N*-(*n*-octyl)-2-pyridylmethanimine/ 90 ^{o}C).	115
			Polystyrene, Mn-3300,Dispersity-1.08 (CuBr,PMDETA/ 130 ^{o}C.	170
5.	Alkyne		PDMAEMA, Mn-10400,Dispersity-1.17 (CuBr,HMTETA/ 60 ^{o}C	107

			Polystyrene, Mn-4650,Dispersity-1.08 (CuBr,CuBr2, PMDETA/ 80 $^{\circ}$C) and PtBA, Mn-4200, Dispersity-1.11 (CuBr,CuBr2, PMDETA/ 60 $^{\circ}$C)	171, 172
			PMA, Mn-7170, Dispersity-1.18 (CuBr, PMDETA/ 90 $^{\circ}$C	173
6.	Epoxy		PMMA, Mn-12100, Dispersity-1.5 (CuBr, PMDETA/ 35 $^{\circ}$C	174
			Polystyrene (CuBr, bpy, 110 $^{\circ}$C)	175
			PHFMA, Mn-6550, Dispersity-1.29 (CuBr$_2$, Cu, PMDETA/ 90 $^{\circ}$C	176
7.	Nitro		PMMA, Mn-6350, Dispersity-1.09 (CuBr, *N*-(*n*-octyl)-2-pyridylmethanimine/ 90 $^{\circ}$C).	115
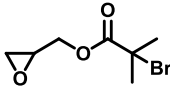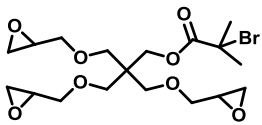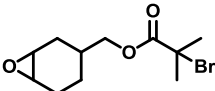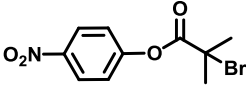
			PMMA, Mn-3800, Dispersity-1.28 , NiBr$_2$ (PPh$_3$)$_2$, 85 ^{o}C)	177
8.	Azido		PDMAEMA, Mn-8800,Dispersity-1.12 (CuBr, HMTETA/ 60 ^{o}C	107
			Polystyrene, Mn-1200-4550,Dispersity-1.2-1.3 (CuBr, bpy/ 130 ^{o}C)	178
			PNIPAAm, Mn-12400 Dispersity-1.19 (CuBr, Me$_6$TREN/ 25 ^{o}C)	179
9.	Allyl		PDMAEMA, Mn- 8600, Dispersity-1.34 (CuBr, BA$_6$TREN/ 60 ^{o}C)	180
			Polystyrene, Mn-6000, Dispersity-1.08 (CuBr, PMDETA/ 90 ^{o}C) and PMMA, Mn-7500, Dispersity-1.2 (CuBr, PMDETA, 70 ^{o}C)	181
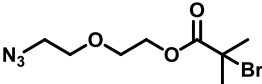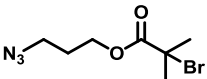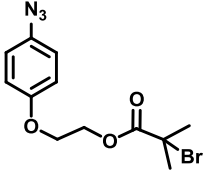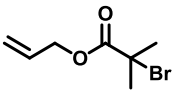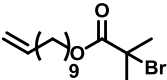
10.	Anhydride		Polystyrene, Mn-7100-12000, Dispersity-1.31-1.42 (CuBr, bpy/ 130 ^{o}C)	182
11	Lactone		PMMA, Mn-2200-3800, Dispersity-1.15-1.22 (NiBr$_2$(PPh$_3$)$_2$) PMA, Mn-3330, Dispersity-1.13 (CuBr, dNbpy/ 110°C) and Polystyrene Mn-4050, Dispersity-1.17(CuBr, dNbpy / 110°C)	183 42
12.	Vinyl ether		PMMA, (silica gel-CuBr, HMTETA) Polystyrene, PDMAEMA, PMMA, PMA, PBA (CuBr, HMTETA)	184 158
13	Oxazoline		Polystyrene (CuBr, bpy/ 110°C) Polystyrene Mn-3700, Dispersity-1.22 (CuBr, bpy/diphenyl ether, 110°C) Polystyrene Mn-2100, Dispersity-1.09 (CuBr, PMDETA/ 70°C)	185 185, 186 185
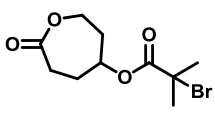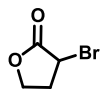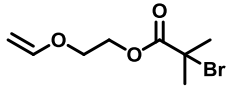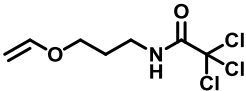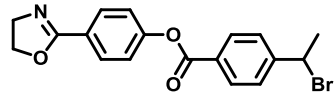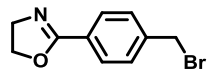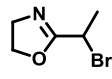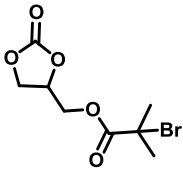
14	Carbonate		PMMA Mn-1740-3500, Dispersity-1.17-1.30 (CuCl, PMDETA/ 60°C)	187
15	Dibenzo-cyclocatyne		PMMA Mn-3860, Dispersity-1.17 (CuBr, PMDETA/ 60°C) and polystyrene Mn-2330, Dispersity-1.07(CuBr, PMDETA/ 90°C)	188
16	Protected maleimide		PMMA Mn-5500-6300, Dispersity-1.12-1.13 (CuCl, PMDETA/ 40°C)	189
17	Anthracene		Polystyrene Mn-3240, Dispersity-1.13 (CuBr, PMDETA/ 110°C)	189
18	Benzophenone		PMMA Mn-2900, Dispersity-1.31 (CuCl, PMDETA/ 70°C) and Polystyrene Mn-1800, Dispersity-1.13 (CuBr, PMDETA/ 110°C)	190
19	Succinimide		Glycopolymers, Mn-4500-10200, Dispersity-1.10-1.31 (CuBr, N-(n-Octyl)-2-pyridylmethanimine/ 70°C)	191
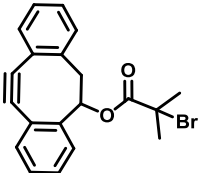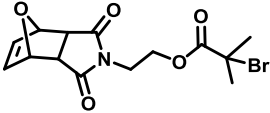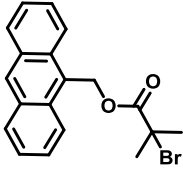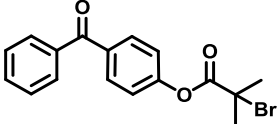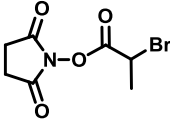
			PEGMA, Mn-6400, Dispersity- 1.14 (CuBr, N-(ethyl) 2-pyridyl-methanimine, 30°C)	192
21	α,α'- Bisallyloxy		PMMA, Mn-9000-21500, Dispersity- 1.23-1.34 (CuBr, PMDETA/ 60 ^{o}C) and polystyrene Mn-14500-29600, Dispersity- 1.06-1.09 (CuBr, PMDETA/ 110 ^{o}C)	65
22	α,α'- Bisaldehyde		Polystyrene, Mn-2200-31500, Dispersity- 1.11-1.16 (CuBr, PMDETA/ 110 ^{o}C)	66
23	α,α'- Aldehyde, allyloxy		PMMA, Mn-3700-19700, Dispersity- 1.19-1.25 (CuBr, PMDETA/ 80 ^{o}C).	67
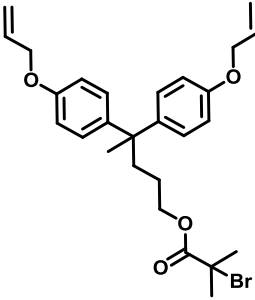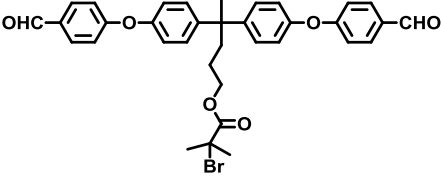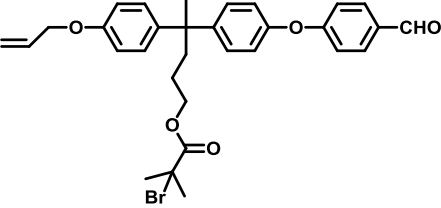
Although, a large number of reactive functional groups have been introduced at polymer chain ends by ATRP technique, there are still unresolved issues in incorporating certain functional groups such as aziridine, furan, isocyanate, isothiocyanate, etc. using ATRP initiator approach due to synthetic complications. However, some of these

functional groups have been introduced in the polymer backbone as pendant groups using respective functional monomers.[193, 194]

1.3.1.2 Difunctional ATRP initiators for synthesis of homo-telechelic polymers

Polymers prepared by ATRP using difunctional initiator retain bromide at their terminals. As the functional groups at α and ω ends are same these polymers are termed as homo-telechelic polymers. These bromide end groups can either be replaced by nucleophilic reagents or transformed into other desired functionalities by some efficient organic reactions.

Cyclopropenone masked dibenzocyclooctyne difunctional ATRP initiator was synthesized and employed for the polymerization of styrene, *t*-butyl acrylate and MMA to obtain homo-telechelic PS (Mn-2400, dispersity-1.06), P*t*BA (Mn-2860, dispersity-1.06) and PMMA (Mn-4800, dispersity-1.11) with terminal bromide groups (**Scheme 1.4**).[195] Polymerization of acrylates using free dibenzocyclooctyne functionalised ATRP initiator showed the non-living behaviour. Use of cyclopropenone masked initiator helped in controlling the ATRP of acrylates and methacrylates. Dibenzocyclooctyne functionality can easily, efficiently and quantitatively be regenerated from the masked cyclopropenone after the polymerization by irradiating the polymer with UV- light and can be used further for the metal-free strain promoted alkyne-azide (SPAAC) click reaction.
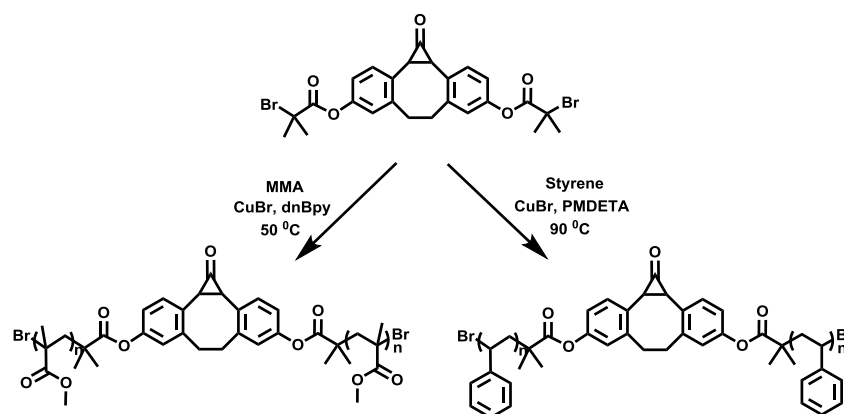
Scheme 1.4 Synthesis of homo-telechelic polystyrene and PMMA using cyclopropenone masked dibenzocyclooctyne difunctional ATRP initiator.

Chen *et al.*[196] attempted the synthesis homo-telechelic PMMA using difunctional ATRP initiator obtained by reaction of ethylene glycol with 2-bromoisobutyryl bromide (**Scheme 1.5**). ABA triblock copolymer with PMMA as glassy middle block and amide

containing dynamic hydrogen bond forming polyacrylate as outer blocks has been synthesized from these homo-telechelic PMMA. The triblock copolymer self assembled into a nanostructure which exhibited the improved mechanical properties and toughness as compared to the previously reported systems showing self healing behaviour based on hydrogen bonding (supramolecular). The mechanical properties were tuned by varying the chain length of outer amide containing hydrogen bonding soft block.
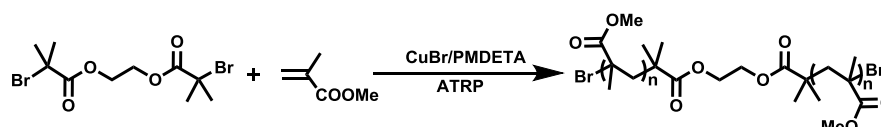
Scheme 1.5 Synthesis of homo-telechelic PMMA from ethylene glycol based ATRP initiator.

Synthesis of molecular architectures with complex topologies such as rotaxanes and catenanes are challenging due to the synthetic difficulties. The design of rotaxanes and catenanes require the use of chemical templates based on hydrogen bonding and donor-acceptor systems. The synthesis of catenane- the interlocked molecular architectures, consisting of two interlocked macrocycles, was demonstrated by Advincula and co-workers. [197] The design was based on the supramolecular 'metal-ligand complex' template approach *via*. ATRP and ATRC using a difunctional ATRP initiator bearing 1,10-phenanthroline as a complexing ligand by taking the advantage of its complex formation with metal and the post-polymerization cyclisation *via*. ATRC resulted in the formation of catenane [198] (**Figure 1.5**).
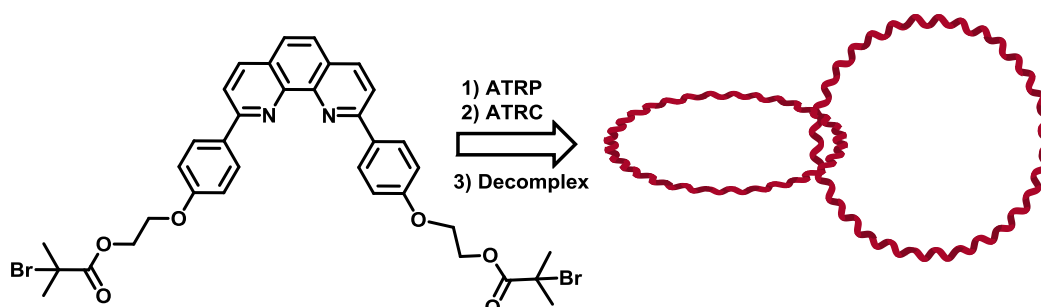
Figure 1.5 1, 10-Phenanthroline containing ATRP initiator for catenane formation *via* homo-telechelic polymer.

1.3.1.3 Multifunctional ATRP initiators for synthesis of star-telechelic polymers

It is well known that the star copolymers show unique properties in solution as well as in bulk in the sense of hydrodynamic volume, viscosity, rheological and mechanical properties and lower critical solution temperature (LCST) as compared to their linear counterparts with same molecular parameters. Various approaches have been explored such as 'core-first', 'arm-first', 'coupling onto', *etc.* to obtain the star architectures involving the use of multifunctional initiators. Multifunctional initiators have been demonstrated based on the molecules with multiple reactive sites. For example, a range of star-telechelic PNIPAAm was demonstrated by Lyngso *et al.* [199] using different multifunctional initiator core molecules (**Scheme 1.6**). The effect of star architecture with different number of arms, arm lengths and arm configurations on the LCST behaviour of PNIPAAm has been investigated. The structural modification of such star-telechelic polymer to 3-arm star-block copolymer may be of interest to carry hydrophobic drugs to the target.
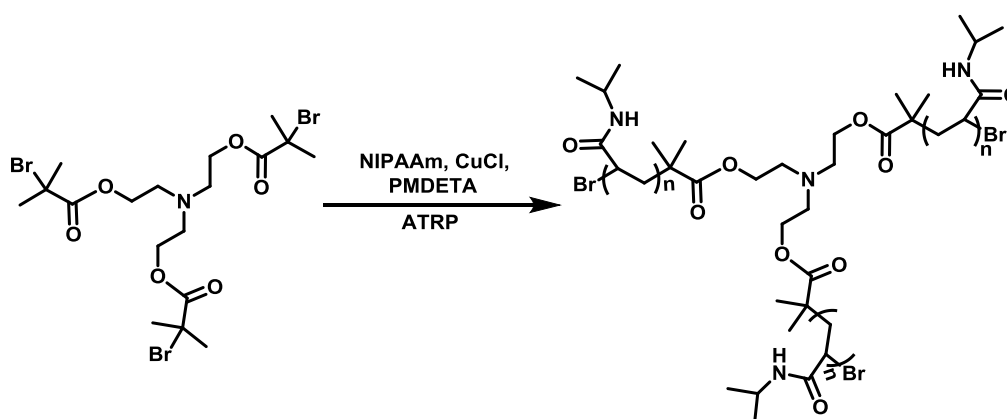
Scheme 1.6 Trifunctional ATRP initiator for 3-arm star telechelic PNIPAAm.

Pentaerythritol is one of the widely used precursors for designing the initiators for star architectures. A multifunctional ATRP initiator, namely, pentaerythritol tetrakis(2-bromoisobutyate) was designed from pentaerythritol to synthesize star telechelic P*n*BA (Mn-70000, dispersity-1.08) (**Scheme 1.7**).[200] Star telechelic P*n*BA with varying arm numbers, arm length and compositions have been studied using ATRP and proved the technique as amenable to design the star-block copolymers for utilization in viscosity modification, and adhesive technologies.
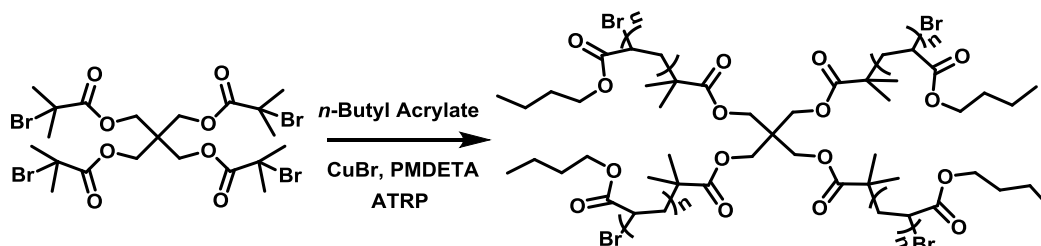
Scheme 1.7 Multi-functional ATRP initiator from pentaerythritol for 4-arm star telechelic polymer.

Phosphazene based organic-inorganic hybrid multifunctional ATRP initiator was designed with six initiating sites to synthesize 6-arm star telechelic PNIPAAm (**Figure 1.6**).[199] Effect of the 6-arm architecture on polymer behaviour in water has been investigated. Star-block polystyrene-*b*-poly(3-hexylthiophene)[201] was synthesized employing a six-armed initiator based on triphenylene using combination of ATRP and click reaction (**Figure 1.6**). Effect of star architecture on microphase separation morphology has been studied by making thin films of polymer. Microphase separation of star-block PS-*b*-P3HT showed larger crystalline domains due to aggregation of P3HT as compared to the linear block copolymer counterparts.
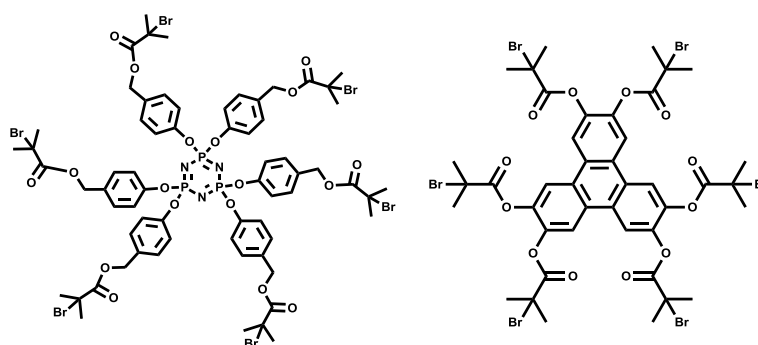
Figure 1.6 Multi-functional ATRP initiators for 6-arm star telechelic polymers.

The commericially available hexakis(bromomethyl)benzene has been used earlier directly to obtain a six-armed star polystyrene using the CuBr/bpy system.[202] Multi-functional polymer additive was reported using functional initiator approach by Narrainen *et al.*[203] A series of multifunctional initiators carrying multiple fluroalkyl groups were synthesized and were used for controlled radical polymerization of vinyl monomers such as styrene and methyl methacrylate to prepare polymer additives carrying fluroalkyl groups at the chain end. Furthermore, temperature and pH dual-responsive 18-arm star-

shaped poly(*N*-isopropylacrylamide)-*co*-poly(itaconamic acid) copolymers were prepared using a 18-arm multifunctional ATRP initiator designed from cyclodextrin (**Figure 1.7**).[204] LCST of the star-shaped copolymer was increased with increasing molar fraction of poly(itaconamic acid). Self assembled aggregates of this star copolymer encapsulate drug in the cavity of cyclodextrin core. Hydrophobic cavity of cyclodextrin helps in drug encapsulation and showed drug release in the intestine due to the pH responsive nature of star polymers. These star copolymers have been utilised for intestinal drug delivery applications.
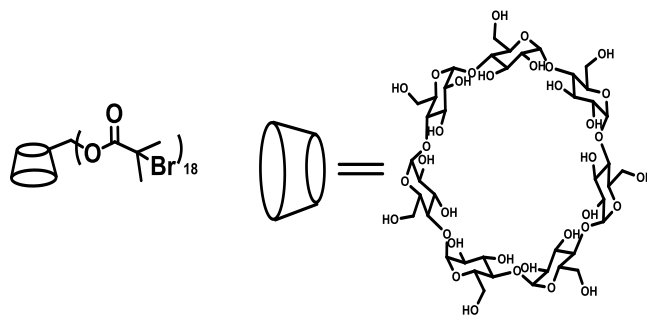
Figure 1.7 Multifunctional ATRP initiator based on cyclodextrin for 18-arm star telechelic polymer.

1.3.2 Use of functional initiator followed by post polymerization transformation of terminal halide

Polymers prepared by ATRP retain halide (bromide) functional group at one of the chain ends which can be transformed into other functional groups using organic transformations. The approach involves the use of functional initiator followed by post-polymerization functionalization of the halogen end group of the polymer into the desired functional groups to obtain α, ω-bifunctionalised polymers.[168, 205, 206] Different routes of post-polymerization transformation of terminal halide obtained by ATRP are represented in Scheme 1.8.
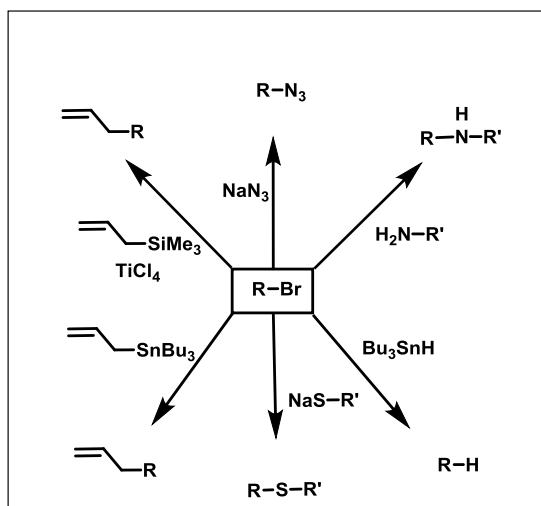
Scheme 1.8 Different routes of post-polymerization transformation of terminal halide.

The transformation of terminal halide to other functional groups can be achieved by two ways.

1.3.2.1 Nucleophilic substitution: Nucleophilic substitution approach was utilized to transform the halogen end group of the polymer into different useful functional groups such as azido, [207] (**Scheme 1.9**), thiol, hydroxyl, carboxylic acid, amine, *etc.* [208, 209]
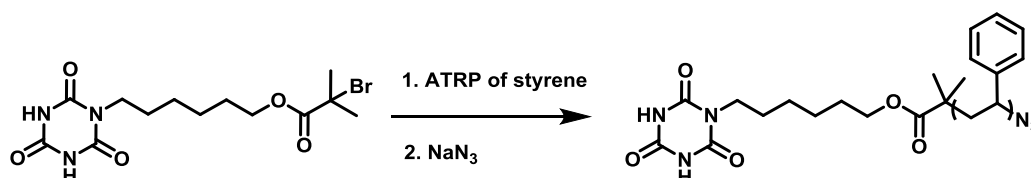
Scheme 1.9 Hetero-telechelic polystyrene with thymine and azido group by post-polymerization transformation.

Use of alkyne containing ATRP initiator followed by transformation of bromide to azido group (**Scheme 1.10**) was useful mainly for synthesis of two architectures: 1) cyclic polymers and 2) linear step growth polymers *via*. click-polymerization. The cyclic polymers such as cyclic PNIPAAm[138] were prepared under high dilution conditions to avoid competing linear polymer formation. These cyclic PNIPAAm showed broad thermal phase transition range, lower LCST and enthalpy change as compared to their linear counterparts due to the absence of chain ends and conformational restrictions of polymer backbone.
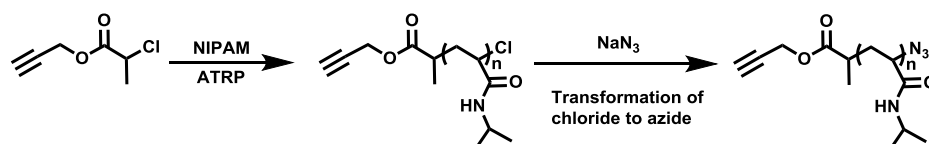
Scheme 1.10 Transformation of terminal halide to azido by nucleophilic substitution.

Matyjaszewski and co-workers [25] attempted the synthesis of α-propargyl ω-azide and α,ω- diazido telechelic polystyrene by transformation approach. The linear step growth polymers were obtained from these telechelic polystyrene by alkyne-azide click homo-coupling and coupling with bispropargyl ether, respectively, *via.* click polymerization. The obtained polystyrene showed broad dispersity due to the competing intra-molecular cyclization of polymer chains in *N,N*-dimethylformamide to form cyclic polystyrene fractions.

A range of functionalities such as dihydroxyl and diamino have been introduced at the ω-chain end *via.* nucleophilic substitution of bromide end group prepared by ATRP.[210-212] Babin *et al.*[212] introduced dihydroxyl and diamino groups onto the ω-chain end *via.* nucleophilic substitution of bromide end group with appropriate amino-diols or triamine, respectively (**Scheme 1.11**). The dihydroxyl chain ends were further modified to ATRP initiators for *t*-butyl acrylate polymerization to obtain water soluble, pH responsive polystyrene-poly(acrylic acid)$_2$ star copolymer while the amino groups were utilised directly for *N*-carboxy anhydride (NCA) polymerization to obtain water soluble, pH responsive polystytrene-poly(L-glutamic acid)$_2$ star copolymer to study the effect of stimuli on the self assembly.
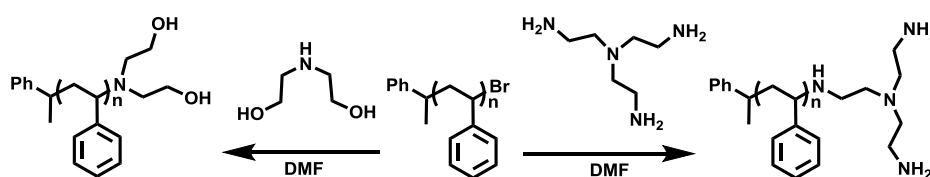
Scheme 1.11 Transformation of terminal halide by nucleophilic substitution.

The reaction of bromine end group with amine nucleophile is slower than that with sodium azide. However, the basicity of the amine is greater than that of azide, which increases the possibility of side reactions. ω- Amino functionalization on polystyrene has been attempted by Postma *et al.*[102] using potassium phthalimide as a nucleophile which leads to the formation of double bond at the ω-terminal due to the elimination of bromide.

Furthermore, general procedure for ω-amino functionalization is the conversion of azide group into phosphoranimine followed by the hydrolysis to amino end group.[213] The direct displacement of bromide from polystyrene, poly(acrylate)s and poly(methacrylate)s with hydroxide ion was not successful and was accompanied by significant elimination. The bromide end group has also been replaced by acetate group using sodium acetate. The cationic groups at the ω-terminal were obtained using phosphines as nucleophiles. For example, tri-*n*-butylphosphine and triphenylphosphine were employed and their feasibility and selectivity with model alkyl halides was investigated.[214] Boyer *et al.* reported thiol terminated poly(*t*-butyl acrylate) using nucleophilic substitution of bromide with sodium methanethiolsulfonate followed by the generation of thiol by hydrolysis using triethylamine (**Scheme 1.12**).[208] Thiol-terminated P*t*BA was amenable for protein conjugation by thiol-ene or thiol-maleimide Michael addition reactions.
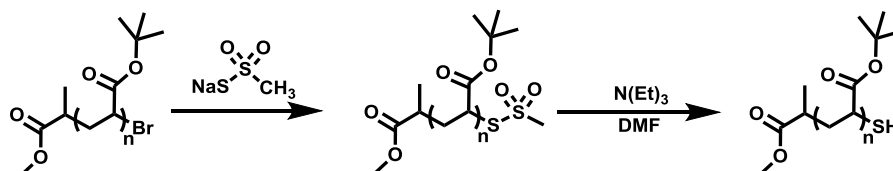
Scheme 1.12 Transformation of terminal halide to thiol using sodium methanethiolsulfonate followed by hydrolysis.

1.3.2.2 Electrophilic addition: Halide end groups on the polymers can also be transformed by addition of electrophiles. For example, Nakagawa *et al.* [215] successfully transformed the bromide end group of polystyrene by titanium tetrachloride (TiCl$_4$) catalysed electrophilic addition of allyltrimethylsilane (**Scheme 1.13**).

Scheme 1.13 Transformation of terminal bromide to allyl group by electrophilic addition reaction.

1.3.3 Chemical modification of a functional group incorporated via functional initiator

If the functional group in the initiator is unstable or capable of participating in side reaction under the ATRP conditions, that group should be protected. Functional groups such as maleimide, amine, alkyne, acid *etc.* should be protected using pre-click strategy or simple organic reaction. After completion of polymerization, the protected group (*t*-

Butoxycarbonyl (*t*-BOC) for amine and *t*-butyl (*t*-Bu) for acid) can be deprotected to obtain desired functionality. Functional groups such as acid and amine interfere in ATRP, thus the telechelic polymers with carboxylic acid and amine groups [216] can be obtained using the masked initiators which after polymerization can selectively be hydrolyzed to obtain the desired functionality (**Scheme 1.14**).
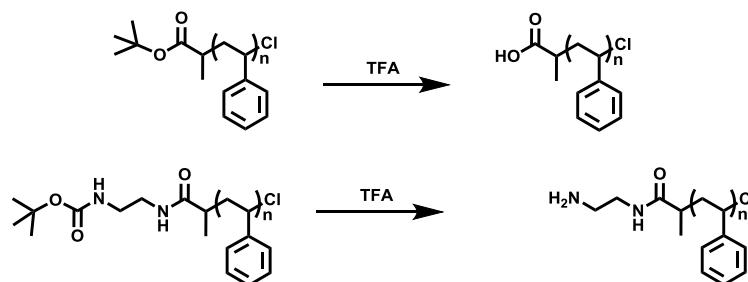
Scheme 1.14 *t*-BOC protected carboxylic acid and amine functionalized polystyrene and their chemical modification to corresponding acid and amine.

Similarly, Haddleton and co-workers[217] obtained the amino telechelic poly(ethyleneglycol methacrylate) (PEGMA) using *t*-Boc-protected amine containing ATRP initiator followed by acid hydrolysis (**Scheme 1.15**).
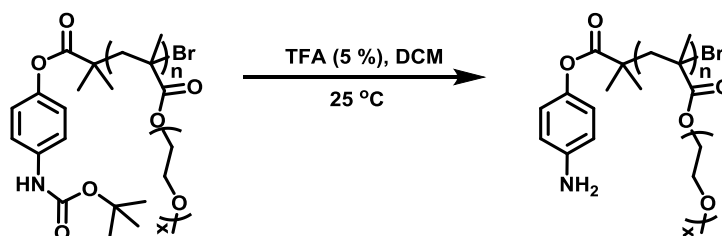
Scheme 1.15 *t*-BOC protected initiator for ATRP and its chemical modification to amine.

α- Primary amine functionalized polystyrene has been synthesized by Postma *et al.* [102] by employing the phthalimido-masked amino-ATRP initiator and post-polymerization hydrazinolysis of phthalimido end groups. The bromide end group was removed by radical induced reduction using tri-n-butylstannane before hydrazinolysis to avoid the reaction of hydrazine hydrate on bromide end (**Scheme 1.16**). This approach has been investigated as applicable for α-functionalization because the ω-functionalization led to the elimination of bromide to generate alkene at the terminal.
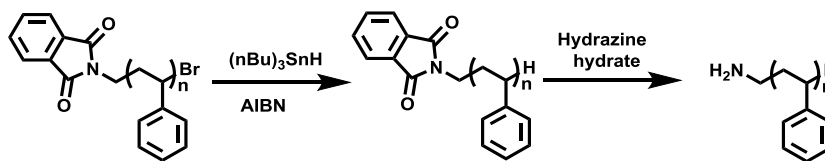
Scheme 1.16 Phthalimido-masked ATRP initiator and its chemical modification to amine by hydrazinolysis.

Caprolactone containing ATRP initiators *viz.* 2-chloro or 2-bromo-caprolactone after ATRP can be hydrolysed or their nucleophilic ring opening led to the formation of telechelic polymers. Bai and co-workers reported a facile strategy to synthesize hetero-bifunctionalised polystyrene combining ATRP and ring opening modification using α-bromocaprolactone as the initiator (**Scheme 1.17**).[218] Polystyrenes with α-hydroxyl, α'-carboxylic acid and α-hydroxyl, α'- amine hetero-telechelic groups have been prepared using amine and water as nucleophiles by ring opening modification of caprolactone incorporated *via* functional initiator and the approach is considered to be useful for the synthesis of miktoarm star copolymers.
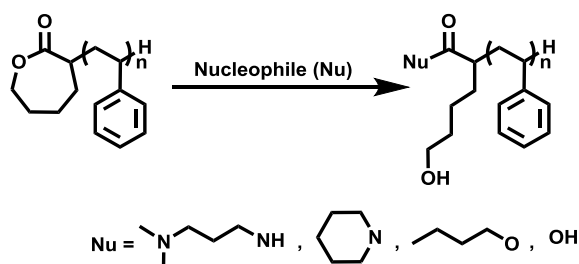
Scheme 1.17 Caprolactone containing ATRP initiator and its chemical modification.

Maleimide bearing initiators should be protected before ATRP as maleimide group interferes in the reaction due to the availability of activated alkene in their structure. Yang *et al.* [219]synthesized maleimide-functionalized PNIPAAm by protecting the initiator in the form of its adduct with furan before the polymerization using pre-click approach (**Scheme 1.18**). Thermo-sensitive electrospun fibres were fabricated by Michael addition reaction of thiol functionalised polysiloxane fibres on these maleimide functionalized PNIPAAm. These graft copolymer fibres showed the thermo-sensitive behaviour to the environment due to temperature sensitive PNIPAAm brushes on the surfaces.
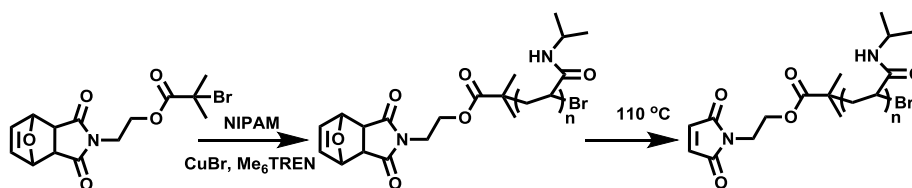
Scheme 1.18 Furan-protected maleimide functionalized ATRP initiator and its thermal deprotection.

1.3.4 Radical-radical coupling reactions

It is one of the widely used approaches to obtain homo-telechelic polymers. Sometimes, halide end groups in the polymer are not desired during the processing of polymer. The terminal halides can be removed by 1) adding double bond containing reactants and 2) direct replacement of bromide terminals to form carbon-carbon bond using activated halides. Both the methods are performed in presence of metal catalysts such as copper or manganese.

The one-pot procedure for the replacement of halide by allyl group after the polymerization has been attempted using allyl tri-*n*-butylstannane which tolerates the other functional groups such as acetals, epoxides, hydroxyl, *etc*. present in the polymer.[220] Monomers such as allyl alcohol and 1, 2-epoxy-5-hexene are non-polymerizable with the available ATRP systems because of the slow activation step due to the formation of unstable radicals. However, using radical coupling approach these less reactive groups have been incorporated at the polymer end.[221] Other non-polymerizable monomers incorporated at the chain end include the divinyl benzene and ethylene on MMA,[222] and maleic anhydride on polystyrene.[223]

Furthermore, the direct replacement of terminal halides using activated halides has been investigated. Visible light irradiation of bromo-terminated polymers prepared by ATRP in the presence of catalysts such as dimanganese decacarbonyl ($Mn_2(CO)_{10}$) and activated halide leads to the formation of telechelic polymer *via* radical-radical coupling (**Scheme 1.19**).[224] The obtained polystyrene bearing ester functionalities at the terminal showed double molecular weight compared to that of precursor.
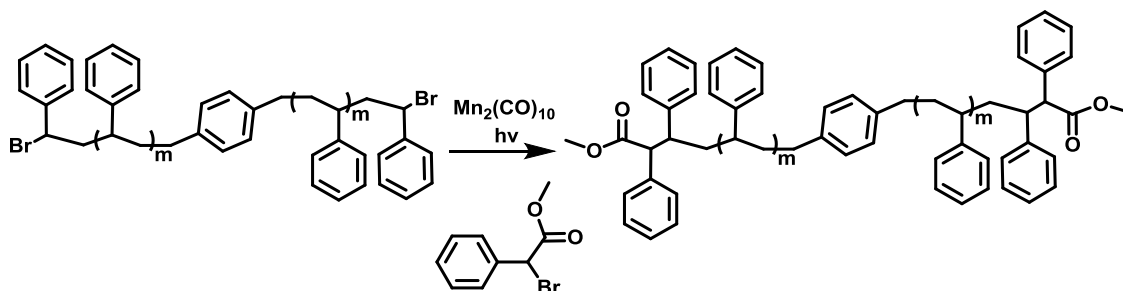
Scheme 1.19 Synthesis of homo-telechelic polymers by radical –radical coupling approach using dimanganese decacarbonyl catalyst.

Synthesis of aldehyde-telechelic polystyrene was attempted by Durmaz *et al.*[225] combining ATRP and atom transfer radical cross-coupling (ATRCC). The bromo-terminated polystyrene prepared by ATRP was cross-coupled with aldehyde functionalised initiator (**Scheme 1.20**). Detailed investigation of the reaction revealed that the efficiency of aldehyde functionalization was found to be 0.85 due to the undesired self-coupling of species generated from polymer and from functional initiator. Influence of different factors such as concentrations of polystyrene, initiator, ligand, and catalyst on the coupling process has also been studied.
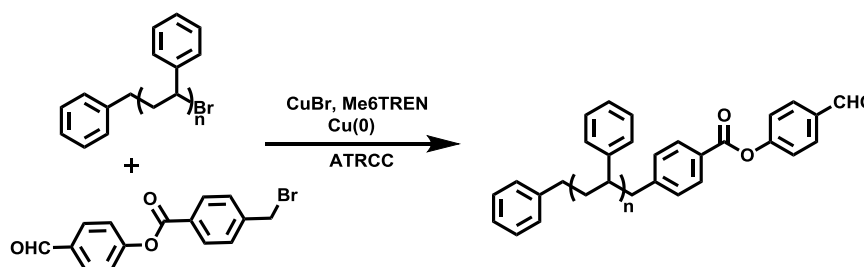
Scheme 1.20 Synthesis of aldehyde telechelic polystyrene combining ATRP and ATRCC.

Similarly, Yagci and co-workers[168] synthesized homo-telechelic polystyrene with acid, aldehyde, aromatic hydroxyl and dimethyl amino groups at α and ω-terminals under copper (0) mediated reductive conditions by ATRC process with double molecular weight compared to that of precursors (**Scheme 1.21**). Polymers prepared by this approach were demonstrated to be attractive for affording telechelic polymers due to the absence of potential undesired side reactions.
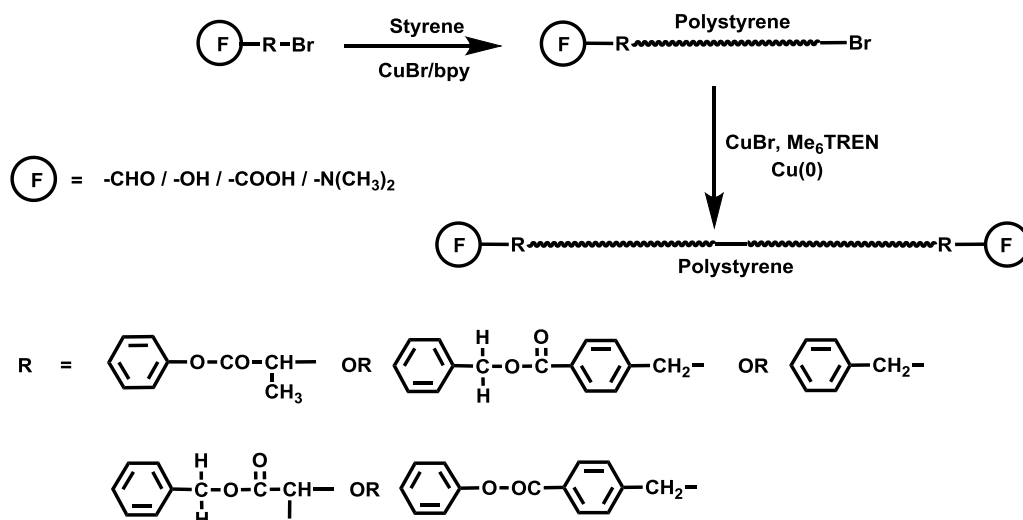
Scheme 1.21 Synthesis of homo-telechelic polymers by copper (0) mediated ATRC.

1.4 Ring opening polymerization (ROP) of lactones

Mainly tin, aluminium and zinc catalytic systems are widely used in ROP of lactones due to their commercial availability, ease of handling and good solubility in organic solvents / monomers. $Sn(Oct)_2$ and $Al(O\text{-}iPr)_3$ are the well known catalysts used for ROP of lactones, lactides and glycolides.[226, 227] ROP of lactones catalyzed by $Sn(Oct)_2$ has been reported to proceed with 'active chain-end' mechanism. The control provided by ROPs allow the convenient synthesis of polyesters with defined molecular weights, functionalized end groups and macromolecular architectures such as random/block, star, graft, comb, brush, hyper-branched, etc. therefrom.[228] ROP of lactones employing metal catalysts is successfully implemented controlled polymerization technique[229] to afford different macromolecular architectures. Scheme 1.22 represents a mechanism of ROP of lactones.
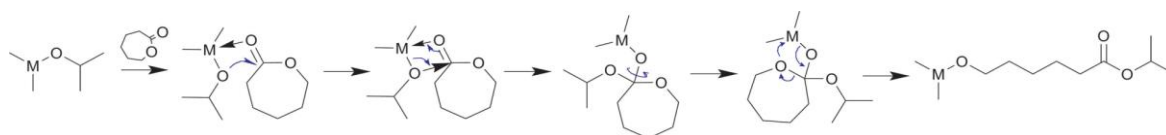
Scheme 1.22 Metal catalyzed coordination-insertion mechanism of ROP of lactones.

Polymers thus obtained are biodegradable and are applicable for degradable suture, tissue engineering and drug delivery purposes.[230] Most of the polymers afforded by ROP are hydrophobic and lacked in functionalities. The lack of functionalities in poly(ε-

caprolactone) restricts some relevant applications. The efforts have been devoted to afford functional polyesters to explore the physical and chemical properties of conventional polyesters to meet the needs related to these properties.

There are several synthetic approaches to afford functional polyesters by ROP which includes the use of functional initiators, [231] end group transformations using organic reactions, etc. However, high end group fidelity is achieved mainly through functional initiator approach.[231]

1.4.1 Major components of ROP

1.4.1.1 Functional ROP initiators

ROP of lactones is mainly initiated by hydroxyl group containing initiators such as alcohols. The reactivity of initiator depends mainly on steric and electronic factors. Some representative functional ROP initiators are listed in Figure 1.8.[231, 232]
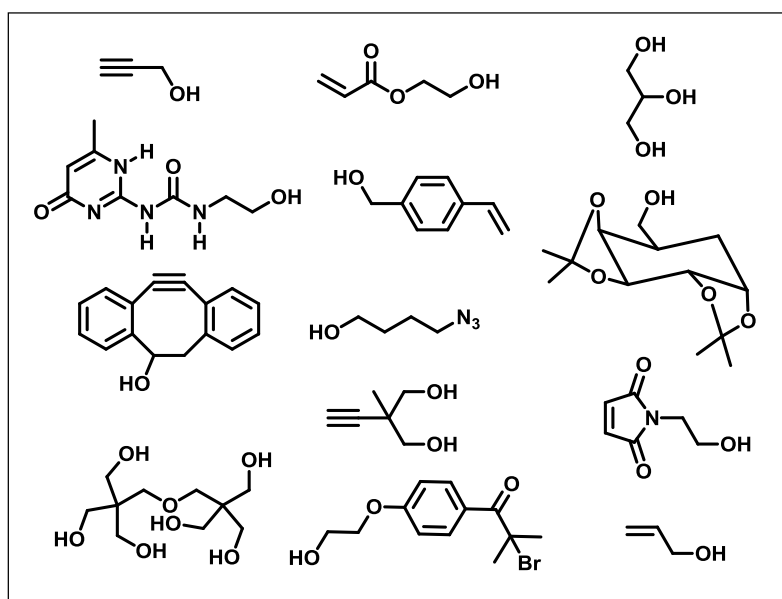
Figure 1.8 Representative functional ROP initiators.

Different functional poly(ε-caprolactones) and macromolecular architectures have been prepared using functional ROP initiators.[232, 233] PEG$_2$-PCL miktoarm star copolymer was prepared by Soliman *et al.* employing a bispropargyl functional ROP initiator to afford bispropargyl-terminated PCL.[234] Furthermore, trinitro-functionalized ROP initiator

based on triazine was employed by Binder and coworkers for synthesis of three arm star PCL bearing photo-cleavable characteristics.[235]

1.4.1.2 Monomers used in ROP

PCL is linear polymer with semicrystalline and hydrophobic nature. The present research is much devoted on functionalization of polymer backbone by using functional lactone monomers. Functional groups such as allyl, halides, propargyl, azido, etc. have been found to be stable under ROP conditions The representative functional ROP monomers are shown in Figure 1.9.

The post polymerization modification of PCL is one of the routes to obtain functional polyesters. Lecomte and Jerome reported several monomers to obtain functional polyesters by performing post polymerization modifications.[236]
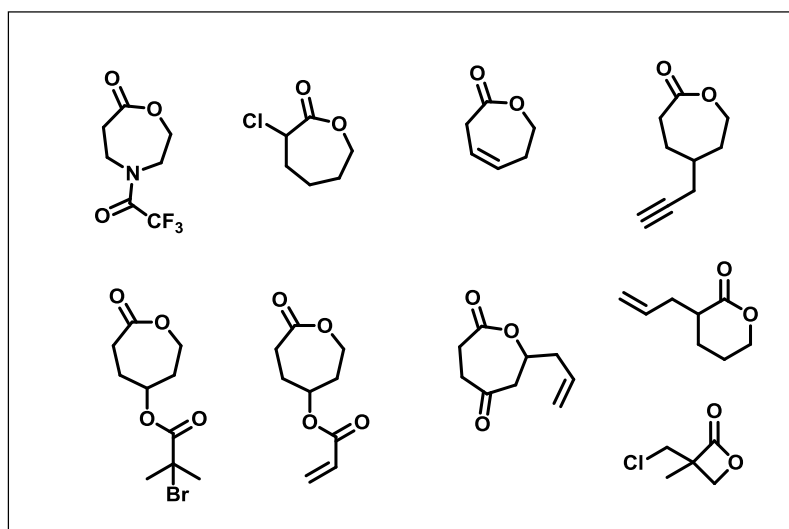
Figure 1.9 Representative lactone monomers containing functional groups.

Functional lactone monomers are useful for synthesis of graft copolymers with desired grafted chains to tune the properties of PCL. The grafting can be performed using three approaches *viz.* 'grafting from', 'grafting onto' and 'grafting through'. A range of polyester graft copolymers have been reported in the literature by these approaches.[237, 238]

1.4.1.3 Catalysts used in ROP

ROP of lactones by aluminium, tin and zinc catalysts are reported in the literature.[239] Polymerizations by these catalysts are much faster and allow the formation of high molecular weight polymers upto 10^6 Da. Although $Sn(Oct)_2$ has been approved by FDI as food additive the toxic effect of tin restricts the use of polymers prepared by these methods for some biomedical applications.[240] The reactivity of ROP catalysts follows the order

$$Sn\ (Oct)_2 > Al(OiPr_3) = Zn\ (Lact)_2$$

Tin (II) ethyl hexanoate is highly active at 140 ^{o}C temperature and requires much less time to complete the reaction. Basically, aluminium alkoxides are used for mechanistic studies which revealed that it is less reactive and require several days for completion of reaction. Zinc derivatives are potential non-toxic ROP catalysts widely used in the polymerization of lactones with a drawback of requirement of several days at 140 ^{o}C. Zinc powder is an acceptable catalyst for ROP of lactones at industrial level. Transesterification is a major problem in ROP, which results into broadening of dispersity and uncontrolled molecular weight of resulting polymer. Some of the representative ROP catalysts are shown in Figure 1.10.
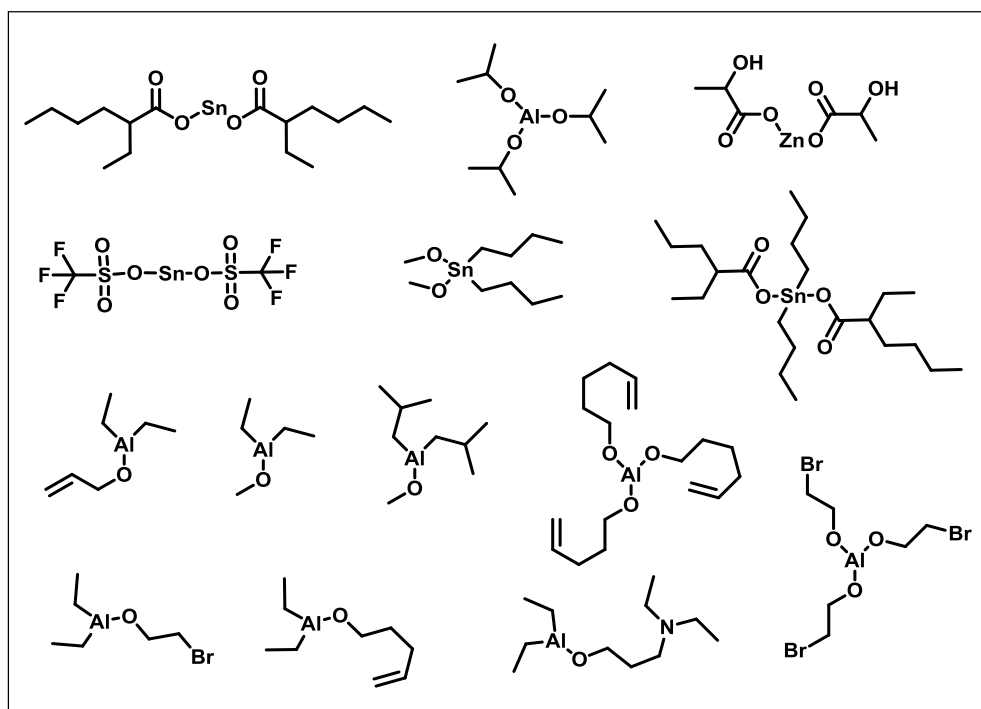
Figure 1.10 Representative examples of catalysts used in ROP.

1.5 Click reactions

The minimum side products, simpler purification of desired product and maximum yield of selective product are some of the basic requirements of organic transformations.

The click-chemistry concept was proposed by Sharpless in 2001 which fulfills the basic criteria of click reactions and was initially applied in organic syntheses.[241] Click reactions are considered to be efficient due to high yields of desired product with simple isolation using non-chromatographic techniques and generation of inoffensive byproducts, if any.[63] Now a days click-reactions are widely used in polymer chemistry to afford different macromolecular architectures. Since last few decades, polymers terminated with clickable functional groups using CRPs and ROP have been much explored. Clickable-telechelic polymers are of particular interest as they can be utilized quantitatively for subsequent transformations or reactions leading to new macromolecular architectures. A large number of research papers, monographs and review articles are available in the literature wherein the clickable polymers and architectures therefrom have been synthesized.[42, 242, 243]

1.5.1 Copper catalyzed alkyne-azide click reaction (CuAAC)

The conventional thermal, non-catalysed alkyne-azide reaction results in the formation of a mixture of 1,4 and 1,5-regioisomers of triazole products which deviate from the criteria of click reactions. However, the copper catalysed alkyne-azide click reactions (CuAAC) give selectively 1,4-disubstituted regioisomer triazole product and are now widely used in combination with CRP and ROP methods to afford new macromolecular architectures. Unlike CuAAC reaction, ruthenium (II) catalysed alkyne-azide reactions results in the formation of polymer with 1,5- disubstituted regioisomer triazole product (**Scheme 1.23**).
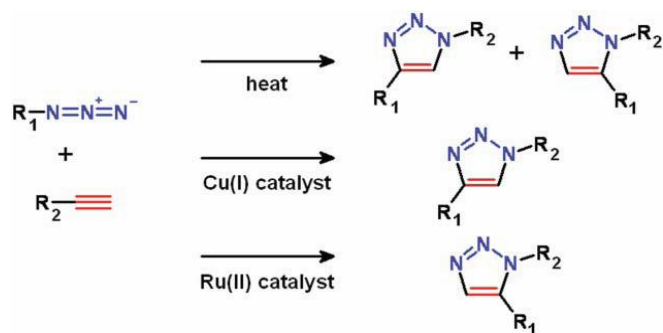
Scheme 1.23 The possible triazole regioisomer products in alkyne-azide click reaction.[244]

Copper bromide /PMDETA or copper sulphate/ sodium ascorbate are mostly used catalytic systems in the CuAAC reactions. The mechanism of CuAAC reaction is shown in Scheme 1.24.
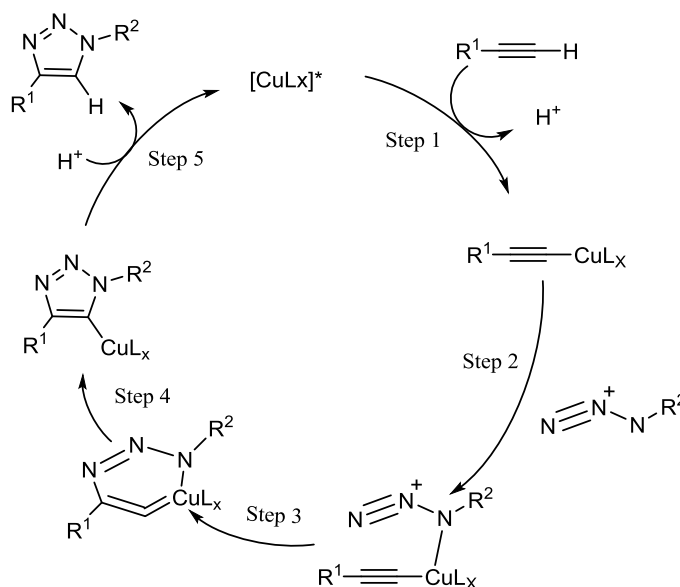
Scheme 1.24 Schematic representation of mechanism of CuAAC reaction.[245]

The range of macromolecular architectures including block, star and graft copolymers were reported in the literature using the combination of CRPs and ROPs with that of CuAAC click reaction[246-248] and are represented in Table 1.2.

Table 1.2 Some representative examples of copolymers by combination of CRPs and ROPs with that of CuAAC click reaction.

Sr. No	Structure of Copolymer	Copolymer	Reactions Used
1		PCL-*b*-PEG-*b*-PCL[246]	ROP and CuAAC click
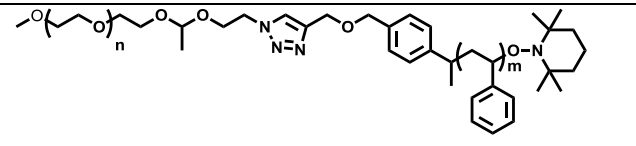
2		PCL-*b*-PS[247]	NMP and CuAAC click
3		PEG-PS-PCL[249]	ATRP, ROP and CuAAC click
4		PEG-PCL-PEEP[232]	ROP and CuAAC click
5		PEG-PS-PCL[250]	CuAAC click (in sequence) and ROP
6		PEG-P*t*BMA-PNIPAAm[136]	ATRP and CuAAC click
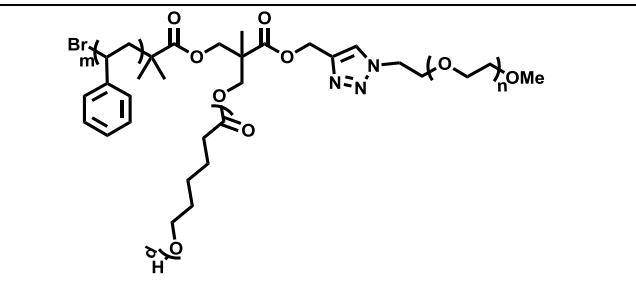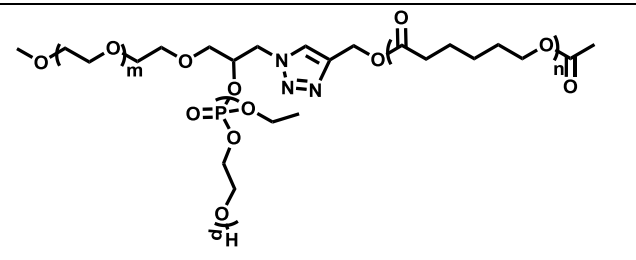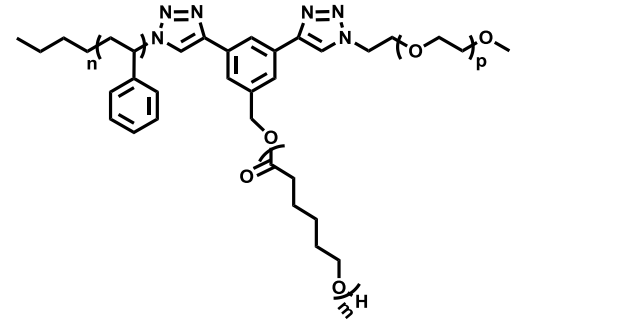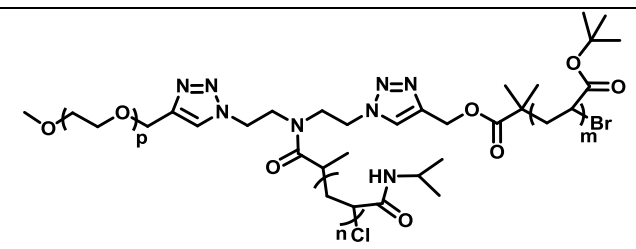
The biomedical applications of the materials obtained from CuAAC reactions are limited due to the toxicity of employed copper catalysts. Strain promoted alkyne-azide click (SPAAC) reaction has been used as an alternative reaction for the synthesis of polymers for medical applications due to their metal free nature.[195] Polymers prepared using 4-dibenzocyclooctynol ROP initiator have been used as a precursor for strain promoted alkyne-azide click (SPAAC) reaction[231] as shown in Scheme 1.25.
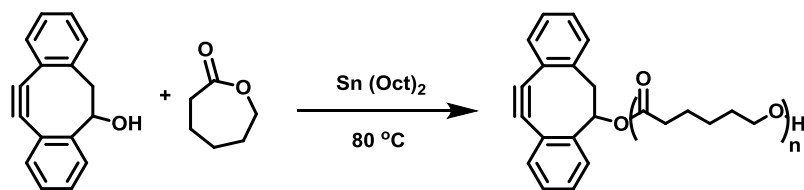
Scheme 1.25 Synthesis of 4-dibenzocyclooctynol end-functionalized PCL useful in metal-free SPAAC click reaction.

1.5.2 Thiol-ene click/coupling reaction

Thiol-ene reaction is one of the widely used click reactions in polymer science with some exceptions due to its metal-free nature. This reaction is performed either thermally or photochemically depending on the choice and the reaction conditions. Thermal and photochemical radical initiators such as AIBN and DMPA, respectively, have been widely used in these reactions. The schematic representation of mechanism of thiol-ene reaction is shown in Scheme 1.26.
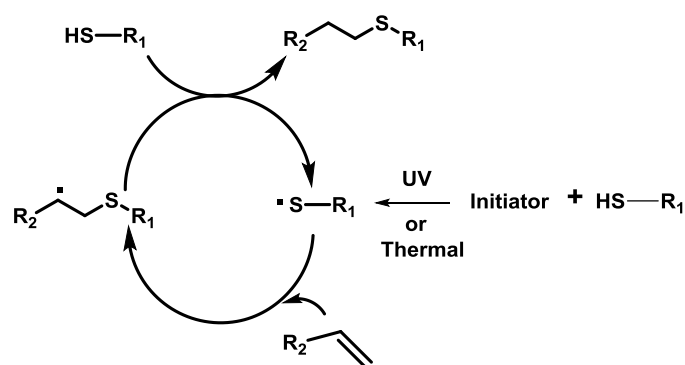
Scheme 1.26 Mechanism of thiol-ene click/coupling reaction.[251]

Thiol-ene reactions of small organic thiols with alkene containing polymers have been considered as 'click reactions' as they fulfil the criteria of 'click' concept.[251] A range of telechelic polymers using thiol-ene click reaction of polymers with small organic thiols have been reported.[252, 253] However, thiol-ene reactions of polymeric thiols with alkene containing polymers have been considered as 'coupling reactions' instead of 'click reactions' due to the formation of different undesirable and difficult to separate side products.[160] The side reactions during thiol-ene reaction are shown in Scheme 1.27. The limited reports are available in the literature concerning the macromolecular architectures afforded using CRP, ROP and thiol-ene coupling reactions.[251-256]
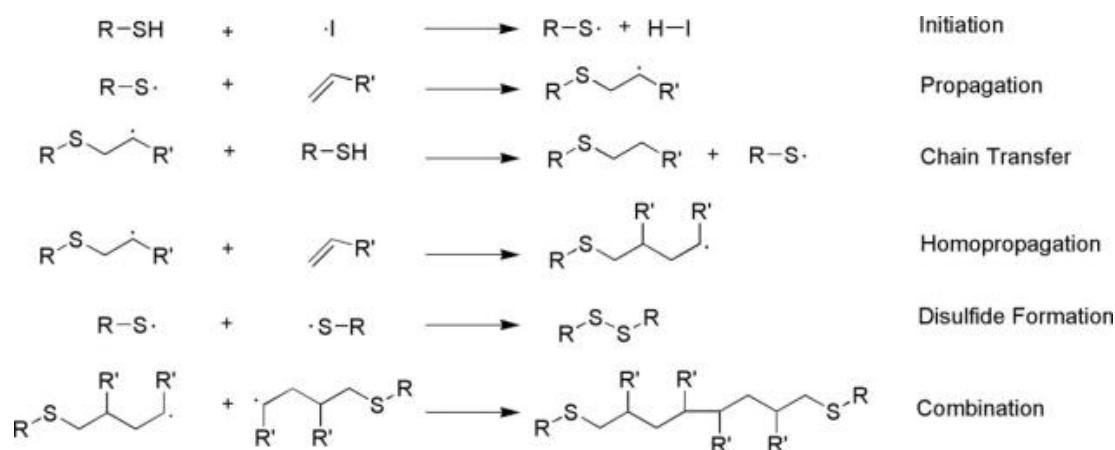
Scheme 1.27 The possible radical pathways in thiol-ene coupling reaction.[160] (Reproduced with permission from S. P. S. Koo, M. M. Stamenovic, R. A. Prasath, A. J. Inglis, F. E. D. Prez, C. B. Kowollik, W. V. Camp and T. Junkers, *J. Polym. Sci. Part A: Polym. Chem.*, 2010, 48, 1699-1713. Copyright © 2010, John Wiley & Sons).

Recently, Hawker and coworkers developed a thiol-yne monoaddition route to overcome these limitations of thiol-ene coupling reactions to afford block copolymers and other macromolecular architectures. [257]

1.5.3 Diels-Alder click reaction

These are thermo-reversible reactions of (4+2) л electron systems where electrons from HOMO molecular orbital of diene to LUMO molecular orbital of dienophile get overlapped (**Scheme 1.28**). These reactions are faster if the energy difference between HOMO and LUMO is less. Furan-maleimide and anthracene-maleimide reactions are widely used Diels-Alder click reactions in polymer and organic chemistry.[258] The equilibrium of reaction can be shifted depending on the temperature of reaction. The forward reaction in case of furan-maleimide reaction occurs at 60 ^{o}C and regeneration of reactants occurs at 110 ^{o}C, whereas, the anthracene-maleimide reaction occurs at 110 ^{o}C. In comparison, furan-maleimide click reactions have been widely used due to ease of operation relative to anthracene-maleimide reaction.

Scheme 1.28 Schematic representation of mechanism of Diels-Alder reaction.

Furan functionalized ATRP and ROP initiators are scarcely explored. However, the polymers with furan in the polymer backbone have been frequently explored.[259, 260] Furan-maleimide click reaction has been frequently used in the polymers where the thermo-reversibility is desired.[261] Self-healing and shape memory materials are the two major areas of the utility of this reaction.

1.6 Macromolecular architectures

Macromolecular architectures such as diblock, triblock, graft, star, cross-linked/network and cyclic copolymers can be obtained from the corresponding homo/hetero-telechelics[31, 234] (**Figure 1.11**).
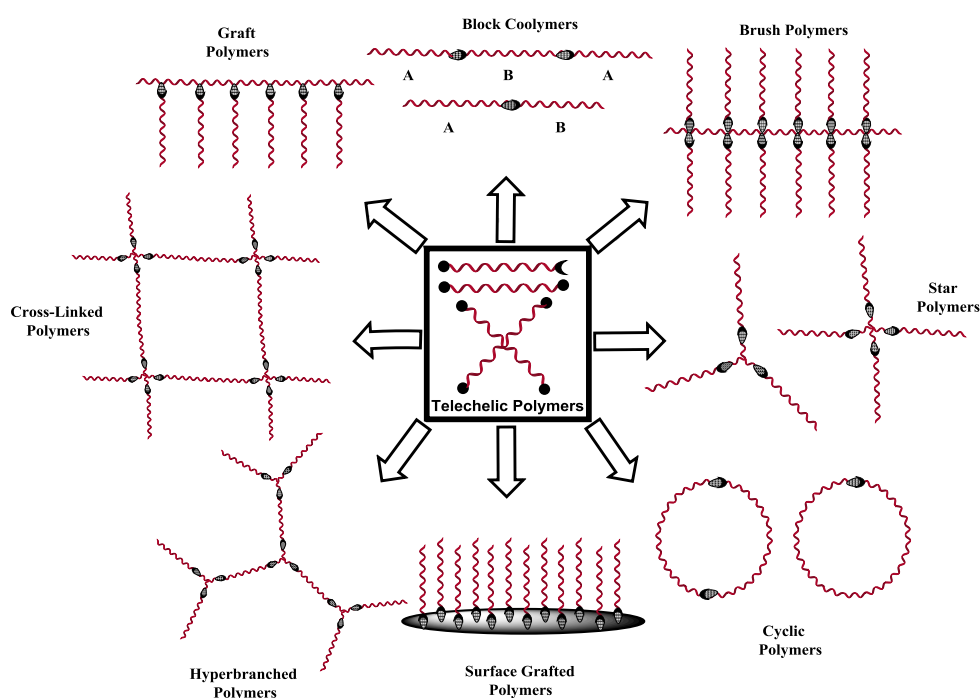
Figure 1.11 Different Macromolecular Architectures derived from telechelic polymers.[31]

1.6.1 Block copolymers

The copolymers where two different blocks are attached at a common junction point are referred as block copolymers. Block copolymers have been synthesized by either attaching two blocks prepared by different CRPs or ROP methods at common junction by some efficient click reactions or by sequential addition of different monomers in living polymer system.[246, 247] Depending on the number of blocks or sequentially added monomers these polymers are classified as diblock, triblock, multiblock, etc.

1.6.2 Star copolymers

Star polymers with symmetric structure and all the arms of similar molecular weight, identical chemical compositions and similar chemical structures are termed as homo-arm star polymers wherein the nature and properties of all the arms are identical (**Figure 1.12**).
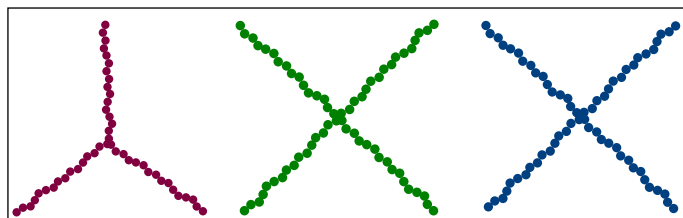
Figure 1.12 Schematic representation of homo-arm star polymers.

Star polymers with different arms are referred as hotero-arm star copolymers or miktoarm star copolymers wherein the nature and properties of arms are different. Schematic representation of hetero-arm star copolymers is shown in Figure 1.13.
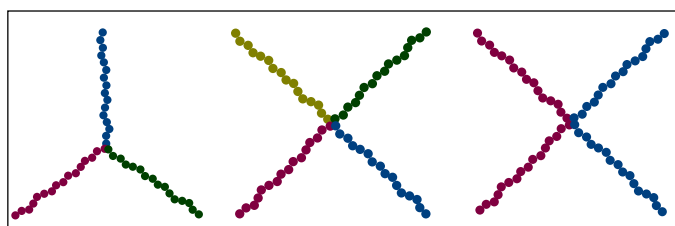
Figure 1.13 Schematic representation of hetero-arm (miktoarm) star copolymers.

1.6.2.1 Approaches for synthesis of 3-miktoarm star copolymers

Multi-armed star polymers can be prepared by various methods. However, star polymers with strictly defined 3-arms have been widely synthesized by three approaches.

1.6.2.1.1 'Core First' approach

Multifunctional initiator core is designed first and polymers are grown outwards by controlled polymerization methods such as ATRP, ROP, NMP or RAFT to synthesize star copolymers with different arms. Schematic representation of synthesis of miktoarm star copolymers by core first approach is shown in Figure 1.14. A variety of polymers have been easily and efficiently obtained by core first approach (**Table 1.3**).
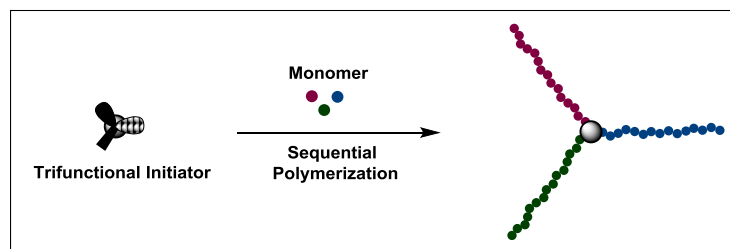
Figure 1.14 Schematic representation of synthesis of hetero-arm (miktoarm) star polymers by core first approach.

Table 1.3 Some representative examples of miktoarm star copolymers by 'core first' approach.

Sr. No.	Structure of Miktoarm Star Copolymer	Star polymer	Reactions Used
1		PDEAEMA-(PHEMA)$_2$[68]	ATRP
2		PCL-(P*t*BA)$_2$[262]	ROP and ATRP
3		(PCL)$_2$-P(*t*BMA)[263]	ATRP and ROP
4		(PCL)$_2$-PS[263]	ATRP and ROP
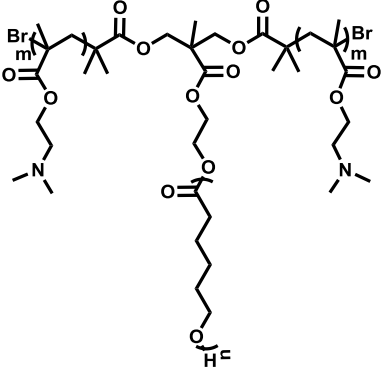
| 5 | | PCL-(PDMAEMA)$_2$[264] | ATRP and ROP |
| 6 | | (PCL)$_2$-PDMAEMA[264] | ATRP and ROP |
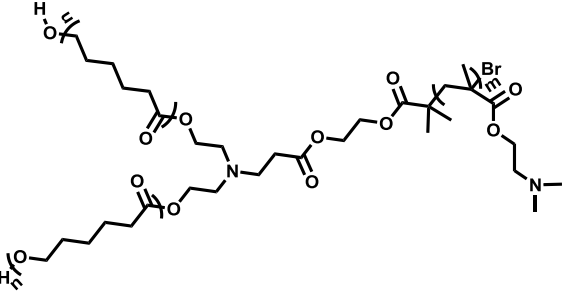
1.6.2.1.2 'Arm-First' or 'Coupling Onto' approach

Multifunctional coupling agent is designed and different functional polymers synthesized by CRP techniques are coupled onto the multifunctional coupling agent by some efficient, high yielding reactions such as "click reactions". These efficient reactions should be orthogonal to each other so as to get high yields of the final star copolymer. Schematic representation of 3-miktoarm star copolymers by coupling approach is shown in Figure 1.15.
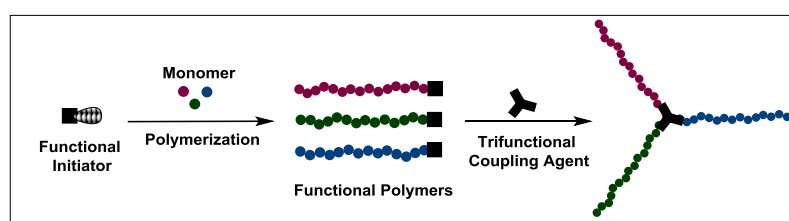
Figure 1.15 Schematic representation of synthesis of hetero-arm (miktoarm) star polymers by coupling approach.

The coupling onto approach and the orthogonality of thiol-ene, Diels-Alder and CuAAC click reactions were demonstrated by Yagci and coworkers to synthesize PS-PCL-PEG star copolymer. This approach was further extended by Tunca and coworkers to afford PS-PCL-PEG star copolymer using Diels-Alder, NRC and CuAAC click reactions.

The orthogonality of Diels-Alder, NRC and CuAAC click reactions were demonstrated (**Table 1.4**).

Table 1.4 Some representative examples of miktoarm star copolymers by 'arm first' or 'coupling onto' approach.

Sr. No.	Structure of Miktoarm Star Polymer	Star Polymer	Reactions Used
1		PS-PCL-PEG[265]	Thiol-ene, CuAAC and Diels-Alder click.
2		PEG-PCL PS[266]	Diels-Alder, NRC and CuAAC click
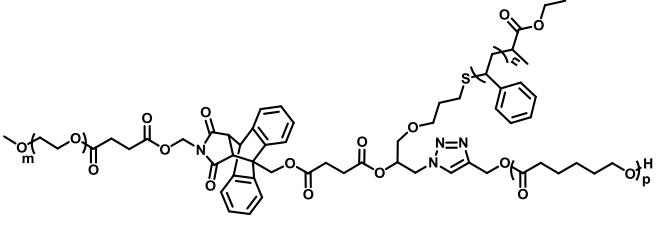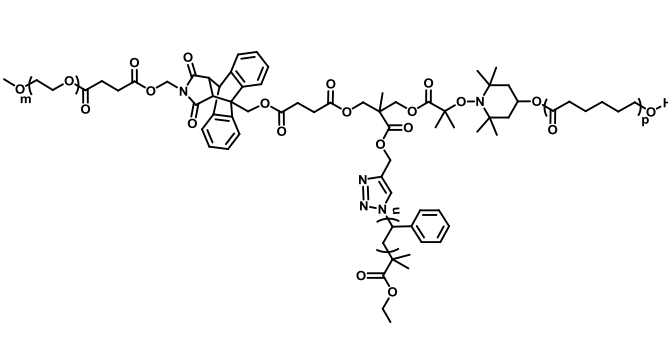
1.6.2.1.3 Combination of 'Core-First' and 'Coupling-Onto' approach

Multifunctional initiator core containing polymerization initiating sites and efficient reactive groups is designed. Polymers are grown outwards first and then on the multifunctional polymer the different orthogonal efficient reactions are performed to couple the functional polymers or vice-versa. Amongst all these approaches, 'Core first-Coupling Onto' approach has been considered as reliable and is widely used to construct miktoarm star copolymers due to its exceptional tolerance towards a variety of functional groups present on the core and different reaction conditions. Schematic representation of synthesis of miktoarm star copolymer by combination of 'core-first' and 'coupling-onto' approach is shown in Figure 1.16.
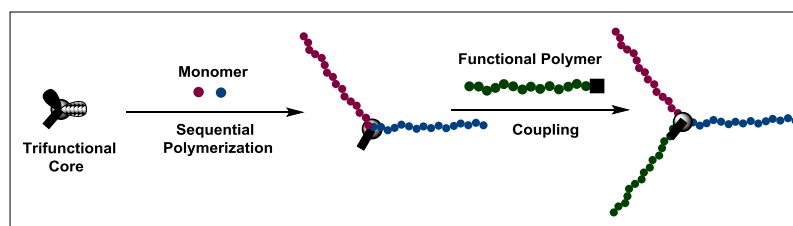
Figure 1.16 Schematic representation of synthesis of hetero-arm (miktoarm) star copolymers by coupling approach.

The miktoarm star copolymers with different arms have been prepared using the combination of different CRP/ROP methods with single or double click reactions[267] (**Table 1.5**). The core first-coupling onto approach and the orthogonality of double click reactions have been frequently demonstrated by various research groups to synthesize the miktoarm star copolymers.[252, 253]

Table 1.5 Some representative examples of miktoarm star copolymers by combination of 'core first' and 'coupling onto' approach.

Sr. No.	Structure of Miktoarm Star Copolymer	Star Polymer	Reactions Used
1		PEG-PDEAEA-PNIPAAm[268]	ATRP and CuAAC click
2		PEG-PMAA (via ATRP of *t*BA)-PDEAEMA[248]	ATRP and CuAAC click
3		PS-PCL-PDMAEMA[269]	ATRP, ROP and CuAAC click
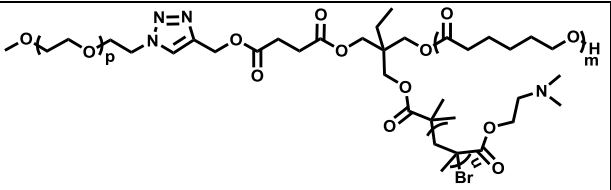
4		PEG-PCL-PDMAEMA[269]	ATRP, ROP and CuAAC click

1.6.3 Network/cross-linked polymers

Network and cross linked polymers have been synthesized from A_2+B_3 and A_3+B_2 monomer systems[270] or by reaction of difunctional cross-linker with polymer containing functional groups as pendant moieties or in the backbone, respectively. [271]A range of self-healing, shape memory polymers and stimuli-responsive gel systems have been designed by these synthetic approaches using CRPs and/or ROP in combination with different click reactions.[272]

1.7 Stimuli-responsive polymers

These are the class of polymers which respond to the applied external stimuli such as temperature, pH, light (UV or visible), magnetic field, redox, enzyme and carbon dioxide, etc.[273, 274] The response of these systems is attributed to the changes in their structure, properties, polarity and hydrophobic-hydrophilic balance. These polymers find applications in detection/sensing and medicinal biology due to the varying temperature, redox and pH conditions in the different organs of body. A range of polymer systems are available in the literature showing response to a single stimulus.[13, 247, 272]

1.7.1 Dual and multi-responsive polymers

Polymers which respond to two or more than two stimuli are referred as dual or multi-responsive polymers, respectively. A range of polymer systems which respond to the combination of two or multiple stimuli have been reported so far.[274-276] Huang *et al*. designed a thermo- and acid-sensitive dual-responsive poly(ethylene glycol)-*b*-poly(*trans*-*N*-(2-ethoxy-1,3-dioxan-5-yl)acryamide (PEG-*b*-P*t*NEA) block copolymer (**Figure 1.17**) which respond to acids and exhibit thermal response.[277] Furthermore, a thermo- and pH-dual responsive *N'*,*N'*-diethylethane-1,2-diamine (DEEDA) modified poly(vinyl alcohol) (PVA) was synthesized by Huo and coworkers[273] which can respond to the changes in temperature and pH.

Temperature and pH Responsive Block Copolymer
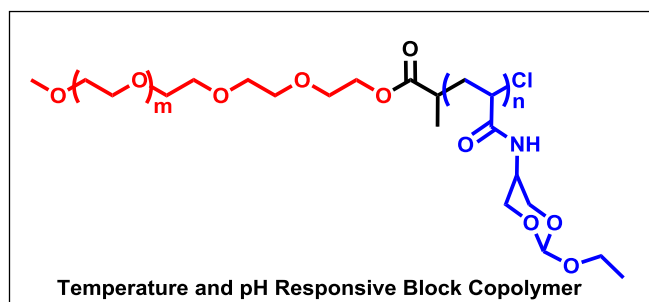
Figure 1.17 Structure of dual-responsive PEG-*b*-P*t*NEA diblock copolymer.[277]

Thayumanavan and coworkers designed a block copolymer system with triple stimuli-response *viz.* temperature, pH and redox (**Figure 1.18**).[153] The polymer was designed in such a way that the hydrophilic block was temperature sensitive (PNIPAAm), hydrophobic block was acid sensitive (acetal protected PHEMA) and the linker at the junction was redox sensitive.

Multi-Responsive Block Copolymer
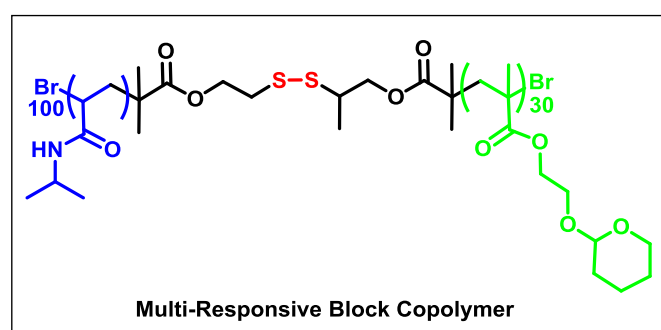
Figure 1.18 Structure of multi-stimuli responsive diblock copolymer.[153]

Quadruple stimuli-responsive poly(2-nitrobenzyl methacrylate)-*b*-poly(dimethylaminoethyl methacrylate) (PNBM-*b*-PDMAEMA) block copolymer system with temperature, pH, photo and redox sensitive groups has been designed by Wang and coworkers (**Figure 1.19**).[278] It has been found that the release of encapsulated guest from the assemblies of these polymers was enhanced under the combined stimulations.
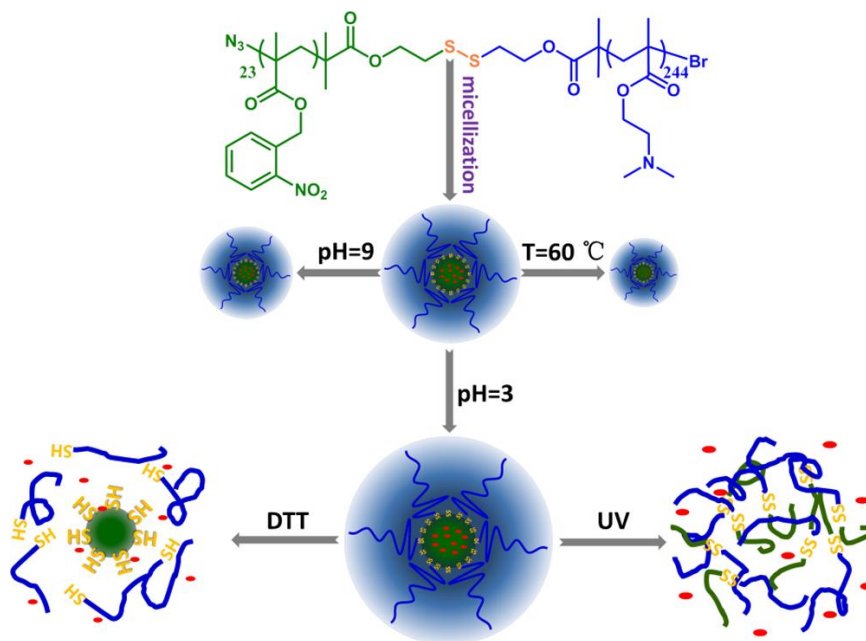
Figure 1.19 Multi-stimuli responsive diblock copolymer.[278] (Reproduced with permission from Z. Cao, H. Wu, J. Dong and G. Wang, *Macromolecules*, 2014, 47, 8777−8783. Copyright © 2014, American Chemical Society).

1.8 Thermo-reversible healable polymers

Hydrogen bonding and Diels-Alder click reactions have been well studied thermo-reversible systems. The self-healing and shape memory materials are mostly based on this chemistry. However, polymers with hydrogen bonding [279] have been found to be weaker compared the systems with Diels-Alder adducts due to the non-covalent (supra-molecular) nature.

Healable linear, network and cross-linked polymers based on furan-maleimide click reactions have been reported in the literature due to the synthetic ease and accessibility. Most of the healable smart materials based on furan-maleimide reactions showed scratch healing in the temperature range of 90-150 °C. There is lack of polymer systems based on these reactions which exhibit healing at moderate to lower temperatures. It has been reported in the literature that, the presence of long flexible chains in the polymer backbone or as pendant moiety imparts chain mobility in these network/cross-linked structures at healing temperature which results into the scratch healing at moderate temperatures.

Thermo-reversible network polymer containing flexible chains in the backbone has been prepared by Yoshie *et al.* using bisfuryl-terminated poly(ethylene adipate) and

trismaleimde.[280] The mending of polymers has been found at around 60 °C due to the reversible cross-linking reaction (**Scheme 1.29**).
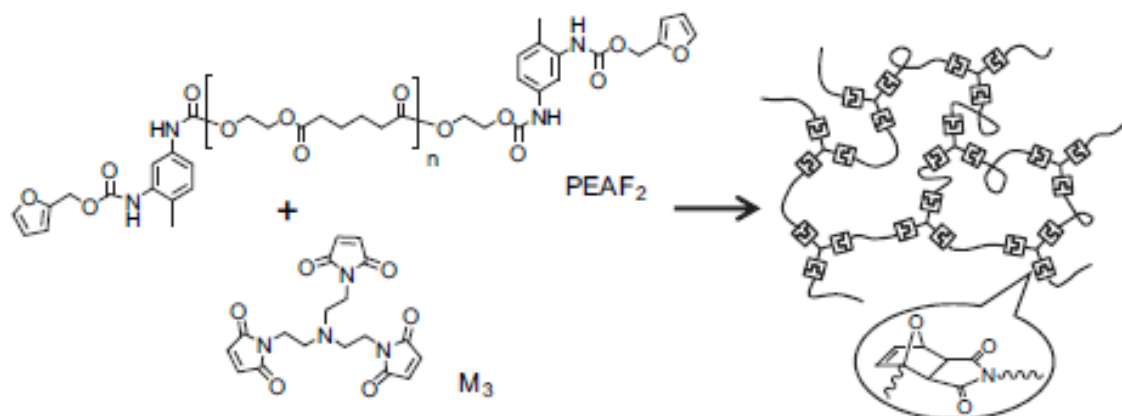
Scheme 1.29 Thermo-reversible network polymer containing flexible chains in the backbone.[280] (Reproduced with permission from N. Yoshie, M. Watanabe, H. Araki and K. Ishida, *Polym. Degrad. Stability*, 2010, 95, 826-829. Copyright © 2010, Elsevier).

A similar observation has been demonstrated by Nguyen *et al*. by designing the network polymer from furyl-telechelic poly(ε-caprolactone) and trismaleimide.[281] The mending process in this network polymer at 60 °C has been observed due to the two simultaneous processes i.e melting of PCL chains at this temperature due to the semicrystalline nature and progressive formation of furan-maleimide Diels-Alder adducts attributed to the flexibility of network structure (**Scheme 1.30**).
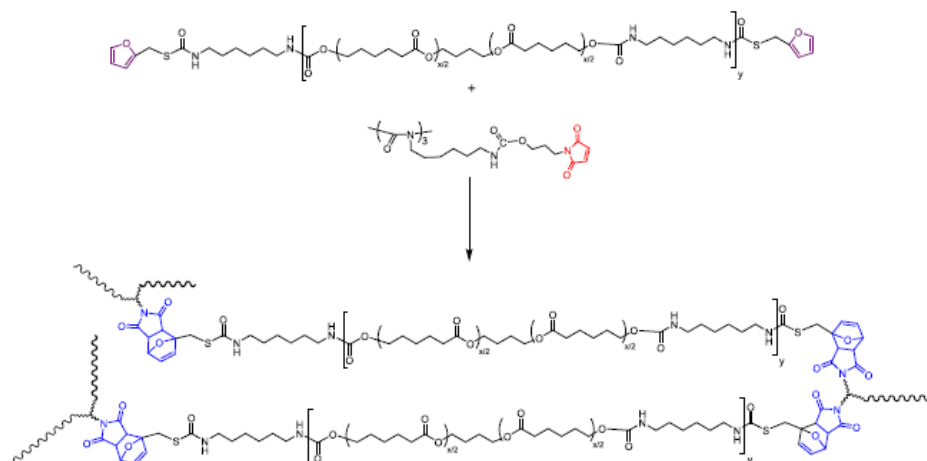
Scheme 1.30 Thermo-reversible network polymer containing PCL chains in the backbone.[281] (Reproduced with permission from L. T. T. Nguyen, H. T. Nguyen and T. T. Truong, *J. Polym. Res.*,2015, 22, 186. Copyright © 2015, Springer).

The effect of incorporation of pendant dodecyl chains in the network or cross-linked polymer have been described by Kotteritzsch [282] and Bose *et al.* [283] Introduction of pendant dodecyl chains in these structures resulted into healability at relatively lower temperatures compared to the healability of polymers without these chains. Polymers with long side chains are flexible and show better reflow of materials into the scratch which results into faster healing process (**Scheme 1.31**).
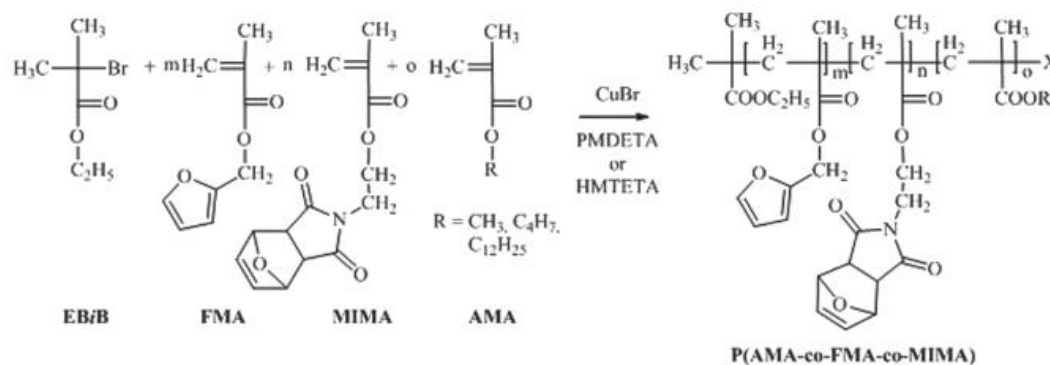
Scheme 1.31 Thermo-reversible network polymer with pendant dodecyl chains.[282] (Reproduced with permission from J. Kötteritzsch, S. Stumpf, S. Hoeppener, J. Vitz, M. D. Hager and U. S. Schubert, *Macromol. Chem. Phys.*, 2013, 214, 1636−1649. Copyright © 2013, John Wiley & Sons).
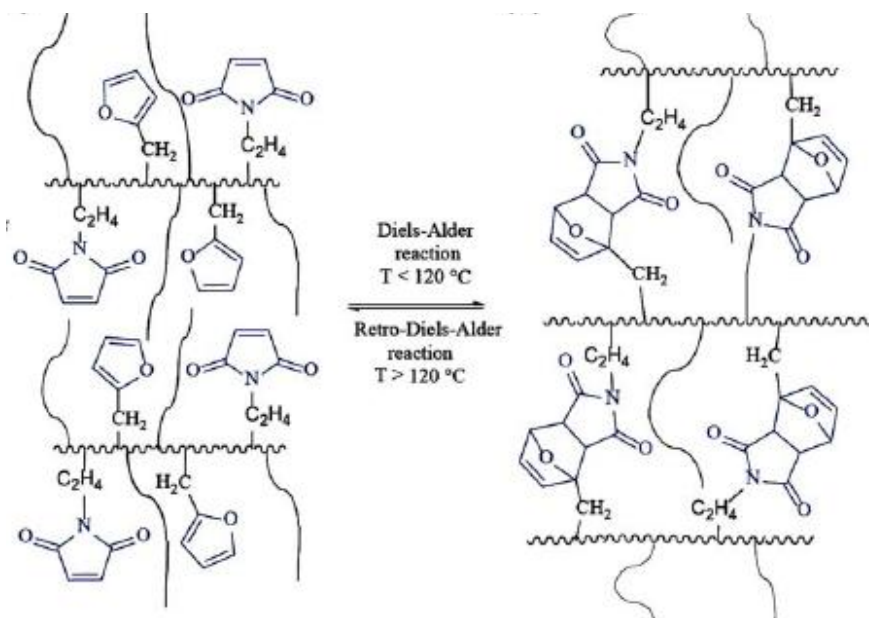
Scheme 1.32 Schematic representation of thermo-reversible network polymer with pendant dodecyl chains.[283] (Reproduced with permission from R. K. Bose, J. Kotteritzsch, S. J. Garcia, M. D. Hager, U. S. Schubert and S. V. D. Zwaag, *J. Polym. Sci. Part A: Polym. Chem.*, 2014, 52, 1669-1675. Copyright © 2014, John Wiley & Sons).

1.9 Scope and Objectives of the Thesis

The present work was focused on exploitation of combination of controlled/living polymerization methods and click chemistry approach for synthesis of designed macromolecular architectures and their smart behaviour with respect to external stimuli.

It has been recognized that the polymeric systems with dual- or multi-responsive groups are advantageous compared to polymeric systems containing single stimulus responsive group. However, there is paucity of polymeric systems containing dual- or multi-responsive groups in a single linear polymeric chain. Thus, there is a need and a wide scope to design simpler responsive polymeric systems which can respond to two stimuli *viz.* temperature and pH compared to relatively synthetically difficult to access macromolecular architectures such as star-branched polymers.

To meet the stated objectives, it was of interest to design and synthesize new ATRP and ROP initiators bearing either one or two clickable functional groups which are either same or different. The following specific objectives were chosen for the research work.

1. To synthesize functionalized ATRP and ROP initiators starting from commercially available inexpensive starting materials and utilize these initiators to obtain end-functional polymers possessing allyl or azido group and macromonomers with reactive functional groups such as allyl, hydroxyl, carboxyl and furyl. Such end-functional polymers and macromonomers represent useful precursors for different macromolecular architectures via click or coupling reactions.

2. Exploitation of controlled polymerization methods such as ATRP and ROP in combination with different click/coupling (orthogonal) reactions to obtain macromolecular architectures *viz.* block, star, network, etc. which could not be otherwise easily accessible by conventional polymerization methods.

3. Preparation of stimuli-responsive macromolecular architectures which respond to stimuli such as temperature and pH either alone or both in a common system by combination of ATRP/ROP and click reactions and study their cargo release profiles under varying conditions of temperature and pH. Such model systems are of interest for potential applications as drug delivery vehicles.

4. Preparation of relatively moderate temperature healable macromolecular architectures such as network systems which take advantage of thermo-reversible furan-maleimide

Diels-Alder click chemistry and enhanced chain mobility offered by flexible chains such as poly(lauryl methacrylate). Such systems are of great interest due to their potential applications in coating industry.

1.10 References

1. E. J. Goethals, *British Polym. J.,* 1990, **22**, 261-262.

2. L. T. Nguyen, H. T. Nguyen and T. T. Truong, *J. Polym. Res.* 2015, **22**, 186.

3. J. Wang, Z.Kang, B. Qi, Q. Zhou, S. Xiao and Z. Shao, *RSC Advances*, 2014, **4**, 51510-51518.

4. A. V. Ruzette and L. Leibler, *Nat. Mater.*, 2005, **4**, 19-31.

5. G. Moreno, C. Valencia, M. V. d. Paz, J. M. Franco and C. Gallegos, *Ind. Eng. Chem. Res.,* 2006, **45**, 4001-4010.

6. N. Hameed, N. V. Salim, T. R. Walsh, J. S. Wiggins, P. M. Ajayanc and B. L. Foxa, *Chem. Commun.,* 2015, **51**, 9903-9906.

7. A. K. Singh, R. Prakash and D. Pandey, *RSC Advances*, 2012, **2**, 10316-10323.

8. J. Huang, J. Xu, K. Chen, T. Wang, C. Cui, X. Wei, R. Zhang, L. Li and X. Guo, *Ind. Eng. Chem. Res.*, 2015, **54**, 1564-1575.

9. B. Dufour, C. Tang, K. Koynov, Y. Zhang, T. Pakula and K. Matyjaszewski, *Macromolecules*, 2008, **41**, 2451-2458.

10. H. Fengab, N. A. L. Verstappena, A. J. C. Kuehnec and J. Sprakel, *Polym. Chem.,* 2013, **4**, 1842-1847.

11. Q. Wei, X. Wang and F. Zhou, *Polym. Chem.*, 2012, **3**, 2129-2137.

12. A. Nomura, K. Ohno, T. Fukuda, T. Satobc and Y. Tsujii, *Polym. Chem.,* 2012, **3**, 148-153.

13. S. Binauld and M. H. Stenzel, *Chem. Commun.*, 2013, **49**, 2082-2102.

14. T. K. Georgiou, *Polym. Int.*, 2014, **63**, 1130-1133.

15. M. Xie, W. Wang, L. Dong, J. Liu, D. Yang, L. Wei and Y. Zhang, *J. Polym. Sci. Part A: Polym. Chem.*, 2010, **48**, 380-388.

16. J. Couthouis, H. Keul and M. Möller, *Macromol. Chem. Phys.*, 2016, **217**, 72-84.

17. N. A. C. Lemus, R. S. Rodriguez and A. L. Claverie, *J. Polym. Sci. Part A: Polym. Chem.,* 2010, **48**, 3033-3051.

18. M. Nagy, M. Zsuga, D. Racz and S. Keki, *J. Polym. Sci. Part A: Polym. Chem.* 2010, **48**, 2709-2715.

19. J. P. Kennedy, V. S. C. Chang and W. P. Francik, *J. Polym. Sci. Part A: Polym. Chem.,* 1982, **20**, 2809-2817.

20. T. Dedeoglu, H. Durmaz, G. Hizal and U. Tunca, *J. Polym. Sci. Part A: Polym. Chem.,* 2012, **50**, 1917-1925.

21. H. Durmaz, A. Dag, G. Hizal and U. Tunca, *J. Polym. Sci. Part A: Polym. Chem.,* 2010, **48**, 5083-5091.

22. O. Altintas, T. Rudolph and C. B. Kowollik, *J. Polym. Sci. Part A: Polym. Chem.,* 2011, **49**, 2566-2576.

23. S. Wallyn, Z. Zhang, F. Driessen, J. Pietrasik, B. G. D. Geest, R. Hoogenboom and F. E. D. Prez, *Macromol. Rapid Commun.*, 2014, **35**, 405-411.

24. N. Rocha, P. V. Mendonça, J. P. Mendes, P. N. Simões, A. V. Popov, T. Guliashvili, A. C. Serra and J. F. J. Coelho, *Macromol. Chem. Phys.* 2013, **214**, 76-84.

25. N. V. Tsarevsky, B. S. Sumerlin and K. Matyjaszewski, *Macromolecules*, 2005, **38**, 3558-3561.

26. E. Bays, L. Tao, C. Chango and H. D. Maynard, *Biomacromolecules*, 2009, **10**, 1777-1781.

27. M. M. Stamenovi, P. Espeel, W. V. Camp and F. E. D. Prez, *Macromolecules* 2011, **44**, 5619-5630.

28. A. Hirao, R. Goseki and T. Ishizone, *Macromolecules*, 2014, **47**, 1883-1905.

29. S. Banerjee, T. Maji and T. K. Mandal, *Colloid. Polym. Sci.*, 2014, **292**, 2217-2226.

30. M. R. Hill, R. N. Carmean and B. S. Sumerlin, *Macromolecules*, 2015, **48**, 5459-5469.

31. M. A. Tasdelen, M. U. Kahveci and Y. Yagci, *Prog. Polym. Sci.*, 2011, **36**, 455-567.

32. A. Anastasaki, V. Nikolaoua and D. M. Haddleton, *Polym. Chem.* 2016, **7**, 1002-1026.

33. A. Anastasaki, V. Nikolaou, G. Nurumbetov, P. Wilson, K. Kempe, J. F. Quinn, T. P. Davis, M. R. Whittaker and D. M. Haddleton, *Chem. Rev.*, 2016, **116**, 835-877.

34. K. Matyjaszewski, Y. Gnanou and L. Leibler, *Macromolecular Engineering. Precise Synthesis, Materials Properties, Applications. Wiley-VCH: Weinheim*, 2007, 1-6.

35. K. Matyjaszewski and T. P. Davis, *Handbook of Radical Polymerization. Wiley Interscience: Hoboken*, 2002, 936.

36. K. Matyjaszewski, *Macromolecules*, 1998, **31**, 4710-4717.

37. K. Matyjaszewski and N. V. Tsarevsky, *Nat. Chem.*, 2009, **1**, 276.

38. K. Matyjaszewski and J. Xia, *Chem. Rev.*, 2001, **101**, 2921-2990.

39. J. S. Wang and K. Matyjaszewski, *J. Am. Chem. Soc.*, 1995, **117**, 5614-5615.

40. M. Kato, M.Kamigaito, M. Sawamoto and T. Higashimura, *Macromolecules*, 1996, **28**, 1721-1723.

41. K. Matyjaszewski and N. V. Tsarevsky, *J. Am. Chem. Soc.,* 2014, **136**, 6513-6633.

42. V. Coessens, T. Pintauer and K. Matyjaszewski, *Prog. Polym. Sci.*, 2001, **26**, 337-377.

43. A. K. Shakya and A. Kumar, *J. Biosci. Biotech.*, 2013, **2**, 1-.

44. M.Ouchi, T. Terashima and M. Sawamoto, *Chem. Rev.*, 2009, **109**, 4963-5050.

45. C. H. Peng, J. Kong, F. Seeliger and K. Matyjaszewski, *Macromolecules*, 2011, **44**, 7546−7557.

46. K. Matyjaszewski, *Macromolecules*, 2012, **45**, 4015-4039.

47. W. Tang and K. Matyjaszewski, *Macromolecules*, 2006, **39**, 4953− 4959.

48. W. A. Braunecker and K. Matyjaszewski, *Prog. Polym. Sci.*, 2007, **32**, 93-146.

49. A. Goto and T. Fukuda, *Macromol. Rapid Commun.,* 1999, **20**, 633-636.

50. K. Matyjaszewski, B. Goebelt, H. J. Paik and C. P. Horwitz, *Macromolecules*, 2001, **34**, 430-440.

51. K. Matyjaszewski, H. J. Paik, P. Zhou and S. J. Diamanti, *Macromolecules*, 2001, **34**, 5125-5131.

52. M.Tatemoto and M.Oka, *Contemporary Topics in Polymer. Science*, 1984, **4**, 763-777.

53. K. Matyjaszewski, S. G. Gaynor and J. S. Wang, *Macromolecules*, 1995, **28**, 2093-2095.

54. K. Matyjaszewski, D. A. Shipp, J. L. Wang, T. Grimaud and T. E. Patten, *Macromolecules*, 1998, **31**, 6836-6840.

55. Q. F. Xu, J. M. Lu, Z. Yang, X. W. Xia and L. H. Wang, *Polym. J.*, 2007, **39**, 213.

56. A. Marsh, A. Khan, D. M. Haddleton and M. J. Hannon, *Macromolecules,* 1999, **32**, 8725-8731.

57. K. Matyjaszewski and J. Spanswick, *Mater. Today*, 2005, **8**, 26-33.

58. L. C. Mei, B. Rui, Q. J. Jun, H. Fen, X. Yan, Z. Chen and Z. Yun, *Polym. Bull.*, 2006, **57**, 139-149.

59. D. P. Chatterjee and B. M. Mandal, *Polymer,* 2006, **47**, 1812-1819.

60. S. S. Patil, S. K. Menon and P. P.Wadgaonkar, *Polym. Int.*, 2015, **64**, 413-420.

61. J. Opsteen and J. Hest, *Chem. Commun.*, 2005, **1**, 57-59.

62. W. Jakubowski, N. V. Tsarevsky, P. McCarthy and K. Matyjaszewski, *Mater. Matters* 2010, **5**, 16.

63. C. B. Kowollik, F. E. D. Prez, P. Espeel, C. J. Hawker, T. Junkers, H. Schlaad and W. V. Camp, *Angew. Chem. Int. Ed.*, 2011, **50**, 60-62.

64. K. Matyjaszewski and N. V. Tsarevsky, *J. Am. Chem. Soc.* , 2014, **136**, 6513.

65. P. S. Sane, D. V. Palaskar and P. P. Wadgaonkar, *Eur. Polym. J.*, 2011, **47**, 1621.

66. P. S. Sane, B. V. Tawade, D. V. Palaskar, S. K. Menon and P. P. Wadgaonkar, *React. Funct. Polym.*, 2012, 72, 713.

67. P. S. Sane, B. V. Tawade, I. Parmar, S. Kumari, S. Nagane and P. P. Wadgaonkar, *J. Polym. Sci. Part A: Polym. Chem.,* 2013, **51**, 2091.

68. Y. L. Cai and S. P. Armes, *Macromolecules*, 2005, **38**, 271-279.

69. G. Deng, L. Zhang, C. Liu, L. He and Y. Chen, *Eur. Polym. J.*, 2005, **41**, 1177.

70. V. Deimede and J. K. Kallitsis, *Chem. Eur. J.*, 2002, **8**, 467.

71. Y. Yamazaki, N. Ajioka, A. Yokoyama and T. Yokozawa, *Macromolecules*, 2009, **42**, 606.

72. S. Yurteri, I. Cianga, A. L. Demirel and Y. Yagci, *J. Polym. Sci. Part A: Polym. Chem.,* 2005, **43**, 879.

73. G. J. Summers, M. P. Ndawuni and C. A. Summers, *Polym. Int.*, 2012, **61**, 1353.

74. M. Kato, M. Kamigaito, M. Sawamoto and T. Higashimura, *Macromolecules*, 1995, **28**, 1721.

75. J. S. Wang and K. Matyjaszewski, *J. Polym. Sci. Part A: Polym. Chem.,* 1995, **117**, 5614.

76. K. Matyjaszewski, J. L. Wang, T. Grimaud and D. A. Shipp, *Macromolecules*, 1998, **31**, 1527.

77. K. Matyjaszewski, D. A. Shipp, J. L.Wang, T. Grimaud and T. E. Patten, *Macromolecules*, 1998, **31**, 6836-6840.

78. T. Ando, M. Kamigaito and M. Sawamoto, *Tetrahedron*, 1997, **53**, 15445-15457.

79. X. Zhang and K. Matyjaszewski, *Macromolecules*, 1999, **32**, 7349-7353.

80. D. M. Haddleton, C. Waterson and P. J. Derrick, *Chem. Commun.*, 1997, **7**, 683-684.

81. A. Likhitsup, A. Parthiban and C. L. L. Chai, *J. Polym. Sci. Part A: Polym. Chem.,* 2008, **46**, 102-116.

82. H. Tai, V. K. Popov, K. M. Shakesheff and S. M. Howdle, *Biochem. Soc. Trans.* 2007, **35**, 516-521.

83. O. Glaied, C. Delaite and P. Dumas, *J. Polym. Sci. Part A: Polym. Chem.,* 2007, **45**, 968-974.

84. S. Ohno, H. Gao, B. Cusick, T. Kowalewski and K. Matyjaszewski, *Macromol. Chem. Phys*, 2009, **210**, 421-430.

85. W. Lin, S. Nie, Q. Zhong, Y. Yang, C. Cai, J. Wang and L. Zhang, *J. Mater. Chem. B.,* 2014, **2**, 4008-4020.

86. H. Matsumoto, T. Nakano, K. Ohkawa and Y. Nagai, *Chem. Lett.*, 1978, **7**, 363-366.

87. J. C. Pelps, D. E. Bergbreiter, G. M. Lee, R. Villani and S. M. Weinreb, *Tetrahedron Lett.*, 1989, **30**, 3915-3918.

88. K. L. Heredia, Z. P. Tolstyka and H. D. Maynard, *Macromolecules*, 2007, **40**, 4772-4779.

89. G. Mantovani, F. Lecolley, L. Tao, D. M. Haddleton, J. Clerx, J. J. L. M. Cornelissen and K. Velonia, *J. Am. Chem. Soc.*, 2005, **127**, 2966-2973.

90. M. Licciardi, Y. Tang, N. C. Billingham, S. P. Armes and A. L. Lewis, *Biomacromolecules*, 2005, **6**, 1085-1096.

91. V. Percec and B. Barboiu, *Macromolecules*, 1995, **28**, 7970-7972.

92. R. M. Broyer, G. M. Quaker and H. D. Maynard, *J. Am. Chem. Soc.,* 2008, **130**, 1041-1047.

93. S. Pfeifer and J. F. Lutz, *Macromol. Chem. Phys.,* 2010, **211**, 940-947.

94. J. Hegewald, J. Pionteck, L. Haussler, H. Komber and B. Voit, *J. Polym. Sci. Part A: Polym. Chem.,* 2009, **47**, 3845-3859.

95. V. B. Sadhu, J. Pionteck, D. Voigt, H. Komber and B. Voit, *Macromol. Symp.*, 2004, **210**, 147-155.

96. V. B. Sadhu, J. Pionteck, D. Voigt, H. Komber, D. Fischer and B. Voit, *Macromol. Chem. Phys.*, 2004, **205**, 2356-2365.

97. G. Toquer, S. Monge, K. Antonova, C. Blanc, M. Nobili and J. J. Robin, *Macromol. Chem. Phys.*, 2007, **208**, 94-102.

98. V. Percec and C. Grigoras, *J. Polym. Sci. Part A: Polym. Chem.,* 2005, **43**, 5283-5299.

99. B. Sun, C. M. Jewell, N. J. Fredin and D. M. Lynn, *Langmuir*, 2007, **23**, 8452-8459.

100. J. T. Kopping, Z. P. Tolstyka and H. D. Maynard, *Macromolecules*, 2007, **40**, 8593-8599.

101. F. Lecolley, C. Waterson, A. J. Carmichael, G. Mantovani, S. Harrisson and H. Chappell, *J. Mater. Chem.*, 2003, **13**, 2689-2695

102. A. Postma, T. P. Davis, G. Moad and M. Shea, *React. Funct. Polym.*, 2006, **66**, 137-147.

103. M. Matsuyama, M. Kamigaito and M. Sawamoto, *J. Polym. Sci. Part A: Polym. Chem.,* 1996, **34**, 3585-3589.

104. C. Boyer, B. Otazaghine, B. Boutevin, C. J. Duhamel and J. J. Robin, *J. Polym. Sci. Part A: Polym. Chem.,* 2005, **43**, 4303-4322.

105. L. Mespouille, M. Vachaudez, F. Suriano, P. Gerbaux, W. VanCamp, O. Coulembier, P. Degee, R. Flammang, F. D. Prez and P. Dubois, *React. Funct. Polym.*, 2008, **68**, 990-1003.

106. L. Mespouille, M. Vachaudez, F. Suriano, P. Gerbaux, O. Coulembier and P. Degee, *Macromol. Rapid Commun.*, 2007, **28**, 2151-2158.

107. W. Agut, D. Taton and S. Lecommandoux, *Macromolecules*, 2007, **40**, 5653-5661.

108. G. Mantovani, V. Ladmiral, L. Tao and D. M. Haddleton, *Chem. Commun.*, 2005, 2089-2091.

109. B. Grignard, C. Calberg, C. Jerome and C. Detrembleur, *J. Supercrit. Fluids*, 2010, **53**, 151-155.

110. C. H. Li, J. M. Hu, J. Yin and S. Y. Liu, *Macromolecules*, 2009, **42**, 5007-5016.

111. G. J. Chen, L. Tao, G. Mantovani, V. Ladmiral, D. P. Burt and J. V. Macpherson, *Soft Matter*, 2007, **3**, 732-739.

112. A. Narumi, K. Fuchise, R. Kakuchi, A. Toda, T. Satoh and S. Kawaguchi, *Macromol. Rapid Commun.*, 2008, **29**, 1126-1133.

113. K. Fuchise, R. Kakuchi, S. T. Lin, R. Sakai, S. I. Sato and T. Satoh, *J. Polym. Sci. Part A: Polym. Chem.,* 2009, **47**, 6259-6268.

114. P. D. Topham, N. Sandon, E. S. Read, J. Madsen, A. J. Ryan and S. P. Armes, *Macromolecules*, 2008, **41**, 9542-9547.

115. D. Haddleton and C. Waterson, *Macromolecules*, 1999, **32**, 8732-8739.

116. J. A. Blazquez, J. Areizaga, J. J. Iruin, O. Miguel, D. Mecerreyes and J. Jouanneau, *React. Funct. Polym.*, 2006, **66**, 1073-1080.

117. C. Granel, P. Dubois, R. Jerome and P. Teyssie, *Macromolecules*, 1996, **29**, 8576-8582.

118. H. Uegaki, M. Kamigato and M. Sawamoto, *J. Polym. Sci. Part A: Polym. Chem.,* 1999, **37**, 3003-3009.

119. K. Matyjaszewski, S. M. Jo, H. J. Paik and S. G. Gaynor, *Macromolecules*, 1997, **30**, 6398-6400.

120. K. Matyjaszewski, M. Wei, J. Xia and N. E. McDermott, *Macromolecules*, 1997, **30**, 8161-8164.

121. V. Percec, B. Barboiu and H. J. Kim, *J. Am. Chem. Soc.*, 1998, **120**, 305-316.

122. V. Percec, H. J. Kim and B. Barboiu, *Macromolecules*, 1997, **30**, 8526-8528.

123. W. K. S. Miller and C. Pugh, *Macromolecules*, 2015, **48**, 3803-3810.

124. M. A. Bennett, *Chem. Rev.*, 1962, **62**, 611-652.

125. R. Nast, *Coord. Chem. Rev.*, 1982, **47**, 89-124.

126. C. J. Duxbury, D. Cummins, A. Heise and . *J. Polym. Sci. Part A: Polym. Chem.,* 2009, **47**, 3795-3802.

127. A. Hasneen, H. S. Han and H. J. Paik, *React. Funct. Polym.*, 2009, **69**, 681-687.

128. B. S. Sumerlin, N. V. Tsarevsky, G. Louche, R. Y. Lee and K. Matyjaszewski, *Macromolecules*, 2005, **38**, 7540-7545.

129. J. Opsteen and J. V. Hest, *J. Polym. Sci. Part A: Polym. Chem.,* 2007, **45**, 2913-2924.

130. I. Singh, Z. Zarafshani, J.-F. Lutz and F. Heaney, *Macromolecules*, 2009, **42**, 5411-5902.

131. Z. Zarafshani, O. Akdemir and J. F. Lutz, *Macromol. Rapid Commun.*, 2008, **29**, 1161-1168.

132. C. Urbani, C. Bell, D. Lonsdale, M. Whittaker and M. Monteiro, *Macromolecules*, 2008, **41**, 76-86.

133. G. D. Fu, L. Q. Xu, F. Yao, K. Zhang, X. F. Wang, M. F. Zhu and S. Z. Nie, *ACS Appl. Mater. Interfaces*, 2009, **1**, 239-243.

134. G. J. Chen, L. Tao, G. Mantovani, V. Ladmiral, D. P. Burt, J. V. Macpherson and D. M. Haddleton, *Soft Matter*, 2007, **3**, 732-739.

135. L. Q. Xu, F. Yao, G. D. Fu and L. Shen, *Macromolecules*, 2009, **42**, 6385-6392.

136. C. Li, Z. Ge, H. Liu and S. Liu, *J. Polym. Sci. Part A: Polym. Chem.*, 2009, **47**, 4001-4013.

137. W. Lin, Q. Fu, Y. Zhang and J. Huang, *Macromolecules*, 2008, **41**, 4127-4135.

138. J. Xu, J. Ye and S. Liu, *Macromolecules*, 2007, **40**, 9103-9110.

139. V. L. G. Mantovani, L. Tao and D. M. Haddleton, *Chem. Commun.*, 2005, **16**, 2089-2091.

140. V. Ladmiral, T. M. Legge, Y. L. Zhao and S. Perrier, *Macromolecules*, 2008, **41**, 6728-6732.

141. S. Pfeifer, Z. Zarafshani, N. Badi and J. F. Lutz, *J. Am. Chem. Soc.*, 2009, **131**, 9195-9197.

142. Y. Li, J. W. Yang and B. C. Benicewicz, *J. Polym. Sci. Part A: Polym. Chem.,* 2007, **45**, 4300-4308.

143. A. Dag, H. Durmaz, G. Hizal and U. Tunca, *J. Polym. Sci. Part A: Polym. Chem.,* 2008, **46**, 302-313.

144. M. Li, P. De, S. R. Gondi and B. S. Sumerlin, *J. Polym. Sci. Part A: Polym. Chem.,* 2008, **46**, 5093-5100.

145. A. Dag, H. Durmaz, E. Demir, G. Hizal and U. Tunca, *J. Polym. Sci. Part A: Polym. Chem.,* 2008, **46**, 6969-6977.

146. O. Altintas, G. Hizal and U. Tunca, *Des. Monomers Polym.*, 2009, **12**, 83-98.

147. H. Durmaz, F. Karatas, U. Tunca and G. Hizal, *J. Polym. Sci. Part A: Polym. Chem.,* 2006, **44**, 3947-3957.

148. B. Gacal, H. Durmaz, M. A. Tasdelen, G. Hizal, U. Tunca, Y. Yagci and A. L. Demirel, *Macromolecules*, 2006, **39**, 5330-5336.

149. H. Durmaz, A. Dag, A. Hizal, G. Hizal and U. Tunca, *J. Polym. Sci. Part A: Polym. Chem.,* 2008, **46**, 7091-7100.

150. M. Erdogan, G. Hizal, U. Tunca, D. Hayrabetyan and O. Pekcan, *Polymer*, 2002, **43**, 1925-1931.

151. V. Vazquez-Dorbatt, Z. P. Tolstyka, C. W. Chang and H. D. Maynard, *Biomacromolecules*, 2009, **10**, 2207.

152. A. Klaikherd, S. Ghosh and S. Thayumanavan, *Macromolecules*, 2007, **40**, 8518.

153. A. Klaikherd, C.Nagamani and S. Thayumanavan, *J. Am. Chem. Soc.*, 2009, **131**, 4830-4838.

154. H. D. Maynard, K. L. Heredia, R. C. Li, D. P. Parra and V. Vazquez-Dorbatt, *J. Mater. Chem.*, 2007, **17**, 4015.

155. A. W. Jackson and D. A. Fulton, *Macromolecules*, 2010, **43**, 1069.

156. Y. Jin, L. Song, Y. Su, L. Zhu, Y. Pang, F. Qiu, G.Tong, D. Yan, B. Zhu and X. Zhu, *Biomacromolecules* 2011, **12**, 3460.

157. V. V. Dorbatt, Z. P. Tolstyka and H. D. Maynard, *Macromolecules*, 2009, **42**, 7650.

158. Y. Shen, S. Zhu, F. Zeng and R. Pelton, *Macromolecules*, 2000, **33**, 5399.

159. F. Zeng, Y. Shen, S. Zhu and R. Pelton, *J. Polym. Sci. Part A: Polym. Chem.,* 2000, **38**, 3821.

160. S. P. S. Koo, M. M. Stamenovic, R. A. Prasath, A. J. Inglis, F. E. D. Prez, C. B. Kowollik, W. V.Camp and T. Junkers, *J. Polym. Sci. Part A: Polym. Chem.*, 2010, **48**, 1699-1713.

161. M. M. Stamenovic, P. Espeel, W. V. Camp and F. E. D. Prez, *Macromolecules* 2011, **44**, 5619.

162. D. J. Liaw, C. C. Huang and C. H. Tsai, *Tamkang J. Sci. Eng.*, 2003, **6**, 133.

163. J. A. Carioscia, L. Schneidewind, C. Obrien, R. Ely, C. Feeser, N. Cramer and C. N. Bowman, *J. Polym. Sci. Part A: Polym. Chem.,* 2007, **45**, 5686.

164. C. F. Hansell, P. Espeel, M. M. Stamenovic, I. A. Barker, A. P. Dove, F. E. D. Prez and R. K. Oreilly, *J. Am. Chem. Soc.*, 2011, **133**, 13828.

165. I. Gadwal and A. Khan, *Polym. Chem.*, 2013, **4**, 2440-2444.

166. L. P. Yang, X. H. Dong and C. Y. Pan, *J. Polym. Sci. Part A: Polym. Chem.,* 2008, **46**, 7757.

167. J. M. Lu, X. W. Xia, X. Guo, Q. F. Xu, F. Yan and L. H. Wang, *J. Appl. Polym. Sci.*, 2008, **108**, 3430.

168. S. Yurteri, I. Cianga and Y. Yagci, *Macromol. Chem. Phys.*, 2003, **204**, 1771.

169. Z. Yang, J. Lu, S.Yao and L. Wang, *J. Macromol. Sci. Part A: Pure and Appl. Chem.*, 2004, **41**, 1105.

170. G. Summers, M. Ndawuni and C. Summers, *Polym. Int.*, 2003, **52**, 158.

171. C. N. Urbani, C. A. Bell, D. Lonsdale, M. R. Whittaker and M. J. Monteiro, *Macromolecules*, 2008, **41**, 76.

172. C. Hou, S. Lin, F. Liu, J. Hu, G. Zhang, G. Liu, Y. Tu, H. Zouab and H. Luo, *New J. Chem.*, 2014, **38**, 2538.

173. J. A. Opsteen and J. C. M. V. Hest, *J. Polym. Sci. Part A: Polym. Chem.,* 2007, **45**, 2913.

174. I. Gadwal and A. Khan, *Polym. Chem.*, 2013, **4**, 2440.

175. M. Degirmenci, O. Izgin, A. Acikses and N.Genli, *React. Funct. Polym.*, 2010, **70**, 28.

176. Y. Sun, W. Liu and Z. Ma, *Polym. Bull.*, 2013, **70**, 1531.

177. G. Carrot, J. Hilborn, J. Hedrick and M.Trollsas, *Macromolecules*, 1999, **32**, 5171.

178. M. Urien, H. Erothu, E. Cloutet, C. R. Hiorns and L. Vignau, *Macromolecules*, 2008, **41**, 7033.

179. S. S. Patil, B. V. Tawade and P. P. Wadgaonkar, *J. Polym. Sci. Part A: Polym. Chem.,* 2016, **54**, 844-860.

180. F. Zeng, Y. Shen, S. Zhu and R. Pelton, *Macromolecules*, 2000, **33**, 1628.

181. L. Campos, K. Killops, R. Sakai, J. Paulusse, D. Damiron, E. Drockenmuller, B. Messmore and C. Hawker, *Macromolecules*, 2008, **41**, 7063.

182. H. Malz, H. Komber, D. Voigt, I. Hopfe and J. Pionteck, *Macromol. Chem. Phys.*, 1999, **200**, 642.

183. D.Mecerreyes, B. Atthoff, K. Boduch, M. Trollsas and J. Hedrick, *Macromolecules*, 1999, **32**, 5175.

184. Y. Shen, S. Zhu, F. Zeng and R. Pelton, *Macromol. Chem. Phys.,* 2000, **201**, 1387.

185. H. Malz, J. Pionteck, P. Potschke, H. Komber, D. Voigt, J. Luston and F. Bohme, *Macromol. Chem. Phys.,* 2001, **202**, 2148.

186. G. J. Summers, R. B. Maseko, B. M. P. Beebeejaun and C. A. Summers, *J. Polym. Sci. Part A: Polym. Chem.,* 2011, **49**, 2601.

187. D. V. Palaskar, P. S. Sane and P. P. Wadgaonkar, *React. Funct. Polym.,* 2010, **70**, 931.

188. X. Yang, S. Wang, Y. Yan, Y. Wu, K. Zheng and Y. Chen, *Polymer*, 2014, **55**, 1128.

189. H. Durmaz, B. Colakoglu, U. Tunca and G. Hizal, *J. Polym. Sci. Part A: Polym. Chem.,* 2006, **44**, 1667.

190. O. S. Taskin, B. A. Temel, M. A.Tasdelen and Y. Yagci, *Eur. Polym. J.*, 2015, **62**, 304.

191. V. Ladmiral, L. Monaghan, G. Mantovani and D. M. Haddleton, *Polymer* 2005, **46**, 8536.

192. F. Lecolley, L. Tao, G. Mantovani, I. Durkin, S. Lautru and D. M. Haddleton, *Chem. Commun.*, 2004, 2026

193. A. A. Kavitha and N. K. Singha, *Macromol. Chem. Phys.*, 2007, **208**, 2569.

194. S. O. Sanchez, F. Marra, A. Dibenedetto, M. Aresta and A. Grassi, *Macromolecules*, 2014, **47**, 7129.

195. P. Sun, G. Yan, Q. Tang, Y. Chen and K. Zhang, *Polymer*, 2015, **64**, 202-209.

196. Y. Chen and Z. Guan, *Chem. Commun.*, 2014, **50**, 10868.

197. A. Bunha, M. C. Tria and R. Advincula, *Chem. Commun.*, 2011, 47, 9173.

198. K. Pangilinan and R. Advincula, *Polym. Int.*, 2014, **63**, 803.

199. J. Lyngsø, N. A. Manasir, M. A. Behrens, K. Zhu, A. L. Kjøniksen, B. Nyström and J. S. Pedersen, *Macromolecules*, 2015, **48**, 2235.

200. K. Matyjaszewski, P. J. Miller, D. C. Pyun, G. Kickelbick and S. Diamanti, *Macromolecules*, 1999, **32**, 6526.

201. D. Han, X. Tong and Y. Zhao, *J. Polym. Sci. Part A: Polym. Chem.,* 2012, **50**, 4198.

202. J. S. Wang, D. Greszta and K. Matyjaszewski, *Polym. Mater. Sci. Eng.,* 1995, **73**, 416.

203. A. P. Narrainen, L. R. Hutchings, I. Ansari, R. L. Thompson and N. Clarke, *Macromolecules*, 2007, **40**, 1969.

204. S. P. Rwei, Y. Y. Chuang, T. F. Way, W. Y. Chiang and S. P. Hsu, *Colloid Polym. Sci.*, 2015, **293**, 493.

205. G. J. Summers, M. P. Ndawuni and C. A. Summers, *Polym. Int.*, 2014, **63**, 876.

206. L. Z. Kong, M. Sun, H. M. Qiao and C. Y. Pan, *J. Polym. Sci. Part A: Polym. Chem.,* 2010, **48**, 454.

207. O. Altintas, P. K. Sidenstein, H. Gliemann and C. B. Kowollik, *Macromolecules*, 2014, **47**, 5877.

208. C. Boyer, A. H. Soeriyadi, P. J. Roth, M. R. Whittaker and T. P. Davis, *Chem. Commun.*, 2011, **47**, 1318.

209. G. Volet, T. X. Lav, J. Babinot and C. Amiel, *Macromol. Chem. Phys.*, 2011, **212**, 118.

210. R. Francis, B. Lepoittevin, D. Taton and Y. Gnanou, *Macromolecules*, 2002, **35**, 9001.

211. R. Matmour, B. Lepoittevin, T. J. Joncheray, E. l. Khouri, R. J., D. Taton, R. S. Duran and Y.Gnanou, *Macromolecules*, 2005, **38**, 5459.

212. J. Babin, C. Leroy, S. Lecommandoux, R. Borsali, Y. Gnanou and D. Taton, *Chem. Commun.*, 2005, **15**, 1993.

213. V. Coessens, Y. Nakagawa and K. Matyjaszewski, *Polym. Bull.*, 1998, **40**, 135.

214. V. Coessens and K. Matyjaszewski, *J. Macromol. Sci., Pure Appl. Chem.*, 1999, **36**, 653.

215. Y. Nakagawa, S. G. Gaynor and K. Matyjaszewski, *Polym. Prepr. (Am. Chem. Soc. Div. Polym. Chem.)*, 1996, **37**, 577.

216. J. Hegewald, J. Pionteck, L. Haubler, H. Komber and B. Voit, *J. Polym. Sci. Part A: Polym. Chem.,* 2009, **47**, 3845.

217. M. W. Jones, R. A. Strickland, F. F. Schumacher, S. Caddick, J. R. Baker, M. I. Gibson and D. M. Haddleton, *J. Am. Chem. Soc.*, 2012, **134**, 1847-1852.

218. Y. Wang, L. Lu, H. Wang, D. Lu, K. Tao and R. Bai, *Macromol. Rapid Commun.*, 2009, **30**, 1922.

219. H. Yang, Q. Zhang, B. Lin, G. Fu, X. Zhang and L. Guo, *J. Polym. Sci. Part A: Polym. Chem.,* 2012, **50**, 4182.

220. V. Coessens and K. Matyjaszewski, *Macromol. Rapid Commun.,* 1999, **20**, 66.

221. V. Coessens, J. Pyun, P. J. Miller, S. Gaynor and K. Matyjaszewski, *Macromol. Rapid Commun.,* 2000, **21**, 103.

222. S. A. F. Bon, A. G. Steward and D. M. Haddleton, *J. Polym. Sci. Part A: Polym. Chem.,* 2000, **38**, 678.

223. E. G. Koulouri and J. K. Kallitsis, *Macromolecules*, 1999, **32**, 6242.

224. B. Iskin, G. Yilmaz and Y. Yagci, *Macromol. Chem. Phys.*, 2013, **214**, 94.

225. Y. Y.Durmaz, I. Cianga and Y. Yagci, *e-Polymers*, 2006, 6.

226. H. R. Kricheldorf, S. R. Lee and S. Bush, *Macromolecules* 1996, **29**, 1375.

227. J. K. Oh, F. Perineau and K. Matyjaszewski, *Macromolecules*, 2006, **39**, 8003−8010.

228. D. Mecerreys, P. Debois and R. Jerome, *Adv. Polym. Sci.*, 1999, **147**, 1-60.

229. M. Degirmenci, A. Acikses and N. Genli, *J. Appl. Polym. Sci.*, 2012, **123**, 2567-2573.

230. B. Parrish, K. Fennifer and T. Emrick, *J. Polym. Sci. Part A: Polym. Chem.*, 2002, **40**, 1983.

231. J. Zheng, S. Xie, F. Lin, G. Hua, T. Yu, D. H. Reneker and M. L. Becker, *Polym. Chem.*, 2013, **4**, 2215-2218.

232. Y. Yuan, Y. Wang, J. Du and J. Wang, *Macromolecules*, 2008, **41**, 8620-8625.

233. J. X. Liu, C. Yuan, Z. Su, T. T. Xu, L. H. Wei and Z. Ma, *J. Polym. Sci. Part A: Polym. Chem.*, 2013, **51**, 1969-1975.

234. G. M. Soliman, R. Sharma, A. O. Choi, S. K. Varshney, F. M. Winnik, A. K. Kakkar and D. Maysinger, *Biomaterials*, 2010, **31**, 8382-8392.

235. A. S. kasegaonkar, H. Barqawi and W. H. Binder, *J. Polym. Sci. Part A: Polym. Chem.*, 2015, **53**, 642-649.

236. P. Lecomte and C. Jerome, *Adv. Polym. Sci.*, 2012, **245**, 173-218.

237. L. Chang, J. Liu, J. Zhang, L. deng and A. Dong, *Polym. Chem.*, 2013, **4**, 1430-1438.

238. B. M. Cooper, D. C. Seng, D. Samanta, X. Zhang, S. parelkar and T. Emrick, *Chem. Commun.*, 2009, 815-817.

239. M. Labet and W. Thielemans, *Chem. Soc. Rev.*, 2009, **38**, 3484.

240. K. Zhang, Y. Wang, W. P. Zhu, X. D. Li and Z. Q. Shen, *J. Polym. Sci. Part A: Polym. Chem.*, 2012, **50**, 2045-2052.

241. H. Kolb, M. Finn and K. Sharpless, *Angew. Chem. Int. Ed.*, 2001, **40**, 2004.

242. U. Mansfeld, C. Pietsch, R. Hoogenboom, C. R. Becer and U. S. Schubert, *Polymer Chemistry*, 2010, **1**, 1560-1598.

243. W. H. Binder and R. Sachsenhofer, *Macromol. Rapid Commun.*, 2007, **28**, 15-54.

244. D. Fournier, R. Hoogenboom and U. Schubert, *Chem. Soc. Rev.*, 2007, **36**, 1369.

245. V. O. Rodionov, S. I. Presolski, D. D. Diaz, V. V. Fokin and M. G. Finn, *J. Am. Chem. Soc.*, 2007, **129**, 12705.

246. H. Wang, J. He, M. Zhang, Y. Tao, F. Li, K. C. Tam and P. Ni, *J. Mater. Chem. B.*, 2013, **1**, 6596-6607.

247. K. Satoh, J. E. Poelma, L. M. Campos, B. Stahl and C. J. Hawker, *Polym. Chem.*, 2012, **3**, 1890-1898.

248. H. Liu, C. Li, H. Liu and S. Liu, *Langmuir*, 2009, **25**, 4724-4734.

249. G. Deng, D. Ma and Z. Xu, *Eur. Polym. J.*, 2007, **43**, 1179-1187.

250. K. Khanna, S. Varshney and A. Kakkar, *Macromolecules*, 2010, **43**, 5688-5698.

251. M. J. Kade, D. J. Burke and C. J. Hawker, *J. Polym. Sci. Part A: Polym. Chem.*, 2010, **48**, 743-750.

252. B. Iskin, G. Yilmaz and Y. Yagci, *J. Polym. Sci. Part A: Polym. Chem.*, 2011, **49**, 2417-2422.

253. S. Ozlem, B. Iskin, G. Yilmaz, M. Kukut, J. Hacaloglu and Y. Yagci, *Eur. Polym. J.*, 2012, **48**, 1755-1767.

254. Y. Xia, H. Yao, Z. Miao, Y. Ma, M. Cui, L. Yan, H. Ling and Z. Qi, *RSC Adv.*, 2015, **5**, 50955-50961.

255. J. W. Chan, B. Yu, C. E. Hoyle and A. B. Lowe, *Chem. Commun.*, 2008, 4959-4961.

256. Q. Zhang, G. Z. Li, C. R. Becer and D. M. Haddleton, *Chem. Commun.*, 2012, **48**, 8063-8065.

257. J. K. Sprafke, J. M. Spruell, K. M. Mattson, D. Montarnal, A. J. McGrath, R. Potzsch, D. Miyajima, J. Hu, A. A. Latimer, B. I. Voit, T. Aida and C. J. Hawker, *J. Polym. Sci. Part A: Polym. Chem.*, 2015, **53**, 319-326.

258. G. Hizal, U. Tunca and A. Sanyal, 2011, **49**, 4103-4120.

259. L. M. Polgar, M. V. Duin, A. A. Broekhuis and F. Picchioni, *Macromolecules*, 2015, **48**, 7096-7105.

260. A. A. Kavitha and N. K. Singha, *ACS Appl. Mater. Interfaces*, 2009, **1**, 1427-1436.

261. C. Zeng, H. Seino, J. Ren, K. Hatanaka and N. Yoshie, *Macromolecules*, 2013, **46**, 1794-1802.

262. T. Erdogan, Z. Ozyurek, G. Hizal and U. Tunca, *J. Polym. Sci. Part A: Polym. Chem.*, 2004, **42**, 2313-2320.

263. O. Glaied, C. Delaite and P. Dumas, *J. Polym. Sci. Part A: Polym. Chem.*, 2006, **44**, 1796-1806.

264. H. Liu, J. Xu, J. Jiang, J. Yin, R. Narain, Y. Cai and S. Liu, *J. Polym. Sci. Part A: Polym. Chem.*, 2007, **45**, 1446-1462.

265. B. Iskin, G. Yilmaz and Y. Yagci, *Polym. Chem.*, 2011, **2**, 2865-2871.

266. U. S. Gunay, H. Durmaz, E. Gungor, A. Dag, G. Hizal and U. Tunca, *J. Polym. Sci. Part A: Polym. Chem.*, 2012, **50**, 729-735.

267. H. Durmaz, F. Karatas, U. Tunca and G. Hizal, *J. Polym. Sci. Part A: Polym. Chem.*, 2006, **44**, 499-509.

268. Y. Zhang, H. Liu, J. Hu, C. Li and S. Liu, *Macromol. Rapid Commun.*, 2009, **30**, 941-947.

269. Y. Zhang, C. Li and S. Liu, *J. Polym. Sci. Part A: Polym. Chem.*, 2009, **47**, 3066-3077.

270. A. Gandini, D. Coelho, M. Gomes, B. Reis and A. Silvestre, *J. Mater. Chem.*, 2009, **19**, 8656-8664.

271. N. Bai, K. saito and G. P. Simon, *Polym. Chem.*, 2013, **4**, 724-730.

272. U. Haldar, K. Bauri, R. Li, R. Faust and P. De, *ACS Appl. Mater. Interfaces*, 2015, **7**, 8779-8788.

273. L. Gao, T. Kong and Y. Huo, *Macromolecules*, 2016, **49**, 7478-7489.

274. E. Blasco, B. V. K. J. Schmidt, C. B. Kowollik, M. Pinol and L. Oriol, *Polym. Chem.*, 2013, **4**, 4506-4514.

275. D. Schmaljohann, *Adv. Drug Del. Rev.*, 2006, **58**, 1655-1670.

276. B. Liu, H. Zhou, S. Zhou, H. Zhang, A. C. Feng, C. Jian, J. Hu, W. Gao and J. Yuan, *Macromolecules*, 2014, **47**, 2938-2946.

277. X. Huang, F. Du, J. Cheng, Y. Dong, D. Liang, S. Ji, S. S. Lin and Z. Li, *Macromolecules*, 2009, **42**, 783-790.

278. Z. Cao, H. Wu, J. Dong and G. Wang, *Macromolecules*, 2014, **47**, 8777−8783.

279. F. Herbst, D. Dohler, P. Michael and W. H. Binder, *Macromol. Rapid Commun.*, 2013, **34**, 203-220.

280. N. Yoshie, M. Watanabe, H. Araki and K. Ishida, *Polym. Degrad. Stab.*, 2010, **95**, 826-829.

281. L. T. T. Nguyen, H. T. Nguyen and T. T.Truong, *J. Polym. Res.*, 2015, **22**, 186.

282. J. Kötteritzsch, S.Stumpf, S. Hoeppener, J. Vitz, M. D. Hager and U. S. Schubert, *Macromol. Chem. Phys.*, 2013, **214**, 1636−1649.

283. R. K. Bose, J. Kotteritzsch, S. J. Garcia, M. D. Hager, U. S. Schubert and S. V. D. Zwaag, *J. Polym. Sci. Part A: Polym. Chem.*, 2014, **52**, 1669-1675.

Chapter 2

Functionalized Polystyrene Macromonomers Using Phenolphthalein-Based ATRP Initiator

2.1 Introduction

Well-defined end functional polymers (telechelic polymers) are useful as building blocks for design and synthesis of various complex macromolecular architectures such as block,[1-4] star,[5-9] graft [10-14]copolymers, etc. and act as the precursors for poly-condensation reactions which find potential applications in biomedical,[15] tissue engineering,[16] materials[17] and surface sciences.[18] Controlled/living polymerization techniques such as nitroxide mediated polymerization (NMP),[19, 20] reversible addition fragmentation chain transfer (RAFT)[20-22] and atom transfer radical polymerization (ATRP) [20, 23] are of much interest to synthesize such end-functional polymers. Retention of living chain end in these polymerization techniques and/or presence of functional groups at their terminals allows the convenient synthesis of such complex architectures. Amongst all these methods, ATRP is a robust, promising and widely used technique due to its tolerance to various functional groups both in the monomer and the initiator, and its suitability to various (meth)acrylic and styrenic monomers over a wide temperature range.[24]

The four approaches generally used to synthesize end functional polymers by ATRP are: A) Functional initiator approach (α- or α,α'-functionalisation),[25-31] B) Chemical modification of functional group incorporated *via* initiator into other useful functional group(s) (α- or α α'- functionalization),[30, 32] C) Transformation of terminal halide into other functional groups (ω- or ω,ω'-functionalization),[33-36] and D) Combination of both i.e. use of functional initiator and transformation of terminal halide into other useful functional group(s) (α,ω-functionalization).[37, 38] Of these approaches, functional initiator approach is preferred as it allows quantitative functionalization and offers flexibility in terms of the choice of functional group(s). ATRP employing functional initiators is a convenient method for synthesis of functionally terminated polymers with a wide range of functional groups depending on the selection and nature of functional initiator. A plethora of ATRP initiators containing functional groups are reported in the literature for synthesis of α-functionalised[9, 20, 26, 34, 39-44] and α,α'-homo-[44, 45] or α,α'-hetero-bifunctionalised polymers.[32] Recently, our group reported synthesis of α-aldehyde α'- allyloxy hetero-bifunctionalised poly(caprolactone), polystyrene and poly(methyl methacrylate) macromonomers employing ROP and ATRP using appropriate functional initiators derived from levulinic acid.[45-47]

However, a limited number of examples of ATRP initiators containing allyl groups are available in the literature. We designed herein a new functional ATRP initiator containing allyl functional groups, namely, 2-(1,1-bis(4-(allyloxy)phenyl)-3-oxoisoindolin-2-yl)ethyl 2-bromo-2-methylpropanoate (**3**) starting from phenolphthalein- a bench top chemical- in fewer number of steps avoiding the protection and deprotection strategies. ATRP initiator containing allyl functional groups is of interest as allyl groups could subsequently be exploited in quantitative thiol-ene click reaction and several other useful organic transformations. α, α'-Bisallyloxy functionalised polystyrene macromonomers with controlled molecular weight and narrow dispersity values were synthesized employing ATRP. α, α' Bis-allyloxy functionalized polystyrene macromonomers represent valuable precursors for the synthesis of polystyrenes containing other interesting functional groups and miktoarm star copolymers by taking advantage of thiol-ene click reaction. Metal-free photochemical thiol-ene click reaction of allyloxy end functional polystyrene with benzyl mercaptan as a model thiol reagent was performed to demonstrate the reactivity of allyloxy groups. Furthermore, the thiol-ene click reaction was extended to thiols containing reactive functional groups, namely, 2-mercaptoethanol and 3-mercaptopropionic acid to obtain α,α'-dihydroxyl and α,α'-dicarboxyl functionalised polystyrene macromonomers which are useful precursors in polycondensation reactions.

2.2 Experimental Section

2.2.1 Materials

2-(2-Hydroxyethyl)-3,3-bis(4-hydroxyphenyl)isoindolin-1-one was synthesized from phenolphthalein as per the reported procedure.[48] Copper(I) bromide (99.99 %, Sigma Aldrich) was washed with dilute acetic acid to remove soluble oxidised species, filtered, washed with ethanol followed by diethyl ether and dried before use. *N,N,N',N'',N''*-Pentamethyldiethylenetriamine (99 %) and α- bromoisobutyryl bromide (98 %) were purchased from Sigma Aldrich and were used as received. Toluene was stirred over calcium hydride and distilled. Styrene was purified by stirring over calcium hydride and distillation under reduced pressure on Linde type (4 A°) molecular sieves. Potassium carbonate (99 %, Fischer Scientific) was dried before use. 2-Ethanolamine (98 %, Fluka) and allyl bromide (98 %, Loba) were used as received. Triethylamine (99.5 %) and acetone were stirred over potassium hydroxide and potassium carbonate, respectively and distilled before use. *N, N*-Dimethylformamide (DMF) was stirred over calcium hydride

and distilled under reduced pressure. Benzyl mercaptan (99 %, Sigma Aldrich), 2-mercaptoethanol (99 %, Sigma Aldrich) 3-mercaptopropionic acid (99%, Sigma Aldrich) and 2, 2-dimethoxy-2-phenyl-acetophenone (DMPA) (99 %, Sigma Aldrich) were used as received.

2.2.2 Characterization and Measurements

FT-IR spectra were recorded on Perkin Elmer Spectrum GX spectrophotometer using chloroform as a solvent. NMR spectra were recorded on Bruker-400 MHz spectrometer in $CDCl_3$ or Acetone-d_6 as a solvent. Molecular weights of polymers were calculated using NMR spectroscopy by comparing the integral ratio of repeating units of polymer with the aromatic proton of initiator fragment. Photochemical thiol-ene click reaction was performed using photochemical reactor with a UV lamp at 365 nm wavelength.

Molecular weights and dispersity of polystyrenes were determined from gel-permeation chromatography (GPC) using chloroform as an eluent at a flow rate of 1 mL/min at 25 °C (Thermo Separation Products) equipped with spectra series UV 100 and spectra system RI 150 detectors. Sample concentration was 2 mg/mL and narrow dispersity polystyrenes were used as calibration standards. Matrix assisted laser desorption ionisation - time of flight (MALDI-TOF) spectrum acquisition was recorded on AB-SCIEX TOF/TOF 5800 using reflector positive method in THF as a solvent using dithranol (5 volume equivalent with polymer) as a matrix and 1 mg/mL concentration of polystyrene at 25 °C.

2.2.3 Synthesis

2.2.3.1 Synthesis of 2-(2-hydroxyethyl)-3, 3-bis (4-hydroxyphenyl)isoindolin-1-one (1)

Into a three necked round bottom flask (500 mL) equipped with a mechanical stirrer, a gas inlet and a reflux condenser were charged phenolphthalein, (5.0 g, 15.7 mmol) and 2-aminoethanol (10.55 g, 172.8 mmol). The solution was refluxed for 24 h. Excess of 2-aminoethanol was distilled under reduced pressure, and residue was poured into ice-cold water to obtain white precipitate. The crude product was recrystallised from a mixture of ethanol and water (30:70, v/v) to afford 4.70 g, (83 %) of 2-(2-hydroxyethyl)-3, 3-bis(4-hydroxyphenyl) isoindolin-1-one **1** as white crystals.

Melting point- 254 °C. (Lit. M.P. - 255-256 °C.)[48]

IR (CHCl$_3$, cm^{-1}): 3023 (-OH) and 1668 (C=O of amide).

^{1}H NMR (Acetone-d$_6$, δ/ppm): 8.55 (s, 2H phenolic OH), 7.75 (d, 1H), 7.55 (t, 1H), 7.47 (t, 1H), 7.40 (d, 1H), 7.08 (d, 4H), 6.84 (d, 4H), 3.95 (t, 1H alcoholic -OH), 3.55 (t, 2H), 3.02 (q, 2H).

^{13}C NMR (Acetone-d$_6$, δ/ppm): 169.51, 158.32, 152.94, 133.12, 132.37, 131.54, 130.30, 128.97, 124.74, 123.89, 116.37, 76.02, 60.57, 45.06.

2.2.3.2 Synthesis of 3, 3-bis(4-(allyloxy)phenyl)-2-(2-hydroxyethyl)isoindolin-1-one (2)

Into a three necked round bottom flask (100 mL) equipped with a mechanical stirrer, an argon inlet and a reflux condenser were charged 2-(2-hydroxyethyl)-3,3-bis(4-hydroxyphenyl)isoindolin-1-one (3 g, 8.3 mmol), dry potassium carbonate (3.44 g, 24.9 mmol) and acetone (40 mL). The reaction mixture was stirred at room temperature for 30 min and was cooled to 5 °C. Allyl bromide (3.0 g, 24.9 mmol) dissolved in acetone (10 mL) was added dropwise over a period of 10 min and the solution was refluxed for 12 h, filtered through the bed of celite, and acetone was evaporated on a rotary evaporator. The crude product was extracted in ethyl acetate and purified by column chromatography using pet ether:ethyl acetate (50:50, v/v) as an eluent to afford 3.2 g (87 %) of 3,3-bis(4-(allyloxy)phenyl)-2-(2-hydroxyethyl)isoindolin-1-one **2** as a thick liquid.

IR (CHCl$_3$, cm^{-1}): 1668 (C=O of amide) and 1506 (C=C)

^{1}H NMR (CDCl$_3$, δ/ppm): 7.86 (d, 1H), 7.49 (t, 1H), 7.43 (t, 1H), 7.25 (d, 1H), 7.12 (d, 4H), 6.86 (d, 4H), 5.98-6.08 (m, 2H), 5.27-5.42 (m, 4H), 4.52 (d, 4H), 3.60 (t, 2H), 3.27 (t, 2H).

^{13}C NMR (CDCl$_3$, δ/ppm): 170.51, 158.54, 151.37, 132.90, 132.47, 131.84, 130.05, 129.24, 128.20, 123.68, 123.40, 117.87, 114.83, 75.60, 68.82, 62.13, 45.32.

2.2.3.3 Synthesis of 2-(1, 1-bis (4-(allyloxy)phenyl)-3-oxoisoindolin-2-yl)ethyl 2-bromo-2-methylpropanoate (3)

Into a two necked round bottom flask (100 mL) equipped with a mechanical stirrer, a gas inlet and an addition funnel were charged 3,3-bis(4-(allyloxy)phenyl)-2-(2-hydroxyethyl)isoindolin-1-one (3.0 g, 6.8 mmol), triethylamine (1.51 g, 14.9 mmol) and dry chloroform (50 mL). The solution of α- bromoisobutyryl bromide (3.44 g, 14.9 mmol) in chloroform (10 mL) was added dropwise over a period of 30 min at 0 °C. The reaction mixture was stirred at 0 °C for 1 h and at room temperature for 12 h and filtered through

the small bed of celite to remove the hydrochloride salt. The solution was washed with a saturated solution of sodium bicarbonate (3×60 mL) and water (60 mL). The combined organic layers were evaporated and the product was purified by column chromatography using pet ether:ethyl acetate (90:10, v/v) as an eluent to afford 3.9 g (97 %) of 2-(1, 1-bis(4-(allyloxy)phenyl)-3-oxoisoindolin-2-yl)ethyl 2-bromo-2-methylpropanoate **3** as a thick liquid.

IR (CHCl$_3$, cm^{-1}): 1735 (C=O of ester) and 1694 (C=O of amide).

^{1}H NMR (CDCl$_3$, δ/ppm): 7.85 (d, 1H), 7.47 (t, 1H),7.41 (t, 1H), 7.26 (d, 1H), 7.14 (d, 4H), 6.86 (d, 4H), 5.98-6.07 (m, 2H), 5.26-5.41 (m, 4H), 4.51 (d, 4H), 3.76 (t, 2H), 3.52 (t, 2H), 1.86 (s, 6H).

^{13}C NMR (CDCl$_3$, δ/ppm): 170.73, 168.45, 158.24, 150.95, 132.61, 132.03, 129.80, 128.92, 127.79, 123.38, 123.10, 117.56, 114.60, 74.44, 68.53, 61.79, 55.55, 38.58, 30.33.

2.2.3.4 Synthesis of α, α'- bisallyloxy functionalized polystyrene

In a typical experiment, the Schlenk tube equipped with a magnetic stirr bar was charged with copper bromide (26.9 mg, 0.192 mmol), and the tube was thoroughly flushed with flowing argon. In a separate sample vial, 2-(1, 1-bis (4-(allyloxy)phenyl)-3-oxoisoindolin-2-yl)ethyl 2-bromo-2-methylpropanoate (111.9 mg, 0.192 mmol), styrene (1 g, 9.61 mmol), and toluene (1 g) were charged (Run-1, Table 2.1).The solution was degassed and transferred to the Schlenk tube using argon purged syringe under argon atmosphere. The reaction mixture was degassed thrice using vacuum freeze pump thaw cycles. *N,N',N',N'',N''*-Pentamethyldiethylenetriamine (32.9 mg, 0.192 mmol) was added to the Schlenk tube under flowing argon followed by two freeze pump thaw cycles and was immersed in an oil bath maintained at 80 °C. Polymerization was quenched after appropriate time by exposing the reaction mixture to air and sudden cooling in liquid nitrogen. The reaction mixture was diluted with tetrahydrofuran (10 mL) and passed through a neutral alumina column to remove copper residue, concentrated and precipitated in tenfold excess of cold methanol, filtered and dried under reduced pressure for 20 h. Conversions of the reaction were calculated gravimetrically.

IR (CHCl$_3$, cm^{-1}): 1640 (C=C of polystyrene rings)

^{1}H NMR (CDCl$_3$, δ/ppm): 7.84 (broad s), 7.45 (broad s), 7.40 (broad s), 6.46-7.05 (m, polystyrene aromatic rings), 6.01-6.04 (m), 5.26-5.42 (m), 4.49 (broad s), 3.40 (broad s), 2.96 (broad s), 0.81-2.07 (m, -CH$_2$-, and –CH- of polystyrene chain)

2.2.4 Polymer modification

2.2.4.1 Photochemical thiol-ene click reaction

Into a Pyrex tube (30 mL) fitted with a rubber septum, bis-allyloxy functionalised polystyrene ($M_{n,GPC}$- 4800 g mol^{-1}, Dispersity-1.05, Run 1. Table 2.1) (100 mg, 0.02 mmol), 2,2-dimethoxy 2-phenyl-acetophenone (0.5 mg, 0.25 wt.% w. r. t. allyl group) and DMF (5 mL) were charged and degassed for 30 min to remove dissolved oxygen. To the deoxygenated reaction mixture was added benzyl mercaptan / 2-mercaptoethanol / 3-mercaptopropionic acid (0.10 mmol) under the positive pressure of argon and reaction mixture was irradiated in the photochemical reactor at 365 nm wavelength for 3 h. DMF was removed under reduced pressure and the polymer sample was precipitated in excess of cold methanol, filtered and dried at 50 °C.

2.2.4.1.1 Synthesis of α, α'-dibenzyl thioether-terminated polystyrene (4a)

Yield- 98 %.

^{1}H NMR (CDCl$_3$, δ/ppm): 7.85 (broad s), 7.44 (broad s), 7.40 (broad s), 7.29 (s, aromatic ring protons of thiol), 6.46-7.09 (m, aromatic rings of polystyrene), 3.97 (q), 3.70 (s), 3.41 (broad s), 2.94 (broad s), 2.57 (q), 1.98 (m), 0.80-2.06 (m, -CH$_2$-, and –CH- of polystyrene chain).

2.2.4.1.2 Synthesis of α, α'-dihydroxyl functionalised polystyrene (4b)

Yield- 96 %

^{1}H NMR (CDCl$_3$, δ/ppm): 7.85 (broad s), 7.44 (broad s), 7.40 (broad s), 6.46-7.09 (m, aromatic rings of polystyrene), 4.03 (q), 3.72 (q), 3.41 (broad s), 2.94 (broad s), 2.72 (s), 2.0-2.2 (m), 0.80-2.06 (m, -CH$_2$-, and –CH- of polystyrene chain).

2.2.4.1.3 Synthesis of α, α'-dicarboxyl functionalised polystyrene (4c)

Yield- 95 %

^{1}H NMR (CDCl$_3$, δ/ppm): 7.85 (broad s), 7.44 (broad s), 7.40 (broad s), 6.46-7.09 (m, aromatic rings of polystyrene), 4.10 (broad s), 3.44 (broad s), 2.94 (broad s), 2.65-2.85 (m), 2.61 (broad s), 2.0-2.2 (m), 0.80-2.06 (m, -CH$_2$-, and –CH- of polystyrene chain).

2.3 Results and Discussion

2.3.1 Synthesis of 2-(1, 1-bis(4-(allyloxy)phenyl)-3-oxoisoindolin-2-yl)ethyl 2-bromo-2-methylpropanoate (3)

Scheme 2.1 depicts the synthesis of a new ATRP initiator, namely, 2-(1,1-bis(4-(allyloxy)phenyl)-3-oxoisoindolin-2-yl)ethyl 2-bromo-2-methylpropanoate **3,** starting from commercially available phenolphthalein as a cheap precursor. Phenolphthalein was reacted with excess of 2-ethanolamine to give 2-(2-hydroxyethyl)-3, 3-bis(4-hydroxyphenyl)isoindolin-1-one **1**. Allylation of **1** in the presence of potassium carbonate, crown ether and dry acetone as solvent resulted in 3,3-bis(4-(allyloxy)phenyl)-2-(2-hydroxyethyl)isoindolin-1-one **2**. 2-(1, 1-Bis(4-(allyloxy)phenyl)-3-oxoisoindolin-2-yl)ethyl 2-bromo-2-methylpropanoate **3** was obtained by reaction of **2** with α-bromoisobutyryl bromide in the presence of triethylamine as an acid acceptor. All the intermediates and initiator were characterized by FT-IR, ^{1}H-NMR and ^{13}C-NMR spectroscopy.
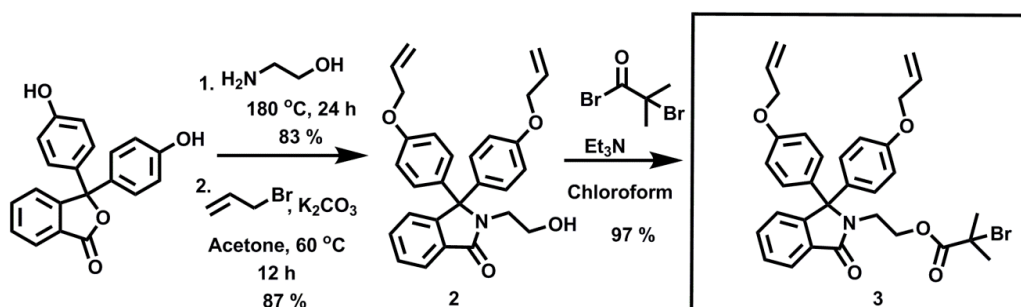
Scheme 2.1 Synthesis of 2-(1,1-bis(4-(allyloxy)phenyl)-3-oxoisoindolin-2-yl)ethyl 2-bromo-2-methylpropanoate (**3**).

FT-IR spectrum of **3** showed a band at 1735 cm^{-1} due to carbonyl stretching frequency of ester (-COO) and at 1694 cm^{-1} due to carbonyl stretching of amide (-CONH) (**Figure 2.1**). The appearance of a singlet at 1.86 ppm in ^{1}H-NMR spectrum (**Figure 2.2**) corresponds to methyl protons of halo-ester. The spectral data for other protons were in good agreement with the proposed structure. [13]C spectrum showed peaks at 170.7 ppm and 168.4 ppm due to carbonyl group of halo-ester and amide, respectively. Appearance of peaks at 132.6 and 117.5 ppm corresponds to the carbon atoms of allyl group. The data corresponding to remaining carbon atoms were in good agreement with the proposed structure.
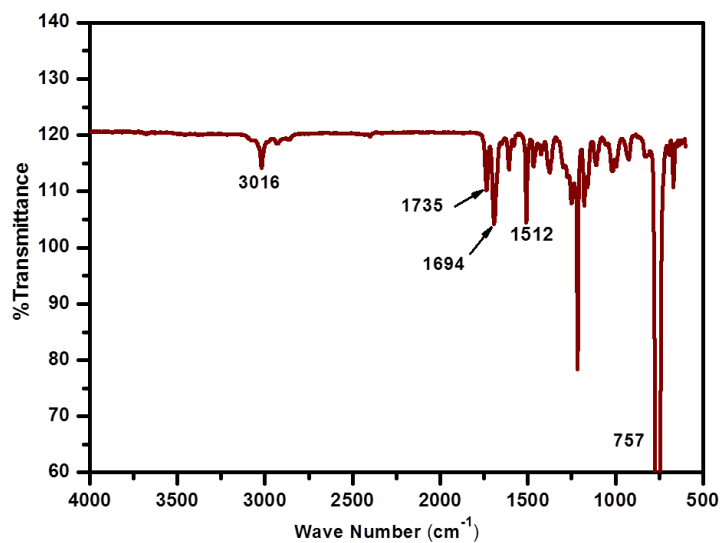
Figure 2.1 FT-IR spectrum (in chloroform) of 2-(1,1-bis(4-(allyloxy)phenyl)-3-oxoisoindolin-2-yl)ethyl 2-bromo-2-methylpropanoate (**3**).
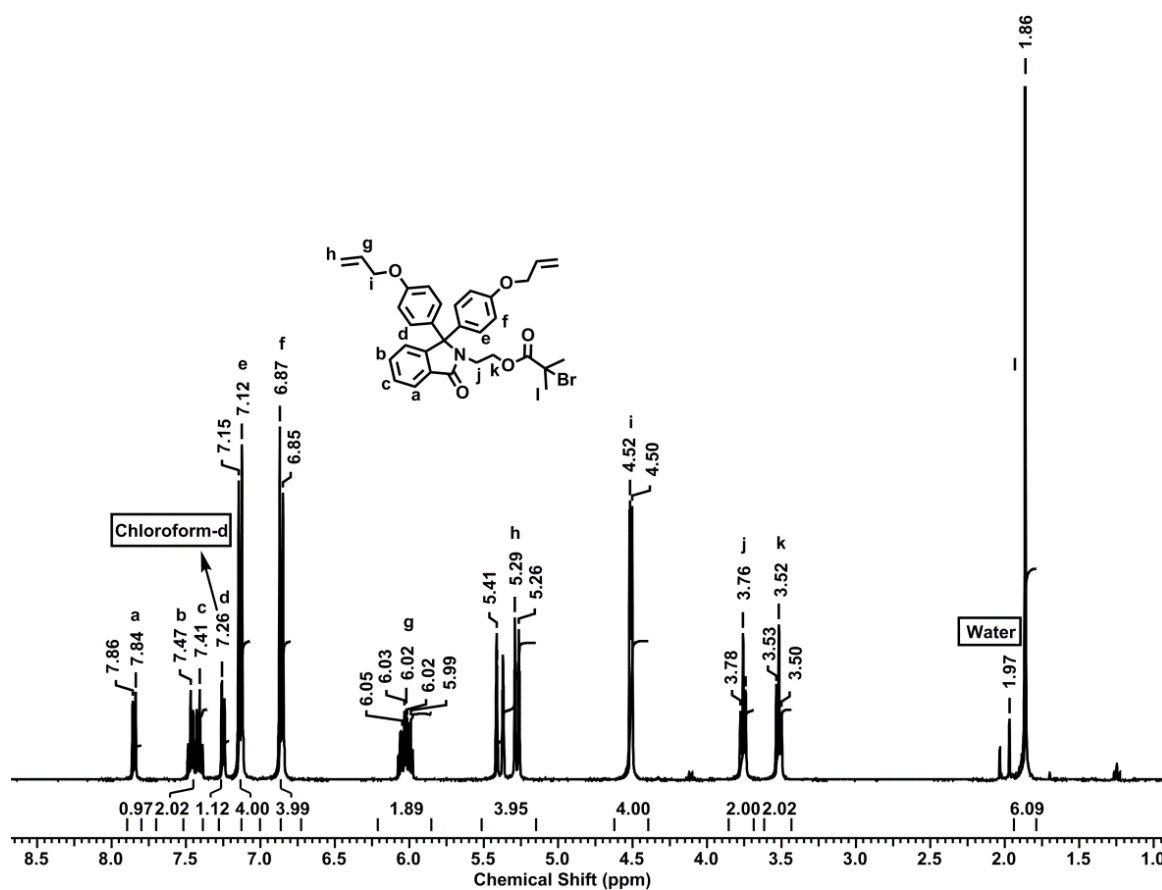
Figure 2.2 ^{1}H-NMR spectrum (in CDCl$_3$) of 2-(1,1-bis(4-(allyloxy)phenyl)-3-oxoisoindolin-2-yl)ethyl 2-bromo-2-methylpropanoate (**3**).

2.3.2 Synthesis of α, α'- bisallyloxy functionalized polystyrene by ATRP

ATRP of styrene was carried out by employing **3** as the initiator using copper (I) bromide as a catalyst, and *N,N',N',N'',N''*-pentamethyldiethylenetriamine as a ligand in toluene as a solvent (**Scheme 2.2**). Polymerization reactions were carried out at 80 $^{\circ}$C in order to minimize the possibility, if any, of potential side reactions involving allyloxy groups. Polystyrenes with molecular weights ranging between 4,800-11,700 g mol^{-1} were synthesized by varying monomer to initiator feed ratio (**Table 2.1**).
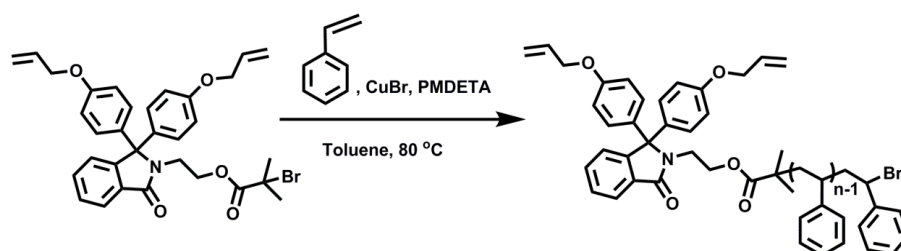
Scheme 2.2 Synthesis of α, α'- bisallyloxy functionalised polystyrene by ATRP.

Polymerization conditions and results of synthesis of bis-allyloxy functionalised polystyrene macromonomers are summarized in Table 2.1.

Table 2.1 Reaction conditions and results of synthesis of α, α'- bisallyloxy functionalised polystyrenes.

Sr. No.	[M]$_0$/[I]$_0$ [a]	Time (h)	Conv. (%) [b]	M$_{n,theo}$ [c]	M$_{n,NMR}$ [d] g mol^{-1}	M$_{n,GPC}$ [e] g mol^{-1}	M$_w$/M$_n$	I^{eff} [f]
1	50	6	74	4500	5600	4800	1.05	0.80
2	100	9	78	8700	10300	10000	1.07	0.84
3	150	9	60	10000	12000	11700	1.06	0.83
4	200	10	47	10400	11000	10000	1.09	0.95

Temperature: 80°C, solvent: toluene (1:1 w/w, w. r. t. monomer)
[a] [M]$_0$/[I]$_0$: [Monomer]$_0$/[Initiator]$_0$ feed ratio.
[b] Gravimetrically (weight of initiator was subtracted from the weight of polymer obtained).
[c] M$_{n,theo}$ = { [M]$_0$/[I]$_0$ ×(% conv.)/100 × mol. weight of monomer} + mol. weight of initiator
[d] M$_{n,NMR}$ = Determined by ^{1}H-NMR spectroscopy.
[e] M$_{n,GPC}$ = Determined by GPC; Polystyrene standard; Chloroform as an eluent.
[f] I^{eff} = M$_{n,theo}$ / M$_{n,NMR.}$

^{1}H-NMR spectrum of polystyrene showed multiplets in the range 6.46-7.05 ppm and 0.81-2.07 ppm for aromatic ring protons of polystyrene and methylene and methine protons of polystyrene backbone, respectively (**Figure 2.3**). Molecular weight of polystyrenes were calculated from ^{1}H-NMR spectrum considering the integral ratios of peak at 6.46-7.05 ppm for phenyl ring of polystyrene to the doublet at 7.84 ppm of phenyl ring of initiator fragment. Degree of polymerization (DP_n) of polystyrene from ^{1}H-NMR spectrum was calculated using the relation

$$DP_n = [(I_{6.46-7.05}/5)_{\text{polystyrene rings}} / (I_{7.84}/1)_{\text{phenyl ring in initiator fragment}}]$$

Molecular weights were calculated using the relation,

$$M_{n\,(\text{NMR})} = [DP_n \times \text{Molecular weight of monomer}] + \text{Molecular weight of initiator}$$
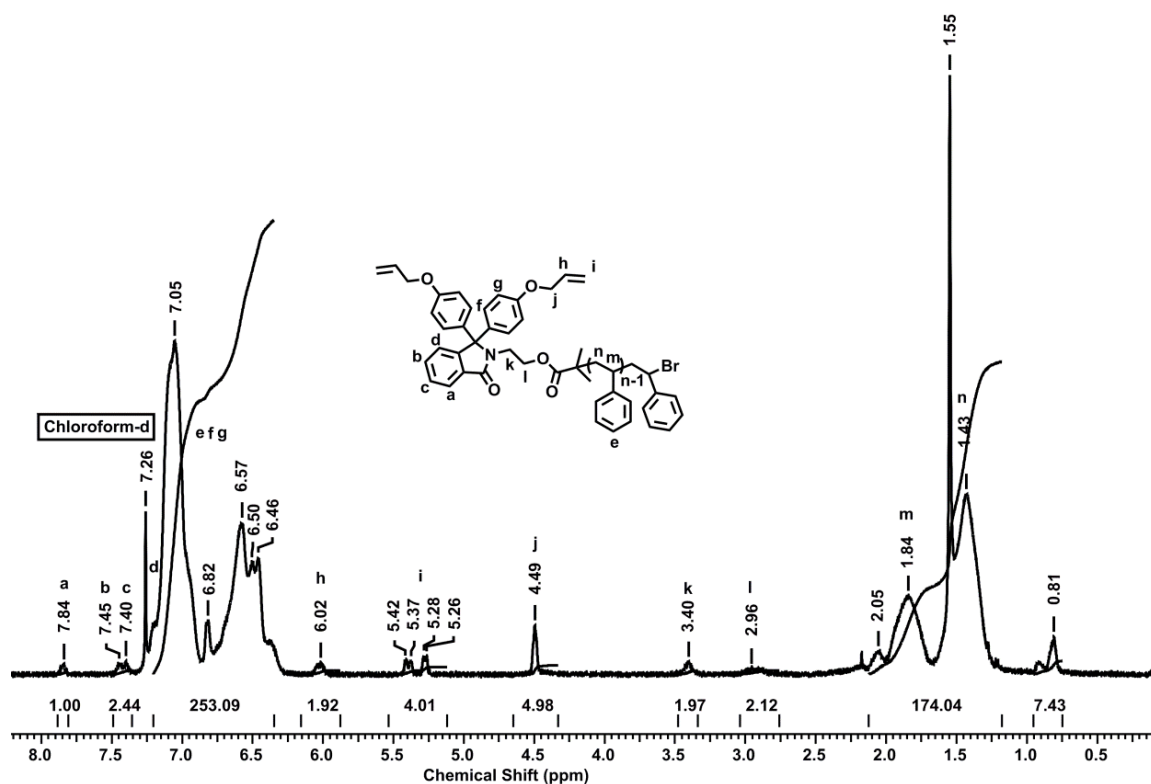
Figure 2.3 ^{1}H-NMR spectrum (in CDCl$_3$) of α, α'- bisallyloxy functionalized polystyrene.

Molecular weights calculated from NMR ($M_{n,\text{NMR}}$) were in good agreement with the molecular weights calculated theoretically ($M_{n,\text{theo}}$) considering monomer to initiator feed ratio. Gel permeation chromatograms of polystyrenes revealed the monomodal curves with dispersity in the range 1.05-1.09. Typical GPC trace for polystyrene ($M_{n,\text{GPC}}$- 4800 g mol^{-1},

Dispersity-1.05, Run 1. Table 2.1) is reproduced in Figure 2.4. Initiator efficiency was calculated by taking the ratio of theoretical molecular weight to the molecular weight determined from ^{1}H-NMR spectroscopy which takes into account the contribution of initiator molecular weight to the overall molecular weight of polymer. Initiator efficiency, thus determined, was found in the range 0.80-0.95.
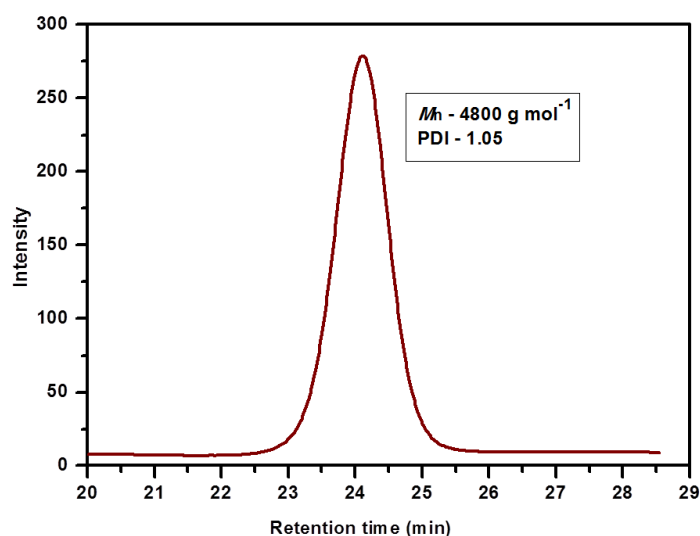
Figure 2.4 Typical GPC trace for α, α'- bisallyloxy functionalised polystyrene ($M_{n,GPC}$- 4800 g mol^{-1}, Dispersity-1.05, Table 2.1, Run 1).

2.3.3 Kinetics of ATRP of styrene

The kinetic study of styrene polymerization employing ATRP initiator **3** was performed. The percentage conversion of monomer was determined gravimetrically. The linear relationship between $\ln(M_o/M_t)$ (where M_o- initial monomer concentration and M_t - monomer concentration at time t) and polymerization time was observed indicating the constant number of growing polymer chains throughout the polymerization reaction and pseudo first order kinetics (**Figure 2.5**).
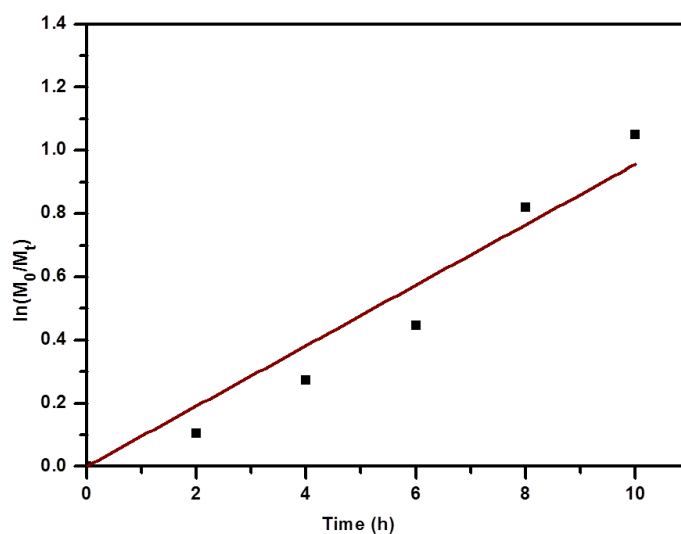
Figure 2.5 Relationship of $\ln[M_0/M_t]$ and polymerization time for ATRP of styrene at 80 °C in toluene.

The linear dependence of molecular weight with percentage conversions and dispersity below 1.11 showed the controlled polymerization behaviour (**Figure 2.6**) and also suggests the absence of significant chain transfer reactions after initiation process of polymerization.
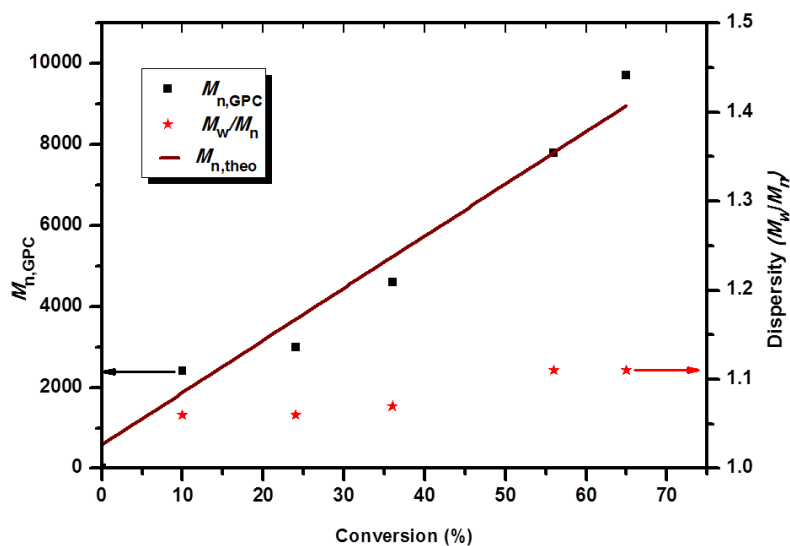
Figure 2.6 Dependence of number average molecular weight ($M_{n,GPC}$) and dispersity on monomer conversion for ATRP of styrene at 80 °C in toluene.

GPC traces of each aliquot were monomodal and Gaussian and showed the increase of molecular weight with polymerization time as an additional support for controlled behavior (**Figure 2.7**).
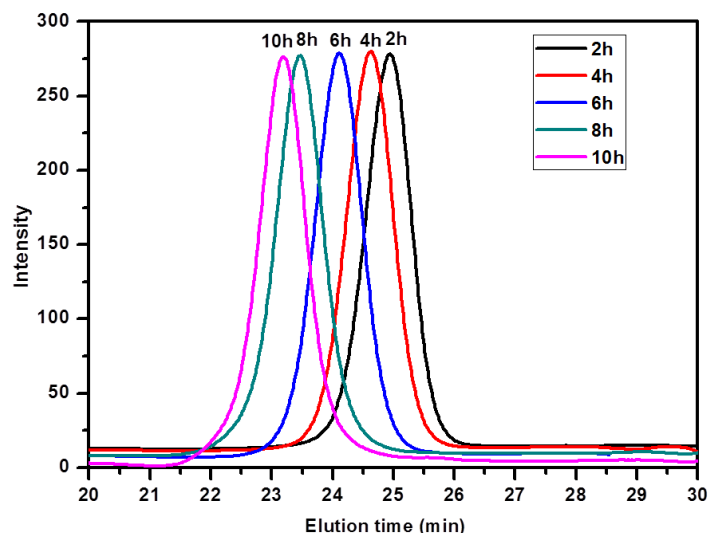
Figure 2.7 Progress of molecular weight of α, α'- bisallyloxy functionalised polystyrene with polymerization time.

MALDI-TOF spectrum of polystyrene (**Figure 2.8**) obtained from the first fraction of kinetic run showed the peak difference equal to molecular weight of styrene monomer and PDI below 1.06 indicating the absence of side reactions during polymerization.

Thus, 2-(1, 1-bis(4-(allyloxy)phenyl)-3-oxoisoindolin-2-yl)ethyl 2-bromo-2-methylpropanoate was found to be an efficient initiator for ATRP of styrene.
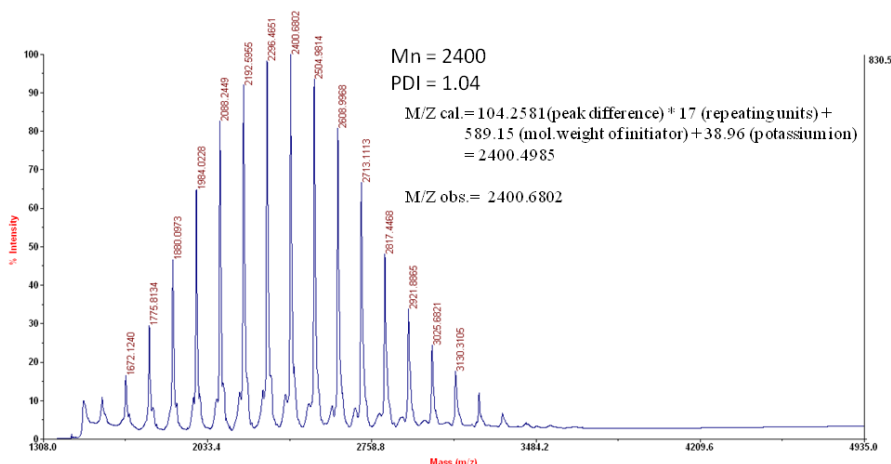
Figure 2.8 MALDI-TOF spectrum of α, α'- bisallyloxy functionalised polystyrene (The sample used was from the first fraction of kinetic run).

2.3.4 Photochemical thiol-ene click reaction

Polymers terminated with allyl functional groups are of great interest as allyl group is capable of undergoing interesting chemical transformations including the well known thiol-ene click reaction. Bis-allyloxy functionality was intentionally incorporated into the polymer to exploit its reactivity with thiols by performing the photochemical thiol-ene click reaction. A model reaction was performed by irradiating the mixture of polystyrene ($M_{n,GPC}$- 4800 g mol^{-1}, Dispersity-1.05), benzyl mercaptan and DMPA catalyst in photochemical reactor at 365 nm wavelength at room temperature (**Scheme 2.3**).

Where 4a, R = Ph−CH₂−
4b, R = HO−CH₂·CH₂−
4c, R = HOOC−CH₂·CH₂−
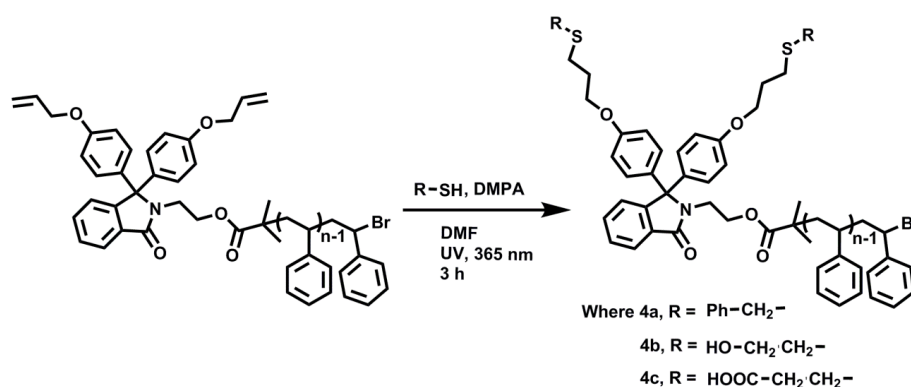
Scheme 2.3 Photochemical thiol-ene click reaction of α, α'- bisallyloxy functionalised polystyrene with benzyl mercaptan (**4a**), 2-mercaptoethanol (**4b**) and 3-mercaptopropionic acid (**4c**).

^{1}H-NMR spectrum of product after click reaction (**4a**) showed the singlets at 7.29 ppm and 3.70 ppm due to phenyl ring and benzylic protons of mercaptan, respectively. Disappearance of peaks corresponding to allyl protons revealed the successful completion of thiol-ene click reaction (**Figure 2.9**). The peaks corresponding to backbone and aromatic ring of polystyrene after the click reaction were found to be intact.

The allyl groups can further be converted to various other functional groups useful for step-growth polymerizations by using functional thiols. A myriad of functional thiols are commercially available for instance, thioglycolic acid, 3-mercaptopropionic acid, 2-mercaptoethanol, 1-thioglycerol, 2-aminoethanol, etc.[49, 50] Thiol-ene click reaction was exploited successfully to introduce other reactive functional groups such as hydroxyl and carboxyl by performing the click reaction of bis-allyloxy functionalised polystyrene with 2-mercaptoethanol (**4b**) and 3-mercaptopropionic acid (**4c**), respectively (**Scheme 2.3**). α, α'-Dihydroxyl and α, α'-dicarboxyl functionalised polystyrene macromonomers, thus

obtained, represent valuable precursors for the synthesis of graft, miktoarm star copolymers and are potentially useful macromonomers for step-growth polymerizations.
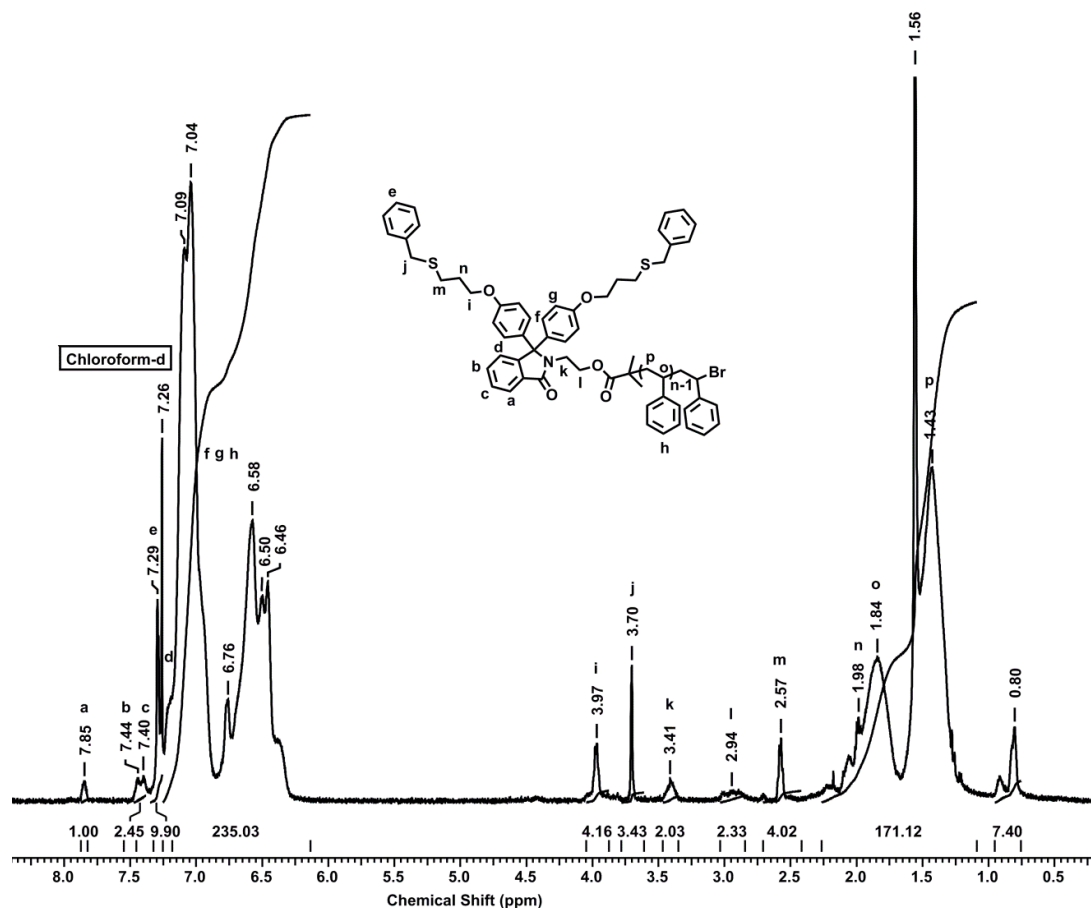
Figure 2.9 ^{1}H-NMR spectrum (in CDCl$_3$) of product obtained by click reaction of α, α'-bisallyloxy functionalised polystyrene with benzyl mercaptan (**4a**).

Polymerization of α,α'-bisallyloxy functionalised polystyrene with a low molecular weight dithiol / thiol-terminated telechelic polymers or with a hydride- terminated telechelic polysiloxane to obtain graft copolymers would be of great interest. Polymers with allyl group can further undergo the efficient reactions such as radical oligomerization, epoxidation, oxidation to diols, hydrosilylation and hydroboration and hence is recognized as a valuable functional group.[51, 52] Thermally or photo-chemically induced cross-linking of the reactive functional group like allyl into the corresponding networked polymers are practically important due to the improvement of thermal stability, mechanical strength and solvent resistance of the resulting polymers.[51] Furthermore, the ring closing metathesis

reaction[53] of allyl functionalised polystyrene can result in networked polymers which are applicable in various fields like surface science and coatings.

2.4 Conclusions

Starting from phenolphthalein as a commercially available cheap precursor, a new ATRP initiator, namely, 2-(1,1-bis(4-(allyloxy)phenyl)-3-oxoisoindolin-2-yl)ethyl 2-bromo-2-methylpropanoate was conveniently synthesized and was employed as an initiator for polymerization of styrene. The notable features of ATRP initiator synthesized in the present work are: 1) utilization of commercially available and inexpensive starting material, namely, phenolphthalein, 2) convenient synthetic methodology and 3) relatively less explored allyloxy functionality which possesses distinct advantages in terms of its reactivity. Well-defined and narrow dispersity α, α' bis-allyloxy functionalised polystyrene macromonomers were synthesized. The kinetic study of polymerization revealed the pseudo first order kinetics. Molecular weight of polystyrene from MALDI-TOF was found to be in good agreement with that determined by GPC. The reactivity of terminal allyl groups for thiol-ene click reaction was demonstrated by performing the model reaction with benzyl mercaptan as a thiol reagent. α,α'-Dihydroxyl and α,α'-dicarboxyl functionalised polystyrene macromonomers were successfully synthesized by reaction of α,α'-bisallyloxy functionalised polystyrene macromonomers with 2-mercaptoethanol and 3-mercaptopropionic acid, respectively. The present approach opens up new avenues for design and synthesis of phenolphthalein-based ATRP initiators containing other useful functional groups and corresponding polymers therefrom.

2.5 References

1. B. Guillerm, S. Monge, V. Lapinte and J. J. Robin, *J. Polym. Sci. Part A: Polym. Chem.*, 2012, **51**, 1118-1128.

2. O. Glaied, C. Delaite and S. Bistac, *Polym. Int*, 2014, **63**, 703-708.

3. V. Raghunadh, D. Baskaran and S. Sivaram, *Polymer*, 2004, **45**, 3149-3155.

4. H. Wang, J. He, M. Zhang, Y. Tao, F. Li, K. C. Tam and P. Ni, *J. Mater. Chem. B*, 2013, **1**, 6596-6607.

5. T. Cai, M. Li, K. G. Neoh and E. T. Kang, *J. Mater. Chem.*, 2012, **22**, 16248-16258.

6. M. W. M. Fijten, C. Haensch, B. M. V. Lankvelt, R. Hoogenboom and U. S. Schubert, *Macromol. Chem. Phys*, 2008, **209**, 1887-1895.

7. C. Li, Z. Ge, H. Liu and S. Liu, *J. Polym. Sci. Part A: Polym. Chem.*, 2009, **47**, 4001-4013.

8. Y. Y. Yuan, Y. C. Wang, J. Z. Du and J. Wang, *Macromolecules*, 2008, **41**, 8620-8625.

9. Y. Zhang, H. Liu, J. Hu, C. Li and S. Liu, *Macromol. Rapid Commun.*, 2009, **30**, 941-947.

10. B. Gacal, H. Durmaz, M. A. Tasdelen, G. Hizal, U. Tunka, Y. Yagci and A. L. Demirel, *Macromolecules*, 2006, **39**, 5330-5336.

11. T. X. Lav, P. Lemechko, E. Renard, C. Amiel, V. Langlois and G. Volet, *React. Funct. Polym.*, 2013, **73**, 1001-1008.

12. M. Ye, D. Zhang, L. Han, J. Tejada and C. Ortiz, *Soft Matter*, 2006, **2**, 243-256.

13. D. Zhang and C. Ortiz, *Macromolecules*, 2004, **37**, 4271-4282.

14. K. Zhang, Y. Wang, W. Zhu, X. Li and Z. Shen, *J. Polym. Sci. Part A: Polym. Chem.*, 2012, **50**, 2045-2052.

15. M. Bauer, S. Schroeder, L. Tauhardt, K. Kempe, U. S. Schubert and D. Fischer, *J. Polym. Sci. Part A: Polym. Chem. *, 2013, **51**, 1816-1821.

16. M. Martina and D. W. Hutmacher, *Polym. int.*, 2007, **56**, 145-157.

17. P. Singh, A. Srivastava and R. Kumar, *J. Polym. Sci. Part A: Polym. Chem.*, 2012, **50**, 1503-1514.

18. J. H. Lee, Y. C. An, D. S. Choi, M. J. Lee, K. M. Kim and J. H. Lim, *Macromol. Symp.*, 2007, **249-250**, 307-311.

19. K. Satoh, J. E. Poelma, L. M. Campos, B. Stahl and C. J. Hawker, *Polym. Chem.*, 2012, **3**, 1890-1898.

20. M. A. Tasdelen, M. U. Kahveci and Y. Yagci, *Prog. Polym. Sci.*, 2011, **36**, 455-567.

21. N. Eschweiler, H. Keul, M. Millaruelo, R. Weberskirch and M. Moeller, *Polym. Int.*, 2014, **63**, 114-126.

22. V. K. Patel, N. K. Vishwakarma, A. K. Mishra, C. S. Biswas, P. Maiti and B. Ray, *J. Appl. Polym. Sci.*, 2013, **127**, 4305-4317.

23. K. Matyjaszewski, *Macromolecules*, 2012, **45**, 4015-4039.

24. K. Matyjaszewski and J. Xia, *Chem. Rev.*, 2001, **101**, 2921-2990.

25. G. J. Summers, M. P. Ndawuni and C. A. Summers, *Polym. Int.*, 2014, **63**, 876-886.

26. X. Yang, S. Wang, Y. Yan, Y. Wu, K. Zheng and Y. Chen, *Polymer*, 2014, **55**, 1128-1135.

27. G. S. Moro, J. Percino, M. Ceron, A. Banuelos, V. M. Chapela and M. E. Castro, *Macromol. Symp.*, 2014, **339**, 112-121.

28. C. Li, J. Hu, J. Yin and S. Liu, *Macromolecules*, 2009, **42**, 5007-5016.

29. D. Colak, L. Clanga, A. E. Muftuoglu and Y. Yagci, *J. Polym. Sci. Part A: Polym. Chem.*, 2006, **44**, 727-743.

30. G. J. Summers, Maseko, R. B. and C. A. Summers, *Polym. Int.*, 2014, **63**, 1785-1796.

31. G. J. Summers, M. P. Ndawuni and C. A. Summers, *Polym. int.*, 2012, **61**, 1353-1361.

32. Y. Wang, L. Lu, H. Wang, D. Lu, K. Tao and R. Bai, *Macromol. Rapid Commun.*, 2009, **30**, 1922-1927.

33. C. Boyer, A. H. Soeriyadi, P. J. Roth, M. R. Whittaker and T. P. Davis, *Chem. Commun.*, 2011, **47**, 1318-1320.

34. J. A. Opsteen and J. C. M. V. Hest, *Chem. Commun.*, 2005, 57-59.

35. G. Volet, T. X. Lav, J. Babinot and C. Amiel, *Macromol. Chem. Phys.*, 2011, **212**, 118-124.

36. R. Matmour, L. B, T. J. Joncheray, R. J. Elkhouri, D. Taton and R. S. Duran, *Macromolecules*, 2005, **38**, 5459-5467.

37. L. Z. Kong, M. Sun, H. M. Qiao and C. Y. Pan, *J. Polym. Sci. Part A: Polym. Chem.*, 2010, **48**, 454-462.

38. S. Yurteri, I. Cianga and Y. Yagci, *Macromol. Chem. Phys.*, 2003, **204**, 1771-1783.

39. G. Chen, L. Tao, G. Mantovani, V. Ladmiral, D. P. Burt, J. V. Macpherson and D. M. Haddleton, *Soft Matter*, 2007, **3**, 732-739.

40. N. Rocha, P. V. Mendonca, J. P. Mendes, P. N. Simoes, A. V. Popov, T. Guliashvili, A. C. Serra and J. F. J. Coelho, *Macromol. Chem. Phys.*, 2013, **214**, 76-84.

41. L. Hou, S. Lin, F. Liu, J. Hu, G. Zhang, G. Liu, Y. Tu, H. Zou and H. Luo, *New J. Chem.*, 2014, **38**, 2538-2547.

42. G. Mantovani, F. Lecolley, L. Tao, D. M. Haddleton, J. Clerx, J. J. L. M. Cornelissen and K. Velonia, *J. Am. Chem. Soc.*, 2005, **127**, 2966-2973.

43. H. Zhang, B. Klumperman and R. V. D. Linde, *Macromolecules*, 2002, **35**, 2261-2267.

44. U. Mansfeld, C. Pietsch, R. Hoogenboom, C. R. Becer and U. S. Schubert, *Polym. Chem.*, 2010, **1**, 1560-1598.

45. P. S. Sane, D. V. Palaskar and P. P. Wadgaonkar, *Europ. Polym. Journal*, 2011, **47**, 1621-1629.

46. P. S. Sane, B. V. Tawade, I. Parmar, S. Kumari, S. Nagane and P. P. Wadgaonkar, *J. Polym. Sci. Part A: Polym. Chem.*, 2013, **51**, 2091-2103.

47. P. S. Sane, B. V. Tawade, D. V. Palaskar, S. K. Menon and P. P. Wadgaonkar, *React. Funct. Polym.*, 2012, **72**, 713-721.

48. Q. Zhang, F. Gong, S. Zhang and S. Li, *J. Membr. Sci.*, 2011, **367**, 166-173.

49. C. E. Hoyle and C. N. Bowman, *Angew. Chem. Int. Ed.*, 2010, **49**, 1540-1573.

50. L. M. Campos, K. L. Killops, R. Sakai, J. M. J. Paulusse, D. Damiron, E. Drockenmuller, B. W. Messmore and C. J. Hawker, *Macromolecules*, 2008, **41**, 7063-7070.

51. H. Oie, A. Sudo and T. Endo, *J. Polym. Sci. Part A: Polym. Chem.*, 2013, **51**, 2035-2039.

52. C. Zona, G. D. Orazio and B. L. Ferla, *Synlett.*, 2013, **24**, 709-712.

53. S. L. Elmer and S. C. Zimmerman, *J. Org. Chem.*, 2004, **69**, 7363-7366.

Chapter 3

(Poly(ethylene glycol))$_2$-Poly(ε-caprolactone) and Poly(ε-caprolactone)-Poly(*N*-isopropylacrylamide)-Poly(ethylene glycol) Star Copolymers by the Combination of ROP, ATRP and Coupling Reactions

3.1 Introduction

Amphiphilic macromolecular architectures such as star copolymers are considered as versatile materials and have attracted the significant attention for applications as rheology modifiers,[1] emulsifiers,[2] compatibilisers in blends,[3, 4] controlled and targeted drug delivery systems[5-8] and stimuli responsive materials[9-12] in biomedical, pharmaceutical, tissue engineering and surface sciences.[13] Miktoarm star copolymers are interesting class of synthetic polymer architectures as they form unique self assemblies due to different phase separation behaviours of various arms attached at a common junction point and their nanostructures possess higher drug loading capacities compared to their linear counterparts.[14, 15] Biodegradable synthetic miktoarm star copolymers mimic the structures of natural polymers and their assembled structures are widely used as potential gene and drug delivery vehicles.[16, 17] The chemical properties of miktoarm star copolymers can be tailored by varying the nature and arm lengths of copolymer.[18] Recent advances in polymer synthesis have made possible the development of sophisticated and efficient synthetic strategies to obtain functional materials and different macromolecular architectures. There are four widely used approaches for precise synthesis of star/miktoarm star copolymers: A) "Core First" approach- multifunctional initiator core is designed first and polymers are grown outwards by controlled polymerization techniques such as atom transfer radical polymerization (ATRP),[19] ring opening polymerization (ROP),[20] nitroxide-mediated radical polymerization (NMP)[21] or reversible addition-fragmentation chain transfer (RAFT)[22] to synthesize star copolymers with different arms.[23-25] The number of arms in the star copolymer depends on the number of different orthogonal initiating sites in the multifunctional initiator core.[26] B) "Arm First" approach- macroinitiators synthesized by different controlled radical polymerization (CRP) techniques are tied at a common junction point.[27, 28] C) "Coupling Onto" approach- multifunctional core is designed first and different functional polymers synthesized by CRP techniques are coupled onto the multifunctional core by some efficient, high yielding reactions such as "click reaction". These efficient reactions should be orthogonal to each other so as to get high yields of the final star copolymer.[29, 30] Yagci *et al* demonstrated the success of this approach by synthesizing ABC miktoarm star terpolymer by orthogonal triple click chemistry.[31] D) "Core First-Coupling Onto" approach- multifunctional initiator core containing polymerization initiating sites and efficient reactive groups is designed. Polymers are

grown outwards first and then on the multifunctional polymer the different orthogonal efficient reactions are performed to couple the functional polymers or vice-versa.[32, 33] Of these approaches, "Core first-Coupling Onto" approach has been considered as reliable and is widely used to construct miktoarm star copolymers due to its exceptional tolerance towards a variety of functional groups present on the core and different reaction conditions.[34] The combinations of controlled polymerization methods *viz.* ATRP, ROP, NMP or RAFT and consecutive reactions such as, copper catalysed alkyne-azide reaction, Diels-Alder reaction, thiol-ene reaction, etc. have been exploited for the precise and modular synthesis of various macromolecular architectures by taking advantages offered by these techniques.[34-40]

Star copolymers bearing poly(ε-caprolactone) arms are mostly focused due to their different phase separation behaviours[41] and special attention has been given to the assemblies obtained from thermoresponsive star copolymers containing PCL which makes them the suitable candidates for biomedical applications such as drug delivery, sensors, gene delivery and stimuli responsive materials.[42, 43] The introduction of poly(ethylene glycol) and thermoresponsive poly(*N*-isopropylacrylamide) blocks on PCL preserves the biocompatibility and biodegradability of PCL and also these polymers are less cytotoxic hence the star copolymers obtained from these systems are considered as suitable for biological applications.[5, 18, 44] PCL-PNIPAAm$_2$ and PEG$_2$-PCL star copolymers have already been reported in the literature and their cell study showed less cytotoxicity and these polymers are found to be biocompatible.[14] Junkers and coworkers have reported the synthesis of biodegradable star copolymers *via* RAFT copolymerization of methyl methacrylate with cyclic ketene acetal.[45]

Polymers with reactive groups such as allyl,[46] propargyl,[47] azido,[48, 49] maleimide,[50] anthracene,[51] or 4-dibenzocyclooctynol[52] at the terminal position were synthesized using appropriate functional initiator and their consecutive click reactions were exploited to obtain different macromolecular architectures. The post-polymerization modification of polymers with multiple functionalities requires the chemistry that is orthogonal which does not interfere with each other during transformations.[53, 54] Yagci et.al reported the use of thiol-ene and CuAAC double click reaction strategy to synthesize PS-PCL-PEG miktoarm star terpolymer.[55] Diels-Alder and CuAAC are widely used orthogonal click reactions for the synthesis of miktoarm star copolymers.[56] However, thiol-ene and CuAAC orthogonal

reactions are scarcely used for this purpose. Our group previously reported the synthesis of α, α'- hetero-bifunctionalised poly(ε-caprolactone)s containing clickable aldehyde and allyloxy groups.[57] In continuation of our work on functional polymers by ROP, we report herein the synthesis of α-allyl, α'-allyloxy and α-allyl, α'-propargyloxy bifunctionalised poly(ε-caprolactone)s and their potential utility for preparation of miktoarm star copolymers using orthogonal chemistry approach.

Towards this end, two new ROP initiators, namely, (3-allyl-2-(allyloxy)phenyl)methanol and (3-allyl-2-(prop-2-yn-1-yloxy)phenyl)methanol containing allyl, allyloxy and allyl, propargyloxy functional groups, respectively, were synthesized from commercially available 3-allylsalicyaldehyde as a starting material. Well defined α-allyl, α'-allyloxy and α-allyl, α'-propargyloxy bifunctionalised poly(ε-caprolactone)s were synthesized with controlled molecular weights in the range 4200-9500 and 3600-10900 g mol^{-1}, respectively, and dispersity in the range 1.16-1.18 and 1.15-1.16, respectively, by varying the monomer to initiator feed ratios employing these ROP initiators. The presence of these reactive functionalities on the polymers was confirmed by FT-IR, NMR spectroscopy and MALDI-TOF analysis. Furthermore, the usefulness of diallyl functionalities in α-allyl, α'-allyloxy bifunctionalized PCL was demonstrated by thiol-ene reaction with poly(ethylene glycol) thiol (mPEG-SH) to synthesize (mPEG)$_2$-PCL star copolymer. α-Allyl, α'-propargyloxy functionalities in α-allyl, α'-propargyloxy bifunctionalized PCL were utilised in orthogonal reactions i.e sequential CuAAC with azido functionalised Poly(NIPAAm) followed by thiol-ene reaction with mPEG-SH, respectively, to synthesize PCL-PNIPAAm-mPEG miktoarm star terpolymer. The preliminary characterization of (mPEG)$_2$-PCL and PCL-PNIPAAm-mPEG star copolymers was performed by NMR spectroscopy and GPC. The issues encountered with utility of thiol-ene chemistry for polymer-polymer conjugation reactions have been highlighted.

Temperature dependence of size and morphological changes of assemblies of PCL-PNIPAAm-mPEG star copolymer were studied under the conditions of varying temperature. Temperature dependant pyrene release kinetics from micelles of PCL-PNIPAAm-mPEG star copolymer showed faster release with increasing temperature.

3.2 Experimental Section

3.2.1 Materials

3-Allylsalicyaldehyde (97 %), propargyl bromide (80 wt. % in toluene) and tin(II) 2-ethylhexanoate (95 %) were purchased from Sigma Aldrich (St. Louis, Missmouri, USA) and were used as received. ε-Caprolactone (99 %, Sigma Aldrich, St. Louis, Missmouri, USA) was stirred over calcium hydride overnight and distilled prior to use and stored over Linde type (4 A^o) molecular sieves. Allyl bromide (98 %, Loba Chemie, Mumbai, India) was used as received. Acetone was stirred over potassium carbonate and distilled before use. Potassium carbonate (99 %, Fischer Scientific, Mumbai, India) and potassium iodide (99.8 %, Thomas Baker, Mumbai, India) were dried before use. Sodium borohydride (99 %, Thomas Baker, Mumbai, India) and 18-crown-6 (99 %, Alfa Aesar, Heysham, England) were used as received. *N, N*-Dimethylformamide (DMF) was stirred over calcium hydride and distilled under reduced pressure. *N*-Isopropylacrylamide (99 %, Sigma Aldrich) was recrystallised from n-hexane and dried prior to use. α-Bromoisobutyryl bromide (98 %, Steinheim, Germany) and 2, 2-dimethoxy-2-phenyl-acetophenone (DMPA) (99 %, Sigma Aldrich) were used as received. Triethylamine (99 %, Spectrochem, Mumbai, India) was stirred over potassium hydroxide overnight and distilled before use. Copper bromide (99.99 %, Missmouri, USA) was stirred in acetic acid, filtered, washed with ethanol and dried at 70 ^{o}C for 6 h. 4-Amino phenol (98 %, Avra, Hyderabad, India) was purified by sublimation under reduced pressure. Sodium azide (99.5 %, Thomas Baker, Mumbai, India), 2-chloroethanol (99 %, Spectrochem, Mumbai, India), methane sulphonyl chloride (98 %, Spectrochem, Mumbai, India), sodium hydrosulfide hydrate (Sigma Aldrich, Missmouri, USA) and DL-dithiothreitol (99 %, Himedia, Mumbai, India) were used as received. Thiol functional poly(ethylene glycol) was synthesized as per the reported procedure with some modifications.[58] *N,N,N',N',N'',N''*-Hexamethyl-[tris(aminoethyl)amine] (Me6TREN) was synthesized by methylation of tris(2-aminoethyl)amine (TREN) as reported in the literature.[59]

3.2.2 Characterization and Measurements

FT-IR spectra were recorded on Perkin Elmer Spectrum GX spectrophotometer using chloroform as a solvent. NMR spectra were recorded on Bruker- 400 or 500 MHz spectrometers in CDCl$_3$ as a solvent and TMS as an internal reference. Melting points of

solid compounds were determined on electrothermal MEL-TEMP apparatus at 230 volt potential. Photochemical thiol-ene reaction on the polymers was performed inside the photochemical reactor equipped with a Hanovia made mercury lamp at 365 nm wavelength and 450 Watt power equipped with a water circulation pump.

3.2.3 Polymer characterization

3.2.3.1 Gel permeation chromatography

Molecular weights and dispersity of poly(ε-caprolactone)s were determined by gel permeation chromatography (GPC) equipped with Viscotek VE-3580 RI and Viscotek VE-3210 UV/VIS detectors and Viscotek VE-1122 pump using 1 mg/mL of polymer sample in tetrahydrofuran (Merck, Lichrosolv) as an eluent at flow rate of 1 mL/min and narrow dispersity polystyrenes as calibration standards with detector and column temperatures at 35 ^{o}C. Sample injection volume for GPC analysis was fixed at 100 μL.

3.2.3.2 MALDI-TOF analysis

Matrix assisted laser desorption ionisation - time of flight (MALDI-TOF) spectrum acquisition was recorded on AB-SCIEX TOF/TOF 5800 instrument with 4500 laser intensity and reflector positive operating method in tetrahydrofuran as a solvent using dithranol (5 volume equivalent with polymer) as a matrix and 1 mg/mL concentration of poly(ε-caprolactone) at 20 ^{o}C. Polymer samples were characterized to determine the end functionalities by spotting the mixture of 4 μL polymer sample (1 mg/mL) with 20 μL of dithranol (10 mg/mL) as matrix and 1 μL of sodium iodide as an ionizing agent (0.2 g/mL) on a metal target plate. Mass range was selected between 2000-5000 g mol^{-1} during MALDI-TOF acquisitions on the basis of molecular weights previously determined from ^{1}H-NMR spectroscopy. Molecular weights and dispersity were also determined from MALDI-TOF analysis. In order to get accurate results, average peak difference of all the peaks were considered and all the calculations were performed by considering four digits after the decimal point. MALDI-TOF MS analysis of initiator was performed by spotting the mixture of 4 μL of sample (1 mg/mL) with 20 μL of HABA (10 mg/mL) as a matrix and 1 μL of sodium iodide as an ionising agent (0.2 g/mL) in THF as a solvent.

3.2.4 Synthesis

3.2.4.1 Synthesis of 3-allyl-2-(allyloxy)benzaldehyde (1)

Into a 100 mL two necked round bottom flask equipped with a mechanical stirrer, a gas inlet and a reflux condenser were charged 3-allylsalicyaldehyde (2.0 g, 12.33 mmol), potassium carbonate (3.41 g, 24.66 mmol), potassium iodide (0.20 g, 1.23 mmol), 18-crown-6 (0.33 g, 1.23 mmol) and acetone (50 mL). The solution of allyl bromide (2.98 g, 24.66 mmol) in acetone (10 mL) was added at room temperature and the reaction mixture was refluxed for 3 h, filtered through a small bed of celite and solvent was removed. The residue was dissolved in chloroform and washed with water (3×100 mL), the combined organic layer was evaporated. The crude product was purified by column chromatography using petroleum ether: ethyl acetate (96:04, v/v) as an eluent to afford 2.3 g, (92 %) of 3-allyl-2-(allyloxy)benzaldehyde as a colourless liquid.

IR (CHCl$_3$, cm^{-1}): 3081 (=C–H), 1688 (–C=O of aldehyde) and 1638 (–C=C– of allyl).

^{1}H-NMR (400 MHz, CDCl$_3$, δ/ppm): 10.36 (s, 1H aldehyde), 7.73 (d, 1H), 7.47 (d, 1H), 7.19 (t, 1H), 6.14-6.03 (m, 1H), 6.03-5.92 (m, 1H), 5.46-5.28 (m, 2H), 5.15-5.05 (m, 2H), 4.46 (d, 2H), 3.47 (d, 2H).

^{13}C-NMR (125 MHz, CDCl$_3$, δ/ppm): 190.33, 160.0, 136.84, 136.31, 134.43, 132.59, 129.64, 126.99, 124.57, 118.58, 116.56, 77.50, 33.33.

3.2.4.2 Synthesis of 3-allyl-2-(prop-2-yn-1-yloxy)benzaldehyde (2)

Into a 100 mL two necked round bottom flask equipped with a mechanical stirrer, a gas inlet and a reflux condenser were charged 3-allylsalicyaldehyde (2.0 g, 12.33 mmol), potassium carbonate (3.41 g, 24.66 mmol), potassium iodide (0.20 g, 1.23 mmol), 18-crown-6 (0.33 g, 1.23 mmol) and acetone (50 mL). The solution of propargyl bromide (2.93 g, 3.6 mL, 24.66 mmol) in acetone (10 mL) was added at room temperature and the reaction mixture was refluxed for 2 h, filtered through a small bed of celite and solvent was removed. The residue was dissolved in chloroform and washed with water (3×100 mL), the combined organic layer was evaporated. The crude product was purified by column chromatography using petroleum ether: ethyl acetate (94:06, v/v) as an eluent to afford 2.2 g, (89 %) of 3-allyl-2-(prop-2-yn-1-yloxy)benzaldehyde as a colourless liquid.

IR (CHCl$_3$, cm^{-1}): 3295 (≡C–H), 3081 (=C–H), 2127 (–C≡C–), 1688 (–C=O of aldehyde) and 1638 (–C=C– of allyl).

^{1}H-NMR (400 MHz, CDCl$_3$, δ/ppm): 10.42 (s, 1H), 7.75 (d, 1H), 7.49 (d, 1H), 7.24 (t, 1H), 6.04-5.92 (m, 1H), 5.16-5.06 (m, 2H), 4.69 (d, 2H), 3.50 (d, 2H), 2.55 (t, 1H).

^{13}C-NMR (100 MHz, CDCl$_3$, δ/ppm): 190.40, 158.48, 136.88, 136.18, 134.43, 130.31, 127.21, 125.17, 116.76, 77.79, 77.32, 63.14, 33.39.

3.2.4.3 Synthesis of (3-allyl-2-(allyloxy)phenyl)methanol (3)

Into a 250 mL round bottom flask equipped with a mechanical stirrer were charged 3-allyl-2-(allyloxy)benzaldehyde (2 g, 9.89 mmol), methanol (80 mL) and water (20 mL). The reaction mixture was cooled to 0 ^{o}C and sodium borohydride (0.45 g, 11.87 mmol) was added portionwise over a period of 20 min. The reaction mixture was stirred for additional 2 h. Methanol was removed and the pH of suspension was adjusted to 4 by addition of dilute hydrochloric acid and the product was extracted into chloroform (3 × 50 mL). The combined organic layer was evaporated and the crude product was purified by column chromatography using petroleum ether: ethyl acetate (90:10, v/v) as an eluent to afford 1.9 g (94 %) of (3-allyl-2-(allyloxy)phenyl)methanol as a colourless liquid.

IR (CHCl$_3$, cm^{-1}): 3382 (O–H broad), 3081 (=C–H) and 1638 (–C=C– of allyl).

^{1}H-NMR (500 MHz, CDCl$_3$, δ/ppm): 7.23 (d, 1H), 7.16 (d, 1H), 7.09 (t, 1H), 6.05-6.15 (m, 1H), 5.92-6.04 (m, 1H), 5.15-5.50 (m, 2H), 5.0-5.15 (m, 2H), 4.72 (s, 2H), 4.39 (d, 2H), 3.44 (d, 2H), 2.25 (broad s, 1H, alcoholic OH)

^{13}C-NMR (100 MHz, CDCl$_3$, δ/ppm): 154.99, 136.94, 134.14, 133.60, 133.14, 130.13, 127.22, 124.43, 117.45, 115.95, 74.92, 61.31, 33.75.

3.2.4.4 Synthesis of (3-allyl-2-(prop-2-yn-1-yloxy)phenyl)methanol (4)

Into a 250 mL round bottom flask equipped with a mechanical stirrer were charged 3-allyl-2-(prop-2-yn-1-yloxy)benzaldehyde (2 g, 9.99 mmol), methanol (80 mL) and water (20 mL). The reaction mixture was cooled to 0 ^{o}C and sodium borohydride (0.45 g, 11.99 mmol) was added portionwise over a period of 20 min. The reaction mixture was stirred for additional 2 h. Methanol was removed and the pH of suspension was adjusted to 4 by addition of dilute hydrochloric acid and the product was extracted into chloroform (3×50 mL). The combined organic layer was evaporated and the crude product was purified by column chromatography using petroleum ether: ethyl acetate (92:08, v/v) as an eluent to afford 1.9 g (94 %) of (3-allyl-2-(prop-2-yn-1-yloxy)phenyl)methanol as a colourless liquid.

IR (CHCl$_3$, cm^{-1}): 3416 (O–H broad), 3304 (≡C–H), 2127 (–C≡C–) and 1638 (–C=C– of allyl).

^{1}H-NMR (500 MHz, CDCl$_3$, δ/ppm): 7.26 (d, 1H), 7.17 (d, 1H), 7.11 (t, 1H), 5.90-6.10 (m, 1H), 5.0-5.15 (m, 2H), 4.77 (d, 2H), 4.60 (d, 2H), 3.47 (d, 2H), 2.56 (t, 1H), 2.14 (broad t, 1H).

^{13}C-NMR (125 MHz, CDCl$_3$, δ/ppm): 154.75, 137.09, 134.71, 133.51, 130.70, 127.89, 125.30, 116.42, 79.25, 75.93, 61.97, 61.62, 34.22.

3.2.4.5 General procedure for synthesis of α,α'-homo and α,α'-hetero-bifunctionalised poly(ε caprolactone)s by ROP

Into a flame dried 100 mL Schlenk tube fitted with rubber septum, an argon inlet and a stir bar were charged ε-caprolactone (20 g, 175.22 mmol), tin(II) 2-ethylhexanoate (1.18 g, 2.92 mmol) and (3-allyl-2-(allyloxy)phenyl)methanol (**3**) / (3-allyl-2-(prop-2-yn-1-yloxy)phenyl)methanol (**4**) (5.84 mmol). The reaction mixture was purged with argon for 10 min and the Schlenk tube was immersed in an oil bath preheated at 95 ^{o}C and quenched after appropriate time by sudden cooling in the liquid nitrogen. The percentage conversion of the polymerization reaction was determined from ^{1}H-NMR spectroscopy by analysing the reaction mixture directly after quenching. The resultant poly(ε-caprolactone)s (**5a** and **5b**) were precipitated into the cold acidified methanol and filtered to afford white solid.

3.2.4.5.1 Synthesis of α-allyl, α'-allyloxy bifunctionalised poly(ε-caprolactone) (5a)

IR (CHCl$_3$, cm^{-1}): 3442 (–O–H broad) and 1730 (–C=O of ester).

^{1}H-NMR (400 MHz, CDCl$_3$, δ/ppm): 7.22 (d, 1H), 7.19 (d, 1H), 7.08 (t, 1H), 5.90-6.02 (m, 1H), 6.02-6.15 (m, 1H), 5.23-5.46 (m, 2H), 5.18 (s, 2H), 5.02-5.12 (m, 2H), 4.36 (d, 2H), 4.06 (t, –CH$_2$–O from poly(ε-caprolactone) backbone), 3.64 (t, 2H), 3.43 (d, 2H), 2.30 (t, –CH$_2$–CO from poly(ε-caprolactone) backbone), 1.53-1.73 (m, –CH$_2$–CH$_2$ from poly(ε-caprolactone) backbone), 1.31-1.45 (m, –CH$_2$–CH$_2$ from poly(ε-caprolactone) backbone).

3.2.4.5.2 Synthesis of α-allyl, α'-propargyloxy bifunctionalised poly(ε-caprolactone) (5b)

IR (CHCl$_3$, cm^{-1}): 3442 (–O–H broad) and 1730 (–C=O of ester)

^{1}H-NMR (500 MHz, CDCl$_3$, δ/ppm): 7.23 (d, 1H), 7.19 (d, 1H), 7.10 (t, 1H), 5.91-6.10 (m, 1H), 5.22 (s, 2H), 5.05-5.12 (m, 2H), 4.55 (d, 2H), 4.05 (t, –CH$_2$–O from poly(ε-caprolactone) backbone), 3.63 (t, 2H), 3.47 (d, 2H), 2.54 (t, 1H), 2.30 (t, –CH$_2$–CO from poly(ε-caprolactone) backbone), 1.59-1.68 (m, –CH$_2$–CH$_2$ from poly(ε-caprolactone) backbone), 1.33-1.42 (m, –CH$_2$–CH$_2$ from poly(ε-caprolactone) backbone).

3.2.4.6 Synthesis of thiol functional poly(ethylene glycol) (mPEG-SH)

Thiol functional poly(ethylene glycol) was synthesized by slight modifications in the reported procedure. [60]

3.2.4.6.1 Synthesis of α-mesyl poly(ethylene glycol) (mPEG-OMs)

Into a two necked round bottom flask equipped with a magnetic stirrer, a nitrogen inlet and an addition funnel were charged mPEG-OH (M_n-2100, Dispersity-1.09, 15 g, 7.14 mmol), triethylamine (1.44 g, 14.28 mmol) and dichloromethane (100 mL). The reaction mixture was cooled to 0 ^{o}C and to the solution was added dropwise methanesulfonyl chloride (1.63 g, 14.28 mmol) dissolved in dichloromethane (10 mL) over a period of 30 min. The reaction mixture was allowed to attain the room temperature and stirred for 8 h, filtered through celite, concentrated and the product was precipitated in cold diethyl ether to afford 15 g (95 %) mPEG-OMs as a white solid.

IR (CHCl$_3$, cm^{-1}): 1352 (–S=O), 1223 (–S=O) and 1112 (–C–O–).

^{1}H-NMR (500 MHz, CDCl$_3$, δ/ppm): 4.37 (t, 2H), 3.76 (t, 2H), 3.63 (s, O–CH$_2$ from PEG backbone), 3.54 (t, 2H, O–CH$_2$), 3.37 (s, 3H, O–CH$_3$), 3.08 (s, 3H, S–CH$_3$).

3.2.4.6.2 Synthesis of thiol functional poly(ethylene glycol) (mPEG-SH)

Into a two necked round bottom flask equipped with an argon inlet and a magnetic stirrer bar were charged mPEG-OMs (10 g, 4.56 mmol), sodium hydrosulfide hydrate (12.79 g, 228.31 mmol) and deionised water (100 mL). The reaction mixture was stirred for 40 min and then heated at 60 ^{o}C for 8 h under argon atmosphere. The reaction mixture was cooled, neutralised by adding dilute hydrochloric acid and product was extracted into dichloromethane (3×100 mL). The solvent was evaporated and the residue was precipitated in cold diethyl ether. The obtained product was dried and charged in a Schlenk tube containing THF (50 mL), purged for 30 min and DL-dithiothreitol (14.5 g, 94.06 mmol) was added as a reducing agent to cleave the possible disulfide linkage formed

during previous procedure. The reaction mixture was heated at 50 ^{o}C for 24 h and precipitated again into cold diethyl ether to obtain mPEG-SH (8.7 g, 92 %) as a white solid.

IR (CHCl$_3$, cm^{-1}): 2538 (–S–H) and 1102 (–C–O–).

^{1}H-NMR (400 MHz, CDCl$_3$, δ/ppm): 3.79 (t, 2H), 3.62 (s, PEG backbone), 3.35 (s, 3H, O–CH$_3$), 2.67 (dt, 2H, S–CH$_2$), 1.58 (t, 1H, –SH).

3.2.4.7 Thiol-ene reaction of α-allyl, α'-allyloxy bifunctionalised poly(ε-caprolactone) with mPEG-SH

A flame dried 10 mL pyrex tube fitted with a rubber septum and equipped with a magnetic stirrer bar was evacuated and refilled with argon and to the tube were charged **5a** (500 mg, 0.119 mmol), DMPA (12.2 mg, 0.4 eq.), mPEG-SH (5 g, 2.38 mmol) and DMF (10 mL). The reaction mixture was again purged for 30 min and sealed under argon and irradiated for 4 h inside the photochemical reactor at 365 nm wavelength. DMF was removed under reduced pressure. The reaction product was dissolved in THF (10 mL) and to the solution was added water (30 mL) dropwise. The solution was treated with DL-dithiothreitol (500 mg) in order to cleave disulfide linkage present in mPEG-S-S-mPEG formed as undesired product during thiol-ene reaction. The solution was dialysed against water using 2 KD dialysis bag to remove mPEG-SH. This procedure was repeated nine times to ensure complete cleavage of mPEG-S-S-mPEG to mPEG-SH and removal of mPEG-SH. The polymer solution was lyophilised to obtain (mPEG)$_2$-PCL miktoarm star copolymer (Yield - 88 %, $M_{n,NMR}$-9100 g mol^{-1}, Dispersity-1.19).

IR (CHCl$_3$, cm^{-1}): 1731 (–C=O of ester) and 1112 (–C–O–).

^{1}H-NMR (400 MHz, CDCl$_3$, δ/ppm): 7.22 (d, 1H), 7.19 (d, 1H), 7.08 (t, 1H), 5.16 (s, 2H), 4.05 (t, CH$_2$–O from poly(ε-caprolactone) backbone), 3.81 (t, 4H), 3.63 (s, O–CH$_2$ from PEG backbone), 3.55 (t, 4H), 3.37 (s, 6H, O-CH$_3$), 2.73 (t, 2H), 2.30 (t, CH$_2$–CO from poly(ε-caprolactone) backbone), 1.58-1.70 (m, –CH$_2$–CH$_2$ from poly(ε-caprolactone) backbone), 1.31-1.44 (m, –CH$_2$–CH$_2$ from poly(ε-caprolactone) backbone).

3.2.4.8 Synthesis of azido-functional poly(*N*-isopropylacrylamide) (PNIPAAm-N$_3$) by ATRP

Azido-functionalised PNIPAAm was synthesized using a new ATRP initiator, namely, 2-(4-azidophenoxy)ethyl 2-bromo-2-methylpropanoate, which in turn was

synthesized starting from 4-aminophenol.

3.2.4.8.1 Synthesis of 4-azido phenol

4-Azido phenol was synthesized by slight modifications in the reported procedure.[61] Into a 250 mL round bottom flask, 4-aminophenol (6 g, 54.98 mmol) was suspended in distilled water (150 mL) and concentrated HCl (13.5 mL) was added dropwise over the period of 10 min. The reaction mixture was cooled to 0 $^{\circ}$C and a solution of $NaNO_2$ (7.59 g, 109.96 mmol) in water (15 mL) was added dropwise and stirred for further 1 h at the same temperature. A solution of NaN_3 (4.29 g, 65.98 mmol) in water (45 mL) was then added portionwise and the reaction mixtue was allowed to attain the room temperature while stirring for 1 h. The product was extracted into ethyl acetate (3×100 mL) and the combined organic layer was evaporated to afford 6.82 g (92 %) of 4-azidophenol as a dark red liquid.

IR (CHCl$_3$, cm^{-1}): 3507 (–O–H, broad) and 2110 (–N$_3$).

^{1}H-NMR (400 MHz, Acetone-d$_6$, δ/ppm): 8.49 (s, 1H, phenolic O–H), 6.93 (d, 2H), 6.88 (d, 2H).

^{13}C-NMR (125 MHz, Acetone-d$_6$, δ/ppm): 154.98, 130.82, 120.02, 116.51.

3.2.4.8.2 Synthesis of 2-(4-azidophenoxy)ethan-1-ol

Into a 250 mL two necked round bottom flask equipped with a magnetic stir bar, an argon inlet and a reflux condenser were charged 4-azidophenol (4 g, 29.60 mmol), potassium carbonate (8.34 g, 59.20 mmol), potassium iodide (0.49 g, 2.96 mmol), 18-crown-6 (0.78 g, 2.96 mmol) and DMF (90 mL). The reaction mixture was stirred for 15 min at room temperature. The solution of 2-chloroethanol (4.79 g, 59.20 mmol) in DMF (10 mL) was added dropwise to the reaction mixture with constant stirring and the reaction mixture was heated at 80 $^{\circ}$C for 12 h. The reaction mixture was cooled, filtered and solvent was evaporated under reduced pressure. Ethyl acetate was added to the residue and washed with water (3×100 mL). The organic layer was evaporated and the crude product was purified by column chromatography using ethyl pet ether: acetate (88: 12, v/v) as an eluent to afford 3.71 g (70 %) of 2-(4-azidophenoxy)ethan-1-ol as a reddish oil.

IR (CHCl$_3$, cm^{-1}): 3404 (–O–H, broad) and 2110 (–N$_3$).

^{1}H-NMR (400 MHz, CDCl$_3$, δ/ppm): 6.96 (d, 2H), 6.91 (d, 2H), 4.07 (t, 2H), 3.96 (broad q, 2H).

^{13}C-NMR (100 MHz, CDCl$_3$, δ/ppm):156.01, 132.86, 120.06, 115.85, 69.59, 61.45.

3.2.4.8.3 Synthesis of 2-(4-azidophenoxy)ethyl 2-bromo-2-methylpropanoate

Into a 100 mL two necked round bottom flask equipped with a magnetic stirrer, an argon inlet and an addition funnel were charged 2-(4-azidophenoxy)ethan-1-ol (1 g, 5.58 mmol), triethylamine (1.13 g, 11.16 mmol) and dichloromethane (40 mL). The reaction mixture was cooled to 0 ^{o}C and the solution of α-bromoisobutyryl bromide (1.54 g, 6.69 mmol) in dichloromethane (10 mL) was added with constant stirring over a period of 30 min and allowed to attain room temperature and stirred overnight. The reaction mixture was filtered through a small bed of celite and washed with saturated sodium bicarbonate solution (3×100mL) and water (2×100 mL). The combined organic layer was evaporated and the crude product was purified by column chromatography using pet ether: ethyl acetate (98: 02, v/v) as an eluent to afford 1.70 g (93 %) of 2-(4-azidophenoxy)ethyl 2-bromo-2-methylpropanoate as a pale yellow solid.

Melting point - 46 ^{o}C.

IR (CHCl$_3$, cm^{-1}): 2110 (–N$_3$) and 1735 (–C=O of ester).

^{1}H-NMR (400 MHz, CDCl$_3$, δ/ppm): 6.95 (d, 2H), 6.91 (d, 2H), 4.51 (t, 2H), 4.20 (t, 2H), 1.94 (s, 6H).

^{13}C-NMR (125 MHz, CDCl$_3$, δ/ppm): 171.60, 155.81, 132.99, 120.02, 116.10, 66.08, 64.06, 55.41, 30.66.

3.2.4.8.4 Synthesis of azido-functional poly(*N*-isopropylacrylamide) (PNIPAAm-N$_3$) by ATRP

Into a 20 mL flame dried Schlenk tube fitted with a rubber septum and an argon inlet were charged 2-(4-azidophenoxy)ethyl 2-bromo-2-methylpropanoate (0.116 g, 0.35 mmol), *N*-isopropylacrylamide (6 g, 53.02 mmol), Me$_6$TREN (0.082 g, 0.35 mmol) and isopropanol (6 g). The reaction mixture was purged with argon while constant stirring for 20 min and then copper (I) bromide (0.051 g, 0.35 mmol) was added under the positive pressure of argon. After three vaccum freeze-pump-thaw cycles the Schlenk tube was allowed to attain the room temperature and stirred for appropriate time. The polymerization reaction was quenched by sudden cooling the Schlenk tube in liquid nitrogen with exposure to air. The solvent was removed under reduced pressure and the crude product was precipitated into cold n-hexane. The percentage conversion of the

reaction was determined by ^{1}H NMR spectroscopy. Polymer was purified by dissolving in THF and passed through a small bed of alumina column to remove the copper salts, concentrated, precipitated into cold diethyl ether, filtered and dried at 50 ^{o}C for 6 h (Yield 74 %, $M_{n,NMR}$-12400 g mol^{-1}, Dispersity-1.19).

IR (CHCl$_3$, cm^{-1}): 3305 (N–H), 2110 (azido) and 1636 (–C=O of amide).

^{1}H-NMR (400 MHz, CDCl$_3$, δ/ppm): 6.95 (broad d, 2H), 6.92 (broad d, 2H), 6.28 (broad peak from N–H of PNIPAAm), 4.37 (broad peak, 2H), 4.16 (broad peak, 2H), 4.0 (s, C–H from PNIPAAm), 1.2-2.5 (m, –CH$_2$ and –CH from PNIPAAm backbone), 1.14 (broad s, –CH$_3$ from PNIPAAm).

3.2.4.9 Orthogonal reactions of α-allyl, α'-propargyloxy bifunctionalised poly(ε-caprolactone) (5b) with PNIPAAm-N$_3$ and mPEG-SH

3.2.4.9.1 Alkyne-azide click reaction of α-allyl, α'-propargyloxy bifunctionalised poly(ε-caprolactone) (5b) with PNIPAAm-N$_3$

A flame dried 10 mL Schlenk tube fitted with a rubber septum and equipped with a magnetic stirrer bar was evacuated and refilled with argon and to the tube were charged **5b** (500 mg, 0.138 mmol), PNIPAAm-N$_3$ (2.06 g, 0.166 mmol), PMDETA (24 mg, 0.138 mmol) and tetrahydrofuran (5 mL). The reaction mixture was degassed twice by vacuum-freeze-pump thaw cycles. Copper bromide (19.9 mg, 0.138 mmol) was then added under the positive pressure of argon and stirred for 24 h at room temperature. The reaction mixture was passed through a small bed of alumina column to remove the copper residues, concentrated and dialysed against water using 12 KD dialysis bag to remove excess of PNIPAAm-N$_3$. The polymer solution was lyophilised to obtain allyl mid-functional PCL-*b*-PNIPAAm copolymer (Yield- 95 %, $M_{n,NMR}$-16400 g mol^{-1}, Dispersity-1.21).

IR (CHCl$_3$, cm^{-1}): 1731 (–C=O of ester) and 1636 (–C=O of amide).

^{1}H-NMR (400 MHz, CDCl$_3$, δ/ppm): 8.07 (s, 1H), 7.67 (d, 2H), 7.23 (d, 1H), 7.13 (t, 1H), 7.07 (d, 2H), 6.55 (broad peak from N–H of PNIPAAm), 5.92-6.03 (m, 1H), 5.23 (s, 2H), 5.05-5.12 (m, 2H), 5.09 (s, 2H), 4.42 (broad peak, 2H), 4.24 (broad peak, 2H), 4.05 (t, –CH$_2$–O from poly(ε-caprolactone) backbone), 3.98 (s, C–H from PNIPAAm), 3.63 (t, 2H), 3.51 (d, 2H), 2.29 (t, –CH$_2$–CO from poly(ε-caprolactone) backbone), 1.2-2.5 (m, –CH$_2$ and –CH from PNIPAAm backbone), 1.58-1.70 (m, –CH$_2$–CH$_2$ from poly(ε-caprolactone), 1.3-1.42 (m, –CH$_2$–CH$_2$ from poly(ε-caprolactone) backbone), 1.12 (broad

s, $-CH_3$ from PNIPAAm).

3.2.4.9.2 Thiol-ene reaction of allyl mid-functional PCL-b-PNIPAAm copolymer with mPEG-SH

A flame dried 10 mL pyrex tube fitted with a rubber septum and equipped with a magnetic stirrer bar was thoroughly purged with argon and to the tube were charged PCL-b-PNIPAAm copolymer (500 mg, 0.030 mmol), DMPA (1.56 mg, 0.2 eq.), mPEG-SH (640 mg, 0.30 mmol) and DMF (2 mL). The reaction mixture was again purged for 30 min and sealed under argon and irradiated for 4 h inside the photochemical reactor at 365 nm wavelength. DMF was removed under reduced pressure. The reaction product was dissolved in THF (2 mL) and to the solution was added water (6 mL) dropwise. The solution was treated with DL-dithiothreitol (64 mg) in order to cleave disulfide linkage present in mPEG-S-S-mPEG formed as undesired product during thiol-ene reaction. The solution was dialysed against water using 2 KD dialysis bag to remove mPEG-SH. This procedure was repeated nine times to ensure complete cleavage of mPEG-S-S-mPEG to mPEG-SH and removal of mPEG-SH. The polymer solution was lyophilised to obtain PCL-PNIPAAm-mPEG miktoarm star terpolymer (Yield- 89 %, $M_{n,NMR}$-18400 g mol^{-1}, Dispersity-1.23).

IR (CHCl$_3$, cm^{-1}): 1731 (–C=O of ester), 1640 (–C=O of amide) and 1112 (–C–O–).

^{1}H-NMR (500 MHz, CDCl$_3$, δ/ppm): 8.06 (s, 1H), 7.67 (broad peak, 2H), 7.23 (d, 1H), 7.13 (t, 1H), 7.08 (broad d, 2H), 7.07 (broad peak, 2H), 6.42 (broad peak from N–H of PNIPAAm), 5.23 (s, 2H), 5.10 (s, 2H), 4.42 (broad peak, 2H), 4.26 (broad peak, 2H), 4.05 (t, $-CH_2$–O from poly(ε-caprolactone) backbone), 3.99 (s, C–H from PNIPAAm), 3.77 (t, 2H), 3.63 (s, O–CH$_2$ from PEG backbone), 3.54 (broad t, 2H), 3.50 (broad t, 2H), 3.37 (s, 3H, O–CH$_3$), 2.73 (t, 2H), 2.30 (t, CH$_2$–CO from poly(ε-caprolactone) backbone), 1.2-2.5 (m, $-CH_2$ and –CH from PNIPAAm backbone), 1.54-1.72 (m, $-CH_2$–CH$_2$ from poly(ε-caprolactone) backbone), 1.3-1.48 (m, $-CH_2$–CH$_2$ from poly(ε-caprolactone) backbone), 1.13 (broad s, $-CH_3$ from PNIPAAm).

3.2.5 Preparation of polymer aqueous solution, dye encapsulation and release studies

The aqueous solution of polymer was prepared by direct dissolution in water for temperature dependant studies. Pyrene was encapsulated in a micellar solution by hydrating a film of pyrene (5×10^{-5} M) using 0.1 wt % aqueous polymer solution. After

stirring for 24 h, the polymer solution was filtered through 0.45 μm PVDF filter and was used for absorbance and release studies. The absorbance of pyrene encapsulated solution was measured at different time intervals by applying varying temperatures to determine the percentage release. The percent release of pyrene was determined based on the decrease in absorbance of encapsulated pyrene in the polymer solution. Rhodamine-B dye (5×10^{-6} M) was encapsulated in 0.1 wt % polymer solution in water and dialysed against water at 26 ^{o}C and 36 ^{o}C to remove non-encapsulated rhodamine-B. The absorbance of rhodamine-B encapsulated solution was measured at these temperatures.

3.3 Results and Discussion

3.3.1 Synthesis of new ROP initiators *viz.* (3-allyl-2-(allyloxy)phenyl)methanol (3) and (3-allyl-2-(prop-2-yn-1-yloxy)phenyl)methanol (4)

Two new ROP initiators, *viz.* (3-allyl-2-(allyloxy)phenyl)methanol (**3**) and (3-allyl-2-(prop-2-yn-1-yloxy)phenyl)methanol (**4**) were synthesized from commercially available 3-allylsalicyaldehyde as a starting material (**Scheme 3.1**). The reaction of 3-allylsalicyaldehyde with allyl bromide or propargyl bromide in the presence of potassium carbonate resulted into formation of 3-allyl-2-(allyloxy)benzaldehyde (**1**) and 3-allyl-2-(prop-2-yn-1-yloxy)benzaldehyde (**2**), respectively. The appearance of peaks at 1638 and 3081 cm^{-1} corresponding to allyl and allyloxy groups in **1** and at 1638, 3081 and at 2127 and 3295 cm^{-1} corresponding to allyl and propargyloxy groups, respectively, in **2** revealed the presence of corresponding functionalities. The presence of a peak at 1688 cm^{-1} in FT-IR spectra showed aldehyde functionality in **1** and **2**.
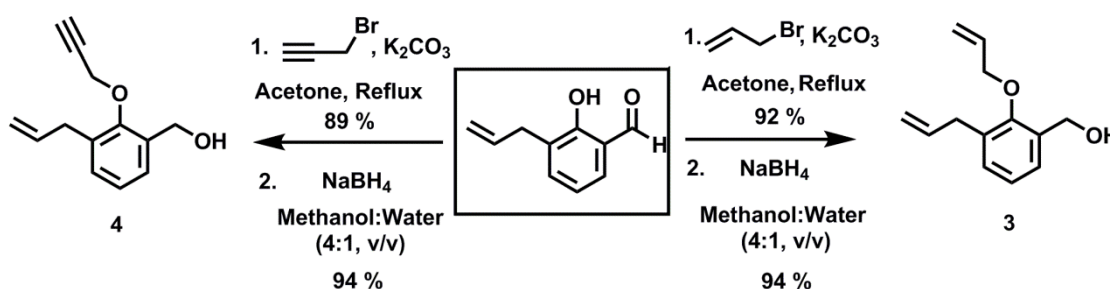
Scheme 3.1 Synthesis of (3-allyl-2-(allyloxy)phenyl)methanol (**3**) and (3-allyl-2-(prop-2-yn-1-yloxy)phenyl)methanol (**4**).

The reduction of aldehyde functional group present in **1** and **2** using sodium borohydride afforded **3** and **4**. The disappearance of a peak at 1688 cm^{-1} in FT-IR

spectrum (**Figure 3.1**) corresponding to carbonyl stretching frequency of aldehyde and appearance of peaks at 3382 cm^{-1} and 3416 cm^{-1} corresponding to hydroxyl group revealed the formation of alcohols.
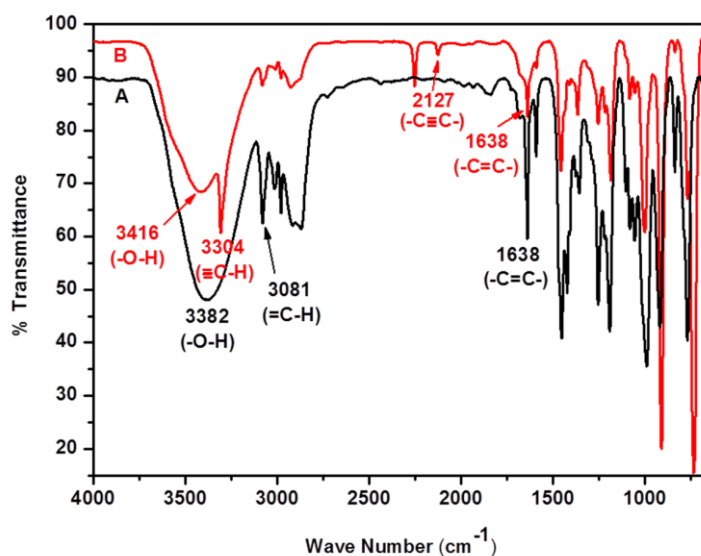
Figure 3.1 FT-IR spectrum (in chloroform) of A) (3-allyl-2-(allyloxy)phenyl)methanol (**3**) and B) (3-allyl-2-(prop-2-yn-1-yloxy)phenyl)methanol (**4**).

^{1}H NMR spectra of **3** and **4** (**Figure 3.2**) showed the disappearance of peaks at 10.36 and 10.42 corresponding to proton of aldehyde functionality, respectively and appearance of peaks at 4.72 and 4.77 ppm and at 2.25 and 2.14 ppm corresponding to benzylic methylene and alcoholic protons revealed the formation of **3** and **4**, respectively. The presence of peaks corresponding to allyl and propargyloxy groups in ^{1}H NMR spectra of **3** and **4** showed the inertness of these functional groups during reduction of aldehyde. ^{13}C NMR spectra of **3** and **4** showed the disappearance of peaks corresponding to carbonyl carbon of aldehyde at 190.33 and 190.40 ppm which gives an additional support for the complete conversion of aldehydes to the corresponding alcohols.
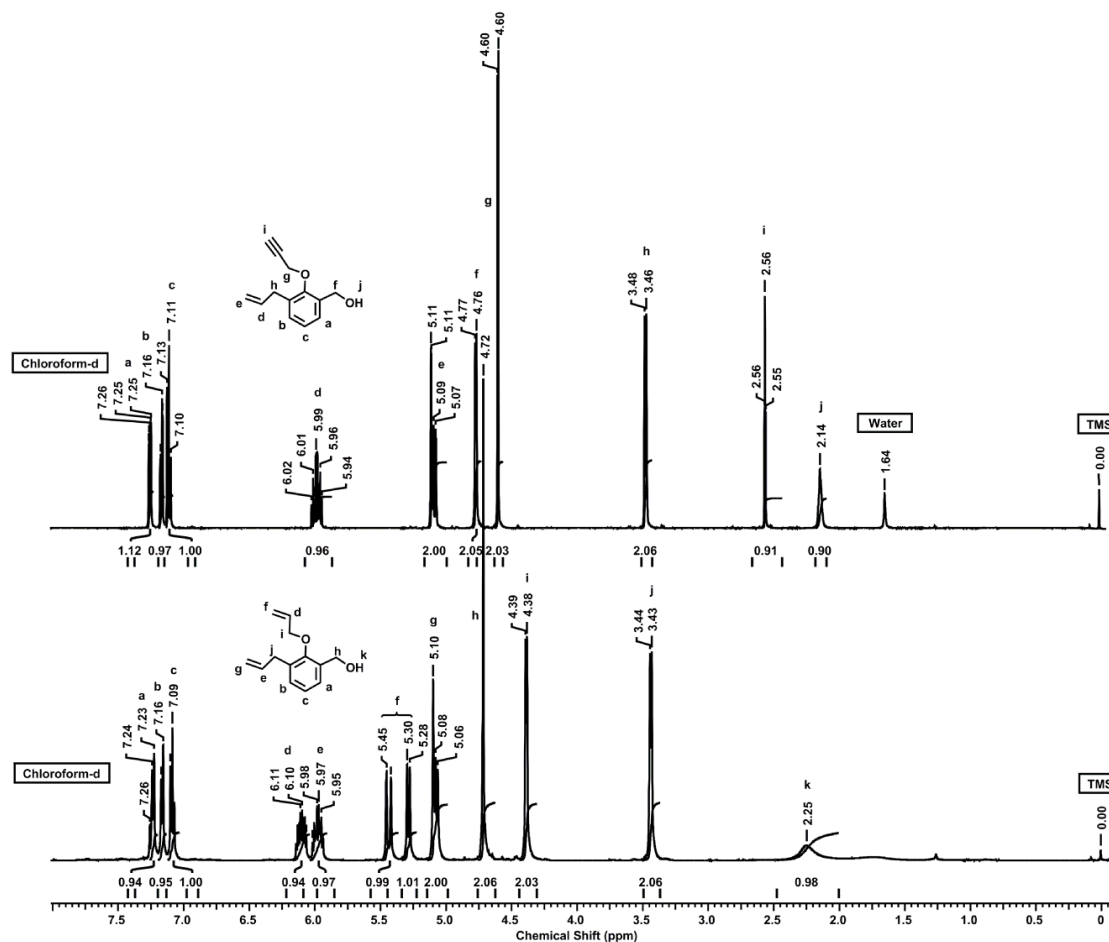
Figure 3.2 ^{1}H NMR spectrum (in CDCl$_3$) of A) (3-allyl-2-(allyloxy)phenyl)methanol (**3**) (Bottom) and B) (3-allyl-2-(prop-2-yn-1-yloxy)phenyl)methanol (**4**) (Top).

3.3.2 Synthesis of α-allyl, α'-allyloxy (5a) and α-allyl, α'-propargyloxy bifunctionalised poly(ε-caprolactone) (5b)

The new functional ROP initiators **3** and **4** were employed for synthesis of poly(ε-caprolactone)s **5a** and **5b**. In a typical experiment, polymerization reaction was carried out at 95 ^{o}C in the presence of Sn(Oct)$_2$ as a catalyst under inert atmosphere (**Scheme 3.2**).
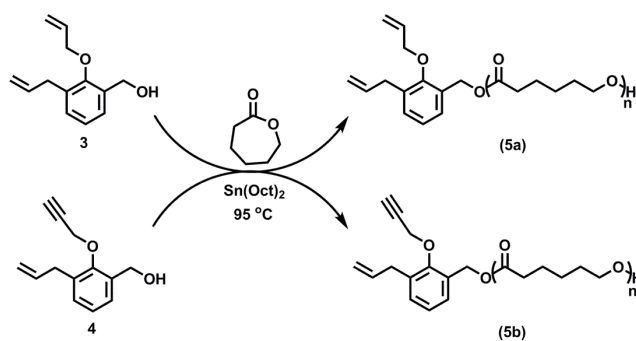
Scheme 3.2 Synthesis of α-allyl, α'-allyloxy (**5a**) and α-allyl, α'-propargyloxy bifunctionalised poly(ε-caprolactone) (**5b**).

^{1}H NMR spectra of **5a** and **5b** showed the peaks corresponding to allyl and propargyl groups at their respective positions as they appeared in the initiators, which revealed the intactness of these reactive functionalities during polymerization reactions (**Figure 3.3**). FT-IR spectra of **5a** and **5b** showed the peak at 1730 cm^{-1} due to carbonyl stretching frequency of ester in the poly(ε-caprolactone) backbone.
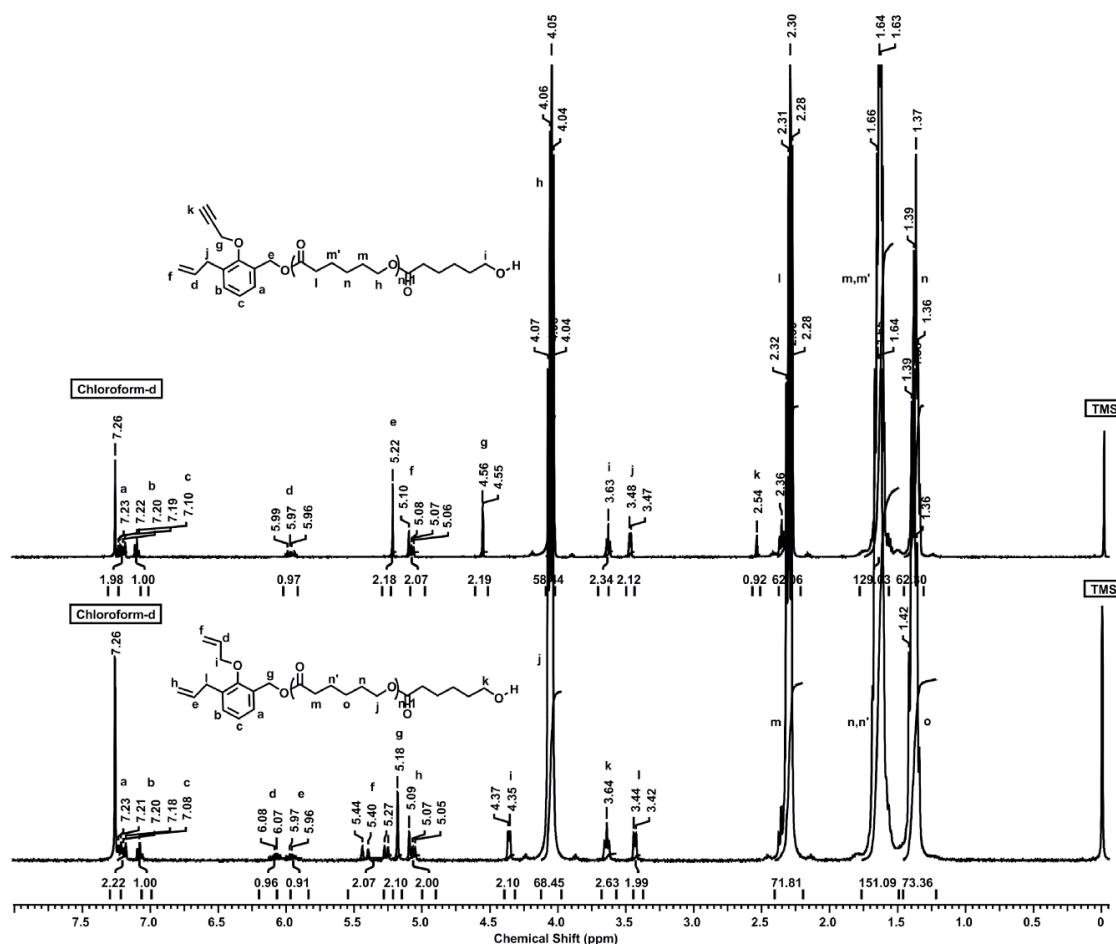
Figure 3.3 ^{1}H NMR spectrum (in CDCl$_3$) of A) α-allyl, α'-allyloxy (**5a**) (Bottom) and B) α-allyl, α'-propargyloxy bifunctionalised poly(ε-caprolactone) (**5b**) (Top).

Well defined α-allyl, α'-allyloxy and α-allyl, α'-propargyloxy bifunctionalised poly(ε-caprolactone)s were synthesized with molecular weights in the range 4200-9500 and 3600-10900 g mol^{-1} and dispersity in the range 1.16-1.18 and 1.15-1.16, respectively, by varying the monomer to initiator feed ratios and keeping catalyst to initiator ratio constant (**Table 3.1** and **3.2**). In both the cases, the percentage conversions were calculated by considering the integral ratio of methylene protons (adjacent to oxygen) of poly(ε-

caprolactone) to the total integration of methylene protons of ε-caprolactone and poly(ε-caprolactone) *i.e* monomer and polymer.

% Conversion = [I] $_{4.03 \text{ or } 4.02}$ / [I] $_{4.21 + 4.03 \text{ or } 4.19 + 4.02}$

Degree of polymerization (DP$_n$) in **5a** and **5b** was calculated by ^{1}H NMR spectroscopy considering the integrated intensity ratios of methylene protons adjacent to oxygen in poly(ε-caprolactone) backbone at 4.06/4.05 ppm to the triplet at 7.08/7.10 ppm originating from initiator fragment, respectively.

DP$_n$ = [I] $_{4.06 \text{ or } 4.05}$ / 2/ [I] $_{7.08 \text{ or } 7.10}$/1

Molecular weight ($M_{n,NMR}$) of poly(ε-caprolactone)s were calculated from degree of polymerization (DP$_n$) as follows,

$M_{n,NMR}$ = [DP$_n$ × Molecular weight of ε-caprolactone] + Molecular weight of initiator.

Table 3.1 Reaction parameters and results of synthesis of α-allyl, α'-allyloxy bifunctionalised poly(ε-caprolactone) (**5a**)

Sr. No.	$[M]_0/[I]_0$ [a]	Time (min)	Conversion (%) [b]	$M_{n,theo}$ [c]	$M_{n,NMR}$ [d]	$M_{n,GPC}$ [e]	M_w/M_n
1	30	100	98	3600	4200	5700	1.18
2	50	165	80	4800	4900	5200	1.16
3	100	210	81	9400	9500	6700	1.16

Temperature: 95 °C (In bulk), Sn(Oct)$_2$= 50 mol % of initiator.

[a] $[M]_0/[I]_0$: [Monomer]$_0$/[Initiator]$_0$ feed ratio.

[b] Conversions were determined by ^{1}H NMR spectroscopy.

[c] $M_{n,theo}$ = { $[M]_0/[I]_0$ ×(% conv.)/100 × mol. weight of monomer} + mol. weight of initiator

[d] $M_{n,NMR}$ = Determined by ^{1}H NMR spectroscopy.

[e] $M_{n,GPC}$ = Determined by GPC; Polystyrene standard; Tetrahydrofuran as an eluent.

Table 3.2 Reaction parameters and results of synthesis of α-allyl, α'-propargyloxy bifunctionalised poly(ε-caprolactone) (**5b**)

Sr. No.	$[M]_0/[I]_0$ [a]	Time (min)	Conversion (%) [b]	$M_{n,theo}$ [c]	$M_{n,NMR}$ [d]	$M_{n,GPC}$ [e]	M_w/M_n
1	30	60	88	3200	3600	5600	1.15
2	50	180	93	5500	6300	6900	1.15
3	100	250	89	10400	10900	8000	1.16

Temperature: 95 °C (In bulk), $Sn(Oct)_2$ = 50 mol % of initiator.

[a] $[M]_0/[I]_0$: $[Monomer]_0/[Initiator]_0$ feed ratio.

[b] Conversions were determined by ^1H NMR spectroscopy.

[c] $M_{n,theo}$ = { $[M]_0/[I]_0$ ×(% conv.)/100 × mol. weight of monomer} + mol. weight of initiator

[d] $M_{n,NMR}$ = Determined by ^1H NMR spectroscopy.

[e] $M_{n,GPC}$ = Determined by GPC; Polystyrene standard; Tetrahydrofuran as an eluent.

Molecular weights and dispersity of PCL synthesized by varying monomer to initiator feed ratios were determined from GPC. Typical GPC chromatograms of **5a** and **5b** are shown in Figure 3.4. GPC chromatograms of **5a** and **5b** appeared symmetric and showed monomodal distributions which support the controlled polymerization behaviour.
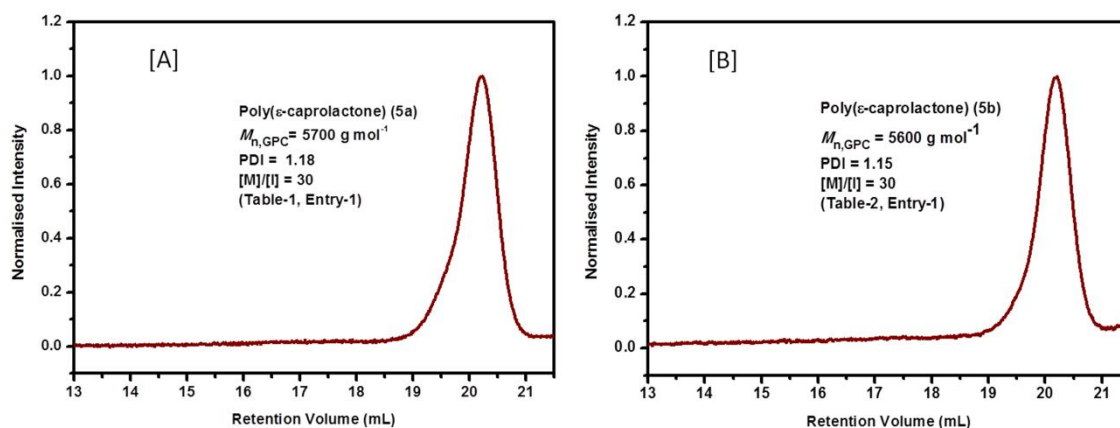
Figure 3.4 Typical GPC trace for A) α-allyl, α'-allyloxy (**5a**) and B) α-allyl, α'-propargyloxy bifunctionalised poly(ε-caprolactone) (**5b**).

MALDI-TOF spectrum of **5a** (Table 3.1, Entry 1) (**Figure 3.5**) and **5b** (Table 3.2, Entry 1) (**Figure 3.6**) showed a mass series **I** corresponding to α-allyl, α'-allyloxy and α-allyl, α'-propargyloxy bifunctionalised poly(ε-caprolactone)s, respectively, with peak

difference equal to the molecular weight of ε-caprolactone monomer repeating unit. The presence of α-allyl, α'-allyloxy and α-allyl, α'-propargyloxy end groups was determined from MALDI-TOF analysis by calculating the molecular weight of initiator fragment and monomer repeating units including the sodium ion. Theoretical molecular weight calculated from MALDI-TOF spectrum considering the initiator fragment for α-allyl, α'-allyloxy and α-allyl, α'-propargyloxy bifunctionalised poly(ε-caprolactone) was in good agreement with observed molecular weight which revealed the presence of the corresponding functionalities.
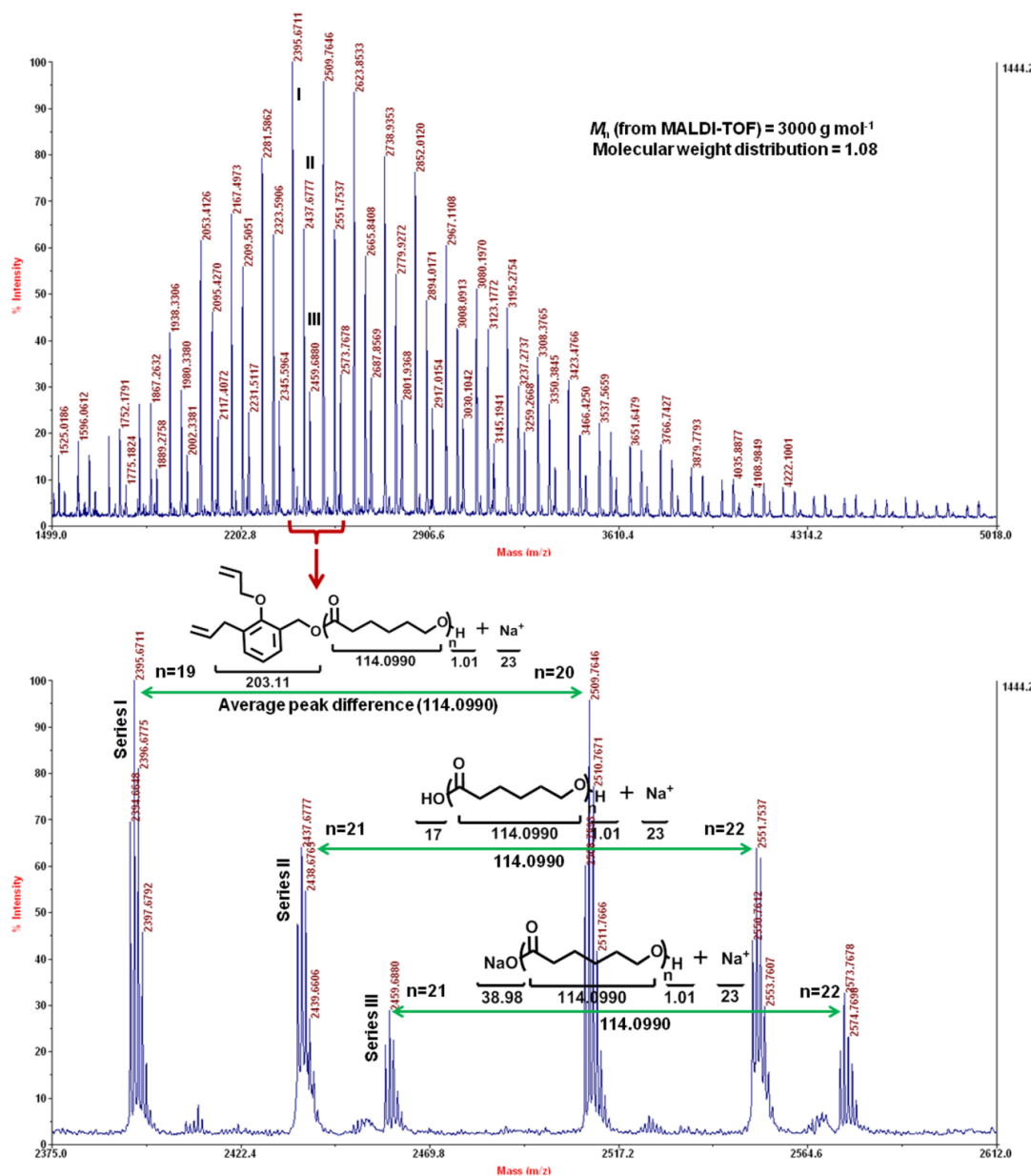
Figure 3.5 MALDI-TOF spectrum of α-allyl, α'-allyloxy bifunctionalised poly(ε-caprolactone) (**5a**) (Top) and a portion from M/Z 2375-2612 (Bottom).
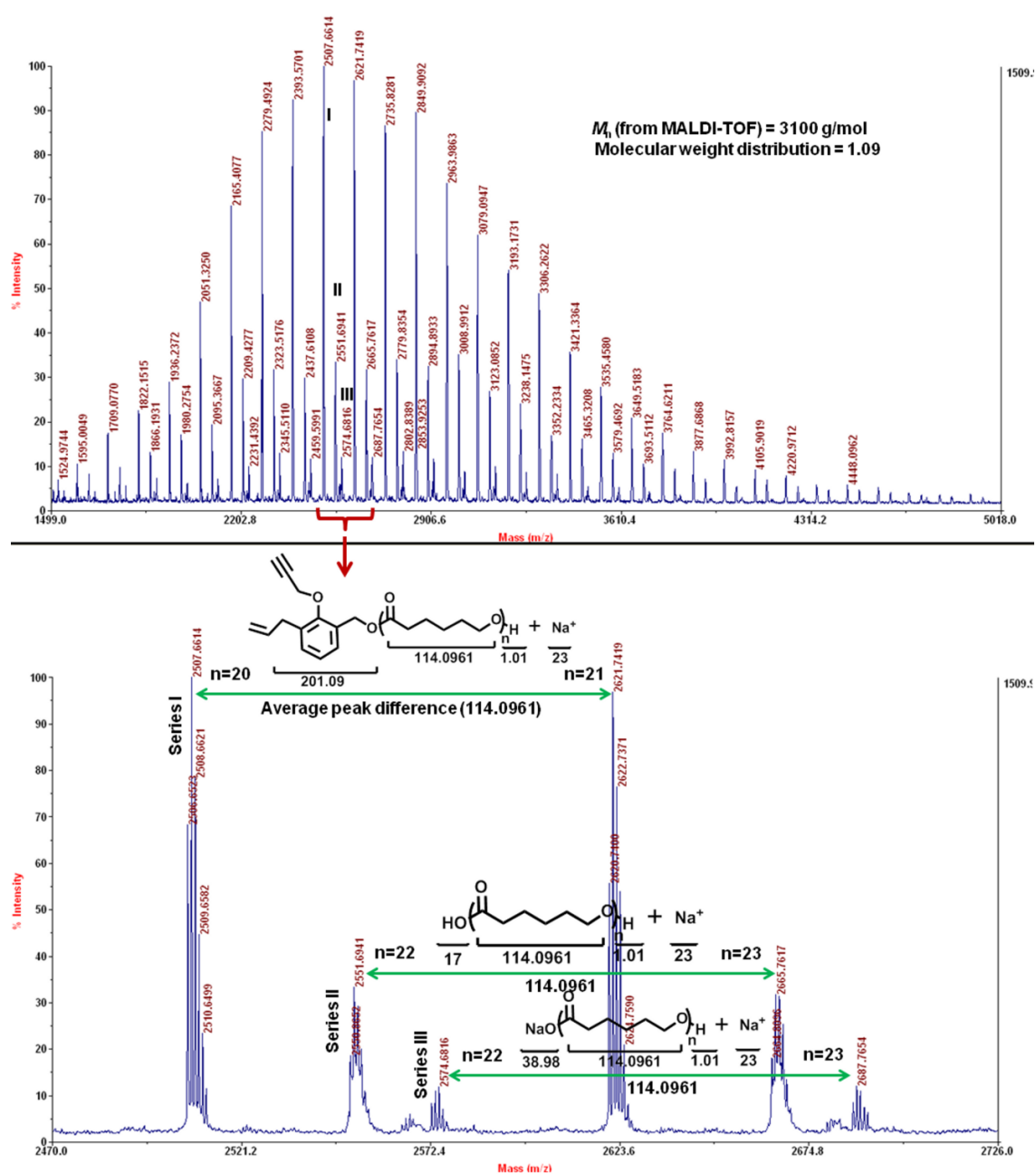
Figure 3.6 MALDI-TOF spectrum of α-allyl, α'-propargyloxy bifunctionalised poly(ε-caprolactone) (**5b**) (Top) and a portion from M/Z 2470-2726 (Bottom).

In addition to the mass series **I**, MALDI-TOF spectrum of **5a** and **5b** showed two additional mass series **II** and **III**, respectively, corresponding to the acid and its sodium salt functionalised poly(ε-caprolactone)s. The appearance of acid functionalised poly(ε-caprolactone)s prompted us to perform ^{13}C-NMR analysis to detect the resonance for carbonyl carbon of acid. However, ^{13}C-NMR spectra of **5a** and **5b** showed the absence of resonance corresponding to the carbonyl carbon of acid (**Figure 3.7**). Thus, the origin of

the acid functionalised poly(ε-caprolactone)s in MALDI-TOF spectra could likely be ascribed to the fragmentation at benzylic site of initiator during the MALDI-TOF acquisition, as exo-cleavage from α-benzyloxy group has been considered as a potential site for fragmentation.[62]
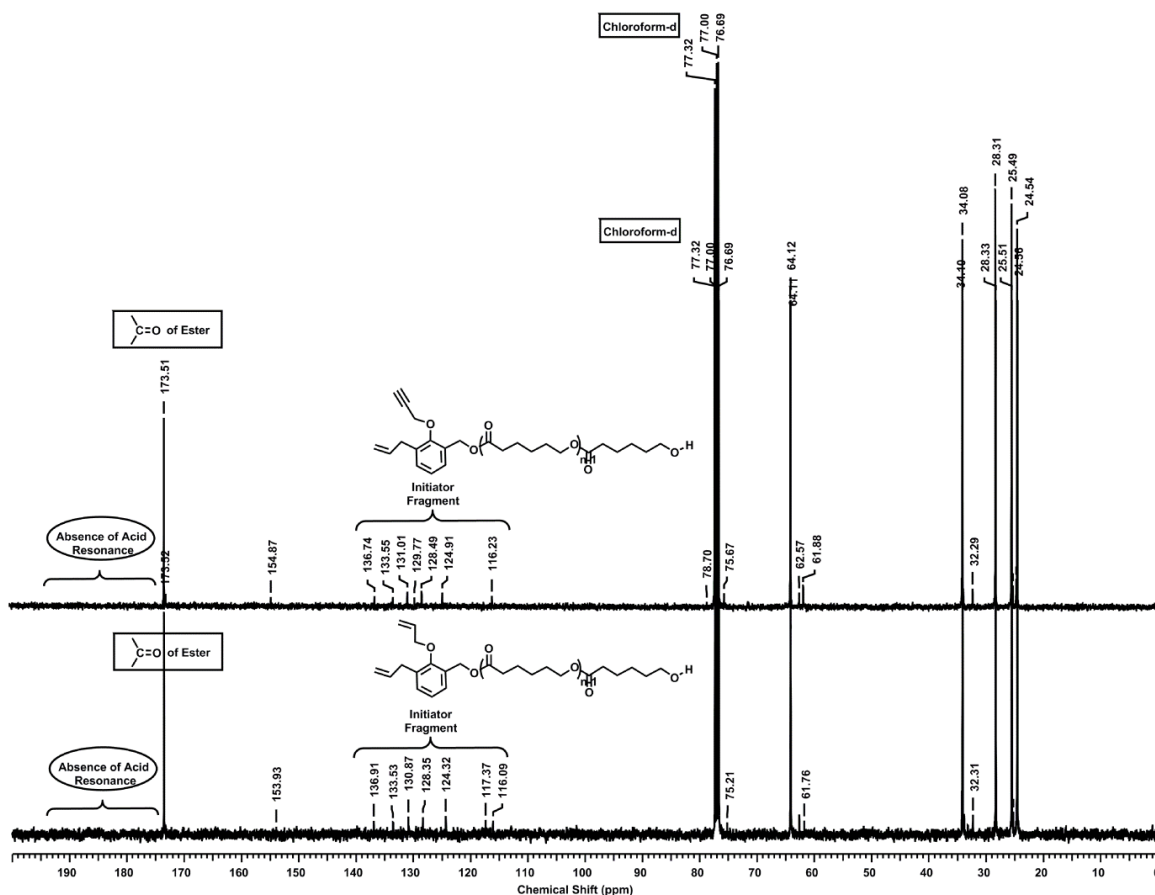
Figure 3.7 ^{13}C NMR spectrum (in CDCl$_3$) of A) α-allyl, α'-allyloxy (**5a**) (Bottom) and B) α-allyl, α'-propargyloxy bifunctionalised poly(ε-caprolactone) (**5b**) (Top).

In order to support the hypothesis that exo-cleavage from α-benzyloxy group occurs, MALDI-TOF MS spectrum of (3-allyl-2-(prop-2-yn-1-yloxy)phenyl)methanol (**4**) was recorded (**Figure 3.8**). The appearance of peak at M/Z 185.26 corresponding to the benzylic cation formed by exo-cleavage from α-benzyloxy group supports the fact that exo-cleavage indeed occurs.
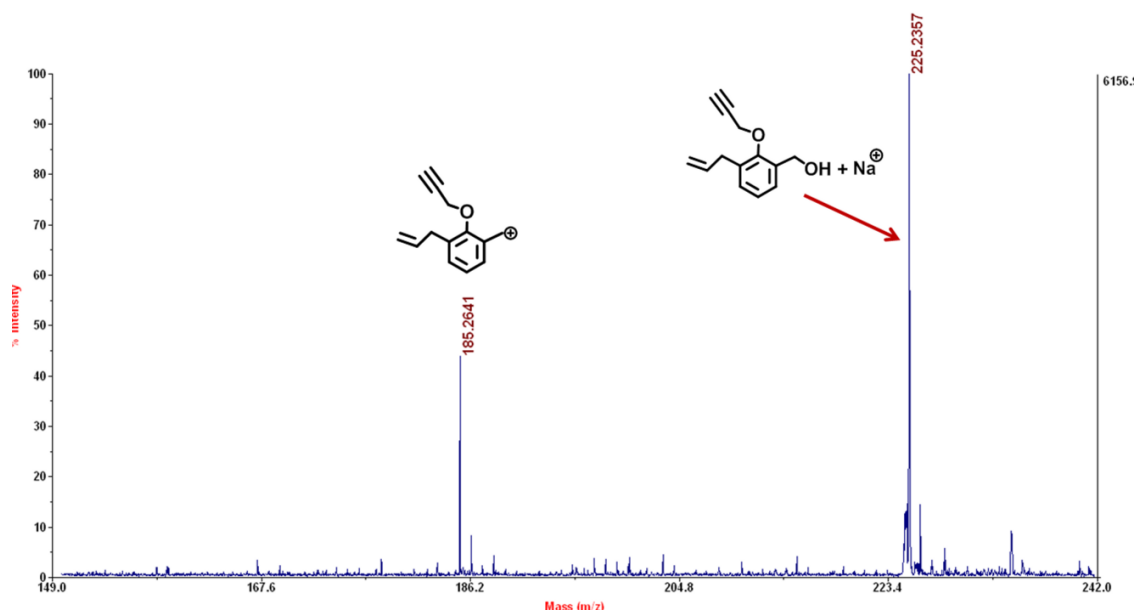
Figure 3.8 MALDI-TOF MS spectrum (in HABA as a matrix) of (3-allyl-2-(prop-2-yn-1-yloxy)phenyl)methanol (**4**) at 4500 laser intensity.

MALDI-TOF MS/MS acquisition of a selected line at M/Z 2393.5 for series **I** was performed to confirm the fragmentation pattern of α-allyl α'-propargyloxy bifunctionalised poly(ε-caprolactone) (**5b**) (**Figure 3.9**). The appearance of peaks at M/Z 2209, 185 and 23 corresponding to acid functional PCL, benzylic cation and sodium ion, respectively, confirmed the exo-cleavage from α-benzyloxy group and presence of sodium ion in series **I**.
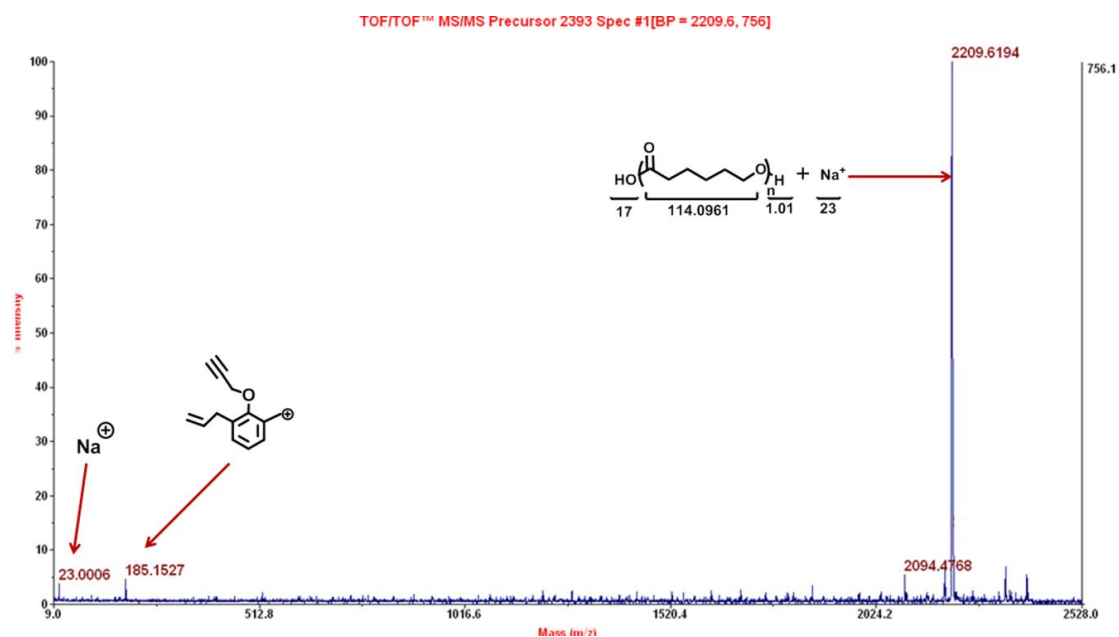
Figure 3.9 MALDI-TOF MS/MS spectrum of a peak at M/Z 2393.51 corresponding to α-allyl α'-propargyloxy bifunctionalised poly(ε-caprolactone) (**5b**).

Additionally, MALDI-TOF MS spectrum of PCL (**5b**) was recorded using HABA as a matrix and potassium iodide as an ion source (**Figure 3.10**). The spectrum indicated the line series corresponding to potassium salt of PCL and the potassium salt of corresponding fragmentation products which further supported the occurence of exo-cleavage from α-benzyloxy group.
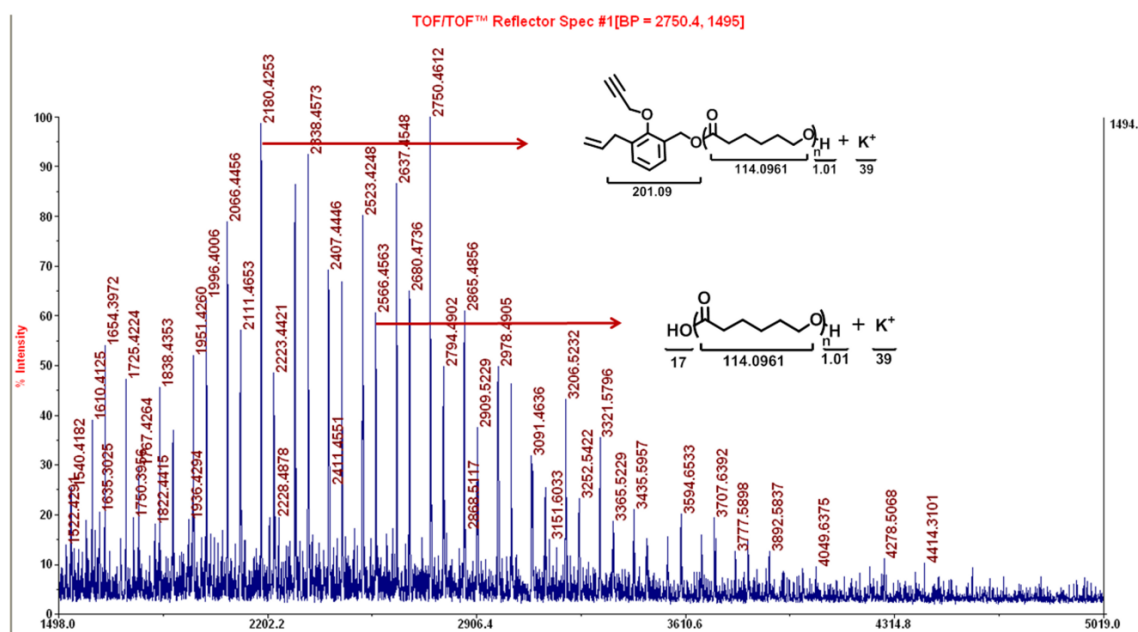
Figure 3.10 MALDI-TOF MS spectrum (in HABA as a matrix) of α-allyl α'-propargyloxy bifunctionalised poly(ε-caprolactone) (**5b**) at 4500 intensity using potassium iodide as an ion source.

MALDI-TOF analysis at higher laser intensity (6000) showed the complete reversal of series **I** and **II** (**Figure 3.11**) which confirmed the origin of acid functionalized poly(ε-caprolactone)s during the acquisition. Furthermore, MALDI-TOF spectra of **5a** and **5b** were symmetric and dispersity obtained from MALDI-TOF analysis was below 1.09 which attested the controlled polymerization behaviour. The model reaction with 1-butanol as the ROP initiator was performed to prepare PCL without the benzyloxy group to verify the exo-cleavage. The absence of lines series corresponding to hydroxyl-terminated PCL in MALDI-TOF spectrum of 1-butanol-initiated PCL (**Figure 3.12**) attested the fragmentation at benzylic site of **3** and **4** initiator during the MALDI-TOF acquisition.
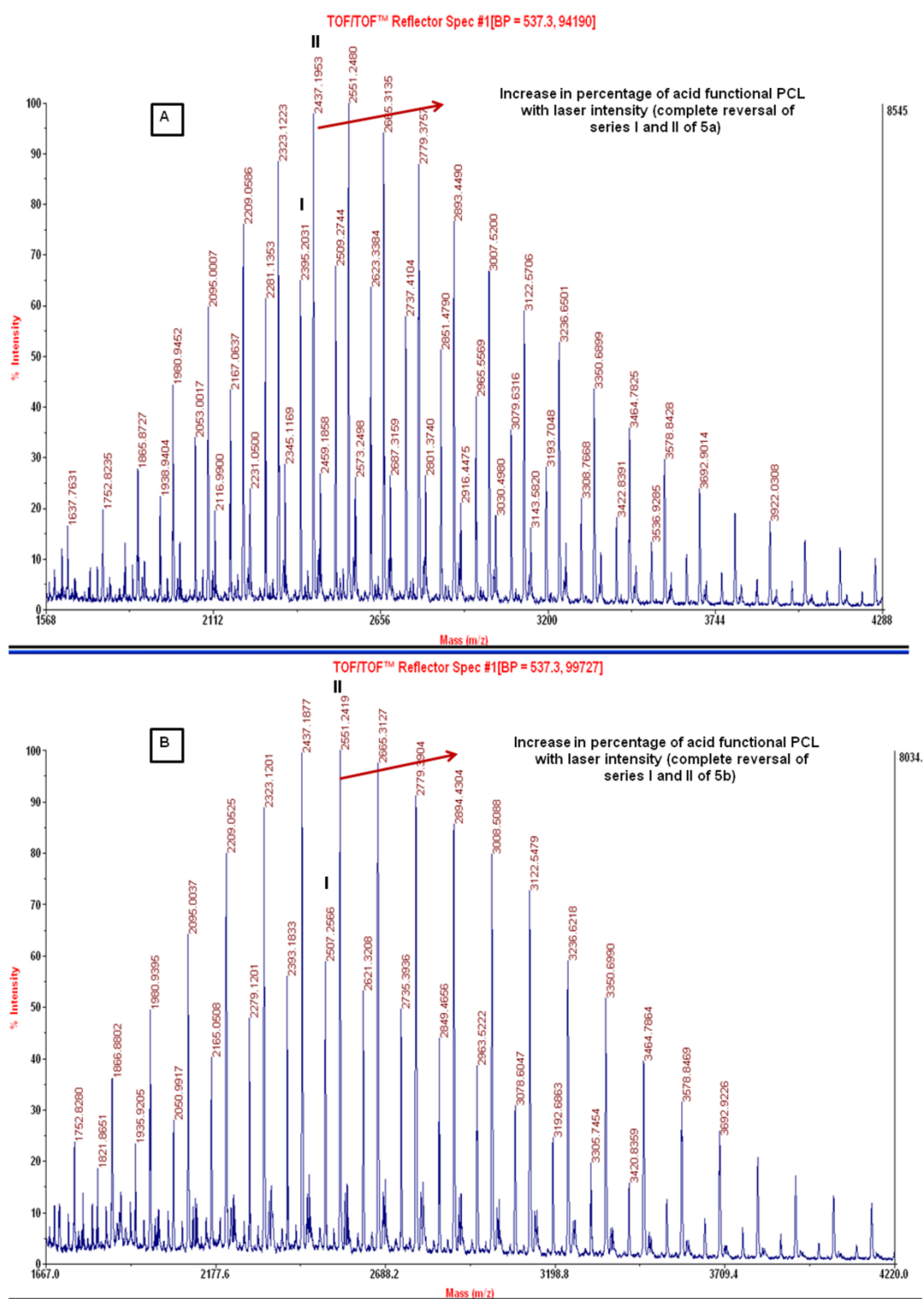
Figure 3.11 MALDI-TOF MS spectrum of A) α-allyl α'-allyloxy bifunctionalised poly(ε-caprolactone) (Top) and B) α-allyl α'-propargyloxy bifunctionalised poly(ε-caprolactone) (Bottom) at 6000 laser intensity (complete reversal of series **I** and **II**).
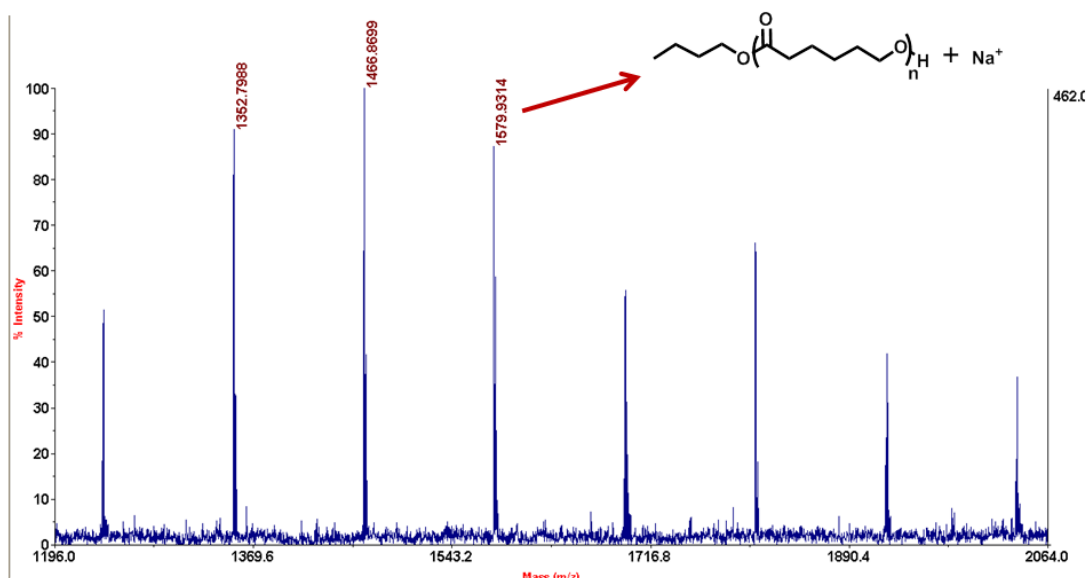
Figure 3.12 MALDI-TOF spectrum of 1-butanol-initiated poly(ε-caprolactone).

3.3.3 Kinetics of ROP of ε-caprolactone using 3 and 4

The kinetics of ε-caprolactone polymerization was performed using ROP initiators **3** and **4** by keeping monomer to initiator feed ratio at 100. The kinetic studies were performed at 95 °C by taking the aliquots from the reaction mixtures at different time intervals and analyzing directly by ^{1}H NMR spectroscopy to determine the percentage conversion. All the samples were further purified by precipitating into cold acidified methanol and molecular weights were determined by ^{1}H NMR spectroscopy. The linear dependence of $\ln[M]_0/[M]_t$ with polymerization time passing through the origin (**Figure 3.13** and **3.14**) in both the systems revealed the pseudo first order kinetic behaviour of polymerization with respect to ε-caprolactone monomer. This suggests the constant rate of consumption of ε-caprolactone monomer and absence of chain terminations, if any, throughout the polymerization. Furthermore, the linear increase of molecular weight with percentage conversions and almost constant polydispersities below 1.2 revealed the controlled polymerization behaviour with constant number of growing polymer chains and absence of significant side reactions (**Figure 3.13** and **3.14**).
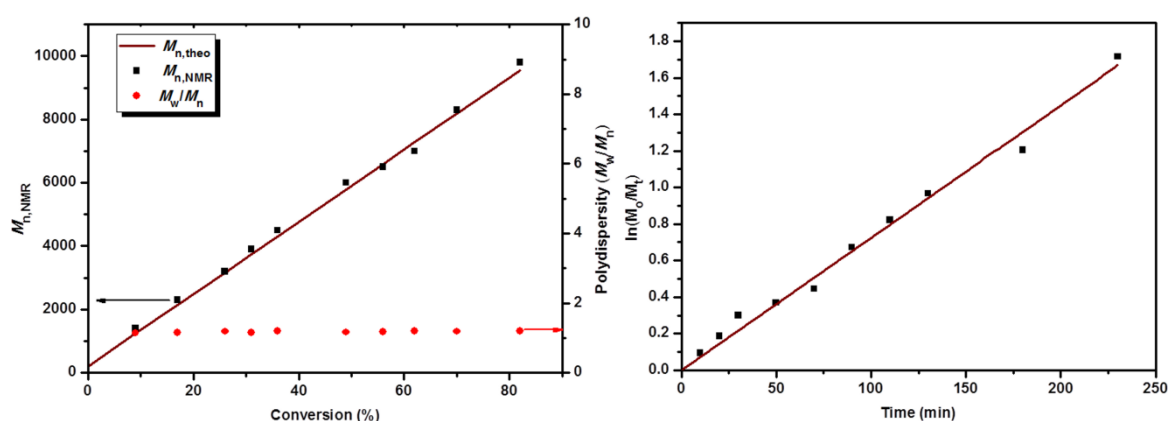
Figure 3.13 Kinetics of ROP of ε-caprolactone using (3-allyl-2-(allyloxy)phenyl)methanol (**3**).
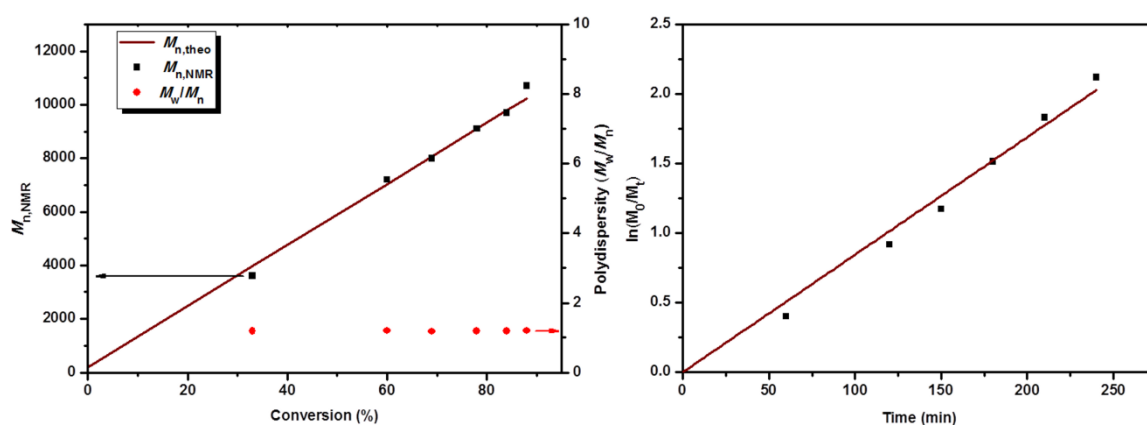
Figure 3.14 Kinetics of ROP of ε-caprolactone using (3-allyl-2-(prop-2-yn-1-yloxy)phenyl)methanol (**4**).

Thus, the initiators **3** and **4** were found to be efficient for ROP of ε-caprolactone affording well defined α-allyl, α'-allyloxy and α-allyl, α'-propargyloxy bifunctionalised poly(ε-caprolactone)s. The in-built allyl functionality in 3-allylsalicyaldehyde offers the flexibility in terms of choice of other functional groups for orthogonal chemistries and hence can be considered as a versatile precursor for synthesis of functional ROP initiator cores for designing homo- and hetero-bifunctionalised polymers. Such functional initiators with non-interferable functionalities offer the reactive sites for orthogonal reactions and post modifications of the polymers.

3.3.4 Synthesis of thiol functional poly(ethylene glycol) (mPEG-SH).

Thiol functional poly(ethylene glycol) was synthesized by slight modifications in the reported procedure. [60]

The transformation of hydroxyl group of PEG monomethyl ether to mesylate followed by the reaction with sodium hydrosulfide hydrate and DL-dithiothreitol afforded the desired thiol-functional mPEG (**Scheme 3.3**).
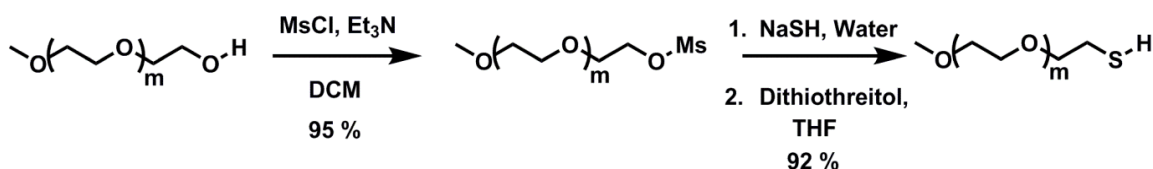
Scheme 3.3 Synthesis of thiol functional poly(ethylene glycol) (mPEG-SH).

3.3.5 Thiol-ene reaction of α-allyl, α'-allyloxy bifunctionalised poly(ε-caprolactone) with mPEG-SH

α-Allyl, α'-allyloxy and α-allyl, α'-propargyloxy bifunctionalised poly(ε-caprolactone)s were considered as useful precursors for synthesis of star copolymers by exploitation of the reactivity of allyl and propargyl groups with appropriate reagents/ prepolymers.

The literature reports indicate that thiol-ene reactions are sensitive to reaction conditions and are accompanied by the formation of side products. Insightful discussion of thiol-ene reaction for polymer-polymer conjugation has been provided in the reported studies.[46, 63-66] It is now accepted that the thiol-ene reaction is far from being satisfactory to be considered as a click reaction. Based on several intricate studies reported in the literature, reaction conditions for thiol-ene reaction have been suggested under which the reaction is likely to proceed with maximum conversion and minimum formation of undesired side products. The favourable thiol-ene reaction conditions recommended are: (1) Thiol:ene molar stoichiometry of 10:1 (2) Use of polar solvents such as *N*-methyl-2-pyrrolidone (NMP) or DMF (3) Minimum quantity of solvent (4) Photoinitiator whose generated radicals are capable of only abstracting proton from thiol (5) Higher ratio of thiol to photoinitiator and (5) Longer reaction time. In the present work, thiol-ene reactions were carried out taking into consideration the above mentioned published information.

α-Allyl, α'-allyloxy bifunctionalised poly(ε-caprolactone) ($M_{n,NMR}$= 4200 g mol^{-1}, DP$_n$-35) was reacted with 10 equivalents (w.r.t. alkene) of mPEG-SH ($M_{n,NMR}$= 2100 g mol^{-1}, DP$_n$-45) in DMF as a solvent using DMPA (0.2 eq. w.r.t. alkene) as a photoinitiator

by irradiating with light of 365 nm wavelength in a photochemical reactor for 4 h (**Scheme 3.4**).
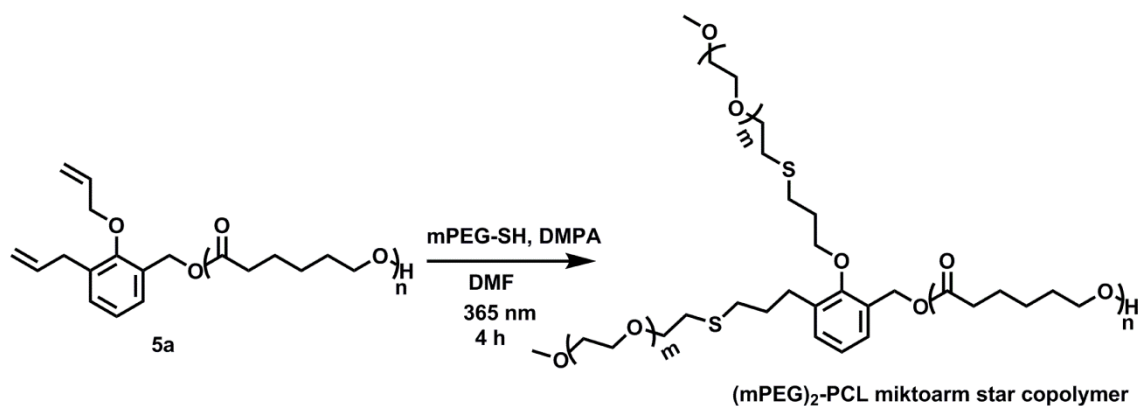
Scheme 3.4 Thiol-ene reaction of α-allyl, α'-allyloxy bifunctionalised poly(ε-caprolactone) (**5a**) with mPEG-SH.

^{1}H NMR spectrum of the reaction mixture at the end of reaction time was recorded after removal of solvent. ^{1}H NMR spectrum (**Figure 3.15**) showed a triplet at 2.88 ppm which could be ascribed to methylene protons adjacent to disulfide linkage.[67] This is an indication of formation of mPEG-S-S-mPEG due to thiyl-thiyl radical coupling reaction which is a prevalent side reaction in thiol-ene coupling reaction. The reaction product was dissolved in a minimum quantity of THF and to the solution was added excess of water dropwise. The solution was treated with DL-dithiothreitol in order to cleave disulfide linkage present in mPEG-S-S-mPEG and form mPEG-SH. The solution was dialysed against water using 2 KD dialysis bag to remove mPEG-SH. This procedure was repeated nine times to ensure complete cleavage of mPEG-S-S-mPEG to mPEG-SH and removal of mPEG-SH. It is to be noted that both mPEG-SH and mPEG-S-S-mPEG are soluble in water which allows their separation from the product polymer by dialysis process.
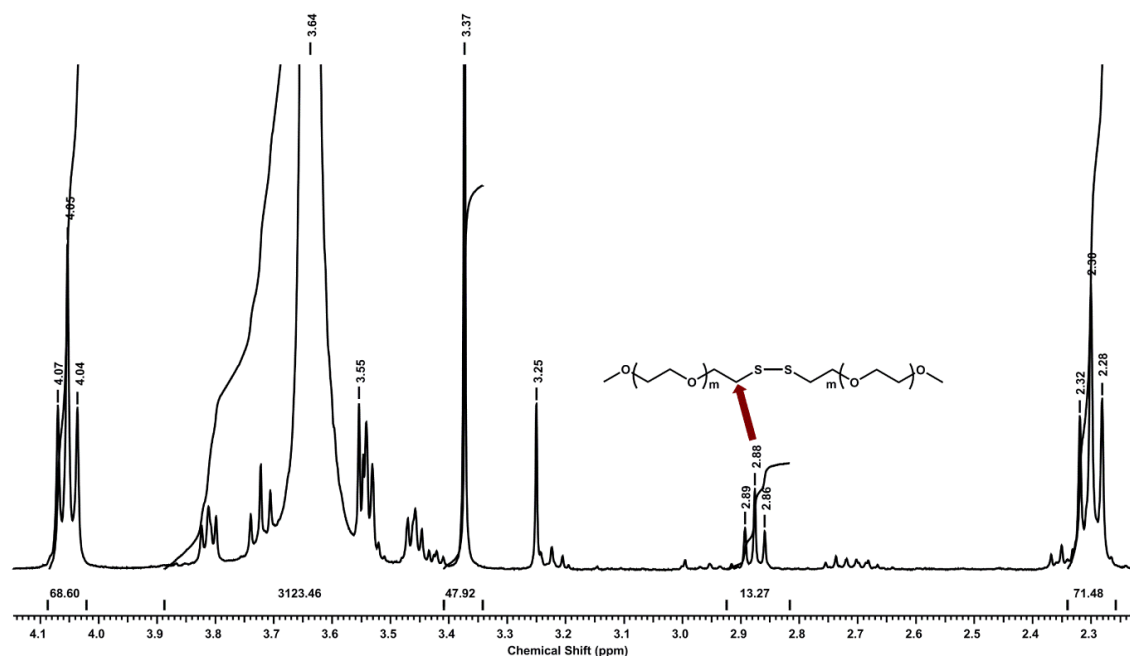
Figure 3.15 ^{1}H NMR spectrum (in CDCl$_3$) of product obtained in the reaction of α-allyl, α'-allyloxy bifunctionalised poly(ε-caprolactone) with mPEG-SH before purification.

^{1}H NMR spectrum (**Figure 3.16**) of the purified product polymer indicated the disappearance of peaks in the region 5.8-6.2 ppm corresponding to allyl functionalities indicating the success of thiol-ene reaction. The peak at 2.88 ppm corresponding to the methylene protons adjacent to disulfide linkage observed in the product polymer before purification was completely absent in the purified product. The relative integration of the peak at 3.63 ppm corresponding to methylene protons adjacent to oxygen in PEG chain with that of the peak at 4.05 ppm corresponding to the methylene protons adjacent to oxygen in PCL chain indicated higher content of PEG units (by 16 mol %) than the theoretical value. The results of ^{1}H NMR spectroscopy studies indicated that the target polymer *viz* (mPEG)$_2$-PCL was formed albeit contaminated with unidentified products. Due to the experimental difficulties involved in isolation of the side products, no efforts were made to establish their identity.
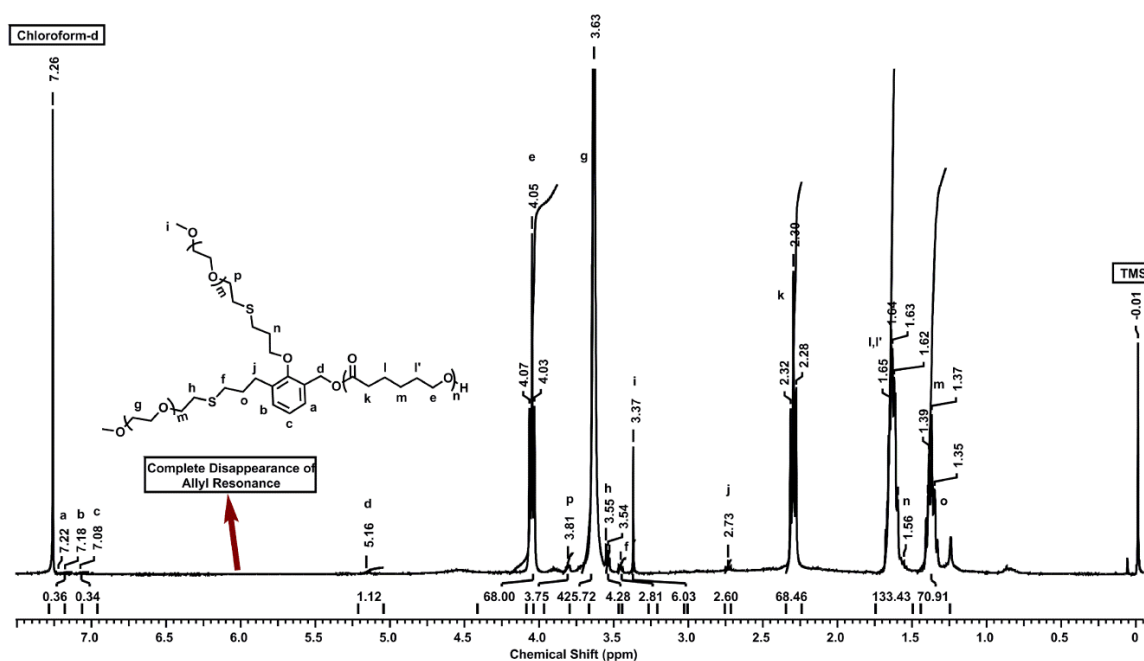
Figure 3.16 ^{1}H NMR spectrum (in CDCl$_3$) of (mPEG)$_2$-PCL miktoarm star copolymer.

Molecular weight and dispersity of (mPEG)$_2$-PCL miktoarm star copolymer was determined by GPC analysis. The shift of GPC curve corresponding to (mPEG)$_2$-PCL miktoarm copolymer to the higher molecular weight side (lower retention volume) revealed the formation of star copolymer (**Figure 3.17**). Star copolymers exhibit lower hydrodynamic volume due to their compact structure as compared to their linear counterparts with same molecular parameters.[68] The observed magnitude of shift of GPC curve corresponding to (mPEG)$_2$-PCL miktoarm star copolymer was not very significant as compared to allyl, allyloxy bifunctionalised poly(ϵ-caprolactone) possibly because of the low molecular weight of mPEG-SH used for thiol-ene reaction and lower hydrodynamic volume of (mPEG)$_2$-PCL miktoarm star copolymer due to the star architecture.
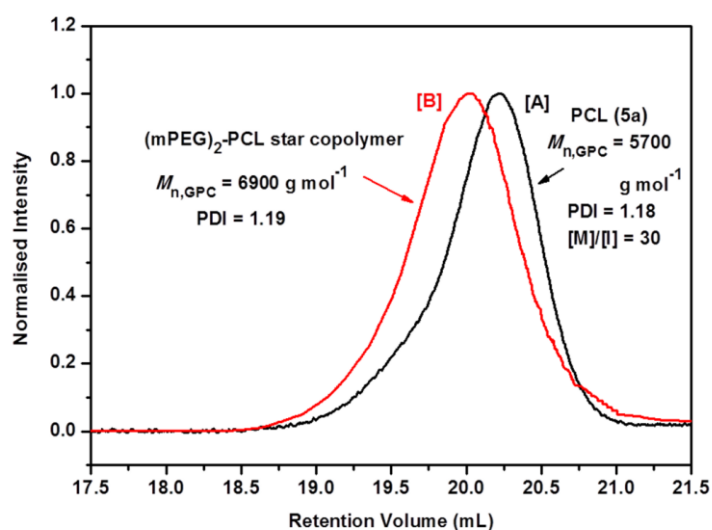
Figure 3.17 GPC trace of A) α-allyl, α'-allyloxy bifunctionalised poly(ε-caprolactone) (**5a**) and B) (mPEG)$_2$-PCL miktoarm star copolymer.

MALDI-TOF MS spectrum of purified (mPEG)$_2$-PCL star copolymer showed the peak series corresponding to (mPEG)$_2$ benzylic cation in addition to the peak series corresponding to acid functionalised PCL which confirmed the formation of the desired star copolymer (**Figure 3.18**).
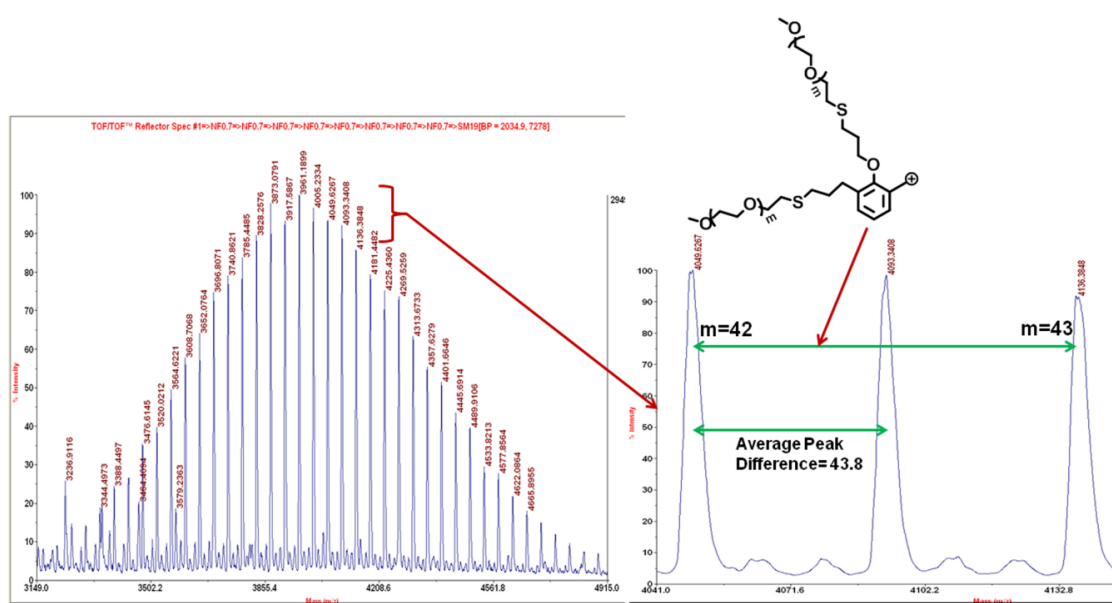
Figure 3.18 MALDI-TOF MS spectrum of (mPEG)$_2$-PCL star copolymer and the region from M/Z- 4041 to 4136.

3.3.6 Synthesis of azido-functional poly(*N*-isopropylacrylamide) (PNIPAAm-N₃) by ATRP

A new ATRP initiator, namely, 2-(4-azidophenoxy)ethyl 2-bromo-2-methylpropanoate was synthesized from 4-aminophenol (**Scheme 3.5**). The nucleophilic substitution of diazonium salt obtained from 4-aminophenol with sodium azide led to the formation of 4-azidophenol. The alkylation of 4-azidophenol followed by the reaction with 2-bromoisobutyryl bromide afforded 2-(4-azidophenoxy)ethyl 2-bromo-2-methylpropanoate initiator. The formation of initiator was confirmed by FT-IR, ^{1}H and ^{13}C NMR spectroscopy. The appearance of a peak at 2110 cm^{-1} in FT-IR spectrum confirmed the presence of azido-functionality. The resonances corresponding to all protons and different sets of carbons in ^{1}H and ^{13}C NMR spectrum, respectively, are in good agreement with the proposed structure (**Figure 3.19**).
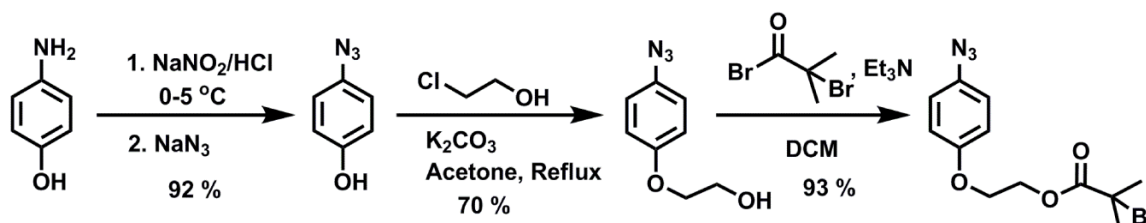
Scheme 3.5 Synthesis of 2-(4-azidophenoxy)ethyl 2-bromo-2-methylpropanoate.
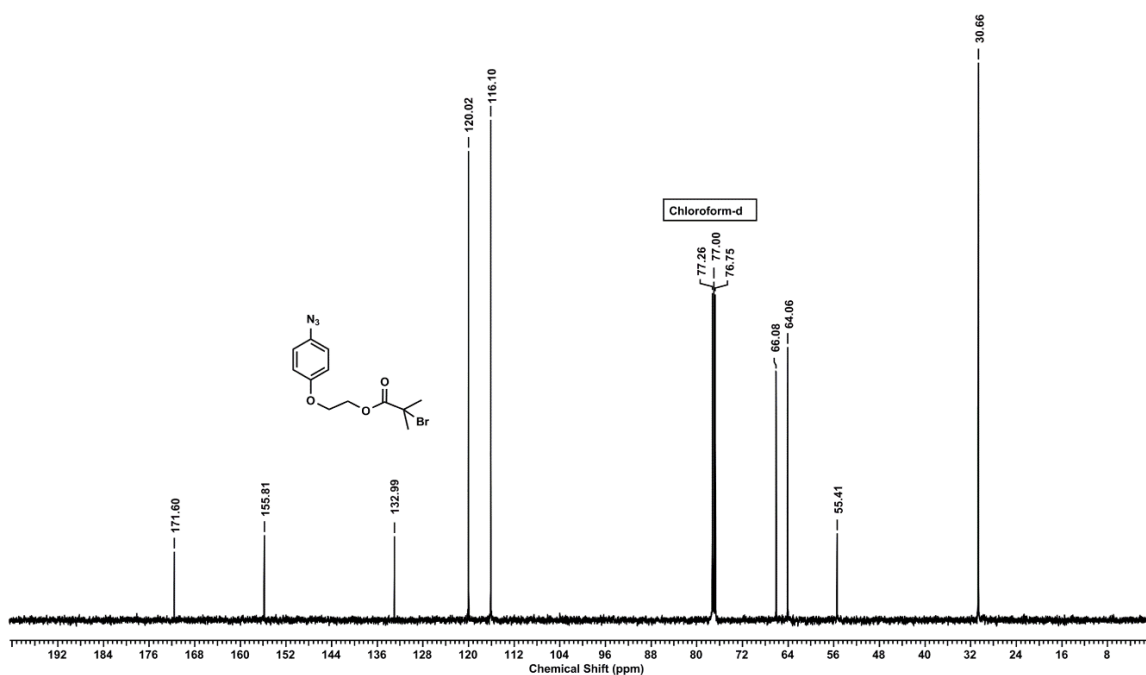
Figure 3.19 ^{13}C NMR spectrum (in CDCl₃) of 2-(4-azidophenoxy)ethyl 2-bromo-2-methylpropanoate.

The requisite azido-terminated PNIPAAm-N$_3$ was synthesized by ATRP of *N*-isopropylacrylamide employing the initiator at 25 $^{\circ}$C in the presence of CuBr/Me$_6$TREN as a catalytic system (**Scheme 3.6**). The percentage conversion of ATRP reaction was determined by ^{1}H NMR spectroscopy.
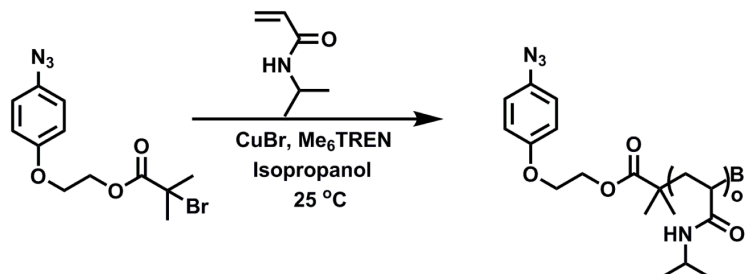
Scheme 3.6 Synthesis of azido functional poly(*N*-isopropylacrylamide) (PNIPAAm-N$_3$) by ATRP in isopropanol.

The presence of clickable azido-functionality in PNIPAAm was confirmed by FT-IR (**Figure 3.20**). Molecular weight and dispersity of PNIPAAm-N$_3$ was determined by GPC analysis and was found to be well controlled with narrow dispersity (1.19).
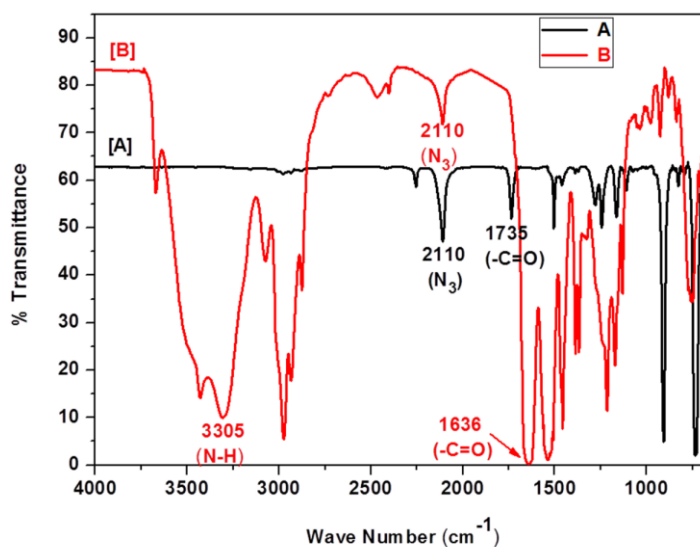
Figure 3.20 FT-IR spectrum (in CHCl$_3$) of A) 2-(4-azidophenoxy)ethyl 2-bromo-2-methylpropanoate and B) azido functional poly(*N*-isopropylacrylamide) (PNIPAAm-N$_3$).
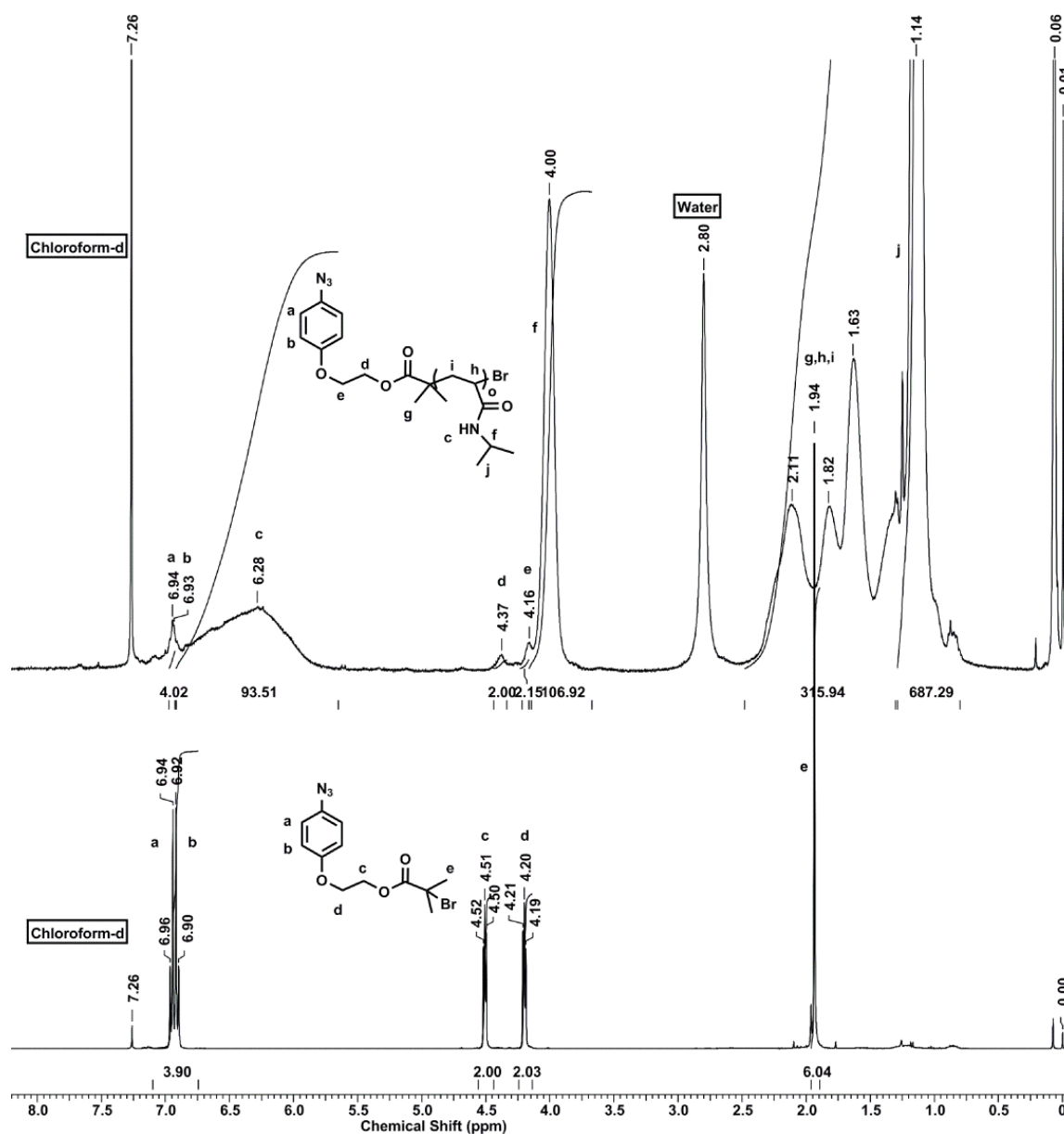
Figure 3.21 ¹H NMR spectrum (in CDCl₃) of A) 2-(4-azidophenoxy)ethyl 2-bromo-2-methylpropanoate (Bottom) and B) azido functional poly(*N*-isopropylacrylamide) (PNIPAAm-N₃) (Top).

3.3.7 Orthogonal reactions of α-allyl, α'-propargyloxy bifunctionalised poly(ε-caprolactone) (5b) with PNIPAAm-N₃ and mPEG-SH

α-Allyl, α'-propargyloxy bifunctionalised poly(ε-caprolactone) was reacted with azido-terminated poly(*N*-isopropylacrylamide) (PNIPAAm-N₃) followed by reaction with poly(ethylene glycol) thiol with an objective to synthesize PCL-PNIPAAm-mPEG miktoarm star terpolymer. The exploitation of alkyne-azide click reaction for synthesis of various macromolecular architectures such as block, star and dendritic structures has been

successfully demonstrated previously by several research groups.[69, 70]

Allyl mid functional PCL-*b*-PNIPAAm copolymer was synthesized by CuAAC reaction of **5b** with PNIPAAm-N$_3$ in presence of CuBr and PMDETA (**Scheme 3.7**).
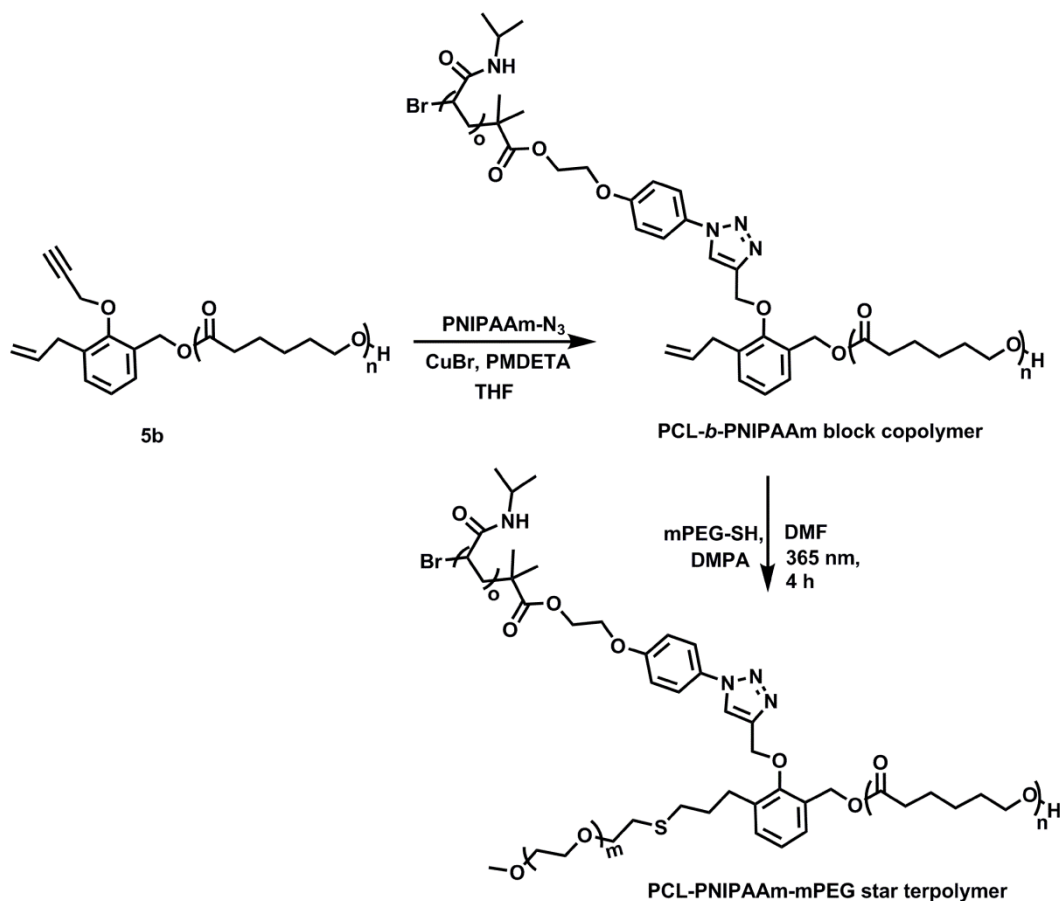
Scheme 3.7 Orthogonal reactions of α-allyl, α'-propargyloxy bifunctionalised poly(ε-caprolactone) (**5b**) with PNIPAAm-N$_3$ and mPEG-SH.

The complete disappearance of protons corresponding to propargyl group and appearance of triazole proton resonance at 8.07 ppm in ^{1}H NMR spectrum revealed the formation of PCL-*b*-PNIPAAm copolymer with allyl functionality at the midpoint (**Figure 3.22**). The relative integration of the triplet at 4.05 ppm attributed to methylene protons adjacent to oxygen in PCL with that of a broad singlet at 3.98 ppm assignable to methine protons in PNIPAAm chain indicated the formation of desired allyl mid-functional PCL-*b*-PNIPAAm. The corresponding shift of GPC chromatogram of PCL-*b*-PNIPAAm to the lower retention volume due to larger hydrodynamic volume compared to **5b** also revealed the formation of PCL-*b*-PNIPAAm.
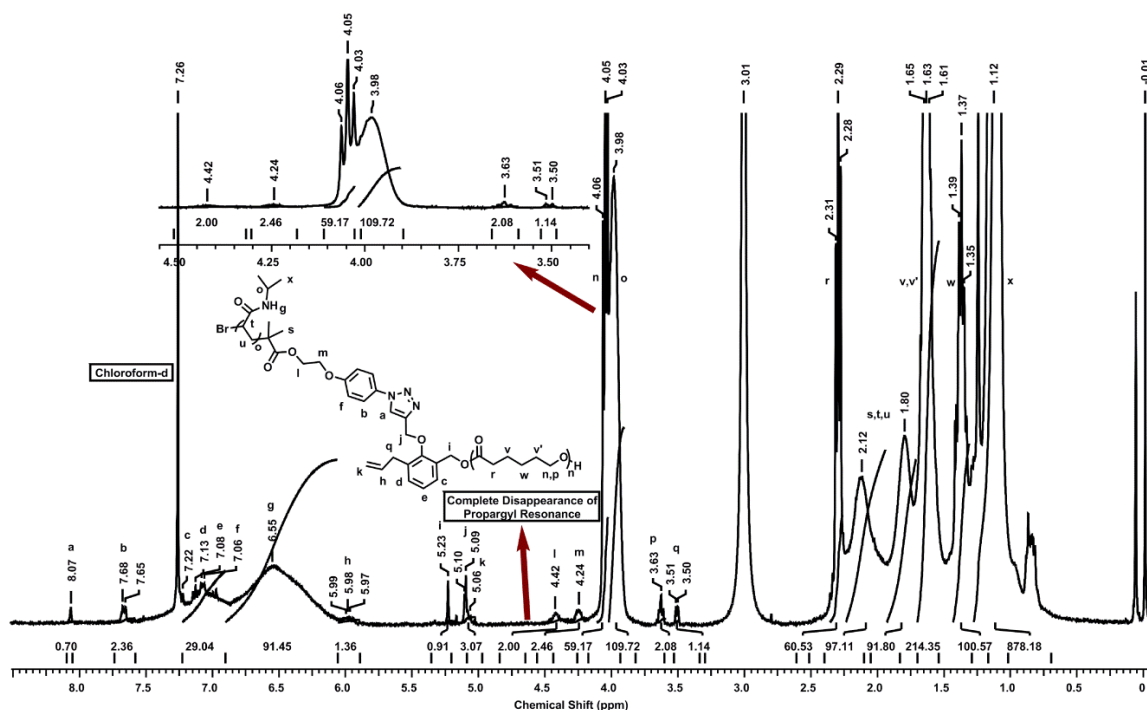
Figure 3.22 ^{1}H NMR spectrum (in CDCl$_3$) of allyl mid-functional PCL-*b*-PNIPAAm block copolymer.

Allyl mid-functional PCL-*b*-PNIPAAm copolymer ($M_{n,NMR}$= 16400 g mol^{-1}) was reacted with 10 equivalents of mPEG-SH ($M_{n,NMR}$= 2100 g mol^{-1}, DP$_n$-45) in DMF as a solvent using DMPA (0.2 eq.) as a photoinitiator by irradiating a reaction mixture with light of 365 nm wavelength in a photochemical reactor for 4 h (**Scheme 3.7**). The reaction product was purified as described for preparation of (mPEG)$_2$-PCL miktoarm star copolymer. ^{1}H NMR spectrum (**Figure 3.23**) of the purified polymer indicated the disappearance of peaks in the region 5.8-6.1 ppm corresponding to allyl functionality indicating the completion of thiol-ene reaction. The relative integration of the peak at 3.63 ppm due to methylene protons adjacent to oxygen in PEG chain with that of the triplet at 4.05 ppm attributed to methylene protons adjacent to oxygen in PCL was in reasonably good agreement, thus, indicating the formation of target miktoarm copolymer namely PCL-PNIPAAm-mPEG.
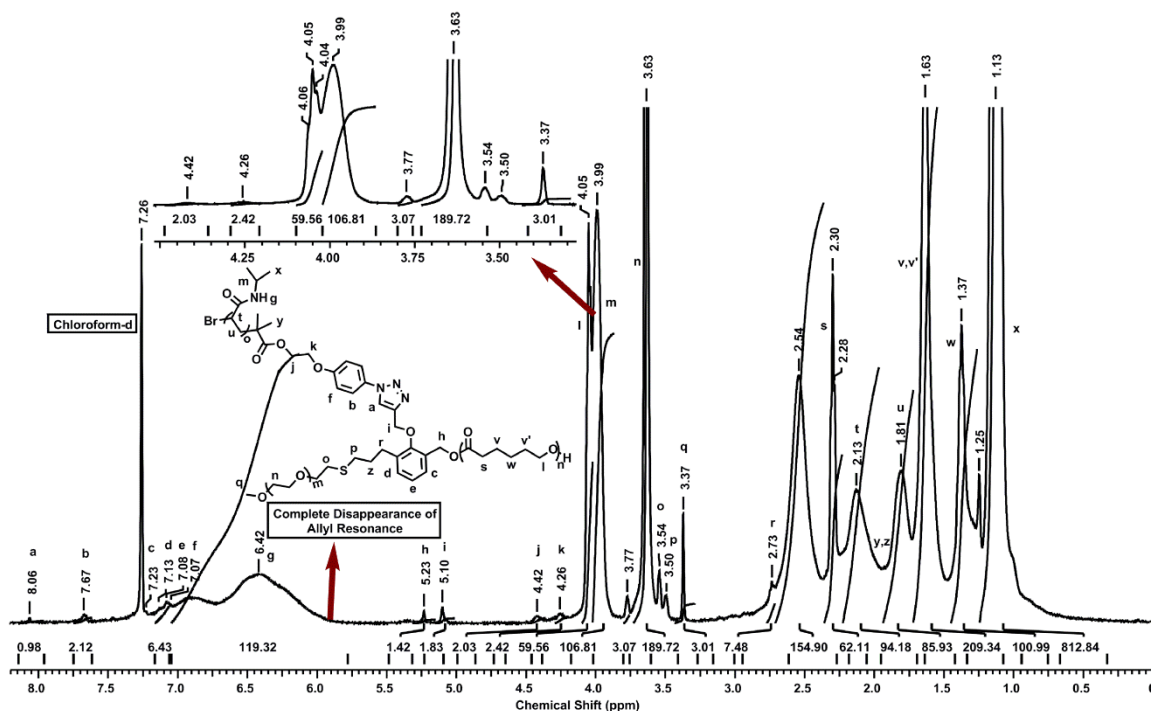
Figure 3.23 ^{1}H NMR spectrum (in CDCl$_3$) of PCL-PNIPAAm-mPEG miktoarm star terpolymer.

The shift of GPC curve of PCL-PNIPAAm-mPEG terpolymer to the higher retention volume confirmed the formation of miktoarm star terpolymer (**Figure 3.24**). The incorporation of poly(ethylene glycol) arm shifts the retention volume of PCL-PNIPAAm-mPEG miktoarm star terpolymer to the higher side due to the greater dipolar interaction of PEG block with the stationary phase of GPC column.[31, 71] The combined results of ^{1}H NMR spectroscopy and GPC measurements indicated that the target polymer *viz* PCL-PNIPAAm-mPEG was formed.
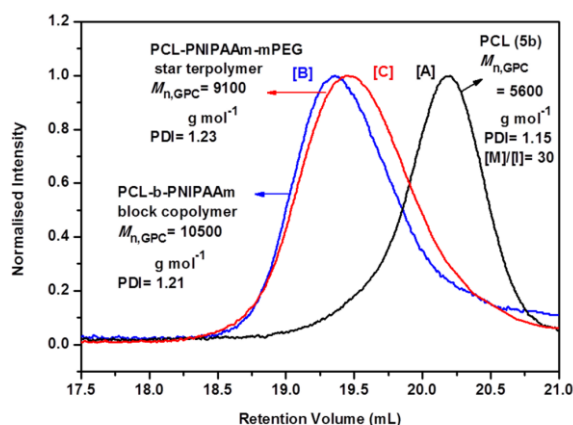
Figure 3.24 GPC trace of A) α-allyl, α'-propargyloxy bifunctionalised poly(ε-caprolactone) (**5b**) B) allyl mid functional PCL-*b*-PNIPAAm block copolymer C) PCL-PNIPAAm-mPEG miktoarm star terpolymer.

Thus, the utility of α-allyl, α'-allyloxy and α-allyl, α'-propargyloxy bifunctionalised poly(ε-caprolactone)s for the synthesis of miktoarm star copolymer was demonstrated. However, considering the need to use high molar excess of thiol-terminated polymer in thiol-ene polymer-polymer conjugation reaction and laborious and extensive purification steps involved, the approach presented herein for synthesizing star copolymers using thiol-ene reaction is of limited scope and utility.

3.3.8 Self-assembly and temperature responsive behaviour of assembly of PCL-PNIPAAm-mPEG star copolymer

The self-assembly of PCL-PNIPAAm-mPEG star copolymer in aqueous solution was studied. To confirm the formation of self-assembly, the polymer solution (0.1 wt %) was prepared in water at 26 ^{o}C and tested for DLS at 90° angle. The average size of assembled structure of PCL-PNIPAAm-mPEG copolymer in water at 26 ^{o}C was found to be 206±2 nm.

PCL-PNIPAAm-mPEG star copolymer exhibited LCST behaviour due to the presence of PNIPAAm arm. LCST of 0.1 wt % solution of PCL-PNIPAAm-mPEG star copolymer was determined in water by measuring the transmittance loss with increasing temperature at a fixed wavelength of 500 nm (**Figure 3.25**). LCST (*i.e*. transmittance of 90 %) of 0.1 wt % aqueous solution of PCL-PNIPAAm-mPEG star copolymer was 34.4 ^{o}C which was higher than that of precursor allyl mid-functionalized PCL-*b*-PNIPAAm copolymer. The attachment of hydrophilic PEG arm to PCL-*b*-PNIPAAm copolymer increased the LCST by 2.4 ^{o}C.
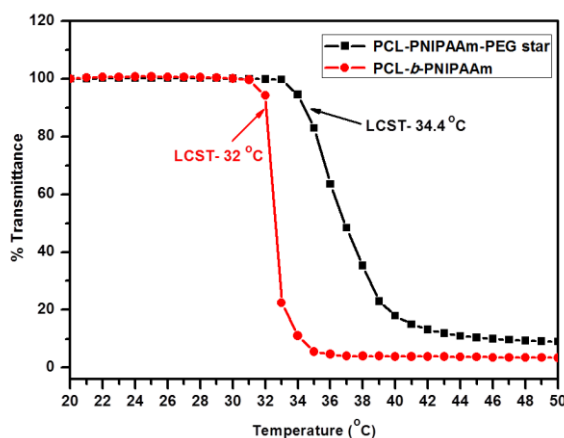
Figure 3.25 LCST determination of PCL-PNIPAAm-mPEG star copolymer by transmittance measurements (500 nm).

The heating and cooling cycle of PCL-PNIPAAm-mPEG copolymer (0.1 wt %) solution showed hysteresis which might be due to the slower rate of equilibration process of thermo-reversible polymers (**Figure 3.26**).
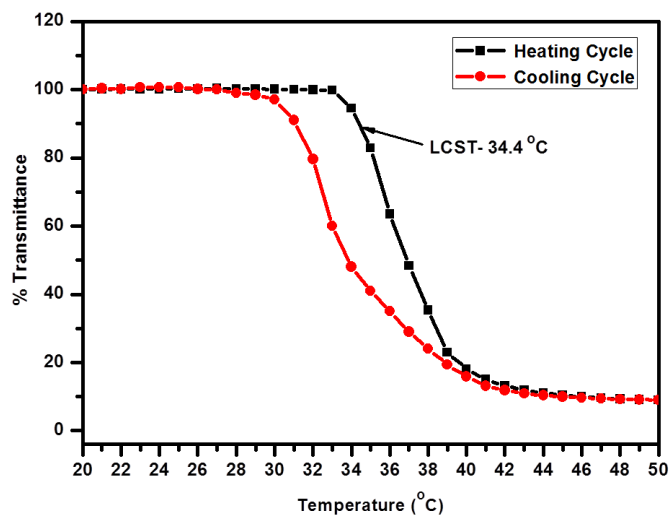
Figure 3.26 Thermo-reversibility (heating-cooling cycle) of PCL-PNIPAAm-mPEG (0.1 wt %) star copolymer.

Temperature dependence of size of assemblies of PCL-PNIPAAm-mPEG star copolymer was monitored using DLS. It was found that with increasing temperature the size of polymer assemblies decreased initially due to swollen to globular transition of PNIPAAm arm on PCL core and finally increased due to precipitation of PCL-PNIPAAm-mPEG copolymer from aqueous solution (**Figure 3.27**).
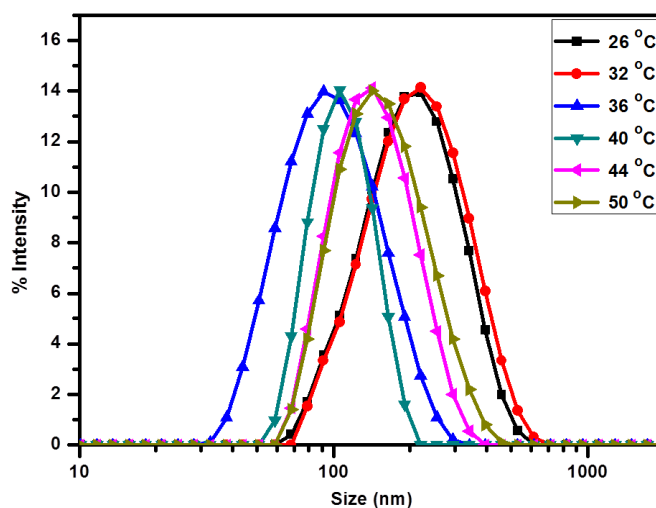
Figure 3.27 Temperature dependence of size of assemblies of PCL-PNIPAAm-mPEG (0.1 wt %) star copolymer in water.

TEM analysis of assembly of PCL-PNIPAAm-mPEG star copolymer at 26±1 ^{o}C (below LCST) showed spherical micelles of average size 180±5 nm. It was found that at 40±1 ^{o}C temperature (above LCST) these micelles squeezed to the size of 100±5 nm due to collapse of PNIPAAm arm on PCL hydrophobic core (**Figure 3.28**).
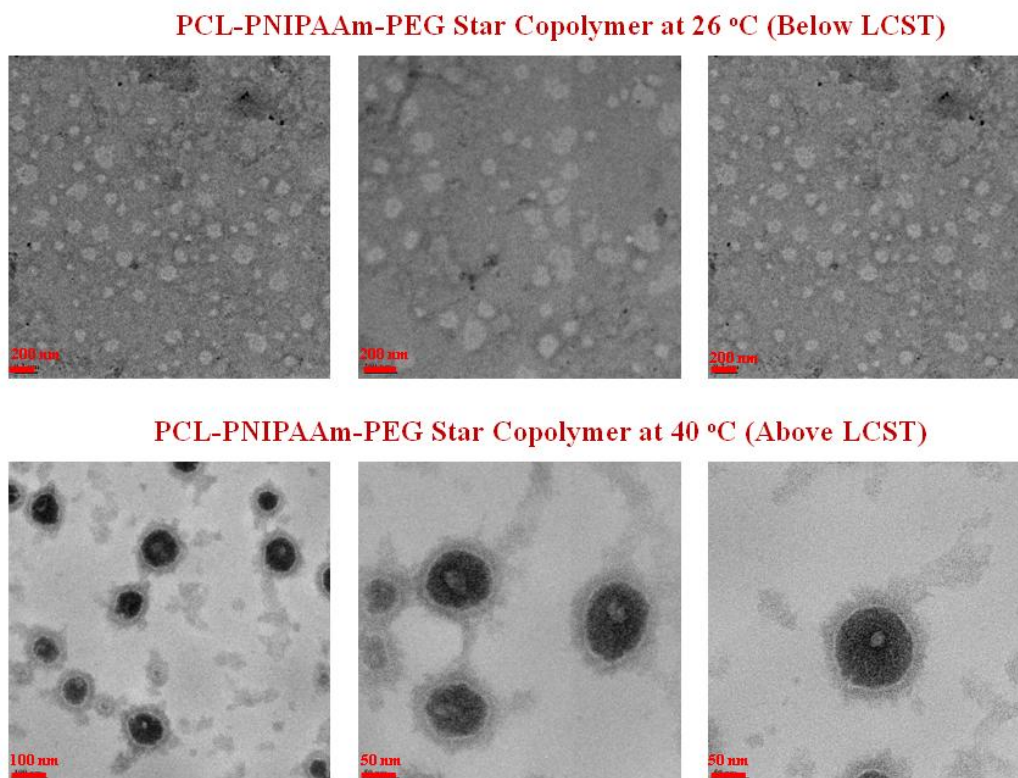
Figure 3.28 TEM images of assemblies of PCL-PNIPAAm-mPEG (0.1 wt %) star copolymer at A) 26±1°C and B) 40±1°C.

To confirm these TEM observations, the encapsulation of hydrophobic fluorescent probe (pyrene) and hydrophilic fluorescent dye (rhodamine-B) in the assemblies of PCL-PNIPAAm-mPEG copolymer at 26 ^{o}C (below LCST) and 36 ^{o}C (above LCST) were performed. It was observed that at 26 ^{o}C the assemblies encapsulated pyrene (**Figure 3.29**), whereas at 26 ^{o}C and 36 ^{o}C the assemblies failed to encapsulate rhodamine-B dye (**Figure 3.30**). These pyrene and rhodamine-B guest encapsulation results were the direct confirmation of formation of micelles with hydrophobic core at 26 ^{o}C which just squeezed to smaller size assemblies at 36-40 ^{o}C (above LCST) due to the collapse of PNIPAAm arm on PCL hydrophobic core.
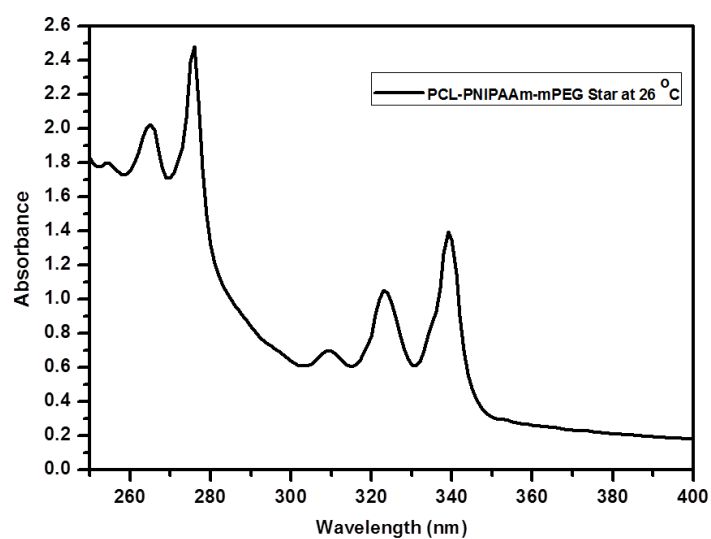
Figure 3.29 Absorption spectra of pyrene in PCL-PNIPAAm-mPEG (0.1 wt %) star copolymer at 26 $^{\circ}$C.
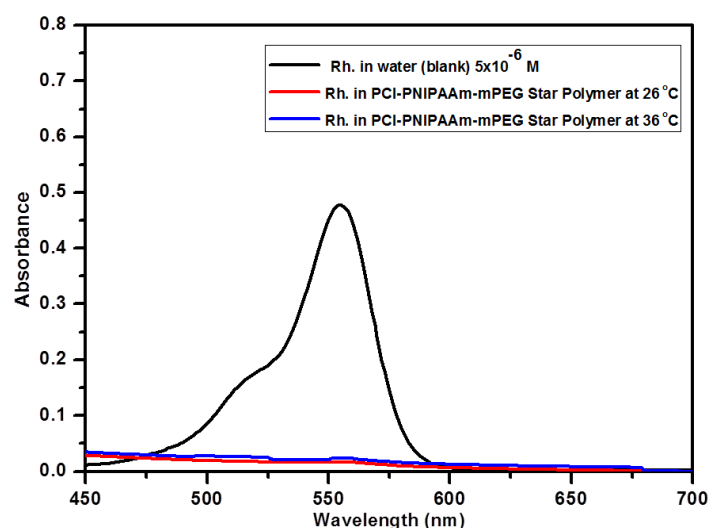
Figure 3.30 Absorption spectra of A) Rhodamine-B in water B) Rhodamine-B in PCL-PNIPAAm-mPEG (0.1 wt %) star copolymer at 26 $^{\circ}$C and C) Rhodamine-B in PCL-PNIPAAm-mPEG (0.1 wt %) star copolymer at 36 $^{\circ}$C.

3.3.9 Temperature responsive release kinetics of pyrene from PCL-PNIPAAm-mPEG star copolymer micelles

Pyrene was encapsulated in the micelles of PCL-PNIPAAm-mPEG star copolymer at 26 $^{\circ}$C and the release studies were performed with increasing temperature (**Figure 3.31**).

It was found that the pyrene release was much faster at 40 $^{\circ}$C and 36 $^{\circ}$C as compared to the release at 26 $^{\circ}$C which could be attributed to the squeezing of micelles due to collapse of PNIPAAm arm on PCL hydrophobic core.
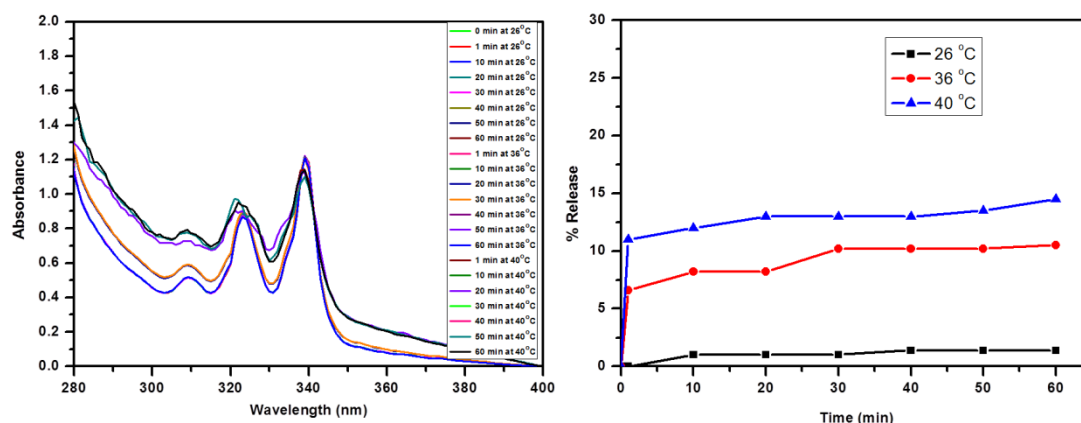
Figure 3.31 A) Absorption spectra of pyrene in PCL-PNIPAAm-mPEG (0.1 wt %) star copolymer at different temperatures and B) Pyrene release profiles of PCL-PNIPAAm-mPEG (0.1 wt %) star copolymer at 26 $^{\circ}$C; 36 $^{\circ}$C and 40 $^{\circ}$C.

3.4 Conclusions

Two new ROP initiators, namely, (3-allyl-2-(allyloxy)phenyl)methanol and (3-allyl-2-(prop-2-yn-1-yloxy)phenyl)methanol containing reactive functionalities such as allyl, allyloxy and allyl, propargyloxy, respectively, were synthesized starting from a common precursor- 3-allylsalicyaldehyde. Well defined α,α'- homo- and α,α'-hetero-bifunctionalised poly(ε-caprolactone)s were conveniently synthesized by controlled polymerization of ε-caprolactone employing these ROP initiators. Thiol-ene reaction and orthogonal alkyne-azide and thiol-ene reactions, respectively, of α-allyl, α'-allyloxy and α-allyl, α'-propargyloxy bifunctionalised poly(ε-caprolactone)s were studied to synthesize (mPEG)$_2$-PCL and PCL-PNIPAAm-mPEG star copolymer. The preliminary characterization of star copolymers was performed by ^{1}H NMR spectroscopy and GPC. The limitations of thiol-ene polymer-polymer conjugation reaction for the synthesis of miktoarm star copolymers were highlighted.

Furthermore, the temperature dependence of size and morphological changes of assemblies of PCL-PNIPAAm-mPEG star copolymer were studied under the conditions of varying temperature. Temperature dependant pyrene release kinetics from micelles of PCL-PNIPAAm-mPEG star copolymer showed faster release with increasing temperature.

It was found that the pyrene release was much faster at 40 $^{\circ}$C and 36 $^{\circ}$C as compared to the release at 26 $^{\circ}$C which could be attributed to the squeezing of micelles due to collapse of PNIPAAm arm on PCL hydrophobic core.

3.5 References

1.   M. Morell, X. F. Francos, J. Gombau, F. Ferrando, A. Lederer, B. Voit and A. Serra, *Prog. Polym. Sci.*, 2012, **73**, 62-69.

2.   Q. Qiu, G. Liu and Z. An, *Chem. Commun.*, 2011, **47**, 12685-12687.

3.   A. K. Singh, R. Prakash and D. Pandey, *Polym. Chem.*, 2012, **2**, 10316-10323.

4.   Y. Cao, J. Feng and P. Wu, *J. Mater. Chem.*, 2012, **22**, 14997-15005.

5.   T. Cai, M. Li, K. G. Neoh and E. T. Kang, *J. Mater. Chem.*, 2012, **22**, 16248-16258.

6.   Y. Chu, H. Yu, Y. Zhang, G. Zhang, Y. Ma, R. Zhuo and X. Jiang, *J. Polym. Sci., Part A: Polym. Chem.*, 2014, **52**, 3346-3355.

7.   J. Hu, J. He, M. Zhang and P. Ni, *Polym. Chem.*, 2015 **6**, 1553-1566.

8.   W. Lin, S. Nie, Q. Zhong, Y. Yang, C. Cai, J. Wang and L. Zhang, *J. Mater. Chem. B*, 2014, **2**, 4008-4020.

9.   P. Theato, B. S. Sumerlin, R. K. O'Reilly and I. T. H. Epps, *Chem. Soc. Rev.*, 2013, **42**, 7055--7056.

10.   J. Zhuang, M. R. Gordon, J. Ventura, L. Li and S. Thayumanavan, *Chem. Soc. Rev.*, 2013, **42**, 7421-7435.

11.   E. Blasco, B. V. K. J. Schmidt, C. B. Kowollik, M. Pinol and L. Oriol, *Polym. Chem.*, 2013, **4**, 4506-4514.

12.   H. Liu, C. Li and S. Liu, *Langmuir*, 2009, **25**, 4724-4734.

13.   G. M. Soliman, A. Sharma, D. Maysinger and A. Kakkar, *Chem. Commun.*, 2011, **47**, 9572-9587.

14.   G. M. Soliman, R. Sharma, A. O. Choi, S. K. Varshney, F. M. Winnik, A. K. Kakkar and D. Maysinger, *Biomaterials* 2010, **31**, 8382-8392.

15.   Y. Zhang, H. Liu, J. Hu, C. Li and S. Liu, *Macromol. Rapid Commun.*, 2009, **30**, 941-947.

16.   W. He, H. Jiang, L. Zhang, Z. Cheng and X. Zhu, *Polym. Chem.*, 2013, **4**, 2919-2938.

17. H. Yin, S. W. Kang and Y. H. Bae, *Macromolecules*, 2009, **42**, 7456-7464.

18. K. Yoon, H. C. Kang, L. Li, H. Cho, M. K. Park, E. Lee, Y. H. Bae and K. M. Huh, *Polym. Chem.*, 2015, **6**, 531-542.

19. K. Matyjaszewski, *Macromolecules*, 2012 **45**, 4015-4039.

20. P. Lecomte and C. Jerome, *Adv. Polym. Sci.*, 2012, **245**, 173-218.

21. E. Harth, C. J. Hawker, W. Fan and R. M. Waymouth, *Macromolecules*, 2001, **34**, 3856-3862.

22. G. Moad, Y. K. Chong, A. Postma, E. Rizzardo and S. H. Thang, *Polymer*, 2005 **46**, 8458-8468.

23. T. Erdogan, Z. Ozyurek, G. Hizal and U. Tunca, *J. Polym. Sci., Part A: Polym. Chem.*, 2004, **42**, 2313-2320.

24. K. V. Bernaerts and F. E. D. Prez, *Prog. Polym. Sci.*, 2006, **31**, 671-722.

25. L. P. Yang, X. H. Dong and C. Y. Pan, *J. Polym. Sci., Part A: Polym. Chem.*, 2008, **46**, 7757-7772.

26. K. Khanna, S. Varshney and A. Kakkar, *Polym. Chem.*, 2010, **1**, 1171-1185.

27. J. Ferreira, J. Syrett, M. Whittaker, D. Haddleton, T. P. Davis and C. Boyer, *Polym. Chem.*, 2011 **2**, 1671-1677.

28. A. Sulistio, A. Blencowe, A. Widjaya, X. Zhang and G. Qiao, *Polym. Chem.*, 2012, **3**, 224-234.

29. U. Tunca, *J. Polym. Sci., Part A: Polym. Chem.*, 2014, **52**, 3147-3165.

30. R. K. Iha, K. L. Wooley, A. M. Nystrom, D. J. Burke, M. J. Kade and C. J. Hawker, *Chem. Rev.*, 2009, **109**, 5620-5686.

31. B. Iskin, G. Yilmaz and Y. Yagci, *Polym. Chem.*, 2011, **2**, 2865-2871.

32. A. Vora, K. Singh and D. C. Webster, *Polymer*, 2009, **50**, 2768-2774.

33. J. Zhu, X. Zhu, E. T. Kang and K. G. Neoh, *Polymer*, 2007, **48**, 6992-6999.

34. Y. Y. Yuan, Y. C. Wang, J. Z. Du and J. Wang, *Macromolecules*, 2008, **41**, 8620-8625.

35. C. Li, Z. Ge, H. Lie and S. Liu, *J. Polym. Sci., Part A: Polym. Chem.*, 2009, **47**, 4001-4013.

36. O. Altintas, A. P. Vogt, C. B. Kowollik and U. Tunca, *Polym. Chem.*, 2012, **3**, 34-45.

37. E. Doganci, M. Gorur, C. Uyanik and F. Yilmaz, *J. Polym. Sci., Part A: Polym.*

Chem., 2014, **52**, 3390-3399.

38. O. Altintas and U. Tunca, *Chem. Asian J.*, 2011, **6**, 2584-2591.

39. R. Riva, S. Schmeits, F. Stoffelbach, C. Jerome, R. Jerome and P. Lecomte, *Chem. Comm.*, 2005, 5334-5336.

40. C. B. Kowollik, F. E. D. Prez, P. Espeel, C. J. Hawker, T. Junkers, H. Schlaad and W. V. Camp, *Angew. Chem. Int. Ed.*, 2011, **50**, 60-62.

41. K. V. Butsele, C. A. Fustin, J. F. Gohy, R. Jerome and C. Jerome, *Langmuir*, 2009 **25**, 107-111.

42. P. Tirino, C. Conte, M. Ordegno, R. Palumbo, F. Ungaro, F. Quaglia and G. Maglio, *Macromol. Chem. Phys.*, 2014 **215**, 1218−1229.

43. Z. Iatridi and C.Tsitsilianis, *Polymers*, 2011, **3**, 1911-1933.

44. L. Sun, L. J. Shen, M. Q. Zhu, C. M. Dong and Y. Wei, *J. Polym. Sci., Part A: Polym. Chem.*, 2010, **48**, 4583-4593.

45. S. Kobben, A. Ethirajan and T. Junkers, *J. Polym. Sci., Part A: Polym. Chem.*, 2014, **52**, 1633-1641.

46. L. M. Campos, K. L. Killops, R. Sakai, J. M. J. Paulusse, D. Damiron, E. Drockenmuller, B. W. Messmore and C. J. Hawker, *Macromolecules*, 2008, **41**, 7063-7070.

47. H. Wang, J. He, M. Zhang, Y. Tao, F. Li, K. C. Tam and P. Ni, *J. Mater. Chem. B*, 2013, **1**, 6596-6607.

48. K. Satoh, J. E. Poelma, L. M. Campos, B. Stahl and C. J. Hawker, *Polym. Chem.*, 2012, **3**, 1890-1898.

49. O. Eren, M. Gorur, B. Keskin and F. Yilmaz, *React. Funct. Polym.*, 2013 **73**, 244-253.

50. H. Yang, Q. Zhang, B. Lin, G. Fu, X. Zhang and L. Guo, *J. Polym. Sci., Part A: Polym. Chem.*, 2012, **50**, 4182-4190.

51. M. A. Tasdelen, *Polym. Chem.*, 2011, **2**, 2133-2145.

52. J. Zheng, S. Xie, F. Lin, G. Hua, T. Yu, D. H. Renekar and M. L. Becker, *Polym. Chem.*, 2013, **4**, 2215-2218.

53. A. Dag, H. Durmaz, V. Kirmizi, G. Hizal and U. Tunca, *Polym. Chem.*, 2010 **1**, 621-623.

54. H. Durmaz, A. Sanyal, G. Hizal and U. Tunca, *Polym. Chem.*, 2012, **3**, 825-835.

55.   B. Iskin, G. Yilmaz and Y. Yagci, *J. Polym. Sci., Part A: Polym. Chem.*, 2011, **49**, 2417-2422.

56.   H. Durmaz, A. Dag, A. Hizal, G. Hizal and U. Tunka, *J. Polym. Sci., Part A: Polym. Chem.*, 2008, **46**, 7091-7100.

57.   P. S. Sane, B. V. Tawade, I. Parmar, S. Kumari, S. Nagane and P. P. Wadgaonkar, *J. Polym. Sci., Part A: Polym. Chem.*, 2013, **51**, 2091-2103.

58.   R. Mahou and C. Wandrey, *Polymers*, 2012, **4**, 561-589.

59.   J. H. Xia, S. G. Gaynor and K. Matyjaszewski, *Macromolecules*, 1998, **31**, 5958-5959.

60.   R. Mahou and C. Wandrey, *Polymers*, 2012, **4**, 561-589.

61.   N. Gimeno, R. M. Rapun, S. R. Conde, J. L. Serrano, C. L. Folcia, M. A. Pericas and M. B. Ros, *J. Mater. Chem.*, 2012, **22**, 16791-16800.

62.   G. Montaudo, F. Samperi and M. S. Montaudo, *Prog. Polym. Sci.*, 2006 **31**, 277-357.

63.   S. P. S. Koo, M. M. Stamenovic, R. A. Prasath, A. J. Inglis, F. E. D. Prez, C. B. Kowollik, W. V. Camp and T. Junkers, *J. Polym. Sci., Part A: Polym. Chem.*, 2010, **48**, 1699-1713.

64.   M. Li, P. De, S. R. Gondi and B. S. Sumerlin, *J. Polym. Sci., Part A: Polym. Chem.*, 2008, **46**, 5093-5100.

65.   J. Xu and C. Boyer, *Macromolecules*, 2015, **48**, 520-529.

66.   N. B. Cramer, J. P. Scott and C. N. Bowman, *Macromolecules*, 2002, **35**, 5361-5365.

67.   E. Q. Rosenthal, J. E. Puskas and C. Wesdemiotis, *Biomacromolecules*, 2012, **13**, 154-164.

68.   M. Trollsas, B. Atthof, A. Wursch and J. L. Hedrick, *Macromolecules*, 2000, **33**, 6423-6438.

69.   W. Agut, D. Taton and S. Lecommandoux, *Macromolecules*, 2007, **40**, 5653-5661.

70.   D. Han, X. Tong and Y. Zhao, *J. Polym. Sci., Part A: Polym. Chem.*, 2012, **50**, 4198-4205.

71.   F. Bahadori, A. Dag, H. Durmaz, N. Cakir, H. Onyuksel, U. Tunca, G. Topcu and G. Hizal, *Polymers*, 2014, **6**, 214-242.

Chapter 4

Temperature and pH Dual Stimuli Responsive PCL-*b*-PNIPAAm Block Copolymer Assemblies and the Cargo Release Studies

4.1 Introduction

Well-defined stimuli-responsive polymers[1-3] are a class of smart materials which undergo significant changes in properties in response to external stimuli. These polymers find potential applications in drug delivery,[4] emulsification,[5] sensing or detection,[6] catalysis,[7] self-healing,[8, 9] etc. The response of these smart polymers to stimuli such as pH,[10] temperature,[11] redox,[12] magnetic field,[13] light (ultra-violet or visible),[14] etc. in macromolecular architectures such as block,[15-18] graft,[19] star,[20, 21] cyclic[22] and cross-linked[23]/hyperbranched[24, 25] polymers has been extensively studied. The combination of controlled/living polymerization methods such as NMP,[26] ATRP,[27] RAFT,[28, 29] ROP,[30] etc. with click reactions have been widely explored to obtain such stimuli-responsive smart macromolecular architectures. Stimuli-responsive amphiphilic macromolecular architectures tend to self-assemble into different morphologies in the aqueous solution and can non-covalently encapsulate hydrophobic dyes/drugs in the self-assembled structures.[31] The release of these encapsulated materials from the self-assembled structures with external stimulus due to the change in morphology or structure, polarity and hydrophilic-hydrophobic balance of amphiphilic polymer has been considered to be of practical interest.[32]

A range of block copolymer systems containing either single or multiple stimuli responsive structural units have been reported in the literature.[27, 28, 33-39] Polymeric systems which respond to the combination of two or multiple stimuli would be more attractive for release of the guest materials. However, a limited number of reports are available in the literature concerning dual stimuli-responsive polymers, which contain polymeric chains and functional groups, capable of responding to temperature as well as pH in a single polymeric system.[40-46] Such dual-stimuli responsive systems gain the advantage of increased temperature and decreased pH environments of cancer tissues compared to the normal healthy tissues to release the encapsulated guest materials without providing the external stimulus source. The development and precisely targeted release of encapsulated materials from the assemblies of such temperature and pH dual stimuli-responsive polymeric systems in response to the tumour environments is a challenging task for research communities and has been relatively less explored.

We herein designed a dual-stimuli *viz.* temperature and pH responsive PCL-*b*-PNIPAAm block copolymer system bearing acetal as a pH- cleavable linkage and

PNIPAAm as temperature responsive block using the combination of ATRP, ROP and CuAAC click reaction. Temperature and pH dependence of size and morphological changes of assemblies of PCL-*b*-PNIPAAm block copolymer were studied under the conditions of varying temperature and pH. The pyrene release kinetics from micelles of PCL-*b*-PNIPAAm block copolymer system with response to these stimuli was found to be faster with increasing temperature and decreasing pH.

4.2 Experimental Section

4.2.1 Materials

2-Azidoethanol was synthesized from 2-chloroethanol according to the literature procedure.[47] Ethylene glycol vinyl ether (97 %), pyridinium p-toluenesulfonate (PPTS) (98 %), α-bromoisobutyryl bromide (98 %), propargyl alcohol (99 %), tin (II) 2-ethylhexanoate (95 %), copper chloride (99 %) and *N,N,N',N'',N''*-pentamethyldiethylenetriamine (PMDETA) (99 %) were purchased from Sigma Aldrich and were used as received. *N*-Isopropylacrylamide (Aldrich) was recrystallised from n-hexane and dried at room temperature before use. Copper bromide (99.99 %, Sigma Aldrich) was stirred over acetic acid to remove copper (II) bromide, washed with ethanol and dried at 60 ^{o}C for 12 h. Me$_6$TREN was synthesized according the literature procedure.[48] Triethylamine was stirred over potassium hydroxide and distilled prior to use. Isopropanol (Merck, India), ε-caprolactone (99 %, Sigma) and dichloromethane were stirred over calcium hydride overnight and distilled before use.

4.2.2 Characterisation and measurements

FT-IR spectra were recorded on Perkin Elmer Spectrum GX spectrophotometer using chloroform as a solvent. NMR spectra were recorded on Bruker- 400 or 500 MHz spectrometer in CDCl$_3$ as a solvent. Molecular weights and dispersity values of PNIPAAm-N$_3$, Pr-PCL and PCL-*b*-PNIPAAm block copolymer were determined by gel permeation chromatography (GPC) equipped with Viscotek VE-1122 pump, two Viscotek (T6000N, General Mixed) columns and Viscotek VE-3580 RI detector and tetrahydrofuran as an eluent at flow rate of 1 mL/min. Polymer concentration for GPC analysis was 5 mg/mL and narrow dispersity polystyrene(s) were used as calibration standards. The detector and column temperatures were set to 30 ^{o}C and the sample injection volume for GPC analysis was fixed at 20 μL.

Matrix assisted laser desorption ionisation - time of flight (MALDI-TOF) spectra were recorded on AB-SCIEX TOF/TOF 5800 instrument with linear/reflector positive operating method in tetrahydrofuran as a solvent using DCTB (10 mg/mL, 5 volume equivalent with polymer) as a matrix at 26 $^{\circ}$C. The end functionality of polymers was determined by spotting the mixture of 4 μL polymer sample (1 mg/mL) with 20 μL of DCTB (10 mg/mL) as matrix and 1 μL of sodium iodide as an ionising agent (0.2 g/mL) on a metal target plate. Mass range was selected on the basis of molecular weights previously determined from ^{1}H-NMR spectroscopy. Molecular weights and dispersity of polymers were also determined from MALDI-TOF analysis. LCST was determined on Agilent UV-Visible spectrophotometer equipped with Agilent 89090A peltier cooling system whereas the pyrene/rhodamine encapsulation or release studies were performed on Specord 210 Plus (analyticjena) UV-Visible spectrophotometer. Fluorescence study was performed on VARIAN CARY Eclipse fluorescence spectrophotometer. Dynamic light scattering (DLS) experiments were performed using a Nano ZS-90 apparatus (Malvern Instruments) with 633 nm red laser (at 90° angle). TEM images were obtained from TEM-Tecnai G2 20S-Twin (200 KV) microscope at different temperature.

4.2.3 Synthesis

4.2.3.1 Synthesis of 2-(vinyloxy)ethyl 2-bromo-2-methylpropanoate (1)

Into a 500 mL round bottom flask equipped with a magnetic stir bar, an argon inlet and an addition funnel were charged ethylene glycol vinyl ether (5 g, 56.74 mmol), triethylamine (11.48 g, 113.48 mmol) and dichloromethane (150 mL). The reaction mixture was cooled to 0 $^{\circ}$C in an ice bath and the solution of α-bromoisobutyryl bromide (15.65 g, 68.09 mmol) in dichloromethane (50 mL) was added dropwise while stirring over a period of 30 min. The reaction mixture was stirred overnight at room temperature, filtered, washed with sodium bicarbonate (2×100 mL) and water (2×100 mL). The combined organic layer was evaporated to afford 11.3 g (84 %) of 2-(vinyloxy)ethyl 2-bromo 2-methyl propanoate (**1**) as a yellowish liquid.

IR (CHCl$_3$, cm^{-1}): 1738 (C=O) and 1620 (C=C).

^{1}H-NMR (200 MHz, CDCl$_3$, δ/ppm): 6.45 (q, 1H), 4.39 (t, 2H), 4.13 (dd, 1H), 4.08 (dd, 1H), 3.91 (t, 2H), 1.92 (6H).

^{13}C-NMR (50 MHz, CDCl$_3$, δ/ppm): 171.51, 151.41, 87.13, 65.44, 64.04, 55.43, 30.65.

4.2.3.2 Synthesis of 2-(1-(2-azidoethoxy)ethoxy)ethyl 2-bromo-2-methylpropanoate (2)

Into a 100 mL round bottom flask equipped with a magnetic stir bar, an argon inlet and an addition funnel were charged **1** (1.49 g, 6.28 mmol), PPTS (0.15 g, 0.62 mmol) and dichloromethane (30 mL). The reaction mixture was cooled to 0 ^{o}C in an ice bath and the solution of 2-azidoethnaol (0.60 g, 6.91 mmol) in dichloromethane (20 mL) was added dropwise while stirring over a period of 30 min. The reaction mixture was stirred additionally for 3 h and quenched by adding dilute sodium caronate solution. The reaction mixture was washed with water (2×100 mL). The organic layer was evaporated and the crude product was purified by column chromatography using pet ether:ethyl acetate (80:20, v/v) as an eluent to afford 1.94 g (95 %) of 2-(1-(2-azidoethoxy)ethoxy)ethyl 2-bromo 2-methyl propanoate (**2**) as a colourless liquid.

IR (CHCl$_3$, cm^{-1}): 2109 (N$_3$) and 1736 (C=O).

^{1}H-NMR (400 MHz, CDCl$_3$, δ/ppm): 4.83 (q, 1H), 4.33 (t, (2H), 3.76-3.86 (m, 2H), 3.69-3.76 (m, 1H), 3.59-3.66 (m, 1H), 3.39 (q, 2H), 1.94 (s, 6 H), 1.35 (d, 3H).

^{13}C-NMR (50 MHz, CDCl$_3$, δ/ppm): 171.54, 99.67, 65.03, 63.63, 62.30, 55.56, 50.82, 30.71, 19.23.

4.2.3.3 Synthesis of azido-terminated poly(*N*-isopropylacrylamide) (PNIPAAm-N$_3$) by ATRP

Into a 20 mL flame dried Schlenk tube fitted with a rubber septum and an argon inlet were charged 2-(1-(2-azidoethoxy)ethoxy)ethyl 2-bromo 2-methyl propanoate (0.095 g, 0.29 mmol), *N*-isopropylacrylamide (5 g, 44.18 mmol), Me$_6$TREN (0.067 g, 0.29 mmol) and isopropanol (10 g). The reaction mixture was purged with argon for 20 min and then copper chloride (0.029 g, 0.29 mmol) was added under the positive pressure of argon. After three vaccum freeze pump-thaw cycles, the Schlenk tube was allowed to attain the room temperature (28 ^{o}C) and stirred for appropriate time under argon. The polymerization reaction was quenched by sudden cooling the Schlenk tube in liquid nitrogen with exposure to air. The solvent was removed under reduced pressure and the crude product was precipitated into cold n-hexane, filtered and dried under reduced pressure. The percentage conversion of the reaction was determined by ^{1}H NMR spectroscopy. Polymer was purified by dissolving in THF and passing through a small bed of neutral alumina

column to remove the copper salts, concentrated, precipitated into cold diethyl ether, filtered and dried at 40 °C to afford white solid.

IR (CHCl$_3$, cm^{-1}): 3309 (N–H), 2110 (–N$_3$) and 1651 (–C=O of amide).

^{1}H-NMR (400 MHz, CDCl$_3$, δ/ppm): 6.47 (broad peak from N–H of PNIPAAm), 4.81 (broad peak, 1H), 4.19 (broad t, 2H), 3.99 (s, C–H from PNIPAAm), 3.76 (broad peak, 2H), 3.54-3.71 (m, 2H), 3.4 (q, 2H), 1.2-2.5 (m, –CH$_2$ and –CH from PNIPAAm backbone), 1.13 (broad s, –CH$_3$ from PNIPAAm).

4.2.3.4 Synthesis of propargyl-terminated poly(ε-caprolactone) (Pr-PCL) by ROP

Into a 30 mL flame dried Schlenk tube fitted with a rubber septum and an argon inlet were charged ε-caprolactone (20 g, 175.43 mmol), tin (II) 2-ethylhexanoate (1.183 g, 2.92 mmol) and propargyl alcohol (0.327 g, 5.84 mmol). The reaction mixture was purged with argon for 30 min and the Schlenk tube was immersed in oil bath preheated at 95 °C and stirred for appropriate time (30 min) under argon. The polymerization reaction was quenched by sudden cooling the Schlenk tube in liquid nitrogen. The conversion of reaction was determined from ^{1}H NMR spectroscopy (50 %). The polymer was purified by repeated precipitations in acidified methanol and filtered to afford white solid (M$_{n,NMR}$-2100 g mol^{-1}).

IR (CHCl$_3$, cm^{-1}): 1737 (C=O) and 2127 (–C≡C–).

^{1}H-NMR (400 MHz, CDCl$_3$, δ/ppm): 4.67 (d,2H), 4.05 (t, –CH$_2$–O from poly(ε-caprolactone) backbone), 3.63 (t, 2H), 2.47 (t, 1H), 2.30 (t, –CH$_2$–CO from poly(ε-caprolactone) backbone), 1.5-1.7 (m, –CH$_2$–CH$_2$ from poly(ε-caprolactone) backbone), 1.31-1.45 (m, –CH$_2$–CH$_2$ from poly(ε-caprolactone) backbone).

4.2.3.5 Synthesis of PCL-*b*-PNIPAAm block copolymer containing acetal linkage by alkyne-azide click reaction

A flame dried 10 mL Schlenk tube fitted with a rubber septum and equipped with a magnetic stir bar was thoroughly evacuated with argon and was charged with Pr-PCL (0.23 g, 0.109 mmol, $M_{n,NMR}$-2100 g mol^{-1}, Dispersity-1.09), PNIPAAm-N$_3$ (1 g, 0.09 mmol, $M_{n,NMR}$-11000 g mol^{-1}, Dispersity-1.2), PMDETA (0.0157 g, 0.09 mmol) and THF (5 mL). The reaction mixture was degassed thrice by vacuum freeze pump-thaw cycles. Copper bromide (0.013 g, 0.09 mmol) was then added under the positive pressure of argon and stirred at room temperature for 24 h. The reaction mixture was passed through a small

bed of alumina column to remove the copper residues, concentrated and precipitated into cold methanol and filtered to remove the excess PCL. The filtrate was evaporated and the product was dried at room temperature to obtain PCL-*b*-PNIPAAm block copolymer containing acetal linkage as a white solid (Yield-95 %, $M_{n,NMR}$-12900 g mol^{-1}, Dispersity-1.2).

IR (CHCl$_3$, cm^{-1}): 1726 (C=O of PCL) and 1649 (C=O of PNIPAAm).

^{1}H-NMR (500 MHz, CDCl$_3$, δ/ppm): 7.73 (s, 1H), 6.10 (broad peak from N–H of PNIPAAm), 5.21 (s, 2H), 4.74 (s, 1H), 4.73 (s, 1H), 4.55 (broad s, 1H), 4.19 (broad peak, 2H), 4.06 (t, –CH$_2$–O from poly(ε-caprolactone) backbone), 4.01 (s, C–H from PNIPAAm), 3.84 (broad peak, 2H), 3.64 (t, 2H), 3.55-3.7 (m, 2H), 3.50 (broad peak, 2H), 2.30 (t, –CH$_2$–CO from poly(ε-caprolactone) backbone), 1.3-2.2 (m, –CH$_2$ and –CH from PNIPAAm backbone), 1.5-1.70 (m, –CH$_2$–CH$_2$ from poly(ε-caprolactone), 1.3-1.42 (m, –CH$_2$–CH$_2$ from poly(ε-caprolactone) backbone), 1.14 (broad s, –CH$_3$ from PNIPAAm).

4.2.4 Preparation of polymer aqueous solution, dye encapsulation and release studies

The aqueous solution of polymer was prepared by direct dissolution in water (for temperature dependant studies) or in buffer solution (for pH dependant studies). Pyrene was encapsulated in a micellar solution by hydrating a film of pyrene (5×10^{-5} M) using 0.1 wt % aqueous polymer solution. After stirring for 24 h, the polymer solution was filtered through 0.45 μm PVDF filter and was used for absorbance and release studies. The absorbance of pyrene encapsulated solution was measured at different time intervals by applying varying temperatures or pH to determine the percentage release. The percent release of pyrene was determined based on the decrease in absorbance of encapsulated pyrene in the polymer solution. Rhodamine-B dye (5×10^{-6} M) was encapsulated in 0.1 wt % polymer solution in water and dialysed against water at 26 ^{o}C and 36 ^{o}C to remove non-encapsulated rhodamine-B. The absorbance and fluorescence of rhodamine-B encapsulated solution was measured to determine percentage encapsulation at these temperatures. The release of rhodamine-B, which was encapsulated in the polymer solution at 36 ^{o}C, was studied at 26 ^{o}C (below LCST) by measurement of the decrease in absorbance at different time intervals under dialysis conditions.

4.3 Results and Discussion

4.3.1 Design and synthesis of 2-(1-(2-azidoethoxy)ethoxy)ethyl 2-bromo-2-methylpropanoate (2) ATRP initiator

A new ATRP initiator *viz.* 2-(1-(2-azidoethoxy)ethoxy)ethyl 2-bromo-2-methylpropanoate containing both cleavable (acetal) and clickable (azido) groups was designed and synthesized starting from commercially available ethylene glycol vinyl ether.

The reaction of ethylene glycol vinyl ether with 2-bromoisobutyryl bromide in the presence of triethylamine afforded 2-(vinyloxy)ethyl 2-bromo-2-methylpropanoate (**Scheme 4.1**).
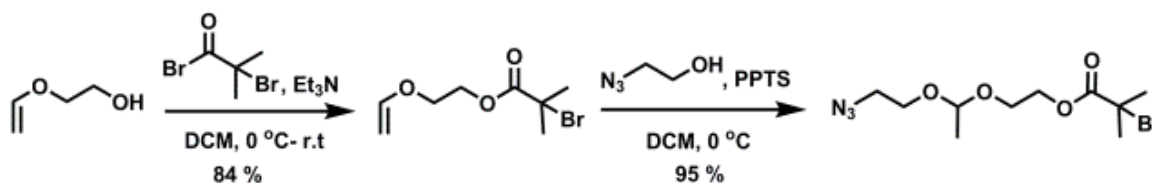
Scheme 4.1 Synthesis of 2-(1-(2-azidoethoxy)ethoxy)ethyl 2-bromo-2-methylpropanoate (**2**).

The formation of 2-(vinyloxy)ethyl 2-bromo-2-methylpropanoate and stability of vinyl ether moiety under reaction conditions was confirmed by FT-IR and NMR spectroscopy. The appearance of peak at 1738 cm^{-1} corresponding to ester linkage in FT-IR spectrum and the presence of a quartet at 6.45 ppm and a singlet at 1.92 ppm corresponding to vinyl ether and methyl protons of ester linkage, respectively in ^{1}H NMR spectrum confirmed the formation of 2-(vinyloxy)ethyl 2-bromo-2-methylpropanoate and stability of vinyl ether moiety.

The reaction of 2-(vinyloxy)ethyl 2-bromo-2-methylpropanoate (**1**) with 2-azidoethanol in the presence of a catalytic amount of PPTS afforded the desired 2-(1-(2-azidoethoxy)ethoxy)ethyl 2-bromo-2-methylpropanoate (**2**). The appearance of a peak at 2109 cm^{-1} in FT-IR spectrum (**Figure 4.1**) and a quartet at 4.83 ppm and a doublet at 1.35 ppm corresponding to the acetal protons in ^{1}H NMR spectrum (**Figure 4.2**) confirmed the formation of 2-(1-(2-azidoethoxy)ethoxy)ethyl 2-bromo-2-methylpropanoate.
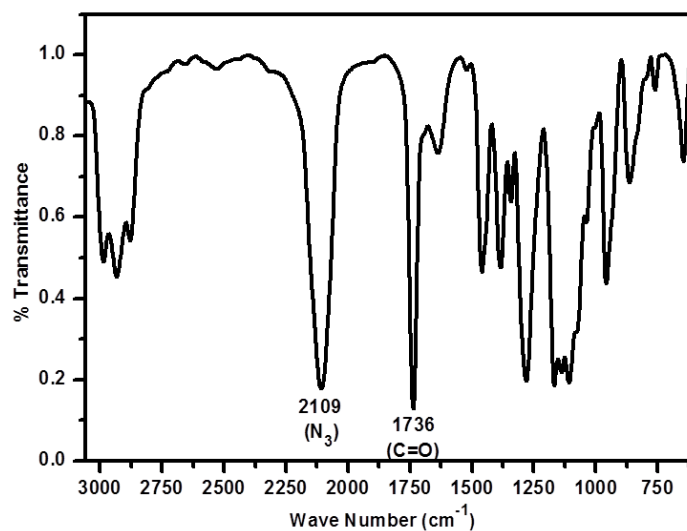
Figure 4.1 FT-IR spectrum (in chloroform) of 2-(1-(2-azidoethoxy)ethoxy)ethyl 2-bromo-2-methylpropanoate (**2**).

Figure 4.2 ^{1}H NMR spectrum (in CDCl$_3$) of 2-(1-(2-azidoethoxy)ethoxy)ethyl 2-bromo-2-methylpropanoate (**2**).

The remaining protons in ^{1}H-NMR spectrum and different sets of carbons in ^{13}C-NMR spectrum (**Figure 4.3**) were found to be in good agreement with the proposed

structure which further supported the formation of desired ATRP initiator *viz.* 2-(1-(2-azidoethoxy)ethoxy)ethyl 2-bromo-2-methylpropanoate (**2**). Furthermore, HR-MS analysis of initiator showed M/Z exactly matching with that of theoretical molecular weight (**Figure 4.4**) which confirmed the structure of (**2**).

Figure 4.3 ^{13}C NMR spectrum (in CDCl$_3$) of 2-(1-(2-azidoethoxy)ethoxy)ethyl 2-bromo-2-methylpropanoate (**2**).

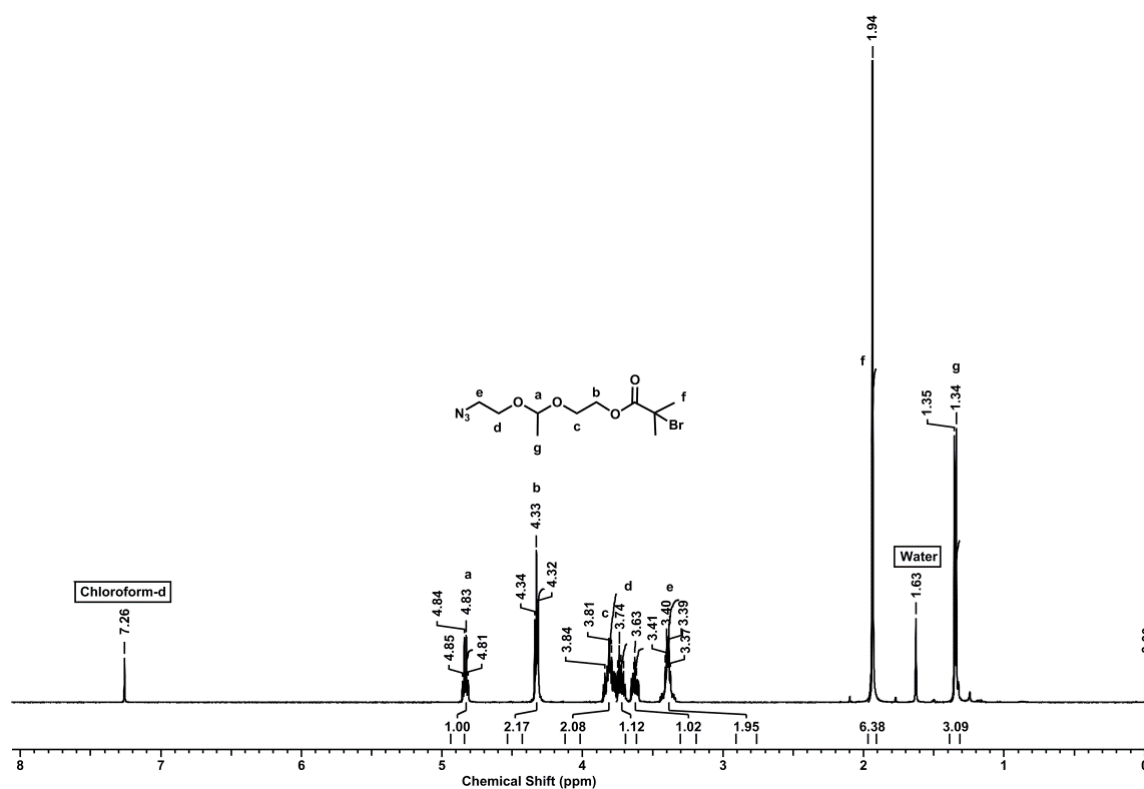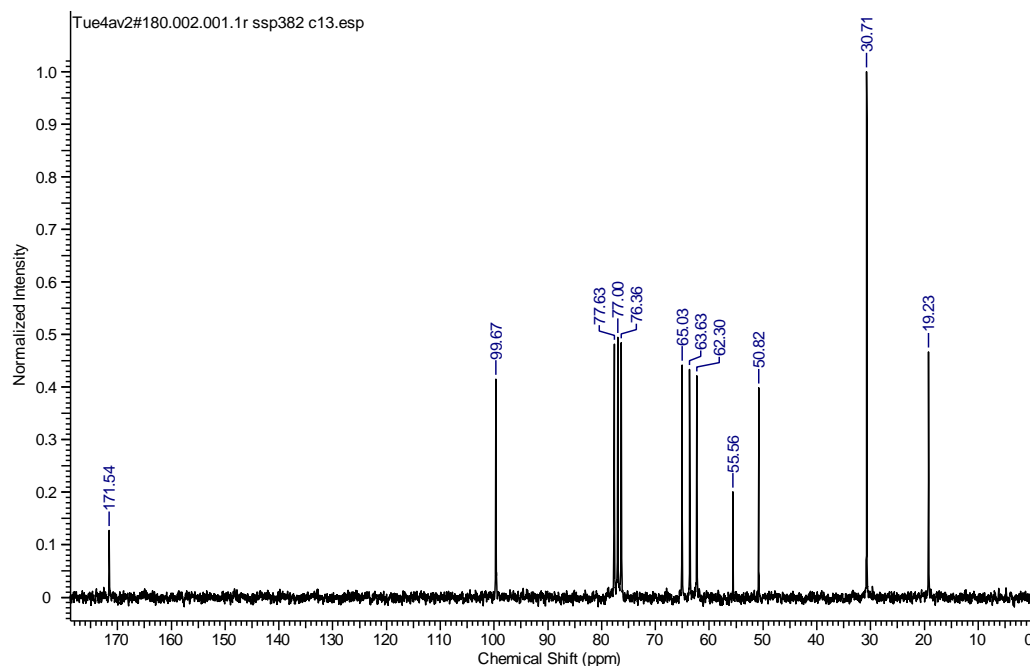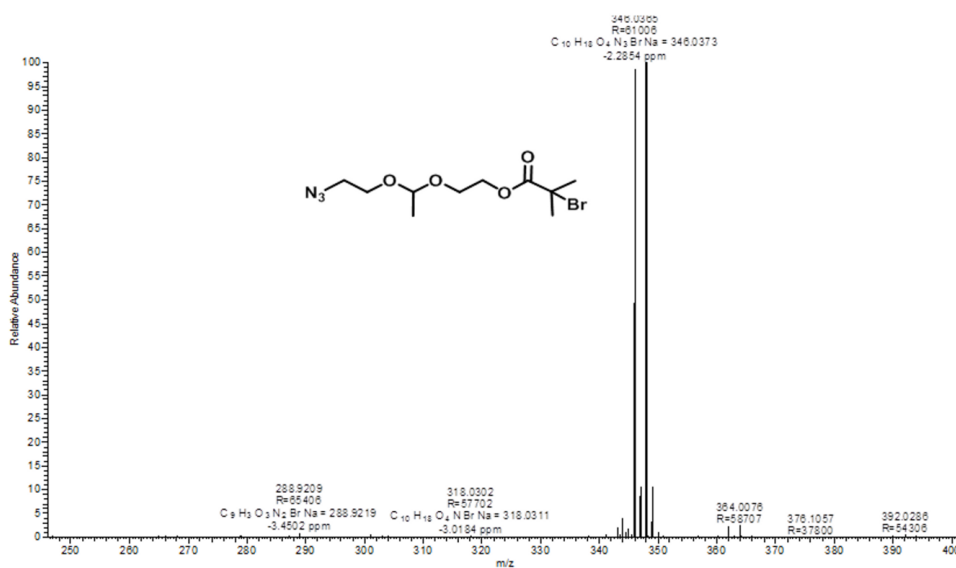**Figure 4.4** HR-MS spectrum of 2-(1-(2-azidoethoxy)ethoxy)ethyl 2-bromo-2-methylpropanoate (**2**).

The vinyloxy group in the intermediate compound **1** offers the opportunity in terms of choice of the incorporation of clickable moieties by reaction with appropriately substituted functional alcohols such as furfuryl alcohol, propargyl alcohol, allyl alcohol, etc. Thus compound **1** can be considered as a versatile precursor to obtain cleavable-clickable initiators potentially useful in controlled polymerization reactions to design smart materials based on stimuli-responsive block/star copolymers.

4.3.2 Synthesis of azido-terminated poly(*N*-isopropylacrylamide)s (PNIPAAm-N₃) by ATRP and their characterization

Azido-terminated PNIPAAm-N$_3$s were synthesized by ATRP of NIPAAm employing 2-(1-(2-azidoethoxy)ethoxy)ethyl 2-bromo-2-methylpropanoate initiator in the presence of copper chloride and Me$_6$TREN as the catalytic system (**Scheme 4.2**).
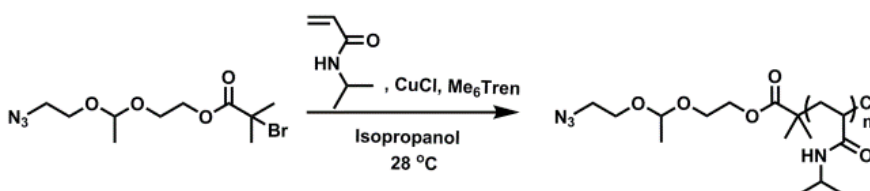
Scheme 4.2 Synthesis of azido-terminated poly(*N*-isopropylacrylamide) (PNIPAAm-N$_3$) by ATRP.

The presence of a peak at 2110 cm^{-1} in FT-IR spectrum of PNIPAAm-N$_3$ corresponding to azido-functionality confirmed the stability of azido-group under ATRP conditions[49] (**Figure 4.5**).

The appearance of acetal proton resonance at 4.81 ppm in ^{1}H-NMR spectrum (**Figure 4.6**) supported the presence of acetal linkage in the initiator fragment. Well defined azido-terminated PNIPAAm-N$_3$ with molecular weights and dispersity in the range 11000-19000 g mol^{-1} and 1.20-1.28, respectively, were prepared by varying monomer to initiator feed ratios. Molecular weights and dispersity of synthesized PNIPAAm-N$_3$ were found to be well controlled and narrow (**Table 4.1**). GPC trace of PNIPAAm-N$_3$ was found to be symmetric and monomodal which further supported the controlled polymerization behaviour.

Figure 4.5 FT-IR spectrum (in chloroform) of azido-terminated PNIPAAm.
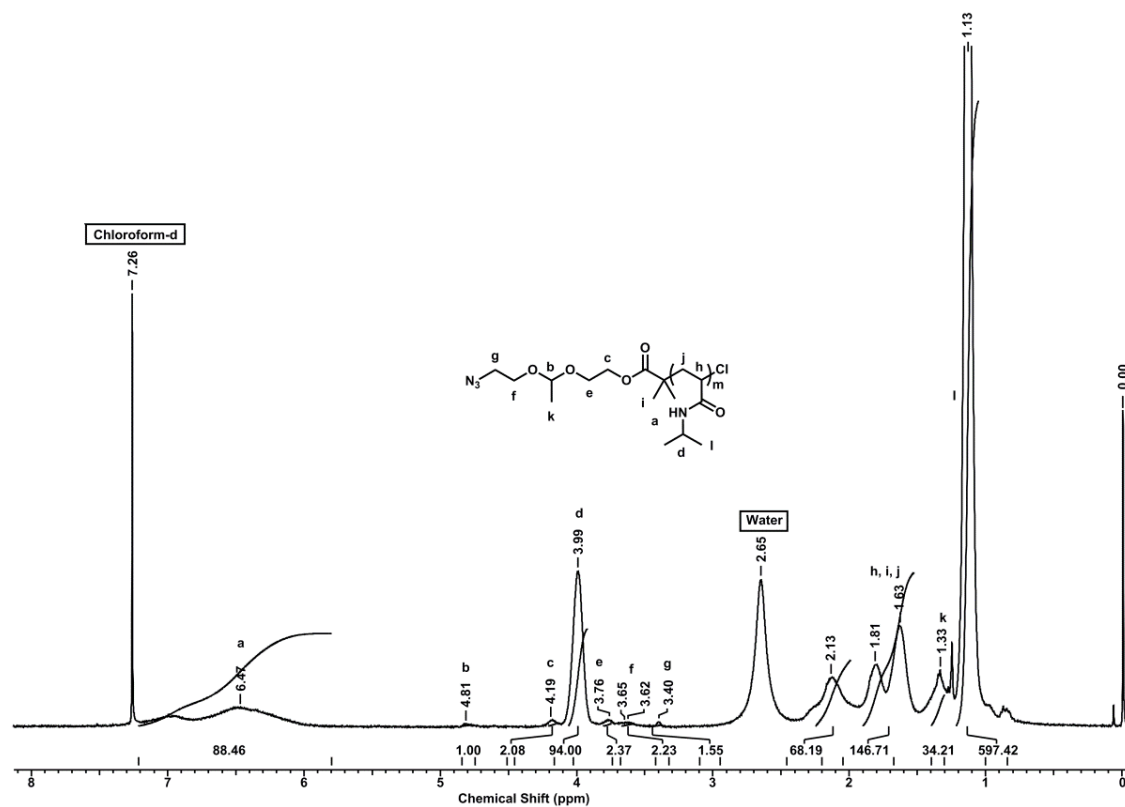
Figure 4.6 ^{1}H NMR spectrum (in CDCl$_3$) of azido- terminated poly(N-isopropylacrylamide) (PNIPAAm-N$_3$).

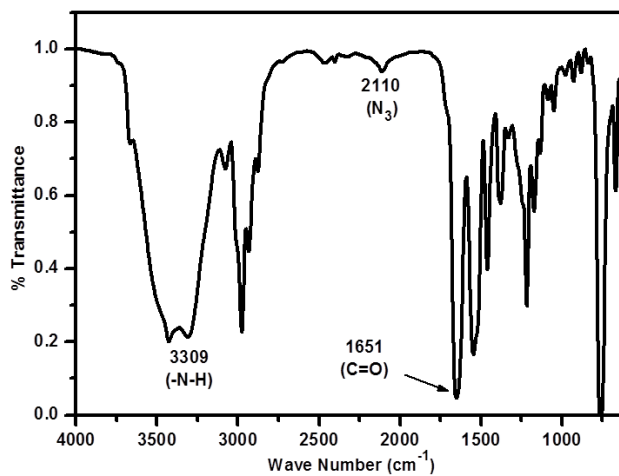**Table 4.1** Reaction parameters and results of synthesis of azido-terminated poly(*N*-isopropylacrylamide) (PNIPAAm-N$_3$).

Sr. No.	$[M]_0/[I]_0$ [a]	Time (h)	Conv. (%) [b]	$M_{n,theo}$ [c]	$M_{n,NMR}$ [d] g mol^{-1}	$M_{n,GPC}$ [e] g mol^{-1}	M_w/M_n	I^{eff} [f]
1	150	7	57	10000	11000	6600	1.20	0.91
2	200	12	70	16200	19000	10100	1.28	0.85

Temperature: 28°C, solvent: Isopropanol (1:2 w/w, w. r. t. monomer);

[a] $[M]_0/[I]_0$: [Monomer]$_0$/[Initiator]$_0$ feed ratio;

[b] Determined from ^{1}H-NMR spectrum;

[c] $M_{n,theo}$ = { $[M]_0/[I]_0$ ×(% conv.)/100 × mol. weight of monomer} + mol. weight of initiator;

[d] $M_{n,NMR}$ = Determined by ^{1}H-NMR spectroscopy;

[e] $M_{n,GPC}$ = Determined by GPC; Polystyrene standard; THF as an eluent;

[f] I^{eff} = $M_{n,theo}$ / $M_{n,NMR}$.

4.3.3 Synthesis of propargyl-terminated poly(ε-caprolactone) (Pr-PCL) by ROP and their characterization

Independently, propargyl-terminated poly(ε-caprolactone) (Pr-PCL) was synthesized (**Scheme 4.3**) by ROP of ε-caprolactone using propargyl alcohol as a counterpart for alkyne-azide click reaction. Molecular weight and dispersity of synthesized PCL was determined from GPC, ^{1}H NMR and MALDI-TOF spectroscopy.
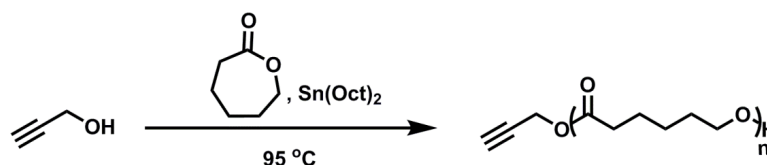
Scheme 4.3 Synthesis of propargyl-terminated poly(ε-caprolactone) (Pr-PCL) by ROP.

The presence of propargyl end group was determined by ^{1}H NMR spectroscopy (**Figure 4.7**) and MALDI-TOF analysis by calculating the molecular weight by addition of initiator fragment and monomer repeating units including the sodium ion. The molecular weight obtained from MALDI-TOF spectrum was in good agreement with calculated molecular weight which confirmed the presence of the propargyl functionality in Pr-PCL.
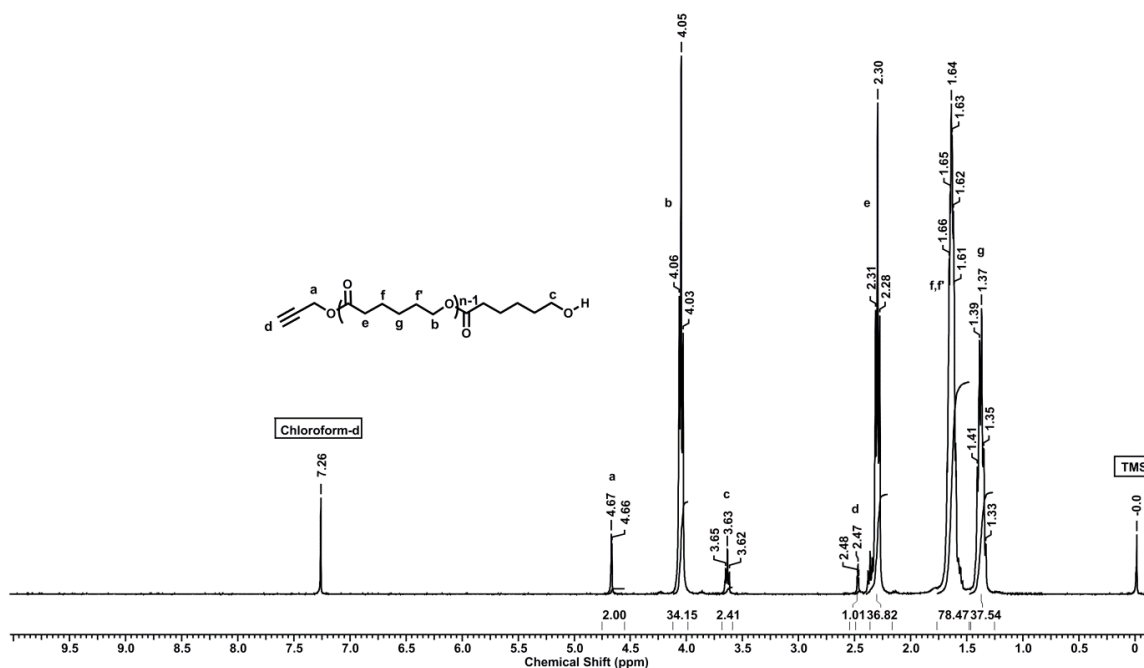
Figure 4.7 ^{1}H-NMR spectrum (in CDCl$_3$) of propargyl-terminated poly(ε-caprolactone) (Pr-PCL).

4.3.4 Synthesis of acetal containing PCL-*b*-PNIPAAm block copolymer by alkyne-azide click reaction and it's self-assembly behaviour

PCL-*b*-PNIPAAm block copolymer bearing acetal as a pH- cleavable linkage close to the junction point was synthesized using alkyne-azide click reaction of azido-terminated PNIPAAm-N$_3$ and propargyl-terminated PCL (**Scheme 4.4**)
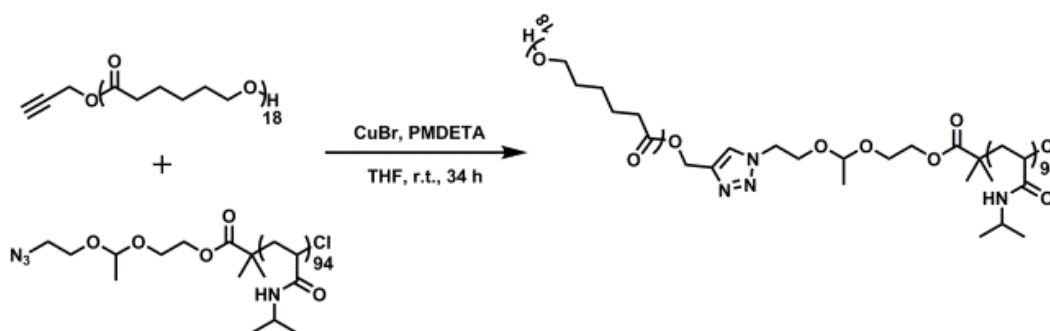
Scheme 4.4 Synthesis of acetal containing PCL-*b*-PNIPAAm block copolymer by alkyne-azide click reaction of PNIPAAm-N$_3$ and Pr-PCL.
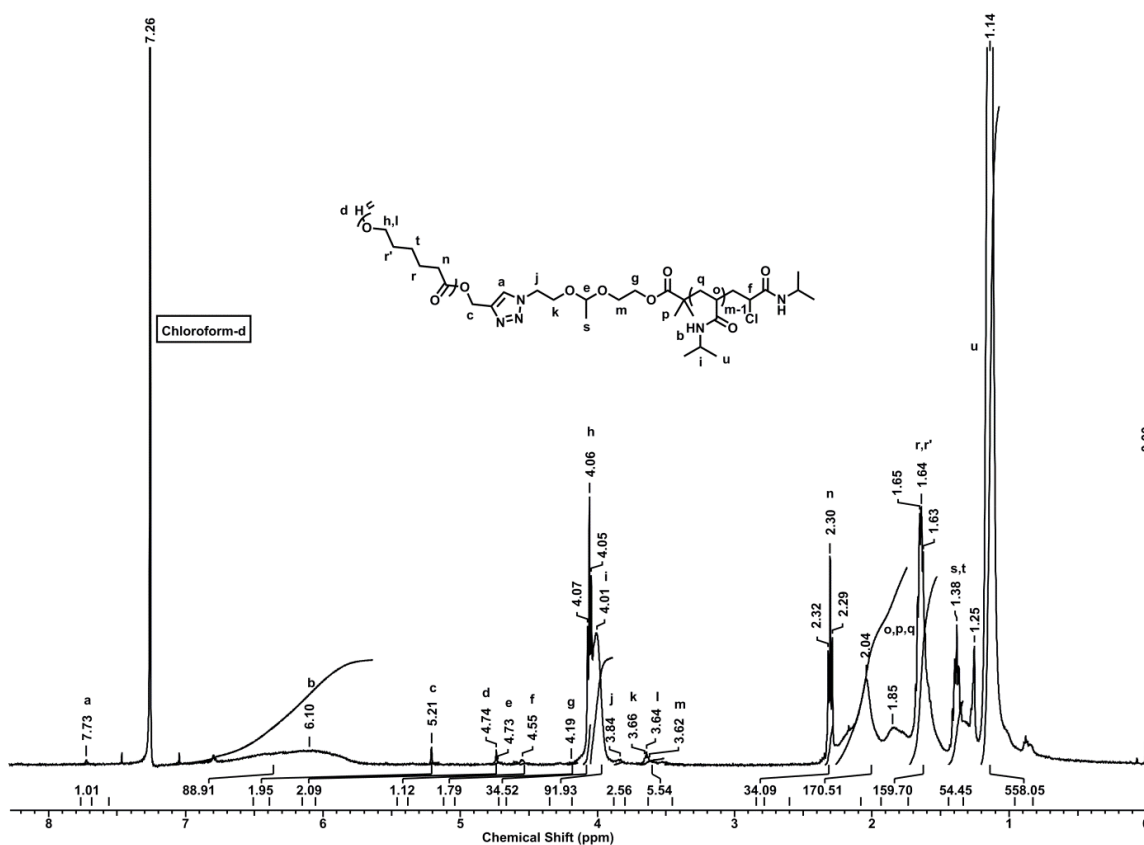
Figure 4.8 ^{1}H NMR spectrum (in CDCl$_3$) of acetal containing PCL-*b*-PNIPAAm block copolymer.

The complete disappearance of resonances at 4.67 ppm and 2.47 ppm corresponding to propargyl group and appearance of a singlet at 7.73 ppm corresponding to triazole proton in ^{1}H-NMR spectrum (**Figure 4.8**) confirmed the formation of PCL-*b*-PNIPAAm block copolymer. The presence of acetal resonance at 4.73 ppm in ^{1}H-NMR spectrum attested the inertness of acetal linkage under the click reaction conditions. Molecular weight and dispersity of PCL-*b*-PNIPAAm block copolymer was determined by GPC analysis. The complete shift of GPC curve of PCL-*b*-PNIPAAm block copolymer to the higher molecular weight side (lower retention volume) compared to GPC curve of PNIPAAm-N$_3$ and Pr-PCL confirmed the formation of block copolymer (**Figure 4.9**).

Critical aggregation concentration (CAC) of PCL-*b*-PNIPAAm block copolymer in water was determined by pyrene probe method using fluorescence spectroscopy.
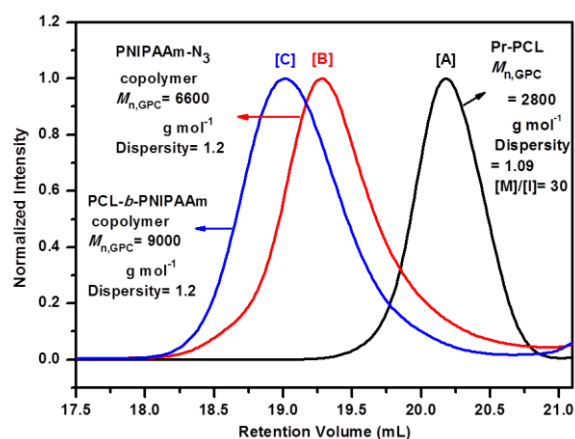
Figure 4.9 GPC trace of A) Pr-PCL B) PNIPAAm-N$_3$ and C) acetal containing PCL-*b*-PNIPAAm block copolymer.

The intersection point where the increase in intensity of a characteristic emission peak of pyrene at 370 nm (excitation at 334 nm) was found is referred to as CAC. To determine CAC value, a known amount of pyrene (5×10^{-6} M) was encapsulated in the aqueous solution of different concentrations of PCL-*b*-PNIPAAm block copolymer and stirred at 26 °C for 48 h. The pyrene emission spectra of all the samples were recorded. CAC of PCL-*b*-PNIPAAm block copolymer was determined by plotting intensity *vs* concentration and was found to be 8.99×10^{-6} M (**Figure 4.10**). Dynamic light scattering experiments (at 90° angle) were performed at 26 °C to verify the formation of assembly and to determine the size of assembled structure in aqueous solution. The polymer solution (0.1 wt %) was prepared in water at 26 °C and tested for DLS. The average size of assembled structure of PCL-*b*-PNIPAAm copolymer in water at 26 °C was found to be 76±2 nm.
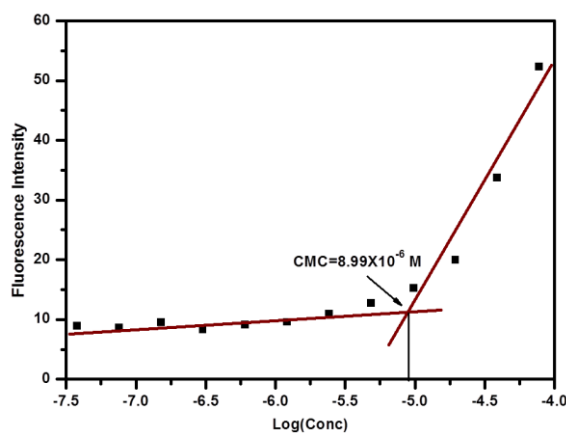
Figure 4.10 Critical aggregation concentration (CAC) of PCL-*b*-PNIPAAm block copolymer in water at 26 °C.

4.3.5 Temperature responsive behaviour of assembly of PCL-*b*-PNIPAAm block copolymer

PNIPAAm is well known to show LCST behavior and is considered as hydrophilic polymer at low temperatures (<LCST).[50] PCL-*b*-PNIPAAm copolymer exhibited LCST behavior due to the presence of PNIPAAm block. LCST of different concentrations of PCL-*b*-PNIPAAm copolymer was determined in water and in 7.4 pH phosphate buffer solution (PBS) by measuring the transmittance loss with increasing temperature at a fixed wavelength of 500 nm (**Figure 4.11**).

A temperature called as LCST where sudden decrease in transmittance (*i.e.* transmittance of 90 %) was obtained for all the samples. LCST of 0.1 wt % aqueous solution of PCL-*b*-PNIPAAm block copolymer was 32 ^{o}C and decreased with increasing polymer concentration (0.2 wt %). LCST of 0.1 wt % buffer solution of PCL-*b*-PNIPAAm block copolymer was found to be 30.1 ^{o}C which was lower than that of the LCST of 0.1 wt % solution of PCL-*b*-PNIPAAm in water. It is known that presence of salts in the solution decreases the LCST of polymers.[51] The attachment of hydrophobic PCL block to PNIPAAm decreased the LCST of precursor PNIPAAm-N$_3$ by 4.4 ^{o}C.
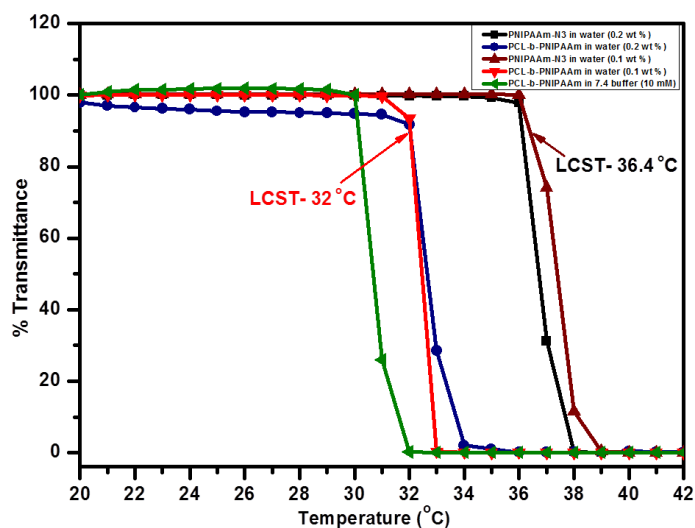
Figure 4.11 LCST determination of PCL-*b*-PNIPAAm block copolymer by transmittance measurements (500 nm).
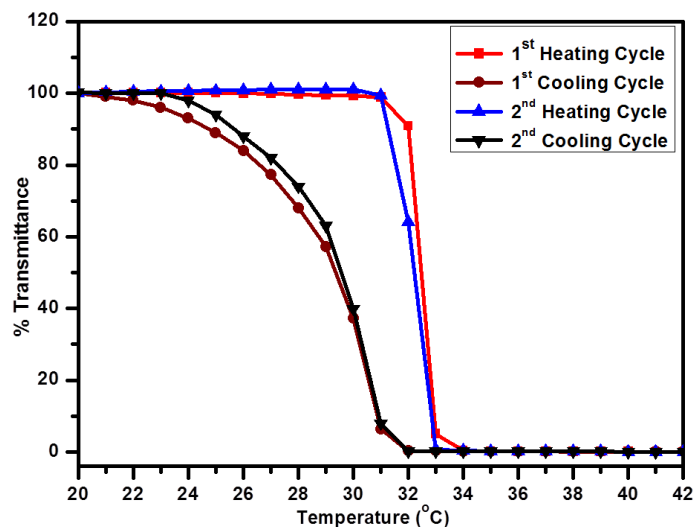
Figure 4.12 Thermo-reversibility (heating-cooling cycles) of PCL-*b*-PNIPAAm (0.1 wt %) block copolymer.

The repeated heating and cooling cycles of PCL-*b*-PNIPAAm copolymer (0.1 wt %) solution attested the thermo-reversibility of these block copolymer systems and the cycles showed hysteresis which might be attributed to the slower rate of equilibration process of thermo-reversible polymers (**Figure 4.12**). In these heating-cooling cycles, the regular and complete appearance and loss of transmittance was observed which confirmed the thermo-reversibility of PCL-*b*-PNIPAAm block copolymer systems (**Figure 4.13**).
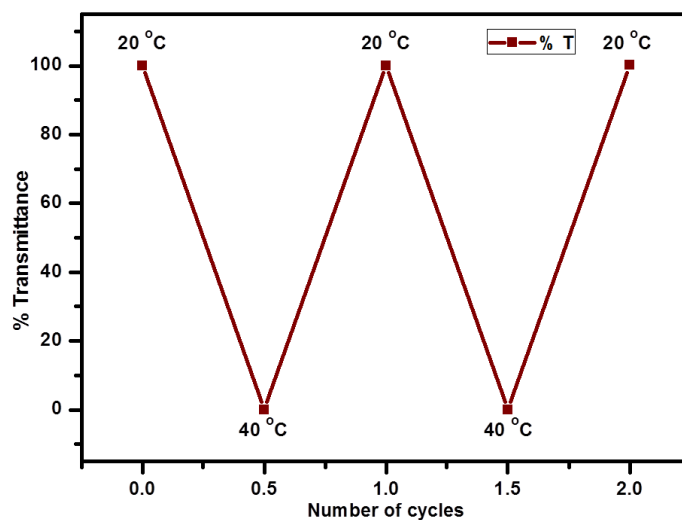
Figure 4.13 Regular appearance and loss of transmittance with different cycles of temperature.
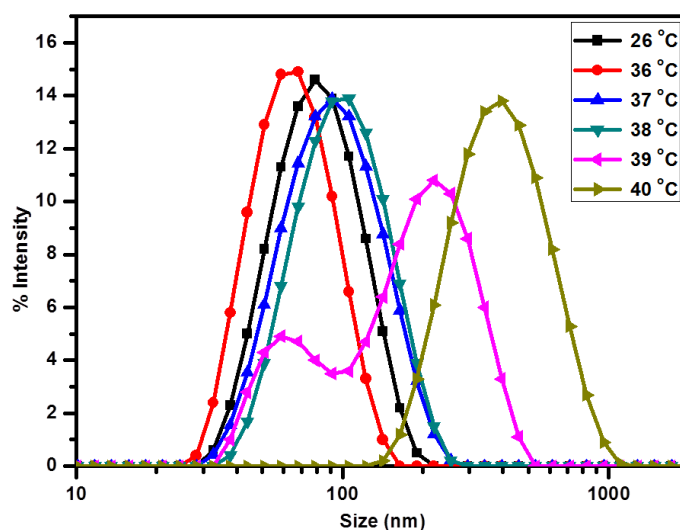
Figure 4.14 Temperature dependence of size of assemblies of PCL-*b*-PNIPAAm (0.1 wt %) block copolymer in water.

Temperature dependence of size of PCL-*b*-PNIPAAm block copolymer assemblies was monitored using DLS which showed that with increasing temperature the size of polymer assemblies decreased initially due to swollen to globular transition of PNIPAAm block on PCL core and finally increased due to complete precipitation of PCL-*b*-PNIPAAm copolymer from aqueous solution (**Figure 4.14**). TEM analysis of assembly of PCL-*b*-PNIPAAm block copolymer at 26±1 ^{o}C (below LCST) showed spherical micelles of average size 75±5 nm and with increasing temperature (above LCST) these initially transformed to vesicles of average size 95±5 nm and finally precipitated above 40 ^{o}C (**Figure 4.15**). To confirm these TEM observations, the encapsulation of hydrophobic fluorescent probe (pyrene) and hydrophilic fluorescent dye (rhodamine-B) in the assemblies of PCL-*b*-PNIPAAm copolymer below and above the LCST were performed. It was observed that at 26 ^{o}C the assemblies encapsulated pyrene but failed to encapsulate rhodamine-B dye, which was the direct confirmation of formation of micelles at 26 ^{o}C with hydrophobic core formed by PCL, whereas the assemblies were able to encapsulate the rhodamine-B dye above the LCST (at 36 ^{o}C). The emission spectrum of encapsulated rhodamine-B above the LCST showed emission wavelength of 573 nm which was 10 nm blue shifted compared to the emission wavelength of blank rhodamine-B in water (583 nm) due to the surrounded hydrophobic environment above the LCST (**Figure 4.16**).
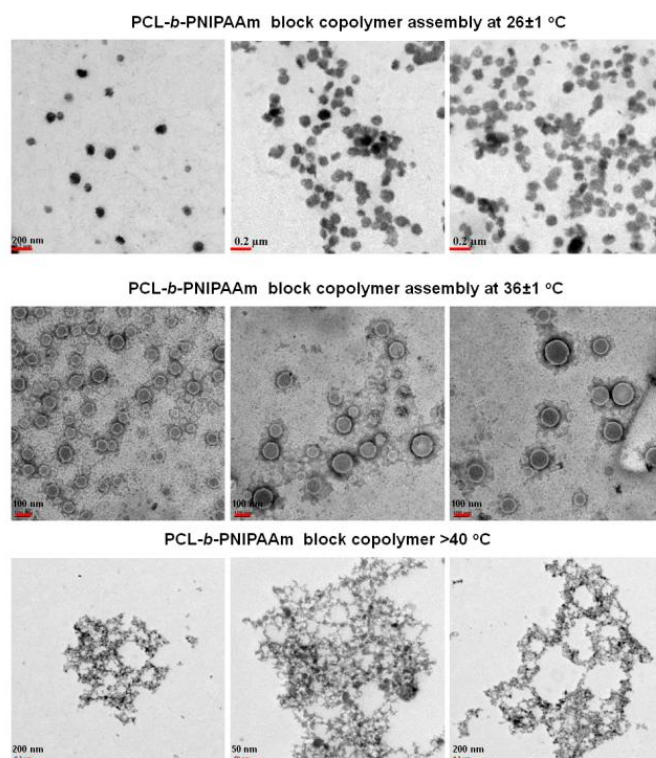
Figure 4.15 TEM images of aggregates of PCL-*b*-PNIPAAm (0.1 wt %) block copolymer at A) 26±1 °C B) 36±1 °C and C) >40 °C.
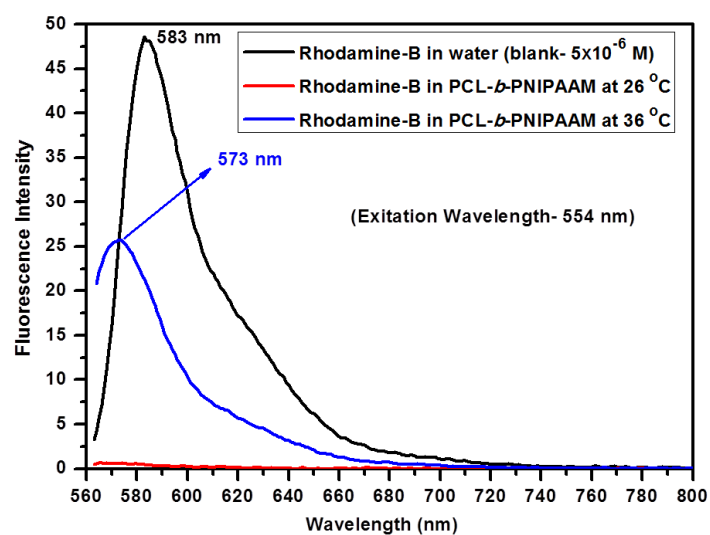
Figure 4.16 Emission spectra of A) Rhodamine-B in water B) Rhodamine-B in PCL-*b*-PNIPAAm (0.1 wt %) block copolymer at 26 °C and C) Rhodamine-B in PCL-*b*-PNIPAAm (0.1 wt %) block copolymer at 36 °C.

To confirm the formation of vesicles above LCST, absorbance of blank rhodamine-B in water and rhodamine-B encapsulated in PCL-*b*-PNIPAAm copolymer at 36 °C was

matched at 0.27 and the fluorescence spectra of samples were measured. The quenching of rhodamine-B in block copolymer at 36 $^{\circ}$C was indeed observed (**Figure 4.17**) albeit the quenching of rhodamine-B was marginal. The release of encapsulated rhodamine-B from these vesicles below LCST (26 $^{\circ}$C) was faster at the initial stages which supported the formation of vesicles at 36 $^{\circ}$C (**Figure 4.18**).
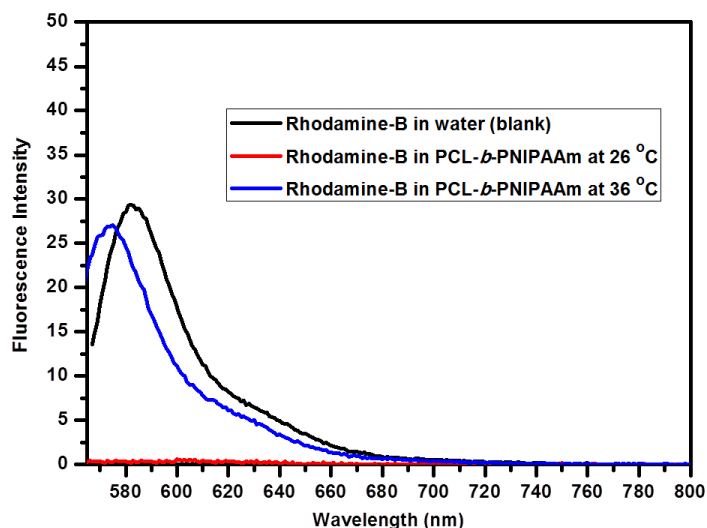
Figure 4.17 Emission spectra of A) Rhodamine-B in water (Absorbance - 0.27) B) Rhodamine-B in PCL-*b*-PNIPAAm (0.1 wt %) block copolymer at 26 $^{\circ}$C and C) Rhodamine-B in PCL-*b*-PNIPAAm (0.1 wt %) block copolymer (Absorbance - 0.27) at 36 $^{\circ}$C.
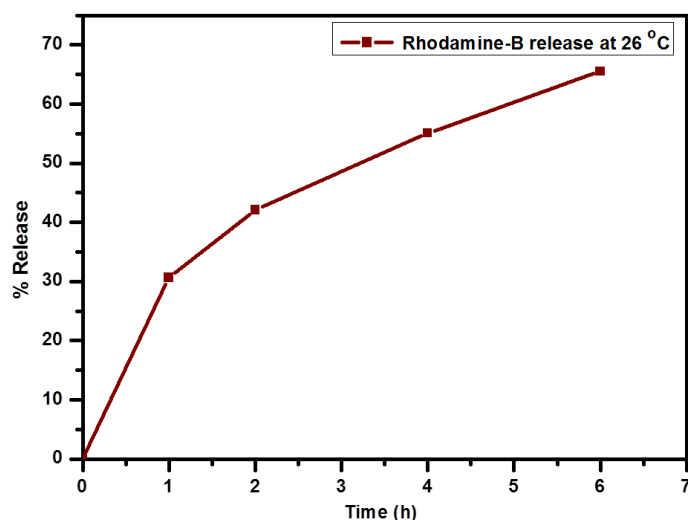
Figure 4.18 Rhodamine-B release from vesicles of PCL-*b*-PNIPAAm block copolymer at 26 $^{\circ}$C.

On the other hand, the encapsulation of rhodamine-B in PCL-*b*-PNIPAAm copolymer at 26 °C was not observed (**Figure 4.19, Inset-A**) due to the hydrophobic core of micellar structures at that temperature. The absorbance and fluorescence values of rhodamine-B in PCL-*b*-PNIPAAm copolymer at 26 °C were found to be insignificant which confirmed the micellar structures at 26 °C.
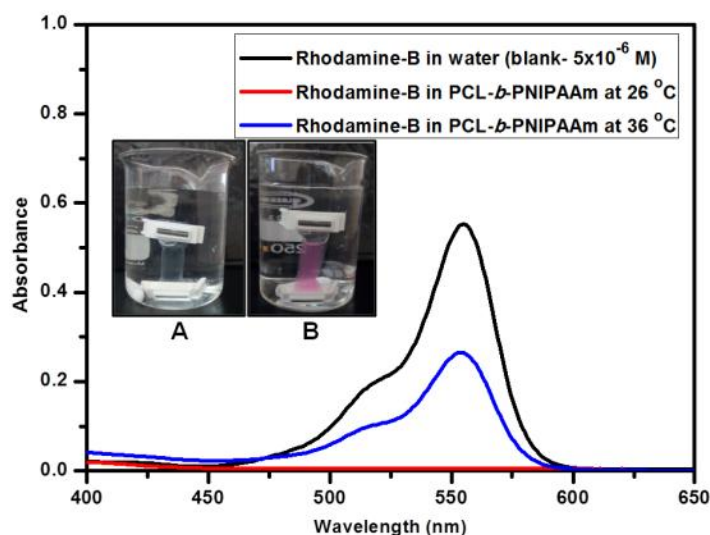
Figure 4.19 Absorption spectra of A) Rhodamine-B in water B) Rhodamine-B in PCL-*b*-PNIPAAm (0.1 wt %) block copolymer at 26 °C and C) Rhodamine-B in PCL-*b*-PNIPAAm (0.1 wt %) block copolymer at 36 °C.

The amount of rhodamine-B encapsulated inside the assemblies of PCL-*b*-PNIPAAm block copolymer above LCST was determined from the absorption spectrum (**Figure 4.19**) and was found to be 48 %. However, the value of absorbance slowly decreased with time which suggests the instability of these vesicular structures above the LCST (32 °C). From the results of hydrophilic-hydrophobic molecule encapsulation studies and TEM analysis, it was confirmed that the aggregates of PCL-*b*-PNIPAAm block copolymer formed spherical micelles in aqueous solution below LCST and transformed to unstable vesicles above the LCST and finally precipitated out at temperatures higher than 40 °C.

4.3.6 Temperature responsive release kinetics of pyrene from PCL-*b*-PNIPAAm block copolymer micelles

Pyrene was encapsulated in the micelles of PCL-*b*-PNIPAAm block copolymer at 26 °C and the release studies were performed with increasing temperature (**Figure 4.20**). It was found that the pyrene release was much faster at 40 °C as compared to the release at 36 °C

and 26 °C i.e below LCST pyrene release was found to be negligible whereas above LCST the release was faster due to the phase separation of PCL-*b*-PNIPAAm block copolymer from the aqueous solution.
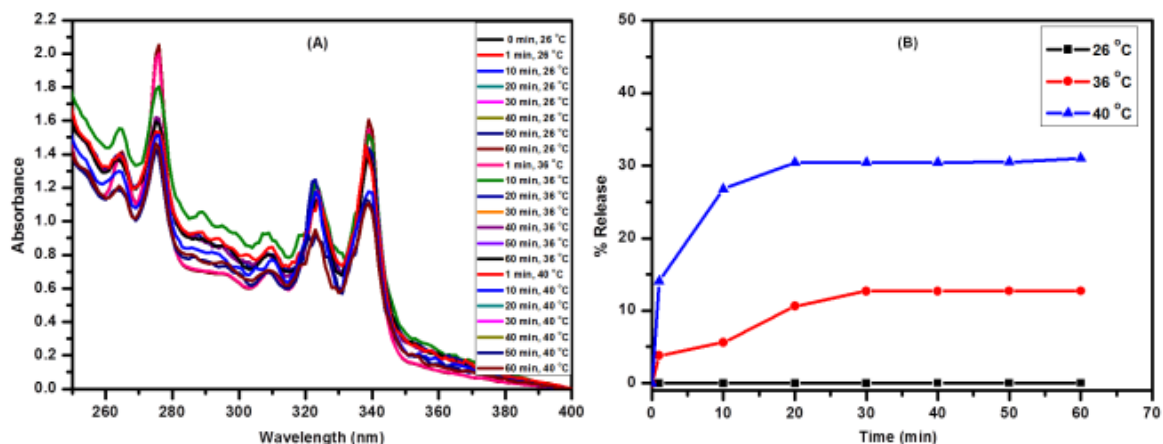
**Figure 4.20** A) Absorption spectra of pyrene in PCL-*b*-PNIPAAm (0.1 wt %) block copolymer at different temperatures and B) Pyrene release profiles of PCL-*b*-PNIPAAm (0.1 wt %) block copolymer at 26 °C; 36 °C and 40 °C.

4.3.7 pH-responsive behaviour of assembly of PCL-*b*-PNIPAAm block copolymer

The pH dependence of size of PCL-*b*-PNIPAAm block copolymer assemblies was studied by DLS analysis. PCL-*b*-PNIPAAm block copolymer sample (1 mg/mL, 0.1 wt %) in phosphate buffer solution was prepared at 26 °C and tested for DLS. PCL-*b*-PNIPAAm block copolymer solution at pH 7.4 showed stable assemblies with hydrodynamic diameter of around 118 nm (**Figure 4.21**). The encapsulation of pyrene at 26 °C confirmed the micellar structure of these assemblies.
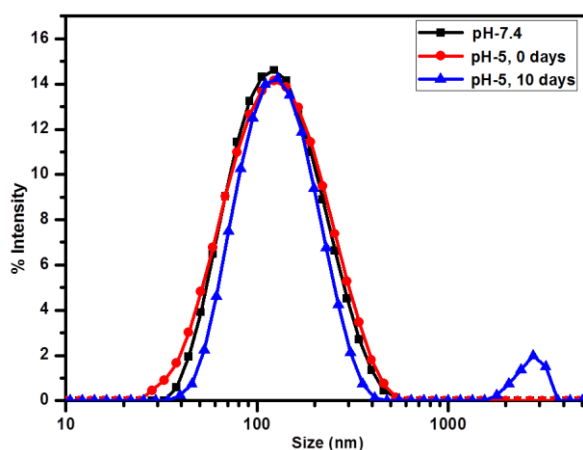
Figure 4.21 The pH dependence of assemblies of PCL-*b*-PNIPAAm (0.1 wt %) block copolymer at 26 °C.
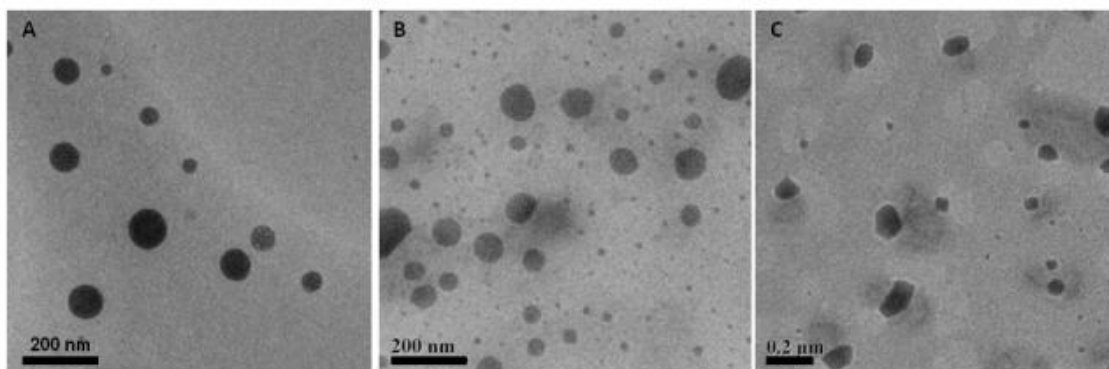
Figure 4.22 TEM images of assemblies of PCL-*b*-PNIPAAm (0.1 wt %) block copolymer in buffer solution after 24 h at pH A) 7.4 B) 5 and C) 2 at 26±1 °C.

TEM analysis of PCL-*b*-PNIPAAm block copolymer micelles at 26±1 °C (below LCST) in buffer solution at pH 7.4 showed the average size of 100±5 nm while with decreasing pH the distortion of micelles was observed (**Figure 4.22**).

The particles of sizes higher than 2000 nm were observed on gently stirring at pH-5 after 10 days at 26 °C (**Figure 4.21**). The reason for the appearance of these larger size particles was the precipitation of hydrophobic PCL block due to the cleavage of acetal linkage of PCL-*b*-PNIPAAm copolymer at pH-5. To confirm the cleavage of acetal linkage at pH-5, a fraction of polymer solution was lyophilized after 20 days and the sample was dissolved in THF and was analyzed by GPC. GPC curve of sample was bimodal and the retention volumes of the bimodal curve correlated with that of the retention volumes of precursor Pr-PCL and PNIPAAm-N$_3$ polymer (**Figure 4.23**) which suggested the appearance of particles due to the cleavage of acetal linkage.
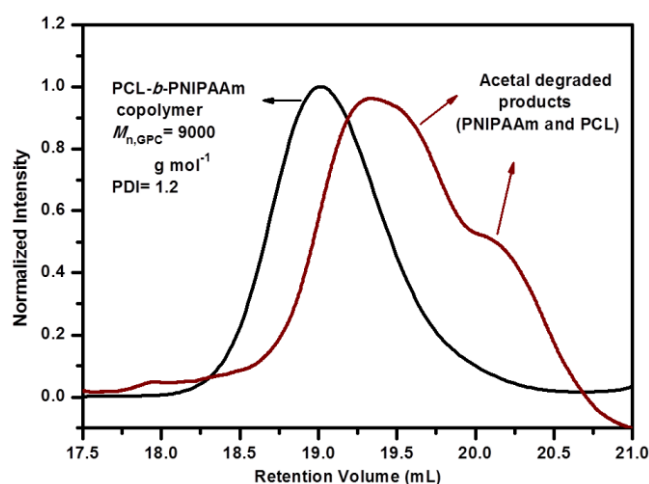
Figure 4.23 GPC trace of A) PCL-*b*-PNIPAAm block copolymer B) acetal degraded products (PCL and PNIPAAm) at pH-5.

The precipitated part of solution was filtered, dried, dissolved in THF and analyzed by MALDI-TOF spectroscopy to determine the end groups. MALDI-TOF spectrum of precipitated part showed line series corresponding to hydroxyl-terminated PCL (**Figure 4.24**) which confirmed the appearance of particles at pH-5 due to the acetal cleavage and precipitation of generated hydroxyl-terminated PCL block.
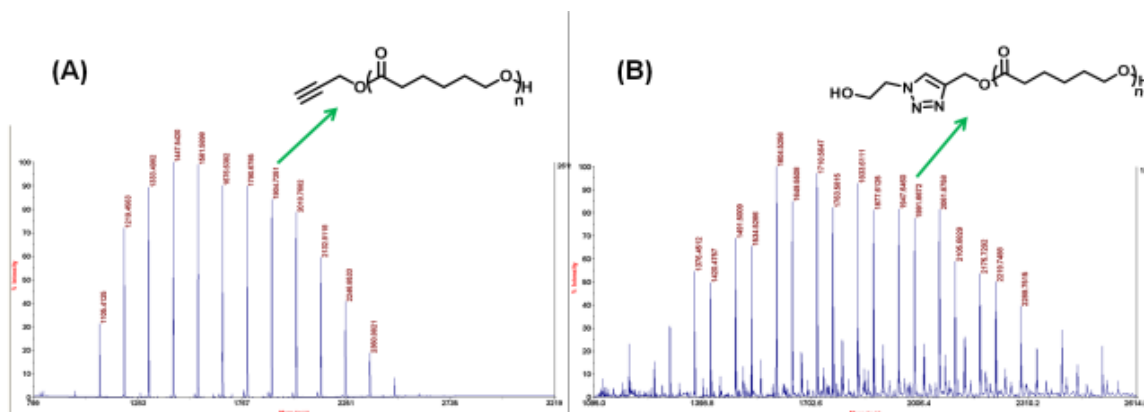
Figure 4.24 MALDI-TOF spectrum of A) Pr-PCL and B) PCL-OH generated after acetal degradation at pH-5.

To support the obtained results, the acetal cleavage of PCL-*b*-PNIPAAm block copolymer at low pH was studied by ^{1}H NMR spectroscopy (**Figure 4.25**).
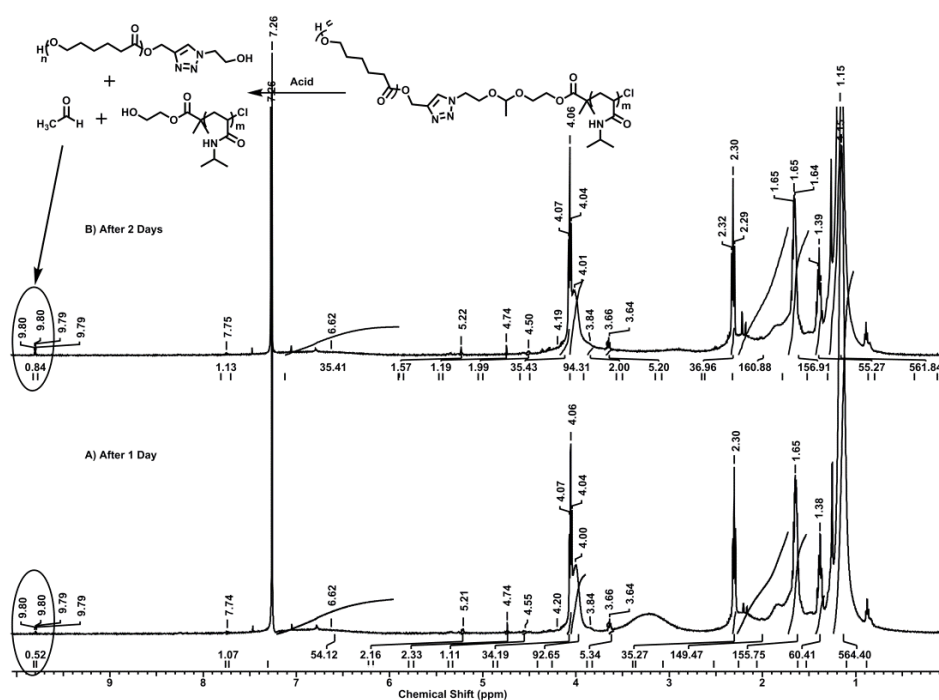
Figure 4.25 Time dependant ^{1}H NMR spectra (in CDCl$_3$) of PCL-*b*-PNIPAAm block copolymer in the presence of deuterated-hydrochloric acid.

The PCL-*b*-PNIPAAm copolymer sample was dissolved in CDCl$_3$ and 1 µL of deuterated hydrochloric acid was added. The integration of a quartet corresponding to aldehyde proton of generated acetaldehyde after cleavage was monitored with respect to time. It was found that after 48 h the acetal linkage of PCL-*b*-PNIPAAm block copolymer was almost completely cleaved (**Figure 4.25**).

4.3.8 pH-responsive release kinetics of pyrene from PCL-*b*-PNIPAAm block copolymer micelles

The hydrophobic pyrene was encapsulated in PCL-*b*-PNIPAAm (0.1 wt %) copolymer prepared in buffer solutions with pH 7.4 (10 mM) and the pH was adjusted to 5 and 2 at the required stages. The pH dependant pyrene release from the micelles of PCL-*b*-PNIPAAm block copolymer at pH-7.4, pH-5 and pH-2 with time was studied at 26 ^{o}C. Typical time dependant absorption spectra of pyrene inside the micelles of PCL-*b*-PNIPAAm block copolymer at pH-5 is shown in **Figure 4.26 A**. It was found that the pyrene release at pH-2 was much faster (**Figure 4.26 B**) compared to the pyrene release at pH-5 and pH-7.4 (**Figure 4.26 C**). The faster pyrene release with decreasing pH suggested pH responsive release due to the cleavage of acetal linkages in PCL-*b*-PNIPAAm block copolymer.

The LCST behavior of PNIPAAm and pH-sensitive nature of acetal linkage confer the dual-stimuli responsive (temperature and pH) characteristics to the PCL-*b*-PNIPAAm diblock copolymer. The straightforward access to such dual stimuli-responsive block copolymer systems is of significant advantage compared to the reported synthetically difficult to access systems such as star, branched, etc. with dual or multi-responsive nature.
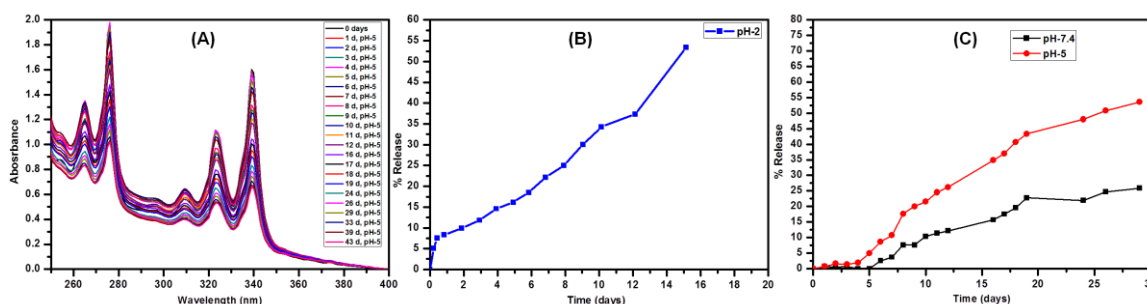
Figure 4.26 A) Time dependant absorption spectra of pyrene inside the micelles of PCL-*b*-PNIPAAm block copolymer at pH-5. B) Pyrene release profile of PCL-*b*-PNIPAAm block copolymer at pH-2 and C) Pyrene release profiles of PCL-*b*-PNIPAAm block copolymer at pH-7.4 and pH-5.

4.4. Conclusions

Well-defined azido-functionalized PNIPAAms with different molecular weights were synthesized by ATRP employing a new initiator containing both cleavable (acetal) and clickable (azido) groups. PCL-*b*-PNIPAAm block copolymer was obtained from these azido-terminated poly(*N*-isopropylacrylamide) (PNIPAAm-N$_3$) by alkyne-azide click reaction with propargyl-terminated poly(ε-caprolactone) (Pr-PCL). Critical aggregation concentration (CAC) of PCL-*b*-PNIPAAm block copolymer in aqueous solution was found to be 8.99×10^{-6} M. LCST of PCL-*b*-PNIPAAm block copolymer was found to be 32 ^{o}C and was dependant on polymer concentration as well as presence of salts in the solution. The effect of dual stimuli *viz*. temperature and pH on the assemblies of PCL-*b*-PNIPAAm block copolymer was studied which revealed that the copolymer below LCST assembled in spherical micelles which successively transformed to unstable vesicles above the LCST. Heating these assemblies above 40 ^{o}C further led to the precipitation of PCL-*b*-PNIPAAm block copolymer. Whereas, at decreased pH, micelles of PCL-*b*-PNIPAAm copolymer disintegrate due to the cleavage of acetal linkage and precipitation of hydrophobic hydroxyl terminated-PCL. The encapsulated pyrene release kinetics from the micelles of synthesized PCL-*b*-PNIPAAm block copolymer system was found to be faster at higher temperature and at lower pH. We presented herein the findings on temperature and pH dual-stimuli response and the morphological changes of self-assemblies of PCL-*b*-PNIPAAm block copolymer with varying temperature and pH which can be useful as model studies for temperature and pH dual-responsive drug-delivery systems.

4.5 References

1.   D. Schmaljohann, *Adv. Drug Del. Rev.*, 2006, **58**, 1655-1670.

2.   S. Binauld and M. H. Stenzel, *Chem. Comm.*, 2013, **49**, 2082-2102.

3.   J. Zhuang, M. R. Gordon, J. Ventura, L. Li and S. Thayumanavan, *Chem. Soc. Rev.*, 2013, **42**, 7421-7435.

4.   P. Du, H. Yang, J. Zeng and P. Liu, *J. Mater. Chem. B*, 2013, **1**, 5298-5308.

5.   A. Salonen, D. Langevin and P. Perrin, *Soft Matter*, 2010, **6**, 5308-5311.

6.   J. Hu and S. Liu, *Macromolecules*, 2010, **43**, 8315-8330.

7.   J. Zhang, M. Zhang, K. Tang, F. Verpoort and T.Sun, *Small*, 2014, **10**, 32-46.

8.   U. Haldar, K. Bauri, R. Li, R. Faust and P. De, *ACS Appl. Mater. Interfaces*, 2015, **7**, 8779-8788.

9.   Y. Cong, K. Chen, S. Zhou and L. Wu, *J. Mater. Chem. A*, 2015, **3**, 19093-19099.

10.   B. J. Saiki, P. Gogoi, S. Sharmah and S. K. Dolui, *Polym. Int.*, 2015, **64**, 437-445.

11.   L. Gao, T. Kong and Y. Huo, *Macromolecules*, 2016, **49**, 7478-7489.

12.   H. Y. Yang, M. S. Jang, G. H. Gao, J. H. Leeb and D. S. Lee, *Polym. Chem.*, 2016, **7**, 1813-1825.

13.   S. F. Medeiros, A. M. Santos, H. Fessi and A. Elaissari, *Int. J. Pharm.* 2011, **403**, 139-161.

14.   C. Yang, L. Chen, Y. Lu and H. Huang, *Polym. Chem.*, 2016, **7**, 6885-6889.

15.   J. Chen, M. Liu, H. Gong, Y. Huang and C. Chen, *J. Phys. Chem. B*, 2011, **115**, 14947-14955.

16.   A. O. Moughton, J. P. Patterson and R. K. Oreilly, *Chem. Comm.*, 2011, **47**, 355-375.

17.   A. Sundararaman, T. Stephan and R. B. Grubbs, *J. Am. Chem. Soc.*, 2008, **130**, 12264-12265.

18.   S. Kashyap, N. Singh, B. Surnar and M. Jayakannan, *Biomacromolecules*, 2016, **17**, 384-398.

19.   Y. He, Y. Zhang, Y. Xiao and M. Lang, *Colloids Surf. B: Biointerfaces*, 2010, **80**, 145-154.

20.   S. Panja, G. Dey, R. Bharti, K. Kumari, T. K. Maiti, M. Mandal and S. Chattopadhyay, *ACS Appl. Mater. Interfaces*, 2016, **8**, 12063-12074.

21.   E. Blasco, B. V. K. J. Schmidt, C. B. Kowpllik, M. Pinol and L. Oriol, *Polym. Chem.*, 2013, **4**, 4506-4514.

22.   X. An, Q. Tang, W. Zhu, K. Zhang and Y. Zhao, *Macromol. Rapid Commun.*, 2016, **37**, 980−986.

23.   M. Burek, Z. P. Czuba and S. Waskiewicz, *Polymer*, 2014, **55**, 6460-6470.

24.   S. Son, E. Shin and B. S. Kim, *Macromolecules*, 2015, **48**, 600-609.

25.   W. Tian, X. Wei, Y. Liu and X. Fan, *Polym. Chem.*, 2013, **4**, 2850-2863.

26.   K. Satoh, J. E. Poelma, L. M. Campos, B. Stahl and C. J. Hawker, *Polym. Chem.*, 2012, **3**, 1890-1898.

27. B. Liu, H. Zhou, S. Zhou, H. Zhang, A. C. Feng, C. Jian, J. Hu, W. Gao and J. Yuan, *Macromolecules*, 2014, **47**, 2938-2946.

28. J. Weiss and A. Laschewsky, *Langmuir*, 2011, **27**, 4465-4473.

29. H. Peng, W. Xu and A. Pich, *Polym. Chem.*, 2016, **7**, 5011-5022.

30. M. Li, P. Pan, G. Shan and Y. Bao, *Polym. Int.*, 2015, **64**, 389-396.

31. N. C. Bell, S. J. Doyle, G. Battistelli, C. L. M. LeGuyader, M. P. Thompson, A. M. Poe, A. Rheingold, C. Moore, M. Montalti, S. Thayumanavan, M. J. Tauber and N. C. Gianneschi, *Langmuir*, 2015, **31**, 9707−9717.

32. C. He, H. Zhao, X. Guo, Z. Guo, X. Chen, X. Zhuang, S. Liu and X. Jing, *J. Polym. Sci. Part A: Polym. Chem.*, 2008, **46**, 4140-4150.

33. J. R. Hernandez and S. Lecommandoux, *J. Am. Chem. Soc.*, 2005, **127**, 2026-2027.

34. R. Cheng, F. Meng, S. Ma, H. Xu, H. Liu, X. Jing and Z. Zhong, *J. Mater. Chem.*, 2011, **21**, 19013-19020.

35. Z. Y. Qiao, R. Ji, X. N. Huang, F. S. Du, R. Zhang, D. H. Liang and Z. C. Li, *Biomacromolecules*, 2013, **14**, 1555-1563.

36. S. Jiang, Y. Yao, Y. Nie, J. Yang and J. Yang, *J. Colloid Interface Sci.*, 2011, **364**, 264-271.

37. Q. Jin, G. Liu and J. Ji, *J. Polym. Sci. Part A: Polym. Chem.*, 2010, **48**, 2855-2861.

38. J. Xuan, D. Han, H. Xia and Y. Zhao, *Langmuir*, 2014, **30**, 410−417.

39. M. Kang and B. Moon, *Macromolecules*, 2009, **42**, 455-458.

40. Q. Zhang, N. Vanparijs, B. Louage, B. G. D. Geest and R. Hoogenboom, *Polym. Chem.*, 2014, **5**, 1140-1144.

41. H. Wei, X. Z. Zhang, H. Cheng, W. Q. Chen, S. X. Cheng and R. X. Zhuo, *J. Controlled Release*, 2006, **116**, 266-274.

42. S. P. Rwei, Y. Y. Chuang, T. F. Way, W. Y. Chiang and S. P. Hsu, *Colloid Polym. Sci.*, 2015, **293**, 493-503.

43. M. T. Savoji, S. Strandman and X. X. Zhu, *Langmuir*, 2013, **29**, 6823-6832.

44. A. Klaikherd, C. Nagamani and S. Thayumanavan, *J. Am. Chem. Soc.*, 2009, **131**, 4830-4838.

45. L. Yang, C. Guo, L. Jia, X. Liang, C. Liu and H. Liu, *J. Colloid Interface Sci.*, 2010, **350**, 22-29.

46. X. Huang, F. Du, J. Cheng, Y. Dong, D. Liang, S. Ji, S. S. Lin and Z. Li, *Macromolecules*, 2009, **42**, 783-790.

47. X. Wu, X. He, L. Zhong, S. Lin, D. Wang, X. Zhu and D. Yan, *J. Mater. Chem.*, 2011, **21**, 13611-13620.

48. M. Ciampolini and N. Nardi, *Inorg. Chem.*, 1966, **5**, 41-44.

49. Y. A. Zhang, H. Liu, H. Dong, C. Li and S. Liu, *J. Polym. Sci. Part A: Polym. Chem.*, 2009, **47**, 1636-1650.

50. J. Xu, J. Ye and S. Liu, *Macromolecules*, 2007, **40**, 9103-9110.

51. F. Jia, S. Wang, X. Zhang, C. Xiao, Y. Tao and X. Wang, *Polym. Chem.*, 2016, **7**, 7101-7107.

Chapter 5

Healable Network Polymers Bearing Flexible Poly(Lauryl Methacrylate) Chains via Thermo-Reversible Furan-Maleimide Diels-Alder Reaction

5.1 Introduction

Smart materials based on healable polymers[1] have contributed significantly to the field of coatings[2, 3] and dielectrics[4]. The response of healable smart materials based on linear and cross- linked/network polymers to temperature has been extensively studied.[5-13] A range of smart materials based on supramolecular chemistry involving hydrogen bonding, л- л stacking, etc. and hydrophobic interactions have been studied.[14, 15] However, these systems have been found to be mechanically weaker than the chemically cross-linked counterparts. The combination of controlled radical polymerization (CRP) methods [16, 17]such as NMP, ATRP, RAFT, etc. and controlled polymerization methods such as ROP, etc. with different click reactions such as thiol-ene, alkyne-azide, anthracene-maleimide, furan-maleimide, aldehyde-aminooxy, etc. have been widely explored to obtain such chemically cross-linked smart materials.[18, 19] Of these, smart materials based on macromolecular architectures obtained by the combination of RDRP or CRP methods with furan-maleimide click reaction have been considered to be of practical interest due to their ease of accessability.[20]

A range of linear and cross- linked/network polymeric systems containing thermo-reversible furan-maleimide Diels-Alder adducts have been reported so far.[21-32] However, a limited number of reports are available in the literature concerning polymeric systems with network/cross linked structure bearing flexible chains.[33, 34] Such systems are expected to show healing ability at relatively moderate temperatures due to the induced chain mobility to the resulting structure.[2]

We designed herein, a network polymeric smart material based on combination of ATRP and thermo-reversible furan-maleimide Diels-Alder click reaction. A new ATRP initiator containing two furyl rings *viz.* bis(furan-2-ylmethyl) 2-bromopentanedioate was synthesized based on L-glutamic acid as a starting material and was utilised to obtain bisfuryl-terminated PLMA macromonomers. Thermo-reversible network polymer bearing flexible PLMA chains was obtained by furan-maleimide click reaction of bisfuryl-terminated PLMA macromonomer with 1,1',1"-(nitrilotris(ethane-2,1-diyl))tris(1H-pyrrole-2,5-dione). The scratch healing study was performed on the films prepared from this network polymer which showed the complete healing at 60 ^{o}C in five days, thanks to the presence of flexible PLMA chains which induced the chain mobility in these systems due to their low Tg (-40 ^{o}C).

5.2 Experimental Section

5.2.1 Materials

L-Glutamic acid (Thomas Baker, 99 %), sodium nitrite (Loba Chemie, 97 %), sodium bromide (Thomas Baker, 99.5 %), *N, N'*-dicyclohexylcarbodiimide (DCC) (Aldrich, 99 %), 4-dimethylaminopyridine (DMAP) (Lancaster, 99 %), copper bromide (Aldrich, 99.99 %), *N,N,N',N'',N''*-pentamethyldiethylenetriamine (Aldrich, 99 %), tris(2-aminoethyl)amine (Aldrich, 96 %) and maleic anhydride (Aldrich, 99 %) were used as received. Furan and furfuryl alcohol were distilled before use. Lauryl methacrylate (LMA) was stirred over calcium hydride and distilled under reduced pressure just before use. Toluene and dichloromethane were stirred over calcium hydride overnight and distilled.

5.2.2 Characterisation and measurements

FT-IR spectra were recorded on Perkin Elmer Spectrum GX spectrophotometer using chloroform as a solvent. NMR spectra were recorded on Bruker- 400 or 500 MHz spectrometer in CDCl$_3$ or tetrachloroethane-d$_2$ as a solvent. Molecular weights and dispersity values of PLMA macromonomers were determined by gel permeation chromatography (GPC) equipped with Viscotek VE-1122 pump, two Viscotek (T6000N, General Mixed) columns and Viscotek VE-3580 RI detector and tetrahydrofuran as an eluent at a flow rate of 1 mL/min. Polymer concentration for GPC analysis was 5 mg/mL and narrow dispersity polystyrene(s) were used as calibration standards. The detector and column temperatures were set to 30 ^{o}C and the sample injection volume for GPC analysis was fixed at 20 μL.

Matrix assisted laser desorption ionisation - time of flight (MALDI-TOF) spectra were recorded on AB-SCIEX TOF/TOF 5800 instrument with linear/reflector positive operating method in tetrahydrofuran as a solvent using *trans*-2-[3-(4-*tert*-butylphenyl)-2-methyl-2-propenylidene]malononitrile (DCTB) (10 mg/mL, 5 volume equivalent with polymer) as a matrix at 26 ^{o}C. The end functionality of polymers was determined by spotting the mixture of 4 μL polymer sample (1 mg/mL) with 20 μL of DCTB (10 mg/mL) as matrix and 1 μL of sodium iodide as an ionising agent (0.2 g/mL) on a metal target plate. Mass range was selected on the basis of molecular weights previously determined from ^{1}H-NMR spectroscopy. Thermograms (TGA) and differential scanning chromatograms (DSC) of polymer samples were obtained from STA 6000 (PerkinElmer) and DSC Q10 or Q100 TA instruments with refrigerated cooling system, respectively. The

extent of crystallinity of polymer samples was determined from MicroMax-007HF (Rigaku) powder XRD machine with rotating anode X-ray generator. The progress of Diels-Alder and retro Diels-Alder reactions was determined on Specord 210 Plus (analyticjena) UV-Visible spectrophotometer using 0.1 cm path length. Scratch healing experiments were performed using OLYMPUS BX60 microscope with OLYMPUS SC30 camera. The polymer films were prepared with thickness of ~50 μm. The precursors were dissolved in TCE, their films were cast on glass plate and heated for 20 days. The thickness of films was determined from optical profilometer. Contact angle measurements were performed on DIGIDROP (GBX model) contact angle instrument. The viscoelastic behavior of network polymer was studied on MCR-301 (Anton Paar) Rheometer using 25 mm parallel plate geometry.

5.2.3 Synthesis

5.2.3.1 Synthesis of 2-bromopentanedioic Acid (1)

Into a 500 mL round bottom flask equipped with a magnetic stir bar and an addition funnel were charged L-glutamic acid (20 g, 135.9 mmol), sodim bromide (27.97 g, 271.8 mmol) and 2.5 M H_2SO_4 (177 mL). The reaction mixture was cooled to 0 ^{o}C in an ice bath and the solution of sodium nitrite (11.72 g, 169.9 mmol) in water (50 mL) was added dropwise while stirring over the period of 20 min. The reaction mixture was stirred at 0 ^{o}C until evolution of nitrogen gas ceased. The progress of reaction was monitored by TLC. The aqueous solution of urea (0.82 g, 13.6 mmol) was added to terminate the reaction. The reaction mixture was extracted with diethyl ether (3×100 mL). The combined organic layer was evaporated and the crude product was recrystallized from ethanol to afford 11.47 g (40 %) of 2-bromopentanedioic acid (1) as a white solid (Melting Point- 40 ^{o}C).

IR (CHCl$_3$, cm^{-1}): 1714 (C=O).

^{1}H-NMR (200 MHz, CDCl$_3$, δ/ppm): 9.38 (broad s, 2H), 4.42 (q, 1H), 2.64 (td, 2H), 2.20-2.55 (m, 2H).

^{13}C-NMR (50 MHz, CDCl$_3$, δ/ppm): 178.52, 174.95, 43.97, 31.15, 29.11.

5.2.3.2 Synthesis of bis(furan-2-ylmethyl) 2-bromopentanedioate (2)

Into a 250 mL round bottom flask equipped with a magnetic stir bar, an argon inlet and an addition funnel were charged **1** (8 g, 37.91 mmol), furfuryl alcohol (8.93 g, 90.99

mmol), DMAP (1.85 g, 15.64 mmol) and DMF (40 mL). The reaction mixture was cooled to 0 °C in an ice bath and the solution of DCC (18.77 g, 90.99 mmol) in DMF (30 mL) was added dropwise while stirring over the period of 20 min. The reaction mixture was stirred additionally for 1 h at 0 °C and at room temperature for 15 h. The reaction mixture was filtered and solvent was evaporated under reduced pressure. The crude product was dissolved in dichloromehane and washed with saturated $NaHCO_3$ solution (2×100 mL) and water (2×100 mL). The combined organic layer was evaporated and the crude product was purified by silica gel column chromatography using pet ether:ethyl acetate (80:20, v/v) as an eluent to afford 11.25 g (80 %) of bis(furan-2-ylmethyl) 2-bromopentanedioate (2) as a colourless liquid.

IR (CHCl$_3$, cm^{-1}): 1738 (C=O) and 1504 (C=C).

^{1}H-NMR (200 MHz, CDCl$_3$, δ/ppm): 7.40-7.44 (m, 2H), 6.33-6.46 (m, 4H), 5.15 (s, 2H), 5.07 (s, 2H), 4.37 (q, 1H), 2.48-2.59 (td, 2H), 2.15-2.46 (m, 2H).

^{13}C-NMR (100 MHz, CDCl$_3$, δ/ppm): 171.62, 168.93, 149.15, 148.46, 143.54, 143.34, 111.27, 110.77, 110.63, 110.57, 59.43, 58.26, 44.47, 31.26, 29.55.

5.2.3.3 Synthesis of bisfuryl-terminated PLMA macromonomers by ATRP

Into a 20 mL flame dried Schlenk tube fitted with a rubber septum and an argon inlet were charged bis(furan-2-ylmethyl) 2-bromopentanedioate (0.437 g, 1.179 mmol), lauryl methacrylate (6 g, 23.58 mmol), PMDETA (0.204 g, 1.179 mmol) and toluene (6 g). The reaction mixture was purged with argon for 10 min and then copper bromide (0.169 g, 1.179 mmol) was added under the positive pressure of argon. After three vaccum freeze pump-thaw cycles, the Schlenk tube was immersed in an oil bath preheated at 50 °C and stirred for appropriate time under argon. The polymerization reaction was quenched by sudden cooling the Schlenk tube in liquid nitrogen with exposure to air. The solvent was removed under reduced pressure. The percentage conversion of reaction was determined by ^{1}H NMR spectroscopy. Polymer was purified by dissolving in dichloromethane and passing the solution through a small bed of neutral alumina column to remove the copper salts, washed with aqueous solution of disodium salt of EDTA, concentrated and precipitated into cold methanol, filtered and dried at 40 °C under reduced pressure to afford a thick liquid.

IR (CHCl$_3$, cm^{-1}): 1730 (C=O).

^{1}H-NMR (200 MHz, CDCl$_3$, δ/ppm): 7.4 (broad peak, 1H), 7.36 (broad peak, 1H), 6.27-6.42 (m, 4H), 5.01 (s, 2H), 4.98 (broad s, 2H), 4.08 (t, 1H), 3.90 (broad s, CH$_2$–O from PLMA), 2.32-2.6 (m, 2H), 2.12-2.3 (m, 2H), 1.67-2.05 (m, –CH$_2$ from PLMA backbone), 1.59 (broad s, –CH$_2$ from lauryl chain), 1.26 (broad s, (–CH$_2$–)$_9$ from lauryl chain and –CH$_3$ from PLMA backbone) and 0.87 (t, –CH$_3$ from lauryl chain).

5.2.3.4 Synthesis of 1,1',1''-(nitrilotris(ethane-2,1-diyl))tris(1H-pyrrole-2,5-dione)

The furan-maleic anhydride adduct (exo-3,6-epoxy-1,2,3,6-tetrahydrophthalic anhydride) was prepared according to the literature procedure.[10]

Into a 50 mL round bottom flask fitted with a rubber septum and an argon inlet were charged tris(2-aminoethyl)amine (1 g, 6.83 mmol), furan-maleic anhydride DA adduct (exo-3,6-epoxy-1,2,3,6-tetrahydrophthalic anhydride) (6.81 g, 41.03 mmol) and methanol (50 mL). The reaction mixture was stirred for four days at 50 ^{o}C, which gave the corresponding trifunctional DA adduct as a yellow solid precipitate. The reaction mixture was precipitated in excess methanol, filtered and dried at 40 ^{o}C.

The dried product was dissolved in toluene and heated at 120 ^{o}C for 3 days to deprotect the trifunctional furan-maleimide adduct. The reaction mixture was precipitated in cold n-hexane and filtered to afford 1.85 g (70 %) of 1,1',1''-(nitrilotris(ethane-2,1-diyl))tris(1H-pyrrole-2,5-dione) as faint yellow solid.

Melting Point- 102 ^{o}C (Lit. Melting Point- 98-100 ^{o}C).[10]

IR (CHCl$_3$, cm^{-1}): 3098 (C=C) and 1687 (C=O).

^{1}H-NMR (400 MHz, CDCl$_3$, δ/ppm): 6.67 (s, 6H), 3.52 (t, 6H), 2.71 (t, 6H).

^{13}C-NMR (100 MHz, CDCl$_3$, δ/ppm): 35.6, 51.6, 134.0 and 170.6.

5.2.3.5 Synthesis of thermo-reversible network polymer with flexible PLMA chains *via* furan-maleimide Diels-Alder click reaction

A flame dried 10 mL Schlenk tube fitted with a rubber septum and equipped with a magnetic stir bar was thoroughly evacuated with vacuum and to the Schlenk tube were charged bisfuryl-terminated PLMA macromonomer (0.4 g, 0.1 molar solution in TCE, Table-5.1, Entry-1, $M_{n,NMR}$-5000 g mol^{-1}, Dispersity-1.3) and 1,1',1''-(nitrilotris(ethane-2,1-diyl))tris(1H-pyrrole-2,5-dione) (30.9 mg, 0.1 molar solution in TCE). The reaction mixture was purged with argon for 20 min, heated initially at 110 ^{o}C for 30 min and stirred for appropriate time at 60 ^{o}C under argon. The solvent was evaporated after completion of

reaction and the insoluble product was dried at 50 °C to obtain network polymer as a sticky solid. The progress of furan-maleimide Diels-Alder click reaction was determined from ^{1}H-NMR spectroscopy and the final spectrum was obtained just before the polymer sample started to precipitate out from the reaction medium.

IR (CHCl$_3$, cm^{-1}): 1730 (C=O).

^{1}H-NMR (500 MHz, TCE-d$_2$, δ/ppm): 7.30-7.50 (m, furyl ring), 6.67 (s, maleimide), 6.47-6.60 (m, 2H), 6.25-6.47 (m, 2H), 5.19 (broad peak, 2H), 5.0 (broad s, 4H), 4.06 (broad t, 1H), 3.90 (broad s, –CH$_2$–O from PLMA), 3.48 (t, –CH$_2$ adjacent to maleimide), 3.44 (broad peak, 6H), 3.15-3.43 (m, 4H, endo), 2.82-3.1 (m, 4H, exo), 2.66 (t, –CH$_2$–N), 2.62 (broad peak, 6H, –CH$_2$–N), 2.32-2.5 (m, 2H), 2.15-2.32 (broad peak, 2H), 1.68-2.05 (m, –CH$_2$ from PLMA backbone), 1.59 (broad s, –CH$_2$– from lauryl chain), 1.25 (broad s, (–CH$_2$)$_9$ from lauryl chain and –CH$_3$ from PLMA backbone), 0.87 (t, –CH$_3$ from lauryl chain).

5.3 Results and Discussion

5.3.1 Design and synthesis of bis(furan-2-ylmethyl) 2-bromopentanedioate (2) ATRP initiator

A new ATRP initiator containing two clickable furyl rings *viz.* bis(furan-2-ylmethyl) 2-bromopentanedioate (2) was designed and synthesized starting from L-glutamic acid-a commercially available and an inexpensive starting material.

The nucleophilic substitution of diazonium salt prepared form L-glutamic acid with sodium bromide afforded 2-bromopentanedioic acid (1). The complete shift of a quartet at 4.42 ppm in ^{1}H NMR spectrum and the appearance of a peak at 748 cm^{-1} corresponding to C-Br stretching in FT-IR spectrum revealed the formation of 1. The esterification reaction of 1 with furfuryl alcohol in the presence of DCC and DMAP resulted into the formation of bis(furan-2-ylmethyl) 2-bromopentanedioate (2) (**Scheme 5.1**).
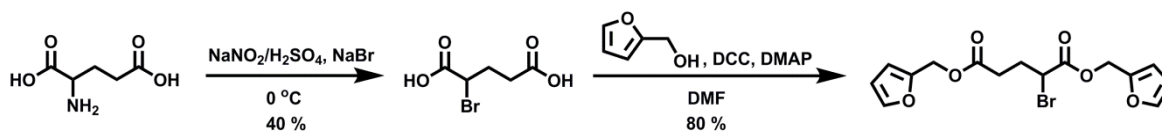
Scheme 5.1 Synthesis of bis(furan-2-ylmethyl) 2-bromopentanedioate (2).

The formation of bis(furan-2-ylmethyl) 2-bromopentanedioate was confirmed by FT-IR, NMR and HR-MS spectroscopy. The appearance of peaks at 1738 cm^{-1} and 1504 cm^{-1} corresponding to carbonyl stretching of ester and C=C stretching of furan rings, respectively, in FT-IR spectrum (**Figure 5.1**) supported the formation of **2**.
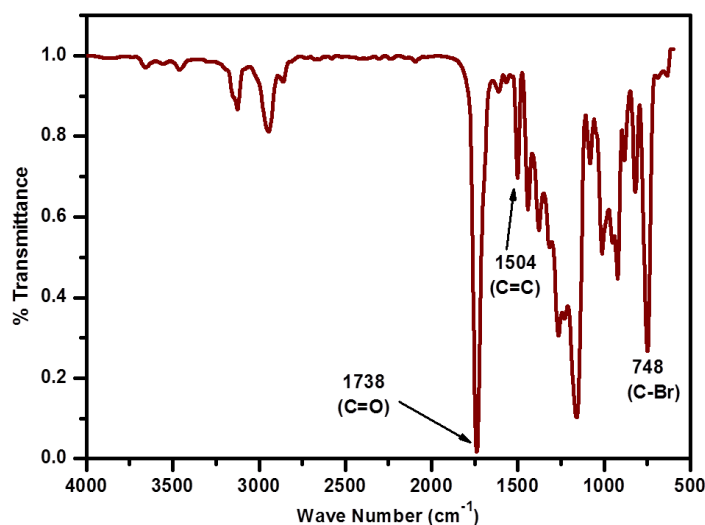
Figure 5.1 FT-IR spectrum (in chloroform) of bis(furan-2-ylmethyl) 2-bromopentanedioate (**2**).

The appearance of multiplets in the range 7.40-7.44 ppm and 6.33-6.46 ppm corresponding to furyl ring protons in ^{1}H NMR spectrum (**Figure 5.2**) confirmed the formation of bis(furan-2-ylmethyl) 2-bromopentanedioate. The remaining sets of protons in ^{1}H-NMR spectrum and sets of carbons in ^{13}C-NMR spectrum (**Figure 5.3**) were found to be in good agreement with the proposed structure. Furthermore, the mass spectrum of **2** showed M/Z of 392.994, which exactly matched with the theoretically calculated molecular weight (**Figure 5.4**).

Figure 5.2 ^{1}H NMR spectrum (in CDCl$_3$) of bis(furan-2-ylmethyl) 2-bromopentanedioate (**2**).

Figure 5.3 ^{13}C NMR spectrum (in CDCl$_3$, 100 MHz) of bis(furan-2-ylmethyl) 2-bromopentanedioate (**2**).
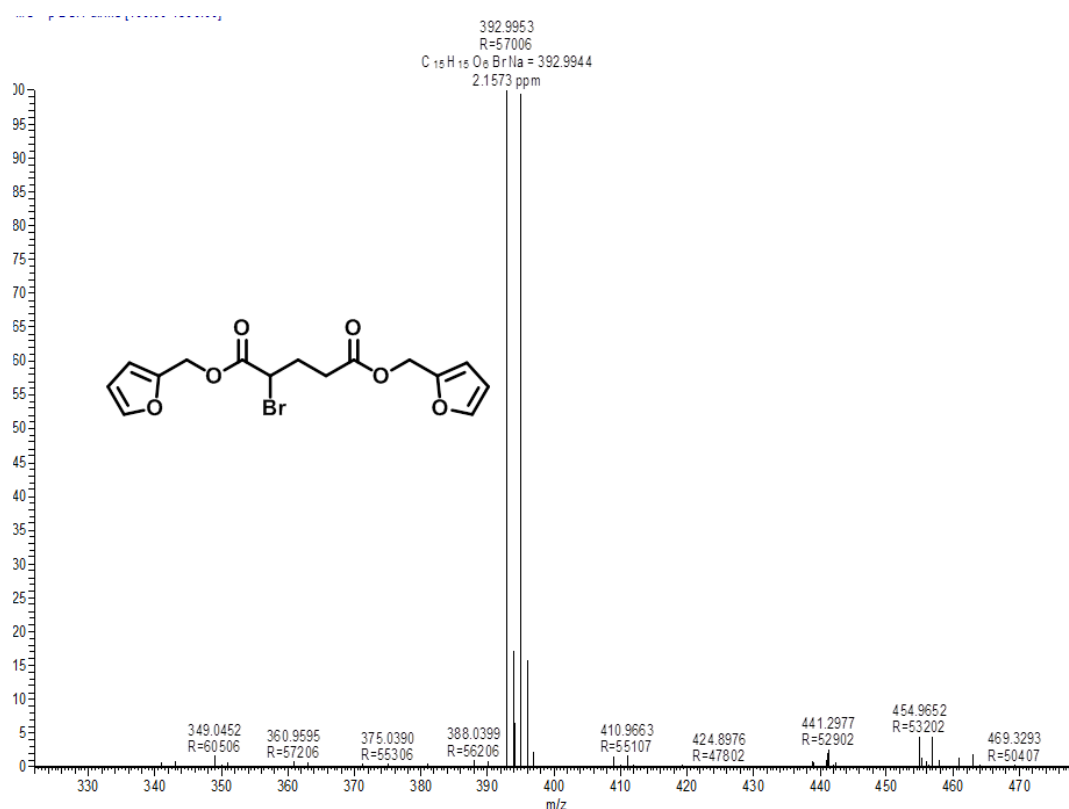
Figure 5.4 HR-MS spectrum of bis(furan-2-ylmethyl) 2-bromopentanedioate (**2**).

5.3.2 Synthesis of bisfuryl-terminated PLMA macromonomers by ATRP and their characterization

Bisfuryl-terminated PLMA macromonomers were synthesized by ATRP of lauryl methacrylate employing bis(furan-2-ylmethyl) 2-bromopentanedioate (**2**) as the initiator in the presence of copper bromide/PMDETA as a catalytic system (**Scheme 5.2**).
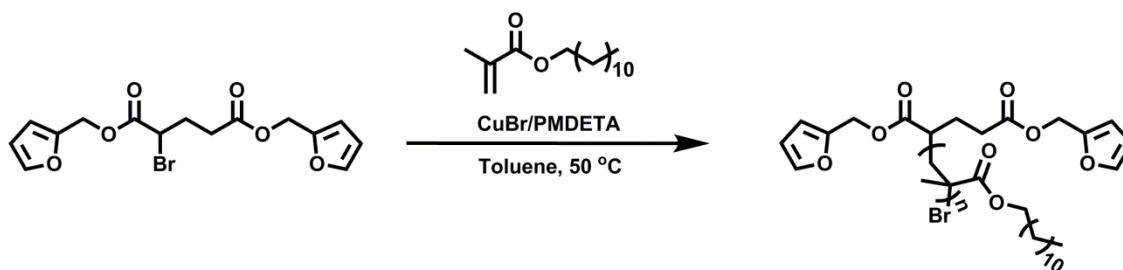
Scheme 5.2 Synthesis of bisfuryl-terminated PLMA macromonomers by ATRP.
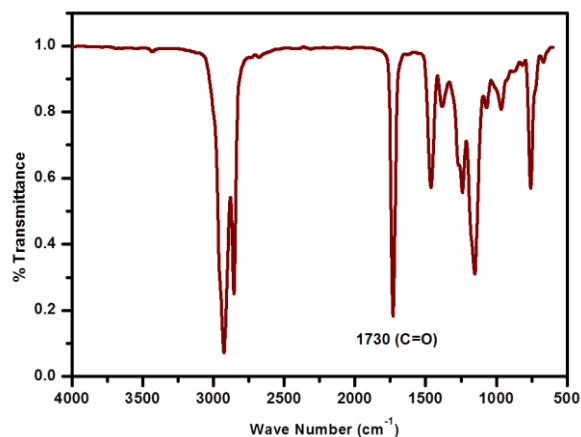
Figure 5.5 FT-IR spectrum (in chloroform) of bisfuryl-terminated PLMA macromonomers.

The appearance of a peak at 1730 cm^{-1} attributed to carbonyl group of PLMA in FT-IR spectrum (**Figure 5.5**) and presence of furyl proton resonances at their respective positions (multiplets in the range 7.3-7.5 ppm and 6.27-6.42 ppm) in ^{1}H-NMR spectrum (**Figure 5.6**) of PLMA macromonomers attested the stability of furan ring under ATRP conditions.

Figure 5.6 ^{1}H NMR spectrum (in CDCl$_3$) of bisfuryl-terminated PLMA macromonomer (Table 5.1, Entry 1).

Well-defined bisfuryl-terminated PLMA macromonomers with molecular weights and dispersity in the range 5000-12000 g mol^{-1} and 1.3-1.37, respectively, were prepared by varying monomer to initiator feed ratios (**Table 5.1**). Molecular weights and dispersities of synthesized PLMA macromonomers were determined from ^{1}H NMR spectroscopy and GPC. Molecular weights of PLMA macromonomers were found to be controlled and dispersities were found to be narrow (**Table 5.1**).

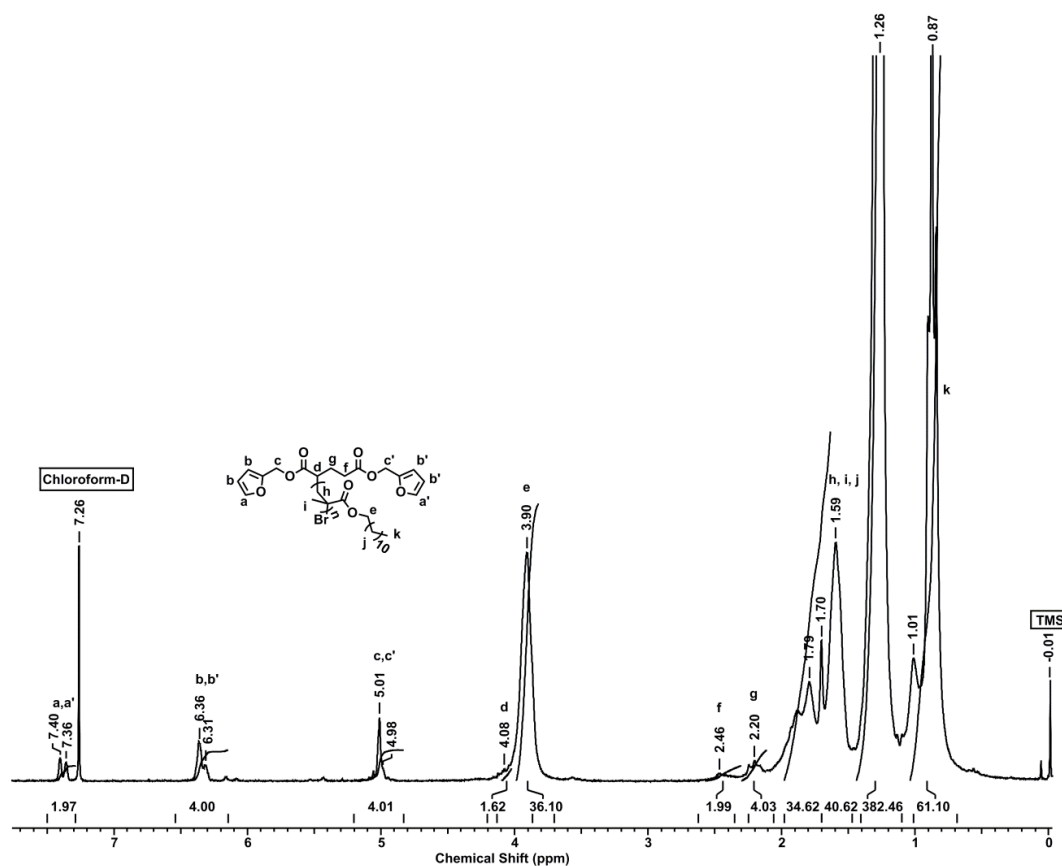**Table 5.1** Reaction parameters and results of synthesis of bisfuryl-terminated PLMA macromonomers.

Sr. No.	$[M]_0/[I]_0$ [a]	Time (min)	Conv. (%) [b]	$M_{n,theo}$ [c]	$M_{n,NMR}$ [d] g mol^{-1}	$M_{n,GPC}$ [e] g mol^{-1}	M_w/M_n	I^{eff} [f]
1	18	30	86	4300	5000	7500	1.3	0.86
2	25	50	94	6300	6700	9300	1.34	0.94
3	50	65	74	9800	12000	15000	1.37	0.82

Temperature: 50 ^{o}C, solvent: toluene (1:1 w/w, w. r. t. monomer)

[a] $[M]_0/[I]_0$: $[Monomer]_0/[Initiator]_0$ feed ratio.

[b] Conversions were determined by ^{1}H NMR spectroscopy.

[c] $M_{n,theo}$ = { $[M]_0/[I]_0 \times$ (% conv.)/100 × mol. weight of monomer} + mol. weight of initiator

[d] $M_{n,NMR}$ = Determined by ^{1}H NMR spectroscopy.

[e] $M_{n,GPC}$ = Determined by GPC; Polystyrene standard; Tetrahydrofuran as an eluent.

[f] I^{eff} = $M_{n,theo}$ / $M_{n,NMR}$.

A typical GPC chromatogram of PLMA macromonomer (Table 5.1, Entry 1) (**Figure 5.7**) was found to be symmetric and monomodal which further supported the controlled polymerization behaviour.
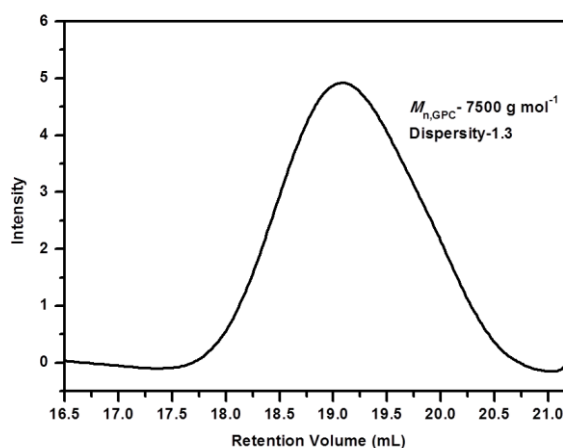
Figure 5.7 GPC trace of bisfuryl-terminated PLMA macromonomer (Table 5.1, Entry 1).

The presence of furyl rings at the initiation end of polymer chain was also determined by MALDI-TOF analysis (**Figure 5.8**). The observed molecular weight of line series of PLMA (Table 5.1, Entry 1) was found to be in good agreement with the molecular weight calculated by taking into consideration the molecular weight of initiator fragment.
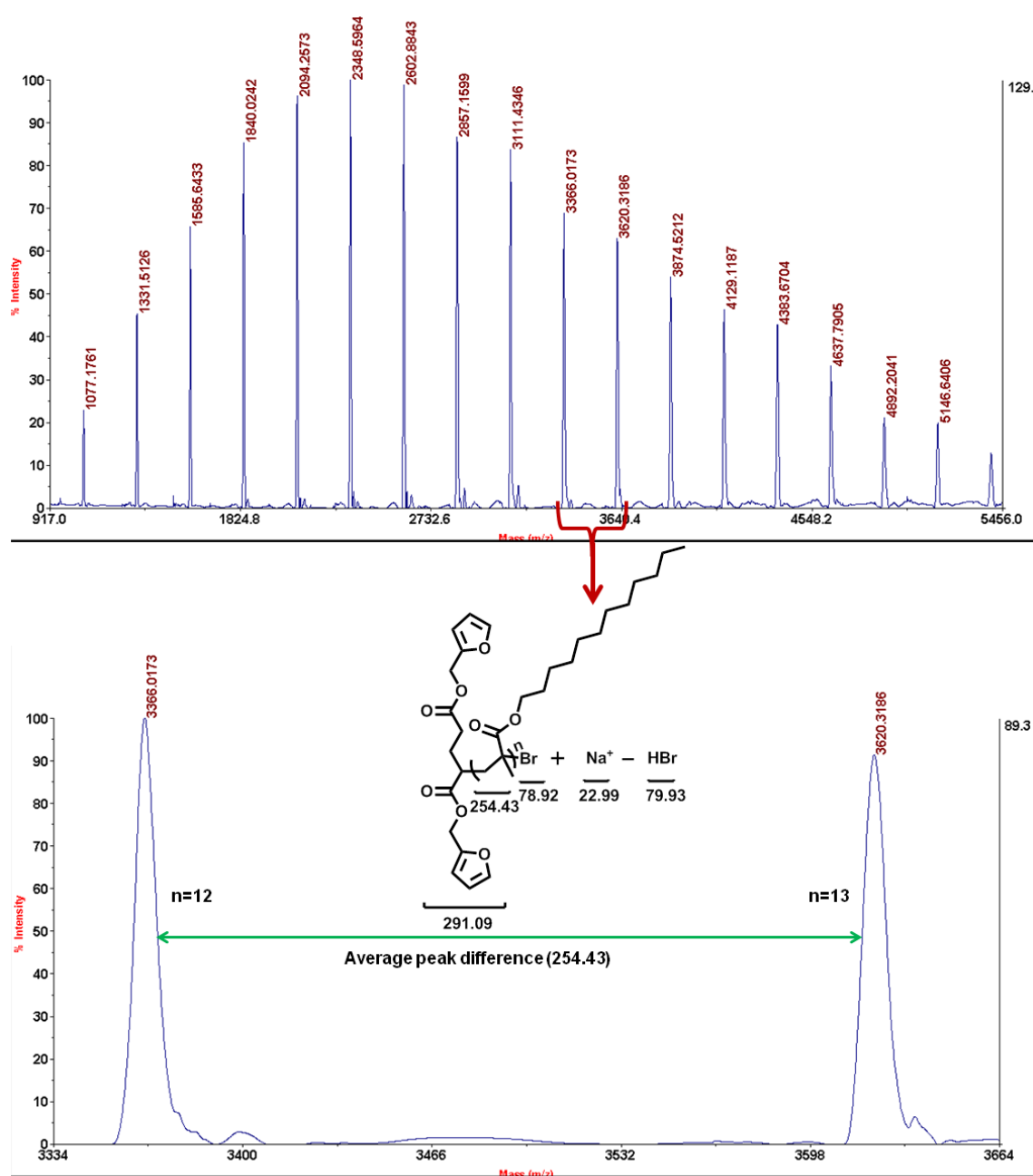
Figure 5.8 MALDI-TOF spectrum of bisfuryl-terminated PLMA macromonomer (Table 5.1, Entry 1).

5.3.3 Synthesis of trismaleimide counterpart *viz.* 1,1',1''-(nitrilotris(ethane-2,1-diyl))tris(1H-pyrrole-2,5-dione)

Independently, a trismaleimide counterpart *viz.* 1,1',1''-(nitrilotris(ethane-2,1-diyl))tris(1H-pyrrole-2,5-dione) for furan-maleimide reaction was synthesized according to the literature procedure with some modifications (**Scheme 5.3**).[10]
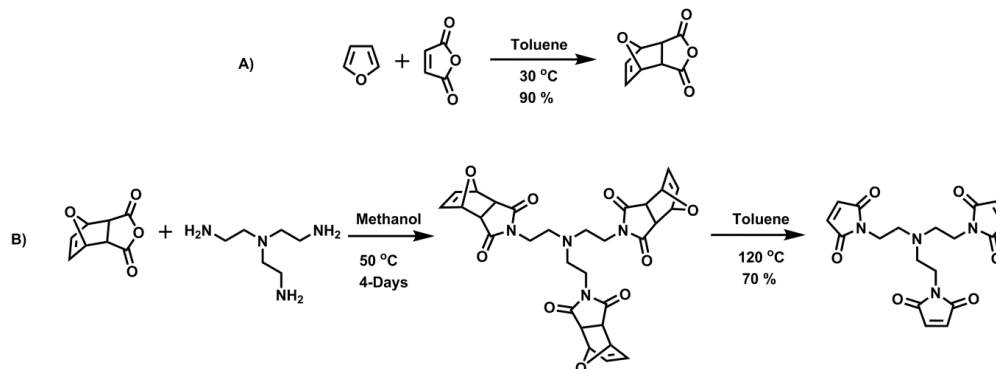
Scheme 5.3 Synthesis of A) exo-3,6-epoxy-1,2,3,6-tetrahydrophthalic anhydride and B) 1,1',1''-(nitrilotris(ethane-2,1-diyl))tris(1H-pyrrole-2,5-dione).

The presence of a singlet at 6.67 ppm corresponding to six protons of maleimide rings in ^{1}H NMR spectrum (**Figure 5.9**) confirmed the formation of 1,1',1''-(nitrilotris(ethane-2,1-diyl))tris(1H-pyrrole-2,5-dione).

Figure 5.9 ^{1}H-NMR spectrum (in CDCl$_3$) of 1,1',1''-(nitrilotris(ethane-2,1-diyl))tris(1H-pyrrole-2,5-dione).

5.3.4 Synthesis of network polymer bearing flexible PLMA chains via furan-maleimide click reaction and the progress of furan-maleimide Diels-Alder and retro Diels-Alder reaction

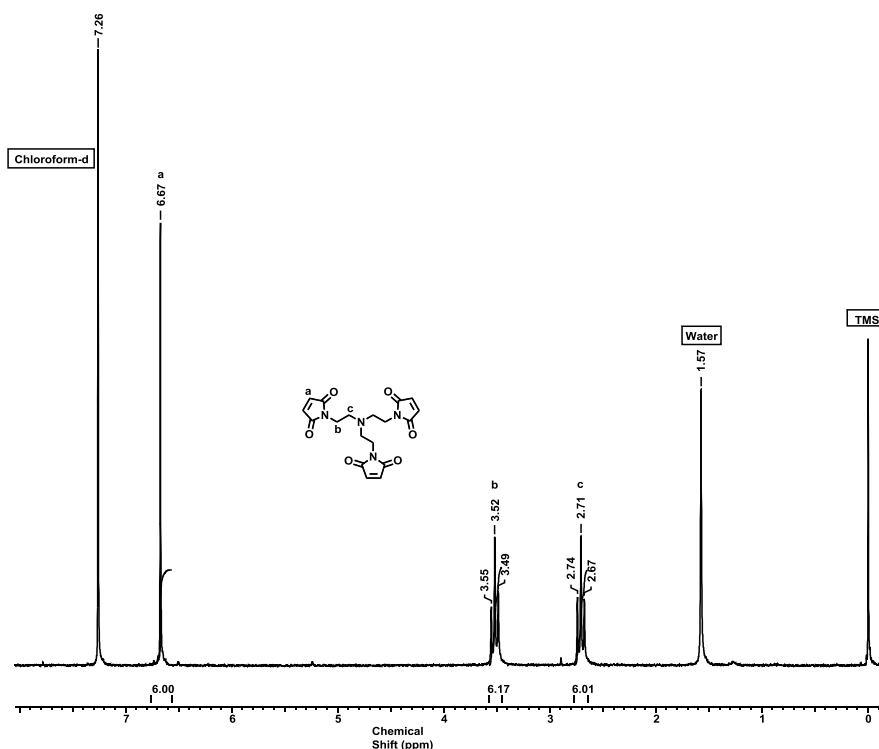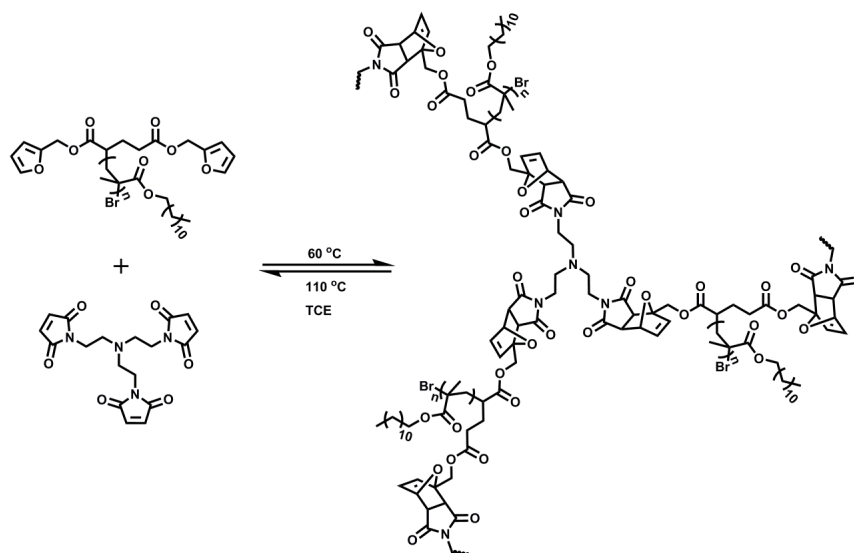The network polymer bearing flexible PLMA chains was synthesized by furan-maleimide Diels-Alder click reaction of equimolar (0.1 M) amounts of bisfuryl-terminated PLMA macromonomer ($M_{n,NMR}$-5000 g mol^{-1}, Dispersity-1.3) and 1,1',1''-(nitrilotris(ethane-2,1-diyl))tris(1H-pyrrole-2,5-dione) in tetrachloroethane (**Scheme 5.4**). These reactions were performed at 60 ^{o}C due to the faster rate of formation of furan-maleimide adducts at this temperature.

Scheme 5.4 Synthesis of thermo-reversible network polymer bearing flexible PLMA chains *via* furan-maleimide click reaction.

The progress of Diels-Alder and retro Diels-Alder reaction was determined by ^{1}H-NMR spectroscopy. The equimolar (0.1 M) amounts of bisfuryl-terminated PLMA and 1,1',1''-(nitrilotris(ethane-2,1-diyl))tris(1H-pyrrole-2,5-dione) in TCE-d$_2$ were reacted at 60 ^{o}C in NMR tube. The progressive decrease in integration of multiplets in the range 7.3-7.5 ppm and 6.27-6.42 ppm corresponding to furyl rings and a singlet at 6.67 ppm corresponding to maleimide rings was observed in ^{1}H-NMR spectrum. The successive increase in integration of multiplets in the range of 6.47-6.60 ppm and 6.25-6.47 ppm corresponding to double bonds of Diels-Alder adduct (**Figure 5.10**) confirmed the formation of furan-maleimide Diels-Alder adducts.
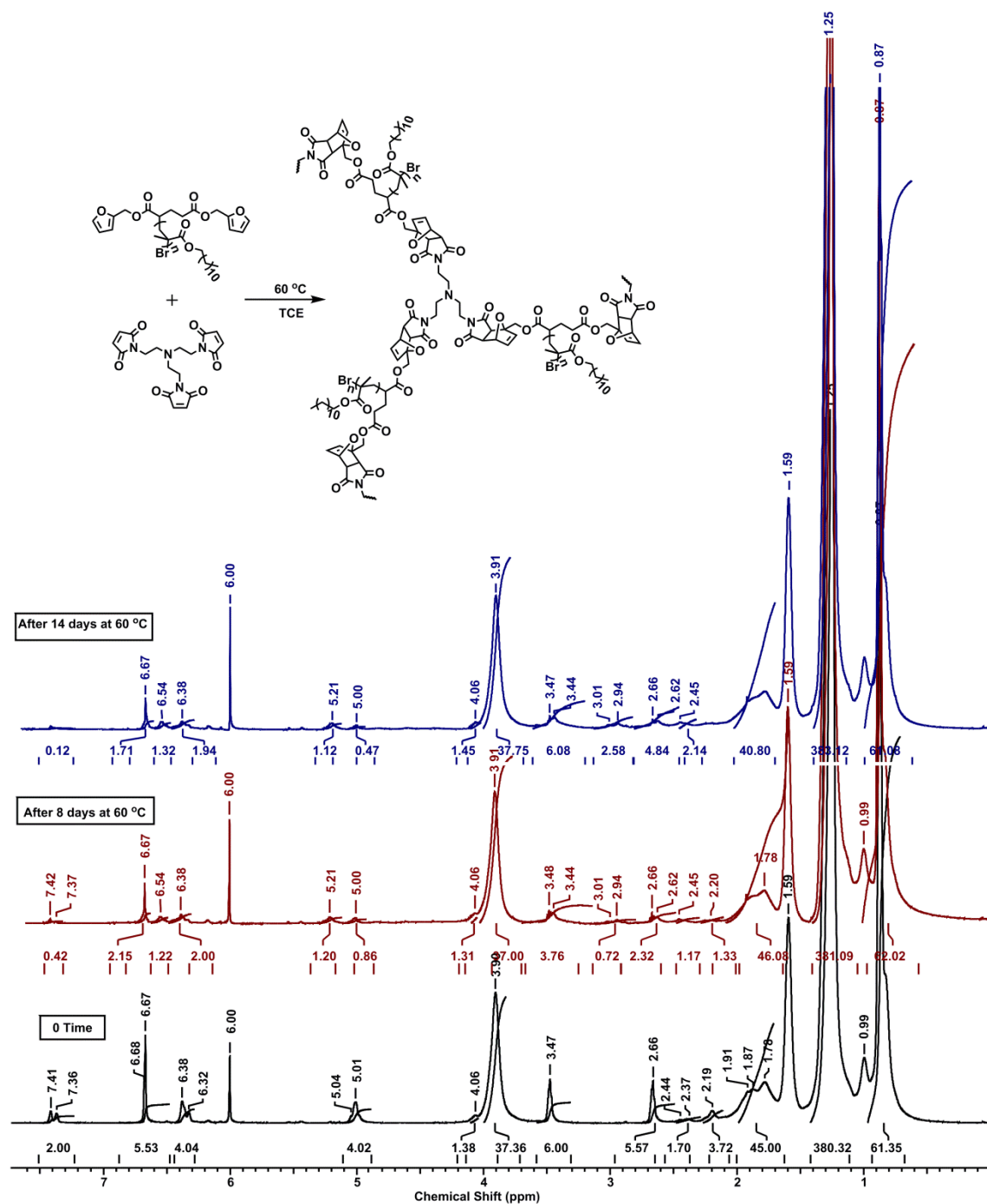
Figure 5.10 The progress of Diels-Alder reaction (in TCE-d$_2$, 0.1 M, 60 ^{o}C) as monitored by ^{1}H-NMR spectroscopy.

The reaction mixture in NMR tube was heated at 110 ^{o}C to determine the progress of retro Diels-Alder reaction. The progressive increase in integration of multiplets and singlet corresponding to furyl and maleimide rings, respectively, (**Figure 5.11**) with time attested the regeneration of bisfuryl-terminated PLMA macromonomer and trismaleimide precursors. The successive decrease in integration of multiplets corresponding to double

bonds of Diels-Alder adducts confirmed the retro Diels-Alder reaction. It should be noted that, the stereochemistry of formed furan-maleimide adducts (endo and exo)[35] may not affect the healing processes and hence determination of their proportion was not of interest in the present studies.

Figure 5.11 The progress of retro Diels-Alder reaction (in TCE-d₂, 0.1 M, 110 °C) as monitored by ¹H-NMR spectroscopy.

The progress of formation of these Diels-Alder adducts and regeneration of respective precursors by retro Diels-Alder reaction was also determined by UV spectroscopy. The reaction of equimolar (0.01 M) amounts of these reactants in TCE at 60 ^{o}C was performed and the absorbance was obtained at different time intervals from UV spectroscopy. The progressive decrease in the value of absorbance at 296 nm corresponding to maleimide ring revealed the formation of these Diels-Alder adducts (**Figure 5.12**).
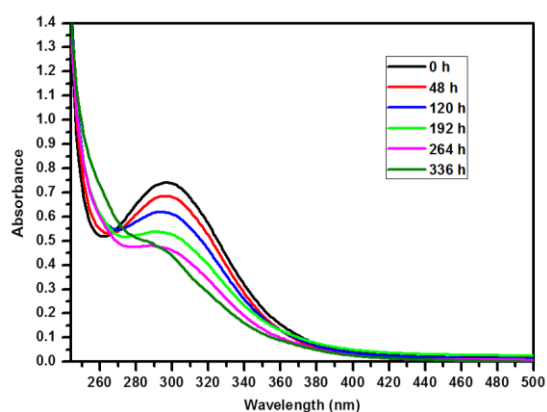
Figure 5.12 The progress of Diels-Alder reaction (in TCE, 0.01 M, 60 ^{o}C) as monitored by UV spectroscopy.

The same reaction mixture was heated at 110 ^{o}C and the value of absorbance with time was obtained to determine the regeneration of respective precursors by retro Diels-Alder reaction. The progressive increase in the value of absorbance corresponding to maleimide rings with time revealed the regeneration of respective precursors by retro Diels-Alder reaction (**Figure 5.13**).
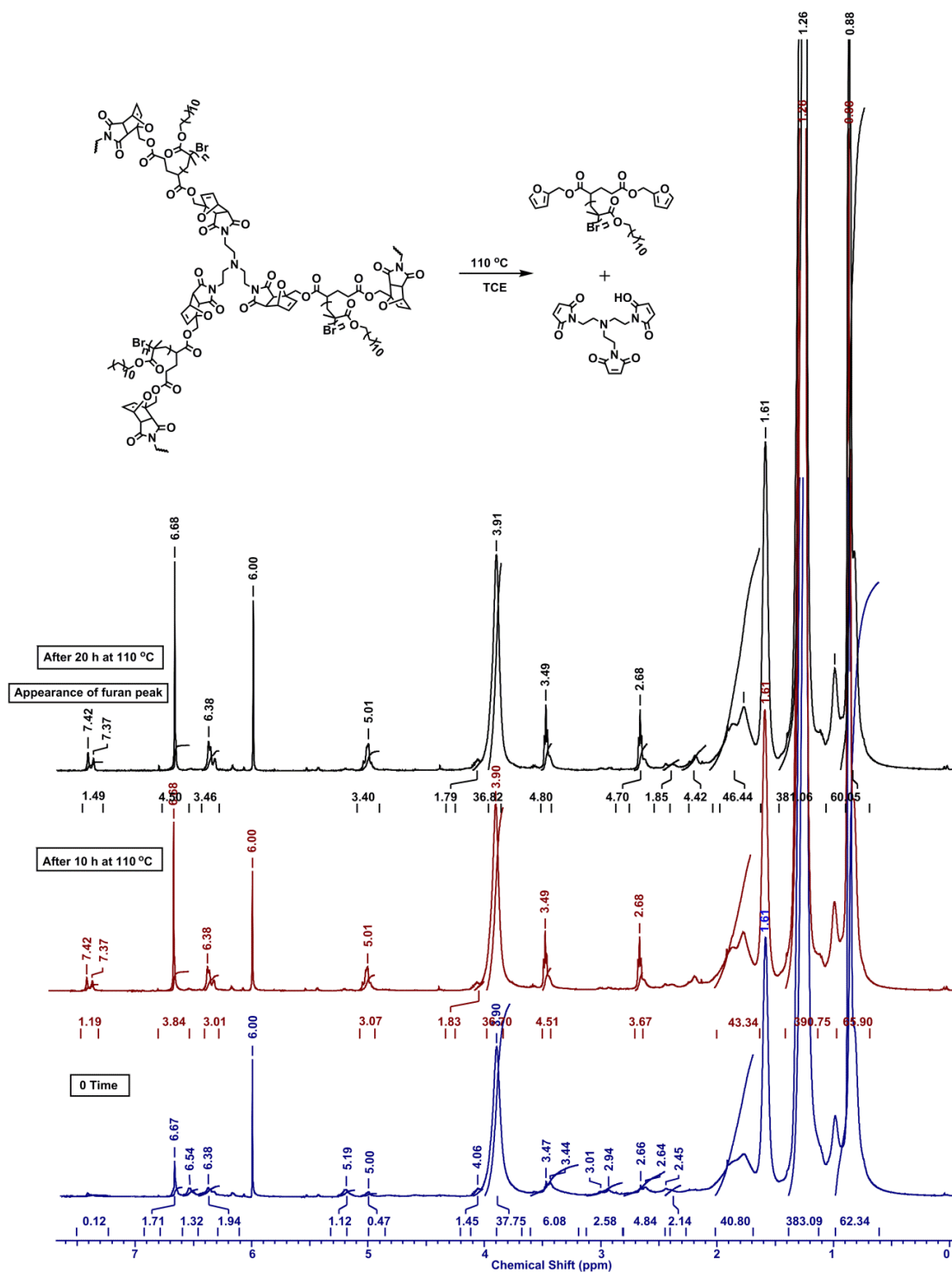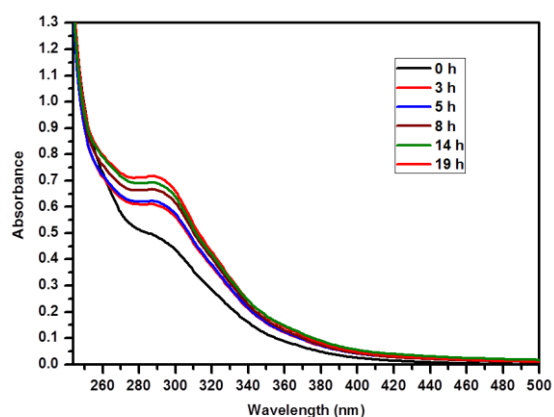

Figure 5.13 The progress of retro Diels-Alder reaction (in TCE, 0.01 M, 110 ^{o}C) as monitored by UV spectroscopy.

The formation of network polymer on heating at 60 ^{o}C due to the formation of furan-maleimide adducts and regeneration of precursors on heating at 110 ^{o}C due to retro Diels-Alder reaction was also confirmed by simple visualization of solubility behavior of polymer in the reaction medium *i.e* TCE (**Figure 5.14**).
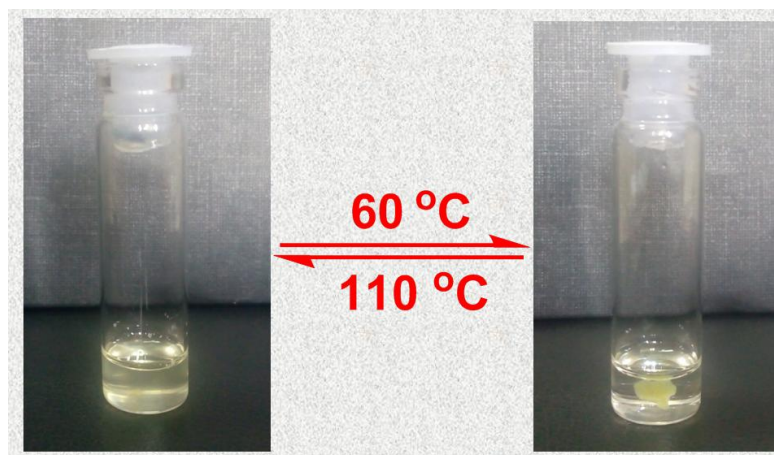
Figure 5.14 The reversible appearance (at 60 ^{o}C) and dissolution (at 110 ^{o}C) of network polymer in TCE.

5.3.5 Thermal properties of bisfuryl-terminated PLMA macromonomer and network polymer bearing flexible PLMA chains

The presence of furan-maleimide adducts confer the thermo-reversible characteristics to the formed network polymer. The repeated heating cycles of PLMA macromonomer in DSC chromatogram showed the glass transition temperature (Tg) of -40 ^{o}C (**Figure 5.15**) while, the repeated heating cycles of a sample of network polymer showed Tg of -44 ^{o}C (**Figure** 5.**16**). The decrease in Tg of network polymer by 4 ^{o}C was ascribed to the introduction of tris-maleimide counterpart in the network structure. In these repeated heating cycles, the regular endothermic transition from 100-170 ^{o}C corresponding to retro Diels-Alder reaction attributed to the cleavage of furan-maleimide adducts to regenerate the precursors were observed.
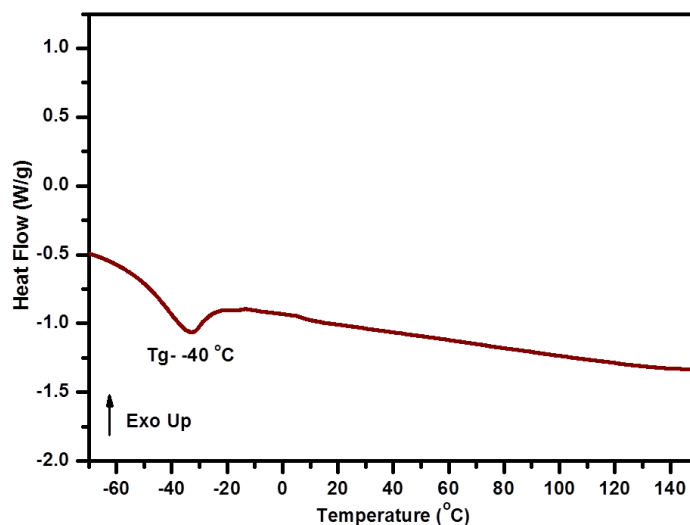
Figure 5.15 DSC trace of bisfuryl-terminated PLMA macromonomer (Table 5.1, Entry 1).
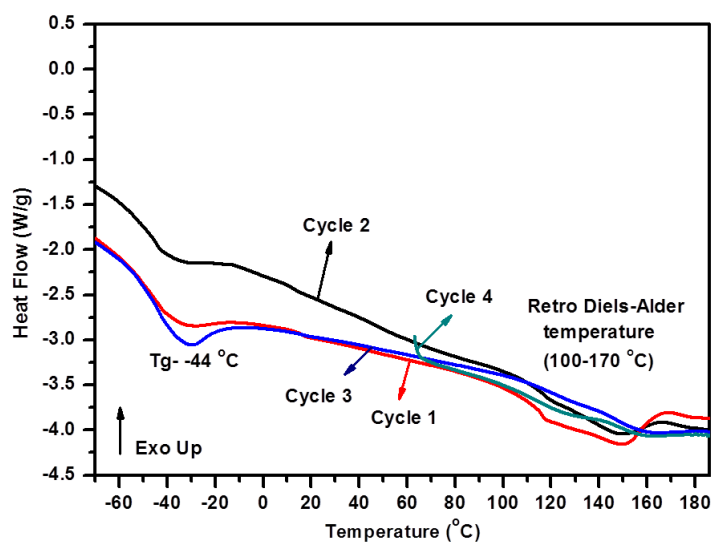
Figure 5.16 DSC traces of repeated heating cycles of network polymer bearing flexible PLMA chains.

Thermo-gravimetric curves of bisfuryl-terminated PLMA and the resulted network polymer showed the stability upto 280 ^{o}C and 295 ^{o}C, respectively, as determined from T_{10} values. In both TG curves, weight loss was observed in two stages. The initial weight loss was observed due to the decomposition of dodecyl chains followed by the decomposition of polymer backbone (**Figure 5.17**).[34]
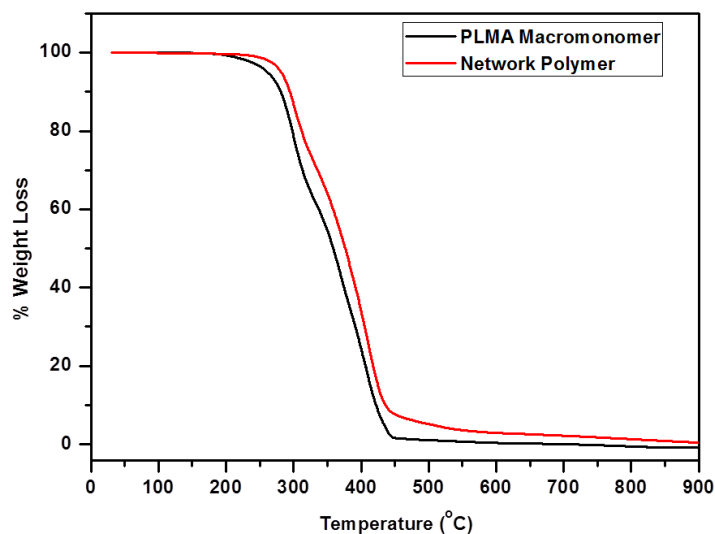
Figure 5.17 TG curves of A) bisfuryl-terminated PLMA macromonomer and B) network polymer.

5.3.6 The visco-elastic behaviour and thermo-reversibility of network polymer bearing flexible PLMA chains with varying temperature

The rheological properties of network polymer were studied to investigate the visco-elastic behavior. The linear region of storage and loss modulus was selected by performing the strain sweep experiment on the network polymer with 1 mm thickness (25 mm parallel plate geometry, 400 mg sample) at 25 $^{\circ}$C. The oscillations at constant angular frequency (5 rad/s) were applied with increasing strain (**Figure 5.18**). It was observed that upto 3 % strain the values of storage and loss modulus were constant. The higher value of storage modulus (G') than loss modulus (G") indicated that the rheological behavior in this network polymer was dominated by an elastic property rather than the viscus property. The angular frequency dependence of storage and loss modulus was also studied by performing the frequency sweep experiment at constant strain (0.5 %). The network polymer showed the reversal of G' and G" at the angular frequency of around 125 rad/sec at 25 $^{\circ}$C (**Figure 5.19**).
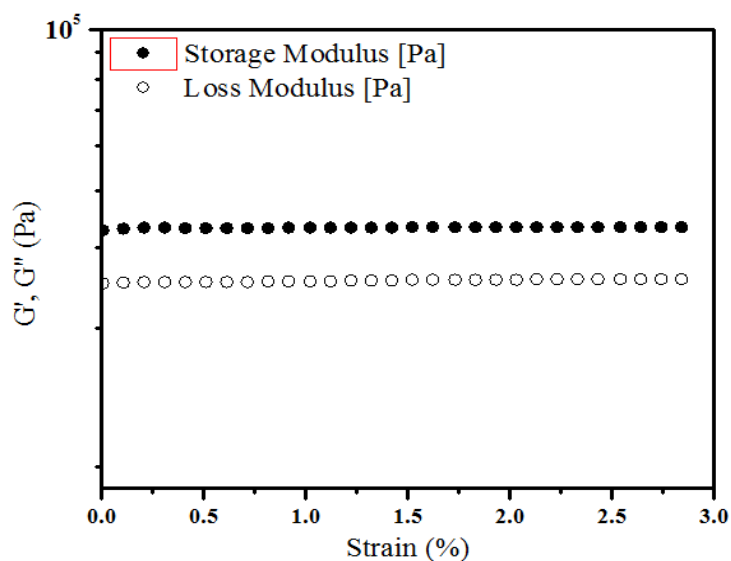
Figure 5.18 The percent strain dependence of storage and loss modulus of network polymer.
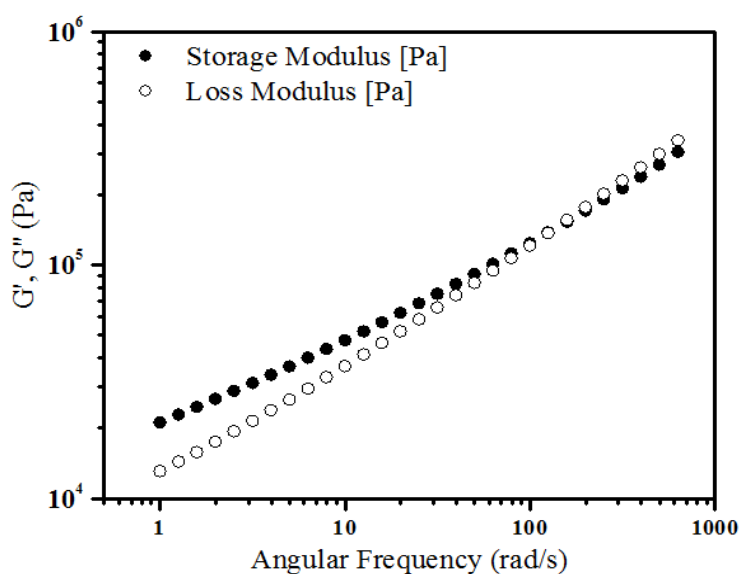
Figure 5.19 The angular frequency dependence of storage and loss modulus of network polymer.

From the experiments of strain and frequency sweep, the values of angular frequency and strain were selected as 5 rad/s and 0.5 %, respectively, for temperature sweep experiment with varying temperatures from 40 -110 ^{o}C. The thermo-reversibility of the prepared network polymer bearing PLMA chains was determined by temperature sweep experiments. The temperature sweep experiment was performed with varying

temperature from 40-110 ^{o}C and 110- 40 ^{o}C. The repeated heating and cooling cycles were performed on the network polymer. In these repeated cycles, the regular reversal of storage (G') and loss modulus (G'') were observed with varying temperature from 40-110 ^{o}C and 110-40 ^{o}C at constant angular frequency and strain (**Figure 5.20**). The initial values of storage (G') and loss modulus (G'') were regained after the completion of each cycle which revealed the thermo-reversibility of network polymers. The thermo-reversibility of the prepared network polymer was demonstrated upto nine repeated cycles which confirmed its recyclability and healability.
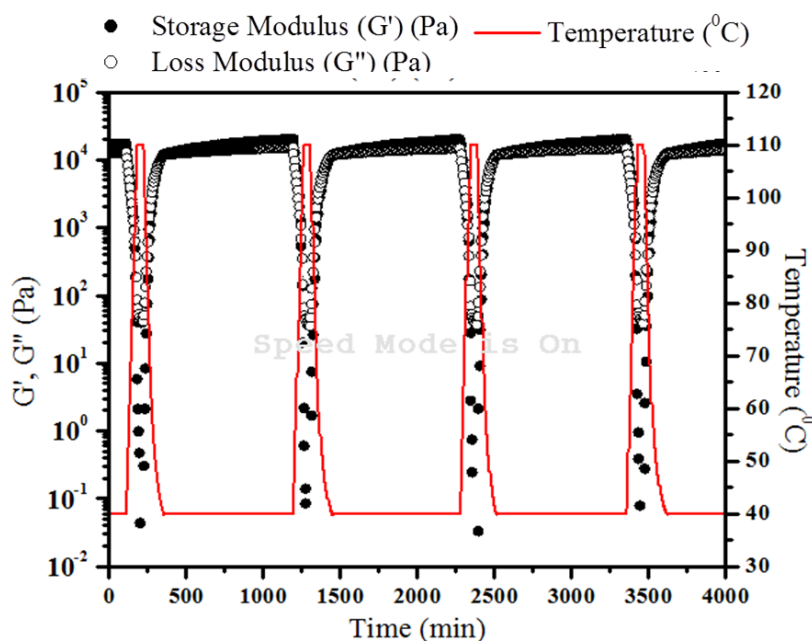
Figure 5.20 Thermo-reversibility of network polymer with repeated heating and cooling cycles from 40-110 ^{o}C and 110-40 ^{o}C.

5.3.7 Crystallinity and water contact angle of network polymer bearing PLMA chains

The crystallinity of the network polymer was found to be lower compared to that of the starting bisfuryl-terminated PLMA macromonomer as indicated by the X-ray diffractogram (**Figure 5.21**). The decrease in crystallinity in the network polymer was attributed to the restricted chain packing. A similar observation has been reported in the literature.[36]
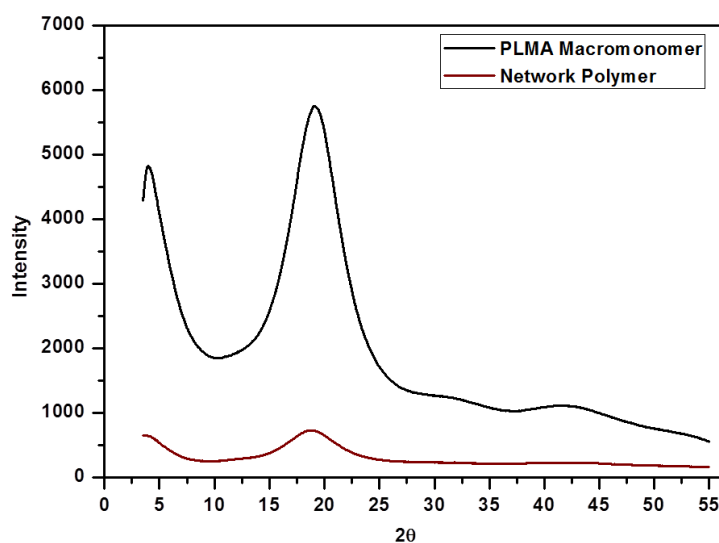
Figure 5.21 X-Ray diffraction patterns of A) bisfuryl-terminated PLMA macromonomer and B) network polymer.

Polymeric materials for several coating applications need hydrophobicity. The hydrophobicity of the designed network polymer bearing PLMA chains was determined by contact angle measurements. The precursor bisfuryl-terminated PLMA macromonomer showed water contact angle of 70° whereas, the contact angle of obtained network polymer with flexible PLMA chains was found to be 102° (**Figure 5.22**). The increase in contact angle (hydrophobicity) may be ascribed to the presence of long PLMA chains and the network structure.
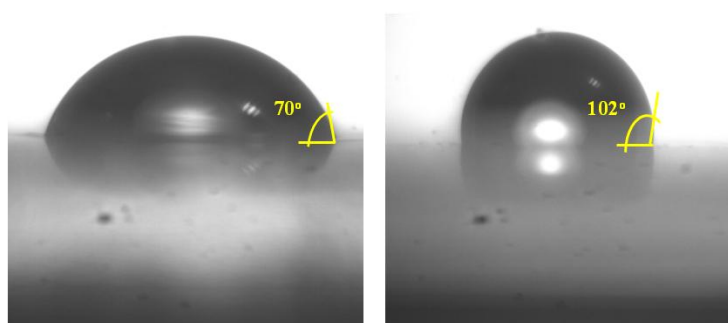
Figure 5.22 Water contact angle of A) bisfuryl-terminated PLMA and B) network polymer.

5.3.8 Scratch-healing behaviour of the network polymer

The healing process requires physical flow of material at the scratch and the chemical re-bonding of cleaved bonds. The scratch healing experiment was performed on polymer film prepared with thickness of ~ 50 μm. The dark spot was made on the glass

plate to identify the exact position of scratch. A scratch with size of ~20 µm was made with a sharp blade on the polymer film. The scratch was completely disappeared after 5 days at 60 ^{o}C temperature (**Figure 5.23**). The presence of low Tg (-40 ^{o}C) PLMA chains induced chain mobility to the network structure which led to the complete scratch healing at 60 ^{o}C in five days.
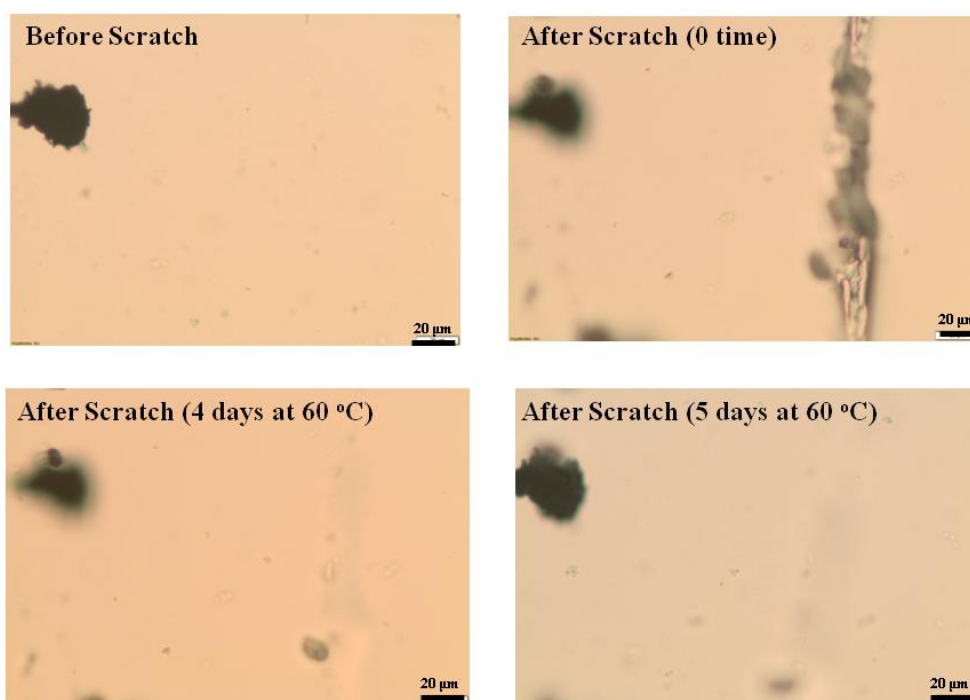
Figure 5.23 The optical microscopy images of network polymer A) before scratch, B) after scratch, C) scratch after 4 days at 60 ^{o}C and D) scratch after 5 days at 60 ^{o}C.

The network polymers with covalent bonding exhibit higher modulus compared to the physically cross-linked (supramolecular) materials. Such hydrophobic thermo-reversible network polymers with chemically bonded structures, comparable storage modulus and healability at 60 ^{o}C or relatively moderate temperatures are potentially useful smart materials in the areas of coating applications.

5.4 Conclusions

A new ATRP initiator containing two furyl rings, namely, bis(furan-2-ylmethyl) 2-bromopentanedioate was synthesized starting from commercially available L-glutamic acid as precursor. Well-defined bisfuryl-terminated PLMA macromonomers were obtained employing the initiator by ATRP. Independently, a trismaleimide counterpart *viz.* 1,1',1''-(nitrilotris(ethane-2,1-diyl))tris(1H-pyrrole-2,5-dione) was synthesized. Thermo-reversible

network polymer bearing flexible PLMA chains was obtained via furan-maleimide Diels-Alder click reaction of bisfuryl-terminated PLMA macromonomer with 1,1',1"-(nitrilotris(ethane-2,1-diyl))tris(1H-pyrrole-2,5-dione). The formation of furan-maleimide Diels-Alder adducts at 60 ^{o}C and regeneration of furan-maleimide precursors on heating at 110 ^{o}C was observed from ^{1}H-NMR and UV-absorbance measurements. Thermo-reversibility of prepared network polymer was demonstrated from rheological measurements upto nine repeated cycles which proved the recyclability and healability of the resulting smart materials. These network polymers exhibited the complete scratch healing at 60 ^{o}C in five days due to the presence of low Tg (-40 ^{o}C) flexible PLMA chains which induced the chain mobility in these systems and Diels-Alder adduct formation. The designed network polymer was found to be quite hydrophobic with water contact angle of 102° due to the presence of long PLMA chains and network structure. Such hydrophobic thermo-reversible network polymers with chemically bonded structures, comparable storage modulus and healability at 60 ^{o}C or relatively moderate temperatures are potentially useful smart materials in coating applications.

5.5 References

1. N. K. Guimard, K. K. Oehlenschlaeger, J. Zhou, S. Hilf, F. G. Schmidt and C. B. Kowollik, *Macromol. Chem. Phys.*, 2012, **213**, 131-143.

2. J. Kotteritzsch, S. Stumpf, S. Hoeppener, J. Vitz, M. D. Hager and U. S. Schubert, *Macromol. Chem. Phys.*, 2013, **214**, 1636-1649.

3. N. Bai, K. Saito and G. P. Simon, *Polym. Chem.*, 2013, **4**, 724-730.

4. R. G. Lorenzini and G. A. Sotzing, *J. Appl. Polym. Sci.*, 2014, **131**, 40179.

5. D. Edelmann and H. Ritter, *Makromol. Chem.*, 1993, **194**, 1183-1195.

6. C. Zeng, H. Seino, J. Ren, K. Hatanaka and N. Yoshie, *Macromolecules*, 2013, **46**, 1794-1802.

7. T. Defize, R. Riva, J. M. Raquez, P. Dubois, C. Jerome and M. Alexandre, *Macromol. Rapid Commun.*, 2011, **32**, 1264-1269.

8. C. Toncelli, D. C. D. Reus, F. Picchioni and A. A. Broekhuis, *Macromol. Chem. Phys.*, 2012, **213**, 157-165.

9. A. Gandini, D. Coelho and A. J. D. Silvestre, *Eur. Polym. J.*, 2008, **44**, 4029-4036.

10. A. Gandini, D. Coelho, M. Gomes, B. Reis and A. Silvestre, *J. Mater. Chem.*, 2009, **19**, 8656-8664.

11. A. M. Peterson and G. R. Palmese, *Macromol. Chem. Phys.*, 2013, **214**, 1798-1805.

12. A. A. Kavitha and N. K. Singha, *ACS Appl. Mater. Interfaces*, 2009, **7** 1427-1436.

13. L. M. Polgar, M. v. Duin, A. A. Broekhuis and F. Picchioni, *Macromolecules*, 2015, **48**, 7096-7105.

14. G. Li, J. J. Wie, N. A. Nguyen, W. J. Chung, E. T. Kim, K. Char, M. E. Mackay and J. Pyun, *J. Polym. Sci., Part A: Polym. Chem.*, 2013, **51**, 3598-3606.

15. F. Herbst, D. Dohler, P. Michael and W. H. Binder, *Macromol. Rapid Commun.*, 2013, **34**, 203-220.

16. J. F. Lutz, B. V. K. J. Schmidt and S. Pfeifer, *Macromol. Rapid Commun.*, 2011, **32**, 127-135.

17. Y. Chen and Z. Guan, *Chem. Commun.*, 2014, **50**, 10868-10870.

18. Y. L. Liu and T. W. Chuo, *Polym. Chem.*, 2013, **4**, 2194-2205.

19. J. A. Syrett, G. Mantovani, W. R. S. Barton, D. Price and D. M. Haddleton, *Polym. Chem.*, 2011, **1**, 102-106.

20. S. O. Sanchez, F. Marra, A. Dibenedetto, M. Aresta and A. Grassi, *Macromolecules*, 2014, **47**, 7129-7137.

21. A. Gandini, *Prog. Polym. Sci.*, 2013, **38**, 1-29.

22. A. Gandini, A. J. D. Silvestre and D. Coelho, *J. Polym. Sci., Part A: Polym. Chem.*, 2010, **48**, 2053-2056.

23. T. Dispinar, R. Sanyal and A. Sanyal, *J. Polym. Sci., Part A: Polym. Chem.*, 2007, **45**, 4545-4551.

24. G. Hizal, U. Tunca and A. Sanyal, *J. Polym. Sci., Part A: Polym. Chem.*, 2011, **49**, 4103-4120.

25. D. Arunbabu, S. M. Noh, J. H. Nam and J. K. Oh, *Macromol. Chem. phys.*, 2016, **217**, 2191-2198.

26. Y. Zhang, A. A. Broekhuis and F. Picchioni, *Macromolecules*, 2009, **42**, 1906-1912.

27. N. Teramoto, Y. Arai and M. Shibata, *Carbohydr. Polym.*, 2006, **64**, 78-84.

28. N. Kuramoto, K. HayashI and K. Nagal, *J. Polym. Sci., Part A: Polym. Chem.*, 1994, **32**, 2501-2504.

29. C. Gousse, A. Gandini and P. Hodge, *Macromolecules*, 1998, **31**, 314-321.

30. C. Gousse and A. Gandini, *Polym. Int.*, 1999, **48**, 723-731.

31. A. Gandini, A. Silvestre and D. Coelho, *Polym. Chem.*, 2013, **4**, 1364-1371.

32. H. L. Wei, K. Yao, H. J. Chu, Z. C. Li, J. Zhu, Y. M. Shen, Z. X. Zhao and Y. L. Feng, *J. Mater. Sci.*, 2012, **47**, 332-340.

33. N. Yoshie, M. Watanabe, H. Araki and K. Ishida, *Polym. Degrad. Stab.*, 2010, **95**, 826-829.

34. R. K. Bose, J. Kotteritzsch, S. J. Garcia, M. D. Hager, U. S. Schubert and S. V. D. Zwaag, *J. Polym. Sci., Part A: Polym. Chem.*, 2014, **52**, 1669-1675.

35. J. Canadell, H. Flscher, G. D. Wlth and R. A. T. M. V. Benthem, *J. Polym. Sci., Part A: Polym. Chem.*, 2010, **48**, 3456-3467.

36. L. T. T. Nguyen, H. T. Nguyen and T. T. Truong, *J. Polym. Res.*, 2015, **22**, 186.

Chapter 6

Conclusions and Future Perspectives

6.1 Conclusions

The synthesis of clickable ATRP and ROP initiators derived from commercially available and inexpensive starting materials by convenient route is a topic of great interest.[1,2] Well-defined telechelic polymers and the respective macromoleular architectures can be obtained from these initiators depending on the functionalities present in their structures. In the first objective of thesis, a new ATRP initiator, namely, 2-(1,1-bis(4-(allyloxy)phenyl)-3-oxoisoindolin-2-yl)ethyl 2-bromo-2-methylpropanoate was synthesized starting from phenolphthalein and was employed for polymerization of styrene. The notable features of ATRP initiator synthesized in the present work are: 1) utilization of commercially available and inexpensive starting material, namely, phenolphthalein, 2) convenient synthetic methodology and 3) relatively less explored allyloxy functionality which possesses distinct advantages in terms of its reactivity. Well-defined and narrow dispersity α, α' bis-allyloxy functionalised polystyrene macromonomers were synthesized. The kinetic studies of styrene polymerization indicated controlled polymerization behaviour. The reactivity of terminal allyl groups for thiol-ene click reaction was demonstrated by performing the model reaction with benzyl mercaptan as a thiol reagent. Thiol-ene click reaction was exploited successfully to introduce other reactive functional groups such as hydroxyl and carboxyl by performing the click reaction of bis-allyloxy functionalised polystyrene with 2-mercaptoethanol and 3-mercaptopropionic acid, respectively. α, α'-Dihydroxyl and α, α'-dicarboxyl functionalised polystyrene macromonomers, thus obtained, represent valuable precursors for the synthesis of graft, miktoarm star copolymers and are potentially useful macromonomers for step-growth polymerizations. The present approach opens up new avenues for design and synthesis of phenolphthalein-based ATRP initiators containing other useful functional groups such as propargyl, furan, azido, etc. and corresponding polymers therefrom.

In another objective of thesis, different macromolecular architectures and their properties with respect to the smart behavior were examined. The initial architectural design to demonstrate smart behaviour was miktoarm star copolymer based on the combination of ROP and ATRP with that of alkyne-azide and thiol-ene coupling reactions. In the present synthetic design, the orthogonality of the thiol-ene and alkyne-azide coupling reactions was also demonstrated. In the beginning the focus of work was laid on the polymers bearing only single stimulus-response.

Two new ROP initiators, namely, (3-allyl-2-(allyloxy)phenyl)methanol and (3-allyl-2-(prop-2-yn-1-yloxy)phenyl)methanol containing reactive functionalities such as allyl, allyloxy and allyl, propargyloxy, respectively, were synthesized starting from a common precursor- 3-allylsalicyaldehyde. The in-built allyl functionality in 3-allylsalicyaldehyde offers the flexibility in terms of choice of other functional groups for orthogonal chemistries and hence can be considered as a versatile precursor for synthesis of ROP initiator cores for designing homo- and hetero-bifunctionalised polymers. Such functional initiators with non-interferable functionalities offer the reactive sites for orthogonal reactions and post modifications of the polymers. Well defined α,α'- homo- and α,α'-hetero-bifunctionalised poly(ε-caprolactone)s were conveniently synthesized by controlled polymerization of ε-caprolactone employing these ROP initiators. Thiol-ene reaction and orthogonal alkyne-azide and thiol-ene reactions, respectively, of α-allyl, α'-allyloxy and α-allyl, α'-propargyloxy bifunctionalised poly(ε-caprolactone)s were studied to synthesize (mPEG)$_2$-PCL and PCL-PNIPAAm-mPEG star copolymer. Thus, the orthogonality of alkyne-azide and thiol-ene coupling reactions was demonstrsted and the limitations of thiol-ene polymer-polymer conjugation reaction for the synthesis of miktoarm star copolymers were highlighted. The temperature responsive behavior, morphological changes of the assemblies of PCL-PNIPAAm-mPEG star copolymer in aqueous solution and the cargo release profiles of hydrophobic probe *viz.* pyrene from these assemblies were studied under varying conditions of temperature. The aggregates of PCL-PNIPAAm-mPEG star copolymer showed faster release of encapsulated pyrene with increasing temperature.

The other architecture to demonstrate smart polymer behaviour was diblock copolymer based on the combination of ROP, ATRP and alkyne-azide click reaction. The advantage of accessability of dual responsive block copolymer system compared to the synthetically difficult to access systems such as star copolymers with dual or multi-responsive nature was also described. Well-defined azido-functionalized PNIPAAms with different molecular weights were synthesized by ATRP employing a new initiator, namely, 2-(1-(2-azidoethoxy)ethoxy)ethyl 2-bromo-2-methylpropanoate containing both cleavable (acetal) and clickable (azido) groups. PCL-*b*-PNIPAAm block copolymer was obtained from these azido-terminated poly(*N*-isopropylacrylamide) (PNIPAAm-N$_3$) by alkyne-azide click reaction with propargyl-terminated poly(ε-caprolactone) (Pr-PCL). Critical

aggregation concentration (CAC) of PCL-*b*-PNIPAAm block copolymer in aqueous solution was found to be 8.99×10^{-6} M. LCST of PCL-*b*-PNIPAAm block copolymer was found to be 32 ^{o}C and was dependant on polymer concentration as well as presence of salts in the solution. The effect of dual stimuli *viz.* temperature and pH on the assemblies of PCL-*b*-PNIPAAm block copolymer was studied which revealed that the copolymer below LCST assembled in spherical micelles which successively transformed to unstable vesicles above the LCST. Heating these assemblies above 40 ^{o}C further led to the precipitation of PCL-*b*-PNIPAAm block copolymer. Whereas, at decreased pH, micelles of PCL-*b*-PNIPAAm copolymer disintegrate due to the cleavage of acetal linkage and precipitation of hydrophobic hydroxyl terminated-PCL. The encapsulated pyrene release kinetics from the micelles of synthesized PCL-*b*-PNIPAAm block copolymer system was found to be faster at higher temperature and at lower pH. The findings on temperature and pH dual-stimuli response and the morphological changes of self-assemblies of PCL-*b*-PNIPAAm block copolymer with varying temperature and pH were investigated. The present design can be useful as model studies for temperature and pH dual-responsive drug-delivery systems. The straightforward access to such dual stimuli-responsive block copolymer systems is of significant advantage compared to the reported synthetically difficult to access systems such as star, branched, etc. with dual or multi-responsive nature.

The next macromolecular architecture to demonstrate smart polymer behaviour was network polymer based on the combination of ATRP and furan-maleimide Diels-Alder click reaction. A new ATRP initiator containing two furyl rings, namely, bis(furan-2-ylmethyl) 2-bromopentanedioate was synthesized starting from commercially available L-glutamic acid as a precursor. Well-defined bisfuryl-terminated PLMA macromonomers were obtained employing the initiator by ATRP. Independently, a trismaleimide counterpart *viz.* 1,1',1''-(nitrilotris(ethane-2,1-diyl))tris(1H-pyrrole-2,5-dione) was synthesized. Thermo-reversible network polymer bearing flexible PLMA chains was obtained via furan-maleimide Diels-Alder click reaction of bisfuryl-terminated PLMA macromonomer with 1,1',1''-(nitrilotris(ethane-2,1-diyl))tris(1H-pyrrole-2,5-dione). The formation of furan-maleimide Diels-Alder adducts at 60 ^{o}C and regeneration of furan-maleimide precursors on heating at 110 ^{o}C was observed from ^{1}H-NMR and UV-absorbance measurements. Thermo-reversibility of prepared network polymer was demonstrated from rheological measurements upto nine repeated cycles which proved the

recyclability and healability of the resulting smart materials. These network polymers exhibited the complete scratch healing at 60 ^{o}C in five days due to the presence of low Tg (-40 ^{o}C) flexible PLMA chains which induced the chain mobility in these systems and Diels-Alder adduct formation. The designed network polymer was found to be quite hydrophobic with water contact angle of 102° due to the presence of long PLMA chains and network structure. Such hydrophobic thermo-reversible network polymers with chemically cross-linked structures, comparable storage modulus and healability at 60 ^{o}C or relatively moderate temperatures are potentially useful smart materials in coating applications.

6.2 Future Perspectives

Results and conclusions of the present research work related to design and synthesis of new functional initiators, end-functionalized polymers and macromolecular architectures have opened up various new prospects in terms of future research.

- The designed new ATRP and ROP initiators have expanded the choice of available functionalities to obtain end-functionalized polymers, macromonomers and macromolecular architectures therefrom. A variety of monomers such as lactides and methacrylates can be polymerized by ROP and ATRP, respectively, employing the respective initiators.

- Diallyl, dihydroxyl and dicarboxyl functionalized macromonomers, thus prepared, are useful precursors for polycondensation reactions. The graft copolymers could be obtained from these macromonomers. For instance, the reaction of α,α'-bisallyloxy functionalised polystyrene macromonomers with hydride- terminated polysiloxane would lead to polysiloxane-g-polystyrene copolymers.

- Bisallyloxy functionalized polystyrene macromonomers could be further utilized in the efficient reactions such as radical oligomerization, epoxidation, hydrosilylation and hydroboration.

- Thermal or photo-chemical cross-linking of allyl groups of bisallyloxy functionalized polystyrene macromonomers into the corresponding networked polymers could be preformed to improve the thermal stability, mechanical strength and solvent resistance of the resulting cross-linked polymers.

- 3-Allylsalicyaldehyde is an interesting precursor for synthesis of a wide variety of ROP and ATRP initiators. The phenolic hydroxyl group provides a reactive handle for introduction of useful functional groups via etherification reaction with appropriately substituted alkyl halides/tosylates. For instance, azido or furyl groups could be introduced via reaction with 2-azidoethyl *p*-methylbenzenesulfonate and 2-(6-bromohexyl)furan, respectively.

- The vinyloxy group in 2-(vinyloxy)ethyl 2-bromo-2-methylpropanoate offers the opportunity in terms of choice of the incorporation of clickable moieties by reaction with appropriately substituted functional alcohols such as furfuryl alcohol, propargyl alcohol, allyl alcohol, etc. Likewise, the number of clickable groups in 2-(vinyloxy)ethyl 2-bromo-2-methylpropanoate could be tuned by appropriate choice of the alcohol containing respective number of clickable groups. ATRP initiators based on these intermediates would eventually provide an access to stimuli-responsive macromolecular architecture such as block or star copolymers.

- It would be of interest to extend the studies concerning structure-molecular parameter-property relationships of the synthesized macromolecular architectures which are needed to assess the viability of these systems in real applications.

6.3 References

1. U. Mansfeld, C. Pietsch, R. Hoogenboom, C. R. Becer and U. S. Schubert, *Polym. Chem.*, 2010, **1**, 1560-1598.

2. V. Coessens, T. Pintauer and K. Matyjaszewski, *Prog. Polym. Sci.*, 2001, **26**, 337-377.

List of Publications

1) **<u>Sachin S. Patil</u>**, Shamal K. Menon and Prakash P. Wadgaonkar, "A New Atom Transfer Radical Polymerization Initiator Based on Phenolphthalein for the Synthesis of Bis-allyloxy Functionalized Polystyrene Macromonomers" *Polym. Int*. 2015, **64**, 413 - 420.

2) **<u>Sachin S. Patil</u>**, Bhausaheb V. Tawade and Prakash P. Wadgaonkar, "A Convenient Synthesis of α,α'-Homo- and α,α'-Hetero-Bifunctionalized Poly(ε-caprolactone)s by Ring Opening Polymerization: The Potentially Valuable Precursors for Miktoarm Star Copolymers" *J. Polym. Sci., Part A: Polym. Chem.* 2016, **54**, 844–860.

3) **<u>Sachin S. Patil</u>** and Prakash P. Wadgaonkar, "Temperature and pH Dual Stimuli Responsive PCL-*b*-PNIPAAm Block Copolymer Assemblies and the Cargo Release Studies" *J. Polym. Sci., Part A: Polym. Chem.,* 2017, DOI-10.1002/pola.20160822.

4) **<u>Sachin S. Patil</u>**, Arun Torris and Prakash P. Wadgaonkar, "Healable Network Polymers Bearing Flexible Poly(Lauryl Methacrylate) Chains via Thermo-reversible Furan-Maleimide Diels-Alder Reaction" (*Manuscript Communicated).*

5) **<u>Sachin S. Patil</u>**, Prakash S. Sane, Dnyaneshwar V. Palaskar, and Prakash P. Wadgaonkar, "Synthesis of Functionally-Terminated Polymers by Atom Transfer Radical Polymerization (ATRP) and Their Applications"-*Book Chapter in Press* (*SMITHERS Rapra-"Functional Polymers by Controlled Radical Polymerization: Concepts, Strategies and Applications" by Nikhil K. Singha and Jimmy W. Mays).*

6) Nilakshi V. Sadavarte, **<u>Sachin S. Patil</u>**, C.V. Avadhani, and Prakash P. Wadgaonkar, "New Organosoluble Aromatic Poly(esterimide)s Containing Pendent Pentadecyl Chains: Synthesis and Characterization" *High Performance Polymers*, 2013, **25**, 735-743.